ULIÈGE

Faculty of Sciences
Laboratory of Virology and Immunology
GIGA-I3

Varicella-Zoster virus ORF9p: role in viral envelopment and cell-cell fusion

---

Author: Julien LAMBERT
Supervisor: Dr. Marielle LEBRUN
Co-supervisor: Pr. Catherine SADZOT

A thesis submitted in fulfillment of the requirements for the degree of Doctor of Philosophy

August 2022

"*Somewhere, something incredible is waiting to be known.*"

Carl Sagan

"*Rien ne sert de courir, il faut partir à point.*"

Jean de La Fontaine

Abstract

Varicella-Zoster virus ORF9p: role in viral envelopment and cell-cell fusion

Varicella-Zoster virus is a double-stranded DNA virus belonging to the *Herpesviridae* family. Its genome encodes 72 ORFs among which ORF9p, the most expressed protein during the lytic cycle of the virus.
Previous work in our laboratory showed that ORF9p plays a role in viral envelopment and that it may interact with the cellular Adaptor Protein-1 (AP-1) complex to do so.
The aim of this work was to better characterize the role of ORF9p during secondary envelopment and to understand the importance of the ORF9p/AP-1 interaction in this process.
First, we confirmed the ORF9p/AP-1 interaction in an infection context and identified the residue leucine 231 of ORF9p as critical for this interaction. We showed that alanine substitution of this residue led to a mislocalization of ORF9p in infected cells as well as a strong replication defect of the virus. Then, we showed that the L231A mutation was also associated with a lack of cell-cell fusion usually seen upon infection by the Wild-type virus. Moreover, naturally occurring compensatory mutations in the coding sequences of gE and/or gH not only restored the fusion phenotype, but also increased cell-cell fusion compared to the Wild-type virus. We have also demonstrated that ORF9p favored the formation of glycoproteins complexes around gE and gH and that the ORF9p L231A mutation destabilized these complexes. Finally, we propose a model explaining the potential role of ORF9p in secondary envelopment of VZV as well as in the cell-cell fusion process.

Résumé

Varicella-Zoster virus ORF9p: role in viral envelopment and cell-cell fusion

Le virus de la Varicelle et du Zona est un virus à ADN double brin appartenant à la famille des *Herpesviridae*. Son génome encode 72 protéines parmi lesquelles ORF9p, protéine la plus abondamment exprimée au cours du cycle lytique du virus.
Différents travaux réalisés précédemment dans notre laboratoire ont démontré qu'ORF9p jouait un rôle dans le processus d'enveloppement du virus et que, pour ce faire, elle pourrait interagir avec le complexe cellulaire AP-1.
L'objectif de ce travail était de caractériser plus en profondeur le rôle de la protéine ORF9p au cours de l'enveloppement secondaire du virus et de déterminer l'importance de l'interaction ORF9p/AP-1 dans ce processus.
Premièrement, nous avons confirmé l'interaction ORF9p/AP-1 dans un contexte d'infection et identifié le résidu leucine 231 d'ORF9p comme critique pour cette interaction. Nous avons montré que la mutation de ce résidu entraîne une mauvaise localisation d'ORF9p au sein des cellules infectées ainsi qu'un grave défaut de réplication du virus muté. Par la suite, nous avons montré que la substitution de la leucine 231 d'ORF9p par une alanine est également associée à une perte de fusion cellule-cellule normalement observée au cours d'une infection par le virus sauvage. Ensuite, nous avons observé que des mutations compensatoires apparaissent dans les séquences codant pour les glycoprotéines gE et/ou gH et que ces mutations non seulement restaurent le phénotype de fusion, mais entraînent également une fusion plus importante qu'observée avec un virus sauvage. De plus, nous avons montré que la protéine ORF9p permettait la formation de complexes de glycoprotéines autour de gE et gH et que ces complexes étaient perturbés par la mutation L231A d'ORF9p. Finalement, nous proposons un modèle expliquant le rôle que pourrait jouer ORF9p dans le processus d'enveloppement secondaire du VZV ainsi que dans le processus de fusion intercellulaire.

Acknowledgements

Je tiens premièrement à remercier le Dr. Catherine Sadzot pour m'avoir accueilli au sein de son laboratoire, d'abord pour réaliser mon mémoire de fin d'études, ensuite pour réaliser cette thèse de Doctorat. Merci pour ta confiance, ton aide et tes conseils tout au long de ce travail, ainsi que pour tes nombreux appels à prendre du recul!

Je remercie bien entendu Marielle. Merci pour ta connaissance encyclopédique du VZV et pour ta mémoire exceptionnelle des expériences et résultats obtenus par mes prédécesseurs au laboratoire. Merci pour ton énergie débordante, même sil est parfois difficile de te suivre dans les couloirs. Merci pour tous tes conseils et pour avoir challengé mes différents modèles, me forçant à revoir ma façon de penser et à me dépasser pour en proposer des nouveaux plus cohérents. Bien plus qu'une promotrice, tu es une véritable amie!

Cédric, merci pour ton soutien logistique, ta connaissance (presque) parfaite de tout ce qui est disponible ou non dans le labo et surtout pour savoir trouver à peu près n'importe quel produit en un temps record!! Encore plus important, merci pour ton humour et la bonne humeur que tu apportes dans le labo.

Merci Tanguy pour ton humour, pour les nombreuses pauses chiques, pour les soirées petits fours, pour m'avoir servi de taxi quand ma voiture était au garage, pour m'avoir sans cesse demandé "bon alors, tu passes quand ta thèse ?" en gros, merci d'avoir été mon collègue préféré durant toutes ces années.

Judit, merci pour ta bonne humeur et ton énergie, merci de m'avoir appris des phrases essentielles en espagnol...ou pas. Et surtout, merci pour les 13287 kilos de saucisson que tu rapportais de chaque voyage en Espagne!!

Merci aux membres du laboratoire PSI et de la plateforme viral vectors pour les nombreux fous rires sur le temps de midi et lors de beer hours, ainsi que pour la bonne ambiance que chacun de vous apporte dans le laboratoire.

Merci aux membres de mon comité de thèse qui m'ont accompagné durant ces quatre années pour leur bienveillance et leurs conseils lors de nos réunions.

Un merci tout particulier à ma famille: maman, merci de m'avoir rappelé qu'il y a des choses bien plus difficiles dans la vie que d'avoir à rédiger une thèse. Papa, merci d'avoir dit à tes collègues que je travaillais sur le virus de la variole, faisant passer mes travaux pour deux fois plus cools que ce qu'ils ont réellement été. Thomas, merci d'avoir choisi de faire un

doctorat en six ans et ainsi me permettre d'être le premier à l'obtenir (même s'il m'a finalement fallu six ans à moi aussi pour terminer), merci également pour ton appui technique pour la rédaction de ce manuscrit. Finalement, merci Céline pour le soutien moral durant toutes ces années et pour la relecture...s'il reste des fautes, tu en seras la seule responsable!

Pour finir, merci Catherine (ma p'tite Demdi d'amour) d'avoir supporté ces nombreux weekends durant lesquels je travaillais sur ma thèse. Merci de m'avoir toujours encouragé et de toujours avoir cru en moi.

Contents

List of Abbreviations

AP	**A**daptin (or Adaptor) **P**rotein complex
ARF	**A**DP **R**ibosylation **F**actor
ATP	**A**denosine **Tri**p**h**osphate
BoHV	**Bo**vine **H**erpes**v**irus
CCV	**C**lathrin **C**oated **V**esicle
CK2	**C**asein **K**inase **2**
CVSC	**C**apsid-**V**ertex **S**pecific **C**omponent
DNA	**D**eoxyribo**n**ucleic **A**cid
dsDNA	**d**ouble-**s**tranded **D**eoxyribo**n**ucleic **A**cid
E	**E**arly
EBV	**E**pstein-**B**arr **V**irus
HCMV	**H**uman **C**yto**m**egalo**v**irus
HHV	**H**uman **H**erpes**V**irus
HRP	**H**orse**r**adish **P**eroxydase
HSPGs	**H**eparan **S**ulfate **P**roteo**g**lycan**s**
HSV	**H**erpes **S**implex **V**irus
IDE	**I**nsulin **D**egrading **E**nzyme
IE	**I**mmediate **E**arly
ILTV	**I**nfectious **L**aryngo **T**racheitis **V**irus
INM	**I**nner **N**uclear **M**embrane
IR	**I**nternal **R**epeat
ITIM	**I**mmunoreceptor **T**yrosine-based **I**nhibition **M**otif
KSHV	**K**aposi's **S**arcoma-associated **H**erpes**v**irus
L	**L**ate
Man6P	**Man**nose-**6**-**P**hosphate
MCP	**M**ajor **C**apsid **P**rotein
MDV	**M**arek's **D**isease **V**irus
M6PR^{ci}	**c**ation-**i**ndependent **M**annose-6-**P**hosphate **R**eceptor
MVB	**M**ulti**v**esicular **B**odies
NEC	**N**uclear **E**xport **C**omplex
NES	**N**uclear **E**xport **S**ignal
NLS	**N**uclear **L**ocalization **S**ignal
ONM	**O**uter **N**uclear **M**embrane
ORI	**Ori**gin of replication
ORF	**O**pen **R**eading **F**rame
PACS	**P**hosphofurin **A**cidic **C**luster **S**orting protein
PHN	**P**ost-**H**erpetic **N**euralgia

PKC	**P**rotein **K**inase **C**
PRV	**P**seudo**r**abies **V**irus
RNA	**R**ibo**n**ucleic **A**cid
SCP	**S**mall **C**apsid **P**rotein
ssDNA	**s**ingle-**s**tranded **D**eoxyribo**n**ucleic **A**cid
TEM	**T**ransmission **E**lectron **M**icroscopy
TGN	*Trans*-**G**olgi **N**etwork
TM	**T**rans**m**embrane
TNTs	**T**unneling **N**ano**t**ube**s**
TR	**T**erminal **R**epeat
U_L	**U**nique **L**ong
U_S	**U**nique **S**hort
VAC	**V**iral **A**ssembly **C**ompartment
VZV	**V**aricella **Z**oster **V**irus
WHO	**W**orld **H**ealth **O**rganization

Part I

State of the art

1 Introduction

1.1 The order *Herpesvirales*

1.1.1 Classification

The *Herpesvirales* is an order of double-stranded DNA (dsDNA) viruses infecting animals. The hallmark of herpesviruses is their ability to establish lifelong latent infections. This order can be divided in three families (Figure 1.1):

1.1.1.1 *Malacoherpesviridae*

This family is composed of only two species, Haliotid herpesvirus 1 and Ostreid herpesvirus 1, which are the only known herpesviruses species with an invertebrate host [175].

1.1.1.2 *Alloherpesviridae*

This family englobes thirteen species of herpesviruses infecting fishes and amphibia [175].

1.1.1.3 *Herpesviridae*

With 107 species, it is by far the largest family. It regroups herpesviruses infecting reptiles, birds, and mammals. This family can be further divided in three subfamilies, differing by the size and structure of the genome, the speed of replication, the host range, and the cell type in which the latent infection is established [175]:

Alphaherpesvirinae

Some genes homologous to those found in HSV-1, contained in the unique short region of the genome and flanking internal and terminal repeats, are characteristic of the subfamily [175]. These viruses can infect a broad host range, have a relatively short reproductive cycle, rapid spread in culture and the capacity to establish a latent infection in sensory ganglia [348].

The most studied viruses in this subfamily are the human Herpes Simplex virus type 1 and 2 (HSV-1, HSV-2) and Varicella-Zoster virus (VZV) or the animal Pseudorabies virus (PRV) and Marek's disease virus (MDV).

Betaherpesvirinae

Genes corresponding to the Human Cytomegalovirus *us22* family are characteristic of the subfamily [175]. Most members of this subfamily can infect a restricted host range, have a long reproductive cycle, and the cells that they infect frequently become enlarged (cytomegalia). These viruses can establish latency in lymphoreticular cells, in secretory glands, kidneys, and other tissues [348].

Well known members of this subfamily are the Human Cytomegalovirus (HCMV) and the Human Roseoloviruses type 6 and 7 (HHV-6 and HHV-7).

Gammaherpesvirinae

Certain genes may be unique to the members of the subfamily, such as *bnrf-1*, *btrf-1*, and *brlf-1* of EBV [175]. Viruses in this group show limited host range, infecting specifically either T or B lymphocytes, but exceptions may occur. They establish latency in lymphoid tissues [348].

The Epstein-Barr virus (EBV) and Kaposi's sarcoma-associated herpesvirus (KSHV) are two human herpesviruses belonging to this subfamily.

1.1.2 Morphology

Herpesviruses are spherical viruses measuring approximately 200 nm and are constituted by four structural elements: the core, the capsid, the tegument, and the envelope (Figure 1.2B). The core is formed by a single copy of a linear dsDNA molecule tightly packed into the capsid. The capsid is an icosahedral structure of around 125 nm in diameter constituted by 162 capsomers, 12 of which are pentons made of five copies of the Major Capsid Protein (MCP) and 150 of which are hexons composed by six copies of the MCP in addition to the Small Capsid Protein (SCP). The capsomers are joined together via triplexes consisting of two viral proteins in a 2:1 ratio (Figure 1.2A). The capsid is then surrounded by a proteinaceous layer called the tegument containing both viral and cellular proteins. The tegument is poorly structurally defined but can be divided into inner and outer tegument depending on the association of its components with the capsid, giving the inner layer an icosahedral aspect. Finally, a lipid envelope containing the viral glycoproteins surrounds the viral particles [72].

The protein composition of the tegument as well as the envelope varies widely across the *Herpesviridae* family: in HSV-1, eight capsid and capsid-associated proteins, 13 viral glycoproteins and 23 potential tegument proteins as well as 49 distinct host proteins were identified by mass spectrometry analysis of virions [245]. In HCMV, 71 viral and more than 70 cellular

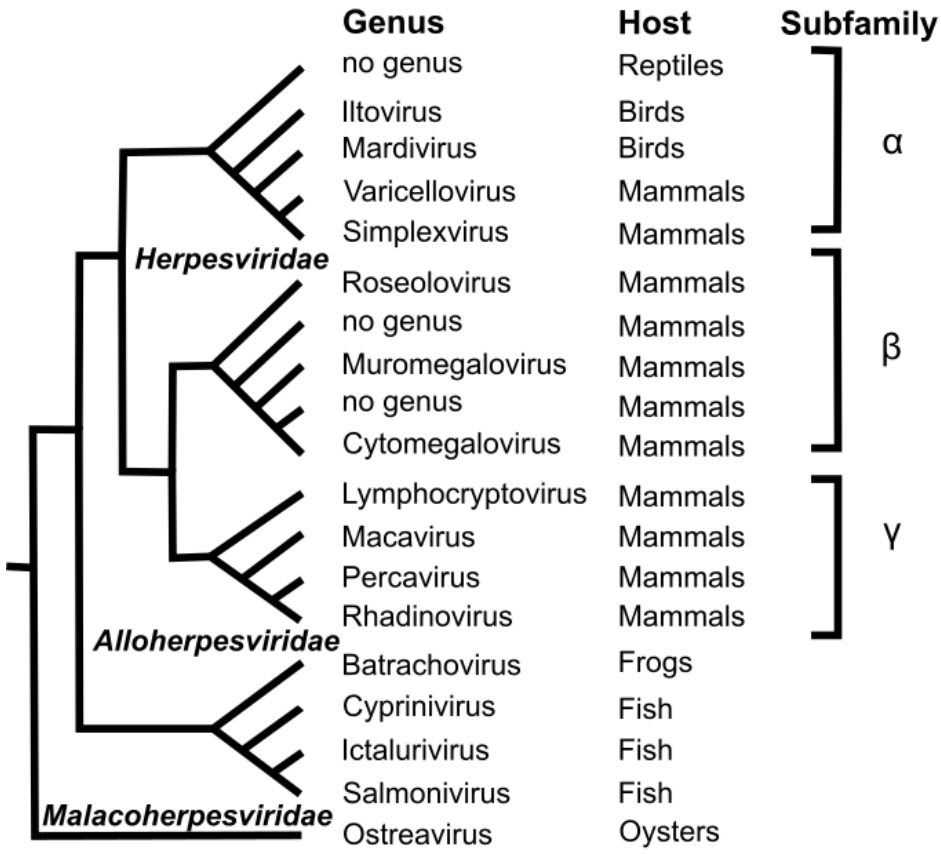

Figure 1.1: ***Herpesvirales*** **classification.** The *Herpesvirales* are double-stranded DNA viruses infecting animals. The order can be subdivided in three families depending on the infected host as well as DNA features. The branching shows relations between the viruses, not evolutionary distances. Figure from [319].

proteins were detected. In KSHV, 21 host proteins were found in addition to the 24 viral proteins [418, 455, 263].

1.2 Varicella-Zoster virus (VZV)

1.2.1 Epidemiology

Varicella-Zoster virus is a highly contagious herpesvirus causing both varicella (chickenpox) and herpes zoster (shingles). Contamination occurs by inhalation of saliva droplets dispersed by subjects with acute infection or by

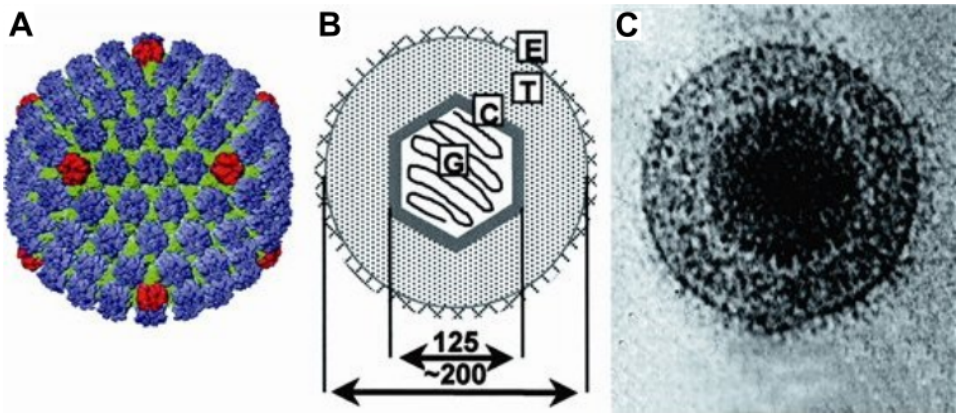

Figure 1.2: **Herpesvirus morphology.** A) Reconstruction of a HSV-1 capsid generated from cryo-electron microscope images. Hexons are shown in blue, pentons in red, and triplexes in green. B) Schematic representation of a Herpesvirus particle. G: genome, C: capsid, T: tegument, E: envelope. Distances are in nm. C) Photo of a Herpesvirus particle taken with a transmission electron microscope. Figure adapted from [175].

direct contact with viral particles present in high amount in vesicular fluid within skin lesions [118]. VZV is present worldwide, and most people are seropositive by mid-adulthood. Geographic variation in the age of infection is usually observed. In the pre-vaccination era, more than 90% of infections occurred before adolescence and less than 5% of adults remained susceptible in temperate countries. In tropical regions, VZV infection generally occurs at older ages resulting in higher susceptibility among young adults. The reasons accounting for these differences are poorly understood but may lie in the properties of the virus, climate, or population density [432].

According to the World Health Organization (WHO), the global annual varicella disease burden in the pre-vaccine era was estimated to include 4.2 million severe complications leading to hospitalization and 4 200 deaths. In the same era, the case fatality rates for varicella were approximately 3 per 100 000 cases [432]. In the United States of America, in the 1990s, an average of 4 million people got chickenpox, 10 500 to 13 000 of which were hospitalized, and 100 to 150 of them died each year. Since a vaccine became available in 1995 and universal varicella vaccination was introduced, it is estimated that, each year, 3.5 million cases of varicella, 9 000 hospitalizations, and 100 deaths are prevented [51]. In Europe, the annual number of varicella cases in each country is close to the countrys birth cohort, with 52 to 78% of the cases occurring in children under six years old and 89 to 95.9% of the cases before 12 years old. In 2015, only eight European countries were

recommending universal varicella vaccination for children at the national or regional level and seventeen countries recommended vaccination for risk groups only [102].

1.2.2 Pathogenesis

1.2.2.1 Varicella

VZV enters the body via the upper respiratory tract where a local replication occurs in epithelial cells and in the tonsils, where T-cells are infected [221, 13]. This process leads to a cell-associated viremia about four to six days after the initial infection (Figure 1.3, left) [141]. During this primary viremia, the virus is disseminated to reticuloendothelial tissues, including liver and spleen, where it further multiplies [118]. VZV is then transported to the skin and mucous membranes with a second viremic phase occurring about 14 days after infection. The characteristic skin rash shows up about two weeks (10 to 21 days) after infection. This exanthema involves principally the trunk, where small pruritic maculopapular vesicles appear before spreading to the neck and limbs. After 12 to 72 hours, the macules turn into pustules that often break down giving rise to scabs. VZV is transmissible 24 to 48 hours before the appearance of the rash, which is often preceded by other symptoms such as nausea, loss of appetite, fever, and headache [118, 141].

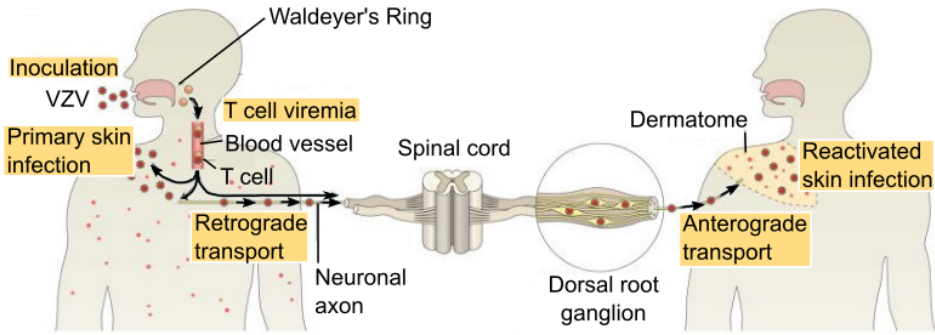

Figure 1.3: **Varicella-Zoster virus replication cycle.** VZV infection occurs via the upper respiratory tract. The virus then spreads and reaches the tonsils where it infects T cells. These T cells transport the virus to the skin and mucous membranes. After the primary infection, VZV establishes latency in sensory ganglia. Reactivation from latency allows the virus to cause a second infection in the skin. The lesions associated with this new infection are usually restricted to the dermatome innervated by the ganglion where the reactivation occurs. Figure adapted from [450].

Varicella usually heals in one to two weeks. Complications are rare in immunocompetent children but are more frequent in immunodeficient patients. The most recurrent complications are bacterial superinfection of the pustules, laryngitis, pneumonia, and neurological problems [118]. VZV infection can have terrible consequences if it is contracted during pregnancy. Indeed, VZV can be transmitted to the fetus causing congenital varicella syndrome. Although its incidence is exceptionally low, it is associated with symptoms including skin lesions, neurological defects, limb hypoplasia, or skeletal anomalies [5]. Fetuses exposed to VZV after the fifth month *in utero* may develop asymptomatic chickenpox and zoster early in life. If the mother develops varicella close to delivery, the newborn can exhibit a serious form of varicella with mortality rates close to 30% [118].

After primary infection causing varicella, VZV becomes latent in sensory neurons, mainly in the trigeminal ganglia (Figure 1.3, center) [131, 199]. Contrary to what has long been believed, VZV reactivations are numerous but are mainly subclinical [118]. The frequent viral replication and subsequent production of antigens stimulate the immune memory and so, attenuate reactivation. When cell-mediated immunity against VZV declines, usually with age or in immunocompromised individuals, the virus reactivates from latency to cause a symptomatic infection termed zoster (Figure 1.3, right) [118].

1.2.2.2 Zoster

Around 10 to 20% of people who contracted varicella are susceptible to develop zoster, with the likelihood increasing over 50 years old [118]. VZV reactivation usually occurs in a single sensory ganglion and the virus is then driven back to the dermis and epidermis, where the virus replicates and causes a vesicular rash (Figure 1.3, right). Since reactivation mainly arises in a single ganglion, the rash is usually restricted to a single dermatome [118]. Skin lesions usually disappear after two weeks, but the pain associated with zoster usually takes 4 to 6 weeks to vanish. Unfortunately, some patients will develop chronic pain after VZV reactivation. This chronic pain, termed post-herpetic neuralgia (PHN), can persist from three months to even years after resolution of the rash [118, 131, 11]. Post-herpetic neuralgia results from damage to peripheral and central neurons, and may be a byproduct of the inflammatory response associated with VZV reactivation [248].

1.2.3 Genome

The first fully sequenced and characterized Alphaherpesvirus genome was the one from VZV, by Davison and Scott in 1986 [74]. The structure of the

genome is similar in all Alphaherpesviruses and is composed of two unique segments designated Unique Long and Unique Short (U_L and U_S, respectively) (Figure 1.4). These two unique regions are flanked by repeats of different length that are termed Internal Repeats (IR) and Terminal Repeats (TR) [25]. Four different genome arrangements can exist differing in the relative orientation of the U_L and U_S segments. In VZV virions, whereas the U_S orientation is present in a 50%-50% repartition, one orientation of the U_L segment is present in approximately 95% of the genomes and the other in only 5%. This overrepresentation of one orientation for U_L might be a consequence of the shorter repeats flanking it, that would reduce the frequency of homologous recombination between the repeats [25]. Finally, the genome possesses an unpaired C residue at the 3' end of U_L and an unpaired G residue at the 3' end of U_S. These unpaired residues are important for circularization during genome replication [25, 74].

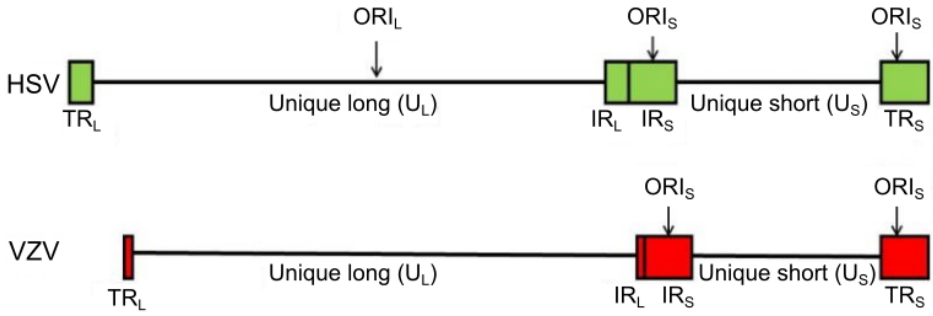

Figure 1.4: **HSV and VZV genomes structure.** Alphaherpesviruses genome structure consists of two unique regions (U_L and U_S) flanked by repeated regions either internal (IR) or terminal (TR). ORI: origin of replication. Adapted from [201].

The genome of VZV is the smallest genome of human herpesviruses and is composed of 124 884 bp. U_L and U_S are respectively 104 836 bp and 5 232 bp while TR_L and IR_L are 88 bp, and TR_S and IR_S are 7 319 bp [74]. VZV also has an overall lower G+C content compared to HSV (46% vs 68% respectively) [25]. Interestingly, Herpesviruses genomes have significantly higher G+C content in the inverted repeats compared to the unique segments. In VZV, this G+C content is about 44% and 43% in U_L and U_S while it is approximately 68% in TR_L and IR_L, and 59% in TR_S and IR_S [74]. Furthermore, the genome of VZV contains five reiterations of short G+C-rich sequences: R1 located in *orf11*, R2 in *orf14* (gC), R3 in *orf22*, R4 between *orf62* and the origin of viral replication, and R5 between *orf60* and *orf61*. The length of the

repeated regions varies among different VZV strains and has been used to distinguish the strains [61].

From the DNA sequence they obtained, Davison and Scott predicted the presence of 71 open reading frames (ORFs) coding for proteins[1] [74]. Three ORFs are in repeated regions flanking U_S and are thus present in two copies: *orf62/71*, *orf63/70*, and *orf64/69* [73]. The VZV genome encodes 41 core genes that are conserved in all Herpesviruses. Some of these genes will be discussed in the coming sections.
Although most VZV genes have homologues in HSV-1 and HSV-2, six ORFs are exclusive to VZV (*orf1*, *orf2*, *orf13*, *orf32*, *orf57* and *orfS/L*). On the other hand, seven genes are encoded by HSV, but not VZV (*ul45*, *ul56*, *us2*, *us5*, *us6*, *us11*, and *us12*) [61].

1.3 Alphaherpesviruses replication cycle

HSV-1 and PRV are the most studied alphaherpesviruses. HSV-1 is the model virus of the subfamily and the envelopment process of PRV has been thoroughly characterized. Thus, most information described hereafter comes from HSV-1 or PRV studies. As most VZV proteins have homologs in HSV-1 or PRV, some details of their replication cycle can be extended to VZV.

1.3.1 Viral entry

Herpesviruses entry into their host cells is a complex mechanism involving two major steps: attachment to the cell surface and binding to specific receptors, and fusion of the viral envelope with cellular membranes (Figure 1.5A) [20].

Tethering of the virion to the cell surface requires the interaction of viral glycoproteins with specific cell receptors. Heparan sulfate proteoglycans (HSPGs) have been identified as important for virion attachment. In HSV-1, gC, and to a lesser extent gB, were shown to bind HSPGs [162, 163]. Interaction of either gC or gB with HSPGs is a relatively nonspecific process based on charge interactions between the highly negatively charged heparan sulfate and positively charged amino acids residues on gC or gB. While these interactions are useful to concentrate the viral particle at the cell surface, it is not sufficient to trigger its entry [20]. Other interactions between the viral particle and the host cell are thus required for successful entry of the

[1] To see the function of VZV proteins and their homologs in HSV-1, please refer to the sheet attached to this thesis or to appendix A.

virion. The glycoprotein gD, which is conserved and essential in most alphaherpesviruses, has been shown to be important for the entry process [46]. In HSV-1 and HSV-2, four gD receptors have been identified: HVEM, a member of the tumor necrosis factor receptor family; the immunoglobulins nectin-1 and nectin-2; and a sulfated form of heparan sulfate (3-O-sulfated heparan sulfate, 3-O-HS) [20, 126, 269, 372, 424]. HVEM was the first gD receptor identified and is expressed on the surface of T and B lymphocytes, epithelial cells, and fibroblasts present in human tissues of the lung, liver, and kidney [20, 269, 378]. Nectin-1 is expressed in virtually all human tissues and is used by both HSV-1 and HSV-2 while nectin-2, also expressed broadly in human tissues, is considered as a weak receptor for HSV-2 and inactive for HSV-1 [20, 379, 241, 47, 217]. Both nectin-1 and nectin-2, as well as the poliovirus receptor CD155, have been shown to mediate the entry of PRV using gD [20, 126, 424]. The last type of gD receptor, 3-O-HS, is a highly sulfated form of heparan sulfate and has been shown to allow the entry of HSV-1 upon interaction with gD [20, 372, 371].

In the case of VZV, attachment of the virions to the cell surface also occurs via heparan sulfate proteoglycans (HSPGs). Indeed, treatment with heparin prevented cell infection with VZV in a concentration-dependent manner [459] and gB has been shown to interact with HSPGs [180]. As VZV does not possess a gD homolog, one or several other glycoproteins and other cellular receptors are needed. Thus far, no unique receptor specific for VZV has been identified, but it has been shown that treatment with mannose-6-phosphate (Man6P) could prevent infection of cells by cell-free VZV [459, 54]. Furthermore, depletion of the mannose-6-phosphate receptor ($M6PR^{ci}$) prevented infection by cell-free, but not cell-associated VZV in five different cell lines [54]. This directly suggests a role for $M6PR^{ci}$ in the entry of VZV into host cells. The $M6PR^{ci}$ is a multifunctional receptor and is essential for normal cell function [128]. Its main task is to deliver newly synthesized acid hydrolases from the *trans*-Golgi network (TGN) to the endosomes for their subsequent transfer to lysosomes [128]. It has also been shown to be implicated in the internalization of several ligands from the cell surface to endosomes [128]. At the cell surface, the $M6PR^{ci}$ is almost exclusively found in clathrin-coated pits [40, 215] and it has been suggested to participate in the entry of HSV via an endocytic pathway [40]. Although at least four VZV glycoproteins have been shown to contain Man6P residues [54], to our knowledge, none of them have yet been shown to interact with $M6PR^{ci}$.
Other cellular proteins could be involved in the process of VZV entry: insulin degrading enzyme (IDE) has been shown to interact with VZV gE, and downregulation of IDE results in 25-75% reduction of VZV infection and cell-to-cell spread [238]. IDE seems to play a role in VZV entry rather than in attachment of the virions to the cell surface [237]. Its interaction with gE has

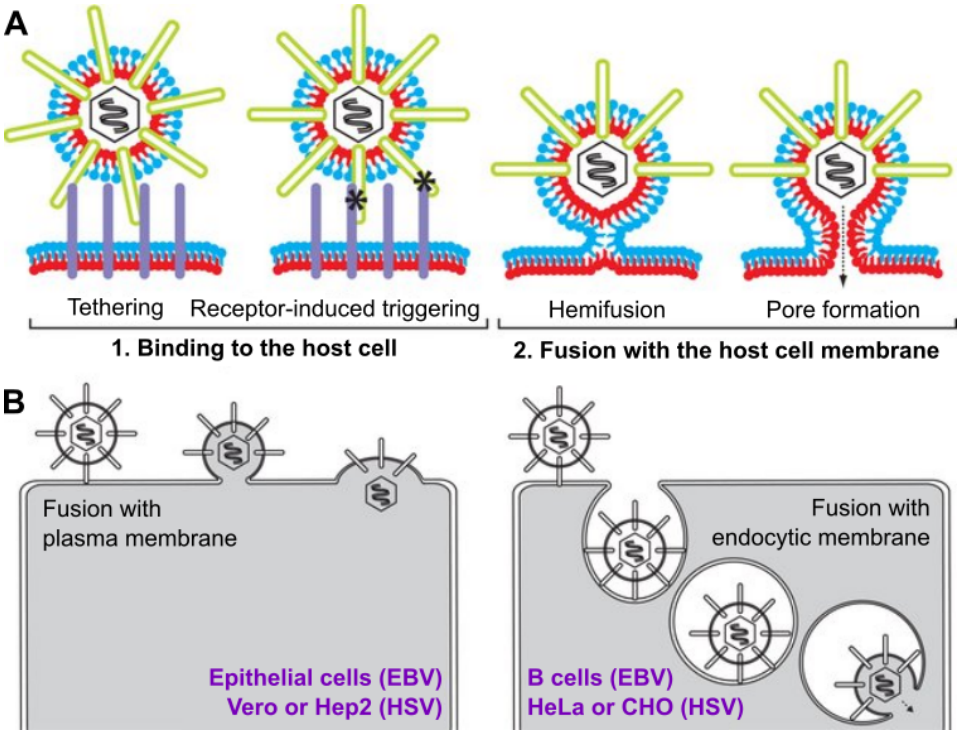

Figure 1.5: **Herpesvirus entry.** A) Two main steps are involved in Herpesviruses entry: tethering to the cell surface and fusion of the viral envelope with the cell membrane. B) Depending on the cell type infected, the viral envelope fuses directly with the cell membrane or with the membrane of an endocytic vesicle. Figure from [65].

been shown to induce a conformational change and a size modification in gE that enhances the stability and infectivity of the virus [237]. Furthermore, deletion of the IDE-binding domain of gE leads to an accumulation of gE at the cell surface and the cell-cell junctions, demonstrating its importance for membrane fusion, syncytia formation and cell-to-cell spread [237]. Moreover, the interaction between gE and IDE may explain the tropism of VZV for a broad range of cell types because IDE is ubiquitously expressed [238]. In addition, Suenaga *et al.*, identified myelin-associated glycoprotein (MAG) as a potential receptor allowing entry of VZV in neural cells [390]. They showed that VZV gB could bind to MAG and that this interaction promotes cell-cell fusion when expressed with gH/gL [390]. The same team later demonstrated that sialic acids residues on VZV gB were required for MAG association and induction of cell-cell fusion [392]. Sialic acids residues on VZV gB have recently been shown to promote entry of VZV in hematopoietic cells [391, 393]. Indeed, gB can interact with Siglec-7, a member of the

sialic acid immunoglobulin-like lectin (Siglec) family of immune regulatory receptors, mainly expressed on hematopoietic cells [391]. The Siglec-7/gB interaction is dependent on the sialic acid residues on gB and is required to induce membrane fusion [391].

Once the viral particle is attached to the cell surface, the viral envelope must fuse with either the plasma membrane or the membrane from endocytic vesicles (Figure 1.5B). The pathway of entry seems to vary upon the cell type to be infected: HSV-1 has been shown to enter Vero cells by direct fusion at the plasma membrane [123] while it enters HeLa or CHO cells via a low-pH endocytic pathway [286]. On the contrary, PRV has been shown to use a low-pH endocytic route to enter PK15 and Vero cells [266]. Regarding VZV, clathrin-dependent endocytosis is required for infection of HELF, MeWo and U373MG cell lines [149]. The reason for the existence of different entry routes is not clear, but it has been suggested that the endocytic pathway could be used to overcome the barrier formed by the subplasmalemmal cortical filament network in some cell types [377]. The mechanism of fusion triggered by Herpesviruses glycoproteins will be discussed in more details further in this thesis.

1.3.2 Capsid delivery to the nucleus

Upon viral envelope fusion with the cellular membrane, the capsid is released and most of the tegument proteins dissociate from the incoming virions [3]. The capsid must then reach the nucleus to deliver the viral genome for its transcription and replication. This translocation of capsids towards the nucleus is not possible by diffusion alone. This is especially true to cover long distances in the axon in the case of infection of nervous cells. Indeed, it was calculated that HSV capsids would need 231 years to travel 1 cm in the axonal cytoplasm in the absence of an active transport mechanism [377]. It has been shown that herpesvirus capsids travel from the cell periphery to the nucleus along microtubules [86]. The inner tegument proteins of HSV-1, including pUL36 and some pUL37, remained associated with the capsid during the transit to the nucleus [3] and PRV pUL36 has been co-immunoprecipitated with dynein and dynactin, suggesting a direct role for pUL36 in motor recruitment for capsids transport [448]. The function of pUL36 and pUL37 in capsid transport will be further detailed in the coming sections.

Once arrived near the nucleus, the capsid docks to the nuclear pore to deliver the viral DNA. In HSV-1, at least two viral proteins, pUL25 and pUL36, were shown to interact with components of the nuclear pore complex [316, 66]. This docking at the nuclear pore is necessary for DNA uncoating [297]

because it triggers the proteolytic cleavage of pUL36 which leads to DNA ejection [190].

1.3.3 Gene expression cascade

Transcription of Herpesviruses genome is performed following a sequentially regulated and ordered cascade in which viral genes can be divided in three classes: Immediate-Early (IE), Early (E), and Late (L) genes [169].

1.3.3.1 Immediate-Early genes (IE)

Immediate-early genes are the first to be expressed in newly infected cells. They are synthesized at highest rates between three to four hours post-infection [169]. Their expression relies only on cellular components such as the RNA polymerase II. The IE transcripts encode regulatory proteins that are carried back into the nucleus where they serve to regulate IE genes transcription and up-regulate the transcription of Early genes [142].

VZV encodes at least four IE proteins regulating viral transcription, three of which (IE4, IE62 and IE63) are in the tegument of virions and one (ORF61) is not present in virions [1, 203, 204].
IE4 is essential for VZV replication and can regulate gene expression alone or in combination with IE62 [361, 76].
ORF61p is synthesized very early post-infection [337] and can *trans*-activate promoters of all three classes of genes [271, 423]. Interestingly, in Vero cells, ORF61p seems to inhibit the transactivation mediated by IE4 and IE62 on all classes of VZV promoters [277].
IE62 is a phosphoprotein and the major *trans*-activator of VZV genes and thus, is essential for viral replication [204, 361]. IE62 can regulate the expression of all classes of genes as well as of its own promoter [320, 174]. It can interact with IE4 and IE63 and both these interactions modulate its *trans*-activation [381, 247].
IE63 has been shown to be heavily expressed during latency, especially in neurons [75]. In co-transfections studies, it was shown to repress the expression of IE62 and to promote the activation of thymidine kinase, suggesting a role for IE63 in the repression of IE genes as well as in the activation of Early genes [178].

1.3.3.2 Early genes (E)

The Early genes are most expressed between five to seven hours post-infection [142]. They mainly encode proteins involved in DNA replication and nucleic acid metabolism, such as the VZV DNA polymerase composed of two subunits (ORF16p + ORF28p), the ribonucleotide reductase (ORF18p

+ ORF19p), the viral thymidine kinase (ORF36p), the two DNA binding proteins (ORF29p + ORF51p), the two viral Ser/Thr kinases (ORF47p + ORF66p), the viral dUTPase (ORF8p), the thymidylate synthetase (ORF13p), the protease (ORF33p), the DNAse (ORF48p), the helicase/primase complex (ORF52p + ORF55p) and the uracil-DNA glycosylase (ORF59p) [61].

1.3.3.3 Late genes (L)

The Late genes are synthesized at increasing rates until at least twelve hours post-infection [142]. They encode structural proteins and require the expression of IE and E genes for their transcription. At first, their expression was thought to depend on viral DNA synthesis, but this concept was modified after the observation that some Late genes can be transcribed relatively early in infection, before the synthesis of new viral DNA [142]. The group of genes with properties intermediary between Early and Late genes has been classified as Early-Late genes while the group of Late genes transcribed after viral DNA synthesis has been called True-Late [142].

The VZV major capsid protein (ORF40p), the scaffold protein (ORF33.5p) which serves in nucleocapsid assembly, the portal protein (ORF54p) which allows viral DNA packaging into the capsid, and most VZV glycoproteins are examples of Late proteins [1].

1.3.4 Genome replication

Viral DNA synthesis begins rapidly after infection and shortly after the appearance of the Early proteins [233]. First, the DNA molecule is converted into a circular form by direct end-to-end ligation mediated by the cellular DNA ligase IV [274, 388]. The DNA synthesis starts at an origin of replication (ORI). In HSV, three origins of replication have been identified: one ORI_L in the middle of the U_L segment, and two ORI_S in the repeated regions flanking the U_S segment [386, 154]. VZV lacks an ORI_L but does have two ORI_S in a position equivalent to that of HSV-1 (Figure 1.4) [154, 387]. DNA synthesis starts bidirectionally at an origin of replication to form a theta structure. It then switches to a rolling circle mode, which generates numerous copies of the genome that are cleaved and packed in the capsid as they are produced [154, 233].

Seven HSV-1 genes have been identified as necessary for DNA replication: *ul9, ul29, ul5, ul8, ul52, ul30* and *ul42* (Figure 1.6) [154, 188, 457, 258, 433]. The first viral protein to intervene is pUL9, which, after homodimerization, binds the origin of replication [154, 306]. pUL9 contains both an ATP-binding motif and a helicase motif, and plays a role in DNA unwinding [135, 37]. pUL9 is stimulated by pUL29 (ICP8), a single-strand

DNA-binding protein, which increases the rate and extent of the helicase activity of pUL9 [154, 36].

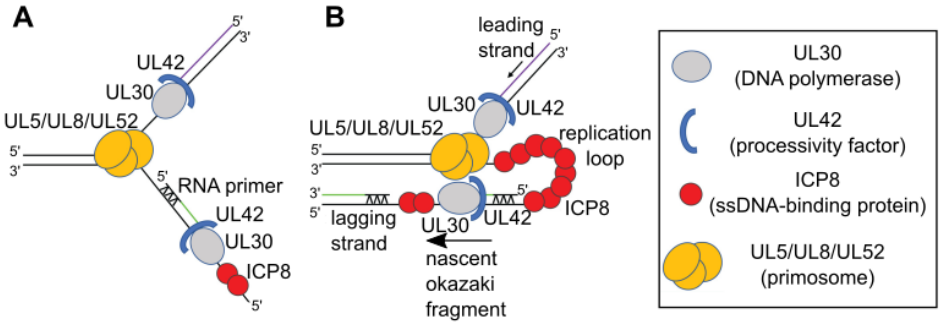

Figure 1.6: **Schematic representation of HSV-1 replication machinery.** A) Replication fork of HSV-1. B) A replication loop is formed for coupled leading- and lagging-strand synthesis. Figure adapted from [31].

After initiation, the primase/helicase complex formed by pUL5, pUL8 and pUL52 is recruited to the replication fork probably by interaction with ICP8 [103]. The pUL5 subunit was shown to contain seven conserved motifs found in members of helicase superfamily I [134, 133] and mutations in these conserved motifs result in viral replication defect and impairement of the helicase but not primase activity *in vitro* [138, 457]. On the other hand, pUL52 contains a conserved DXD motif, which is found in DNA primases. Mutation of this motif abolishes primase but not helicase activity *in vitro* [205]. While pUL5 seems to be the helicase subunit and pUL52 the primase subunit, the integrity of the pUL5/pUL8/pUL52 complex is required for its function [55]. The exact function of the pUL8 subunit is not known, but it is necessary for the function of the complex and has been shown to increase the rate of pUL5/pUL52 primer synthesis [403, 369]. Furthermore, pUL8 has been shown to interact with both ICP8 and the catalytic subunit of the viral DNA polymerase, suggesting its role in keeping the replisome intact [103, 253]. The last essential component of the replication machinery is the viral DNA polymerase, composed of the catalytic (pUL30) and processivity (pUL42) subunits [129, 332, 136]. The viral polymerase has an architecture closely resembling that of other alpha polymerases despite being at least 300 amino acids longer and having a low sequence homology [243]. pUL30 also shows a 3'-5'-exonuclease activity, which serves as a proofreading activity to ensure high fidelity during DNA replication. In addition to its exonuclease activity, pUL30 possesses a RNase H activity that probably serves to remove the RNA primers that initiates the

synthesis of Okazaki fragments [243]. The pUL42 protein, with its dsDNA-binding activity, increases the polymerase activity by tethering pUL30 to the DNA molecule [233, 243, 336].

Apart from these seven essential proteins, a set of auxiliary proteins have been identified. These proteins, although non-essential in cell culture, appear to be crucial for infectivity in animal models. These include thymidine kinase, ribonucleotide reductase, alkaline endo-exo-nuclease, deoxyuridine triphosphatase and uracil N-glycosylase. In addition to these viral proteins, some cellular proteins such as DNA ligase and topoisomerases play a role in viral DNA replication [154].

1.3.5 Capsid assembly and genome encapsidation

Once the viral genome has been synthesized, it must be packed into the nucleocapsid to form a new viral particle. As already mentioned above, Herpesvirus capsids are composed of 162 capsomers forming an icosahedron. One of the capsid vertex is occupied by the portal complex, which is a dodecamer of the pUL6 protein forming a ring structure allowing the passage of the genome in or out of the capsid [283, 67, 284]. The capsomers are linked together by 320 triplexes, each formed by two copies of pUL18 and one copy of pUL38 (Figure 1.7) [283, 67, 299]. In addition, the tip of each pUL19 protein in the hexons is decorated with one copy of the small capsid protein pUL35 [67]. Finally, pUL17 and pUL25 are forming a heterodimer found in five copies associated with each penton. These complexes are called the capsid vertex-specific component (CVSC) and are important for capsid stability as well as for association of the capsid with the tegument (Figure 1.7) [67, 412, 408, 404].

During the lytic infection, four types of capsids are formed in the nucleus of infected cells: procapsids, which are quite fragile, are the precursor form of the stable A-, B-, and C-capsids (Figure 1.8) [279, 130, 346, 160]. The assembly of the procapsid starts around a scaffold composed of two related proteins: VP22a, that contains the scaffold core domain, and a chimeric protein formed by the viral protease (VP24) attached to the N-terminus of VP22a via a linker [67, 242]. The initiation of procapsid formation is thought to start with assembly of the portal ring associated with the scaffold protein VP22a [282, 280]. Then, the major capsid protein VP5, in association with VP22a, would be incorporated by self-assembly of the scaffold protein and finally, the preformed triplexes would be incorporated by interaction with the VP5-VP22a complex [279, 380, 285, 347].

The maturation of the procapsid occurs at the time of DNA packaging and is driven by activation of the VP24 protease which, via an auto-proteolytic

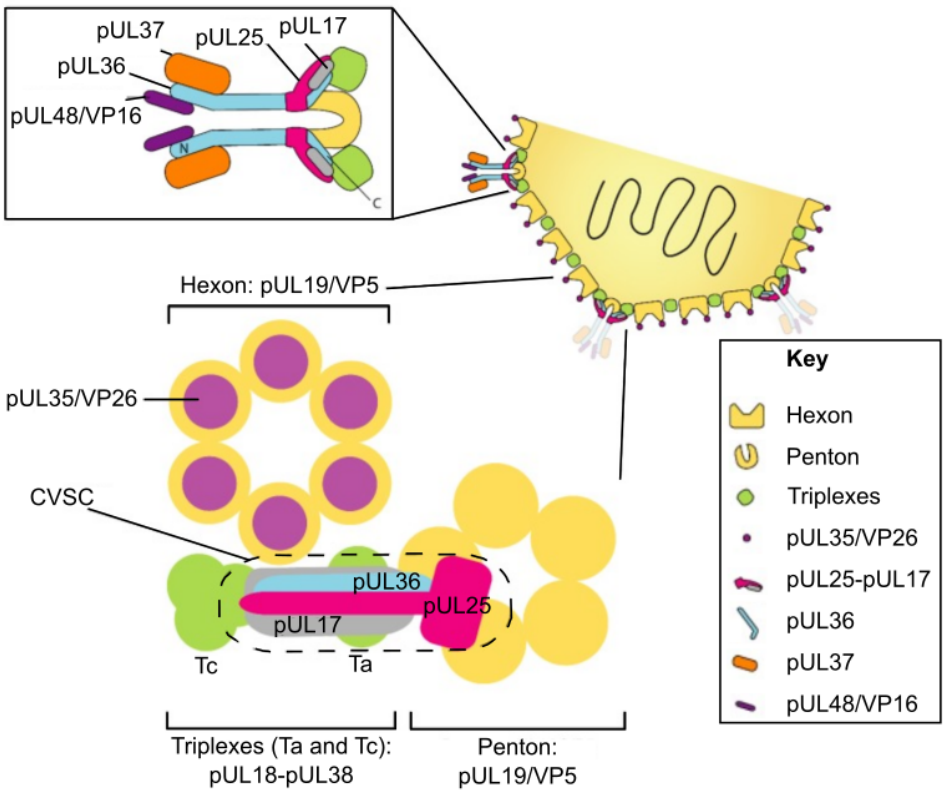

Figure 1.7: **Structure of HSV-1 capsid and CVSC.** Herpesvirus capsids are composed of 162 capsomers (yellow; 150 hexons, 11 pentons and 1 portal). In HSV-1, the hexons are formed by six copies of pUL19, each decorated by one copy of pUL35. The pentons are constituted by five copies of pUL19. The capsomers are linked together by triplexes (green). Finally, on top of the pentons lies the CVSC (Top inset). Figure from [309].

cleavage, frees itself from preVP22a [242, 24]. During this maturation process, the outer shell of the procapsid changes from a roughly unstable spherical form to a highly stable icosahedral form [24, 166, 411]. Three different outcomes can occur during capsid maturation [279, 24, 411] and lead to the appearance of A-, B- or C-capsids (Figure 1.8): C-capsids are the type of capsids found in mature virions. They are formed if the procapsid encounters the DNA packaging machinery and DNA is inserted inside. B-capsids are a dead-end product obtained when the DNA packaging machinery is not engaged and the angularization of the capsid traps the scaffold protein inside. Finally, A-capsids are capsids from which the scaffold has been expelled, but the DNA is not successfully sealed within.

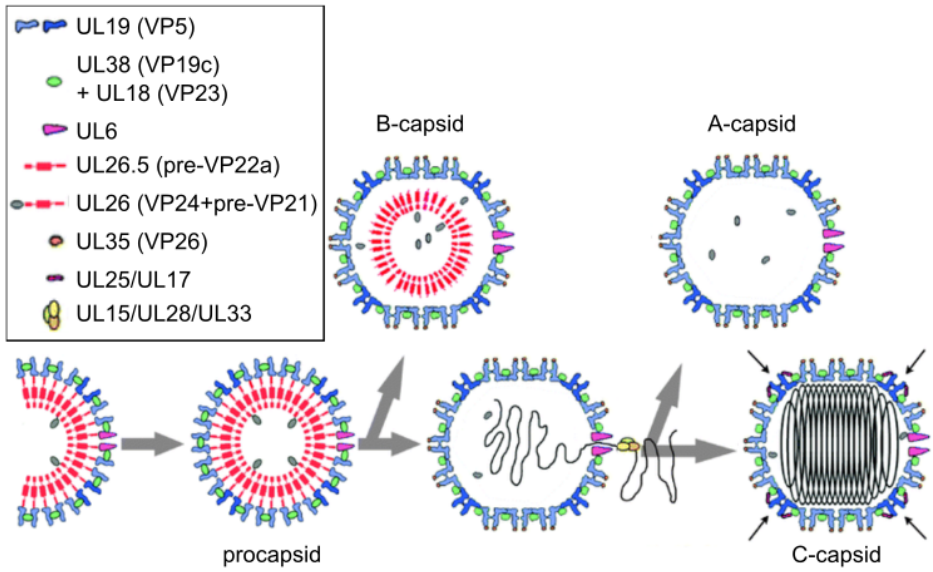

Figure 1.8: **HSV-1 capsid assembly and maturation.** Four types of capsids are formed during infection: procapsids are the precursor form of the three other types. The maturation occurs when pUL26, the viral protease, cleaves preVP22a and itself. B-capsids are a dead-end product, which contains the degraded scaffold proteins but no DNA. A-capsids are capsids from which the scaffold protein was ejected but the DNA was not retained. Finally, C-capsids are mature capsids containing the viral genome. Figure adapted from [50].

The viral DNA encapsidation requires seven essential proteins: pUL32, pUL6, pUL15, pUL28, pUL33, pUL17, and pUL25. Although its exact role in viral DNA packaging is still unresolved, pUL32 seems to be important for the correct localization of capsids to the replication compartment [223]. pUL32 is the only protein involved in DNA cleavage/packaging which has not been shown to associate with capsids. It contains two highly conserved oxidoreductase-like C-X-X-C motifs that are essential for cleavage/packaging of the viral genome. Mutations in these motifs alter the disulfide profile of pUL6, pUL25, VP19C and VP24, suggesting a role for pUL32 in modulating disulfide bond formation during capsid assembly and maturation [8].
As already mentioned above, pUL6 forms the portal by which DNA is incorporated into the capsid during packaging and through which it is released during viral entry, and is thus required for DNA encapsidation [284].
pUL15 and pUL33 are linked together by pUL28 and form a heterotrimer with terminase activity [443]. pUL15 is homologous to HCMV pUL89,

which has been shown to have a RNase H activity [275]. The crystal structure of the C-terminal domain of pUL15 shows a conformation resembling those of RNAse H-like enzymes [160, 367]. This directly suggests a role for pUL15 in cleavage of viral concatemeric DNA. Furthermore, pUL15 contains conserved amino acids motifs known as Walker A and Walker B boxes found in proteins that metabolize ATP, suggesting that pUL15 also serves as a motor for the translocation of DNA into the newly formed capsid [160, 445]. pUL28 is a regulator of the terminase complex. It has been shown to bind to specific sequences that are required for the cleavage and packaging of the genome [2]. The exact role of the last component of the terminase complex, pUL33, is unknown. It has been shown to interact with capsids [28] and with pUL28 [443]. This interaction with pUL28 seems to facilitate the interaction between pUL28 and pUL15. One role for pUL33 could therefore be to stabilize the terminase complex [443].
Finally, two components of the capsid vertex-specific component, pUL17 and pUL25, are required for DNA packaging. It has been hypothesized that the presence of the CVSC surrounding the portal vertex could serve in the assembly of the portal/terminase DNA packaging complex [408]. The precise role of pUL17 is not known, but it has been shown to be important for the correct localization of capsids within the replication compartment [402]. From the seven proteins essential for viral DNA packaging, only pUL25 is not required for DNA cleavage [259]. It is found in increasing amounts from procapsids, to B-, A-, and then C-capsids, which suggests a role in capsid stabilization as the encapsidation progresses [259, 281, 368]. Based on structural studies, Huet *et al.* suggested a model to explain the role of the CVSC in DNA packaging. They showed that the interaction of the pUL15 and pUL28 subunits of the terminase complex with capsids, and the initial cleavage of the genome requires the presence of pUL6 as well as pUL17. The interaction of the terminase with pUL17 and pUL6 leads to the cleavage and packaging of the viral DNA. During the process, the portal is displaced, probably in response to the packaged DNA. The displacement of the portal would then modify the orientation of pUL17 leading to the disengagement of the terminase and favoring the binding of pUL25, sealing the viral DNA inside the capsid [172].

1.3.6 Primary envelopment and nuclear egress

Once the viral genome has been packed into the capsid, the latter must be enveloped and transported to the cell surface to infect a new cell. The envelopment/de-envelopment/re-envelopment model is the most widely accepted to explain how Herpesviruses acquire their final envelope (Figure 1.9). According to this model, a first, temporary, envelope is acquired by budding of the viral capsid at the inner nuclear membrane (INM), leading

to enveloped virions in the perinuclear space. This primary envelope is then lost by fusion with the outer nuclear membrane (ONM) and naked capsids are released into the cytoplasm, where the final envelope is then acquired [382].

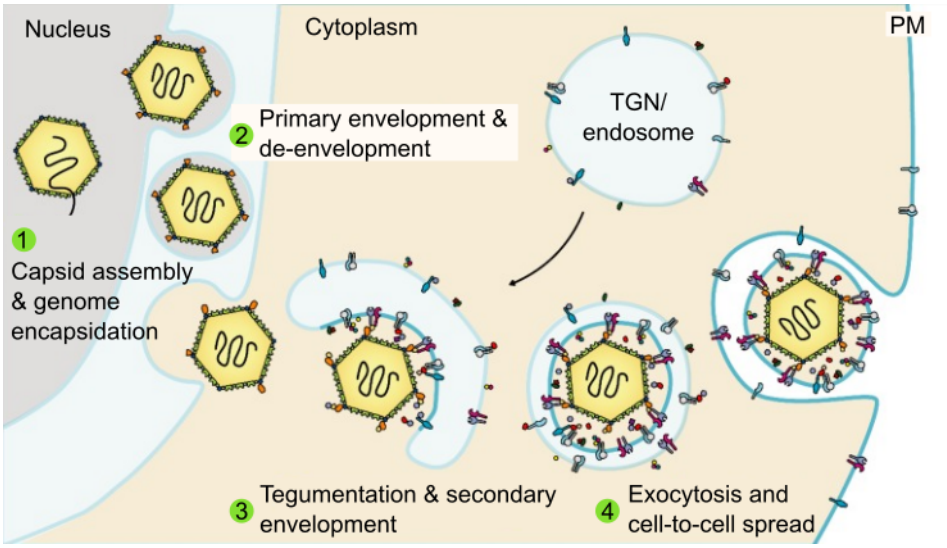

Figure 1.9: **Model of Alphaherpesviruses envelopment and egress.** Capsid assembly and genome encapsidation occur inside the nucleus. The capsid then acquires a first envelope by budding through the inner nuclear membrane. Primary enveloped viruses are thus found in the perinuclear space. This primary envelope is lost upon fusion with the outer nuclear membrane and naked capsids are released in the cytoplasm. There, the capsids acquire the tegument and their final envelope by budding through vesicles derived from the TGN or endosomes. The result from this second budding step is that enveloped virions are inserted in transport vesicles that will fuse with the plasma membrane to release the enveloped virions from the cell. Figure adapted from [309].

The process of nuclear envelopment and egress consists of four main steps: formation of a nuclear egress complex (NEC) at the INM, phosphorylation-induced reorganization of the nuclear lamina, docking of capsids at the NEC, and budding through the nuclear membrane (Figure 1.10) [397].

Herpesviruses nuclear egress is mainly orchestrated by a heterodimer of pUL31 and pUL34 forming the NEC, which is conserved throughout the whole Herpesvirus family [350]. The formation of this complex is required for the correct localization of both proteins at the inner nuclear membrane [350, 122, 341, 342, 210, 222]. The NEC has been shown to be incorporated into perinuclear virions [342] and *in vitro* experiments with the HSV-1 or PRV NEC have shown that the NEC alone is sufficient for

membrane budding and vesicles formation [33, 213]. Furthermore, both pUL31 and pUL34 have been shown to be required for nuclear lamina disruption [373].

The nuclear lamina is a filamentous network mainly constituted of lamins, strongly associated with the inner nuclear membrane and maintaining the structural integrity of the nucleus. Lamins are classified as type V intermediate filaments. Four lamin isoforms compose the nuclear lamina in mammalian cells: two A-type lamins (A and C) and two B-type lamins (B1 and B2) [230]. This nuclear lamina represents a steric barrier which Herpesviruses nucleocapsids must cross to gain access to the INM for primary envelopment, even if the gaps naturally occurring in the lamin mesh should allow some capsids to reach the INM [350, 370]. Moreover, the rigidity of the nuclear lamina and its tight interaction with the INM likely prevent the curvature of the INM, which is needed during the budding of the capsids [350]. Herpesviruses have developed mechanisms to overcome these obstacles and allow access and budding at the INM.

Apart from the NEC, different virus- or cellular-encoded kinases play a role in nuclear lamina disruption. All Herpesviruses encode a conserved serine/threonine kinase mimicking the function and substrate specificity of the cellular cdc2 kinase [195, 127, 179]. This function similarity is particularly present in Beta- and Gammaherpesviruses, whereas it is less obvious in Alphaherpesviruses [179]. In HCMV, HSV-2 and EBV, this kinase has been shown to phosphorylate lamins [49, 228, 252]. In HSV-1, this homolog, called pUL13, has not been shown to phosphorylate the nuclear lamina, but instead, it phosphorylates pUS3, another viral kinase, which in turn is implicated in lamins phosphorylation [193]. The pUS3 kinase is found in all Alphaherpesviruses and, while it is not essential for viral replication, its deletion impairs viral production [77, 364, 333, 268, 357]. In HSV-1-infected cells, pUS3 phosphorylates lamin A/C. However, pUS3 seems to negatively regulate disruption of the nuclear lamina. Indeed, mutation of pUS3 leads to the formation of large holes in the lamina instead of failure to reorganize it [34]. Thus, one role of pUS3 has been suggested to be a negative regulator of lamina disruption, perhaps to conserve nuclear function during infection [350].

Besides the two viral kinases, different isoforms of cellular PKC have been shown to be recruited to the nuclear rim during HSV-1 infection. Nonetheless, the role of these different isoforms is unclear. Indeed, specific inhibition of these isoforms has limited impact on HSV replication or nuclear egress. On the contrary, inhibition of PKC with a broad-spectrum inhibitor blocks viral replication as well as nuclear egress [350, 313, 226]. In addition, the cellular protein p32 has been reported to participate in the nuclear lamina

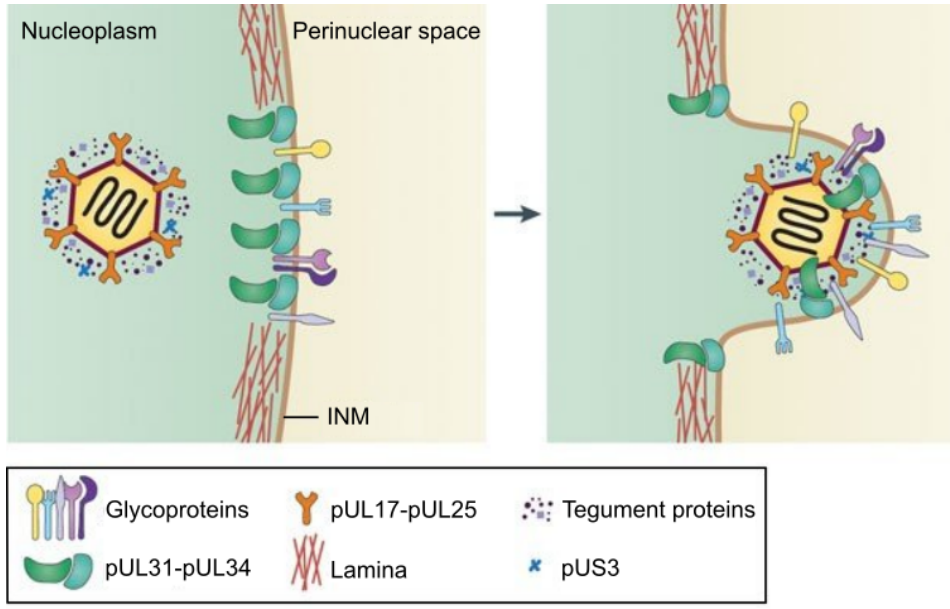

Figure 1.10: **Schematic representation of HSV-1 primary envelopment.** The nuclear lamina is disassembled upon phosphorylation by the viral kinase pUS3 in combination with pUL13 and the cellular PKC. The NEC is associated to the inner nuclear membrane (INM) and its interaction with CVSC components allows capsid docking at the INM. Figure from [186].

disruption after its recruitment to the NEC. In HSV-1-infected cells, p32 has been suggested to participate in the recruitment of cellular PKC to the NEC for lamina phosphorylation and disruption [435].

After assembly of the NEC and disruption of the nuclear lamina, the next step is docking of the capsid at the inner nuclear membrane (Figure 1.10). In both HSV-1 and PRV, pUL25 from the CVSC has been found to be required for nuclear egress of newly formed capsids [291, 212]. Furthermore, in HSV-1-infected cells, the CVSC has been shown to interact with pUL31, one subunit of the NEC [442]. These results suggest that capsid docking at the NEC is mediated by the CVSC. As previously mentioned, the CVSC is found in increasing amount from procapsids, to B-, A-, and then C-capsids, which probably represents a way of selection of capsids having packed a copy of the genome for nuclear egress [412, 281, 442].

Once the capsid has docked to the INM, it must bud through it to acquire its primary envelope. *In vitro* studies showed that expression of both components of HSV-1, PRV, or KSHV NEC is sufficient to induce membrane budding [33, 213, 78]. Studies on both HSV-1 and PRV NEC have shown

that it forms a honeycomb-like hexagonal lattice at the inner surface of the luminal vesicles (Figure 1.11) [350, 33, 148]. The crystal structures of HSV-1, PRV, or HCMV NEC are quite similar [32, 421, 449]. Each hexagonally symmetric unit is composed of six copies of the NEC (Figure 1.11) [350, 32, 421]. The crystal structure of HSV-1 NEC also showed extensive interactions intra- and inter-hexamers. Within each hexamer, pUL34 interacts with both pUL34 and pUL31, while pUL31-pUL31 interactions link neighboring hexamers [350, 32]. Bigalke *et al.* demonstrated that mutations disrupting the hexagonal lattice of the NEC reduced budding *in vitro*, which demonstrates that assembly of the NEC scaffold is required for budding. Nevertheless, some distortions of the flat hexagonal lattice found in NEC crystals must occur to obtain the spherical honeycomb coat found in infected cells. A closed spherical lattice is usually achieved through a regular inclusion of pentagons, which generates a polyhedral particle [32]. Interestingly, recent *in vitro* studies using HSV-1 proteins have shown that binding of pUL25 promotes the formation of NEC pentagons rather than hexagons. This observation raised the hypothesis that during budding at the INM, pUL25 located at the pentagonal capsid vertices binds to the NEC, thus promoting the formation of NEC pentagons that would anchor the NEC coat to the capsid (Figure 1.12). This incorporation of NEC pentagons at the point of contact with the capsid vertices would also promote assembly of the curved hexagonal NEC coat around the capsid, leading to primary envelopment of the capsids [89].

The last step of the nuclear egress is a poorly understood process during which the primary envelope is lost after fusion with the outer nuclear membrane, releasing naked capsids in the cytoplasm. Once more, the pUS3 kinase seems to play a role in the process. In HSV-1, MDV, and PRV, pUS3 has been shown to be required for efficient de-envelopment at the ONM [364, 357, 206]. In HSV-1, pUS3 is incorporated into perinuclear virions and phosphorylates pUL31 [342]. Serine to alanine mutations in the N-terminal part of pUL31 caused an accumulation of viral particles in the perinuclear space. On the contrary, serine to glutamic acid mutations prevented budding at the INM [273]. These data suggest that the regulation of the phosphorylation status of pUL31 by pUS3 modulates both the primary envelopment and de-envelopment of HSV capsids [273]. In the de-envelopment process, the phosphorylation of pUL31 by pUS3 could lead to the disassembly of the NEC lattice or its detachment from the capsid [350].
As for viral entry, the fusion of the primary envelope with the ONM may involve viral glycoproteins. In HSV, deletion of both gB and gH prevents de-envelopment and enveloped virions accumulate in the perinuclear space. By contrast, deletion of gB or gH alone has minor to no defect in nuclear egress [108]. These two proteins thus seem to be involved, probably in a

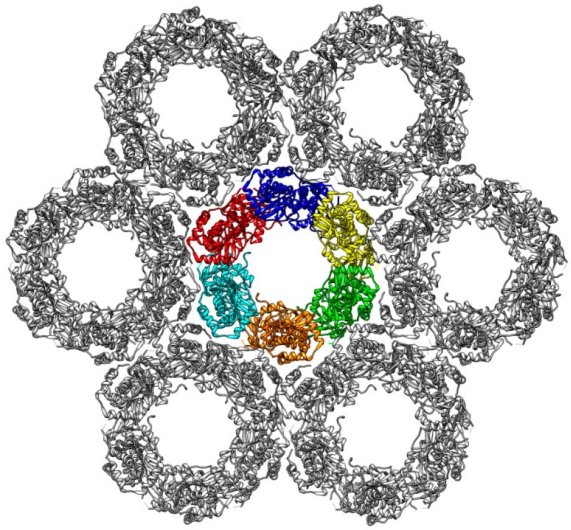

Figure 1.11: **Structure of the hexagonal lattice of PRV NEC derived from cryo-EM study.** The NEC forms a honeycomb-like hexagonal lattice. Each hexagon is composed of six NEC heterodimers (colored individually in the central hexagons). Figure from [82].

redundant manner, in de-envelopment. Furthermore, phosphorylation of the cytoplasmic domain of gB by pUS3 seems important for its function in nuclear egress [430]. In HSV-infected cells, gD and gM localize to the INM and at least gM is incorporated into virions during nuclear envelopment [428, 26]. Also, overexpression of gK impedes de-envelopment of perinuclear virions [173]. In PRV, gB, gD, gH and gL are dispensable for nuclear egress and have not been detected at the INM nor in primary virions [209].

Although the most common way out of the nucleus is via budding through the nuclear membrane, two other minor mechanisms have been suggested (Figure 1.13). In cell cultures, during both HSV-1 or BoHV-1 infections, enlargement of the nuclear pores compatible with the passage of viral capsids have been observed, and capsids have indeed been seen passing through these enlarged nuclear pores (Figure 1.13A) [235, 427]. However, other studies on HSV-1 showed that the nuclear permeability barrier remained intact throughout infection and no evidence for major perturbation of the nuclear pores was observed [167]. Another mechanism for nuclear egress has been identified using pUL34- or pUL31-deficient PRV in cell culture. After several passages, reversion occurred, and titers of the mutants were comparable to the Wild-type. These reversions induced nuclear envelope breakdown and

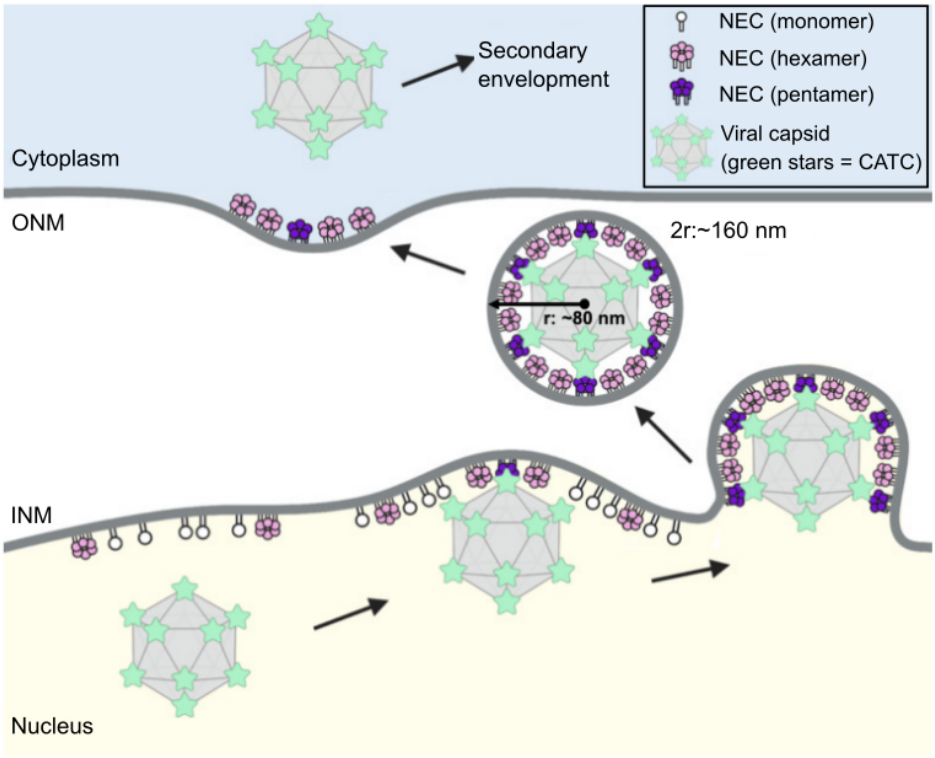

Figure 1.12: **Model of NEC-mediated budding in HSV-1-infected cells.** Binding of pUL25 from CVSC to the NEC induces the formation of pentagonal insertions (purple pentamers) within the NEC lattice. Insertion of NEC pentamers in the coat allows the curvature of the lattice around the capsid. INM: inner nuclear membrane, ONM: outer nuclear membrane, CATC: capsid-associated tegument complex. Figure adapted from [89].

capsids were released in the cytosol (Figure 1.13C) [207]. When pUL34 was reintroduced in the pUL34-deficient virus, capsids were shown to exit the nucleus by the nuclear egress pathway and simultaneously after induction of nuclear envelope breakdown [363]. The precise biochemical mechanisms involved in both these minor pathways are unknown. It is also not known whether or not they exist *in vivo*.

1.3.7 Secondary envelopment and egress

Shortly after its arrival in the cytoplasm, the capsid associates with tegument proteins [4]. The tegument is composed of viral and host proteins,

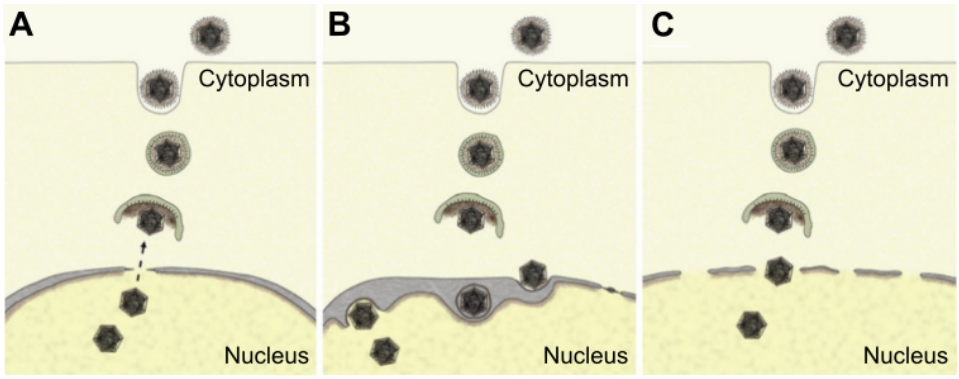

Figure 1.13: **Models of Herpesvirus exit from the nucleus.** A) Capsids exit through dilated nuclear pores. B) Envelopment/de-envelopment/re-envelopment model. C) Capsids exit after nuclear envelope breakdown. Figure modified from [264].

which serve different purposes such as motor recruitment and microtubule-directed transport of capsids, attachment of capsids to envelopment organelles, and cytoplasmic envelopment to form the mature virion [4]. Eleven viral proteins have been implicated in the secondary envelopment of HSV-1 and PRV among which seven (pUL7, pUL11, pUL16, pUL21, pUL36, pUL37 and pUL51) are conserved in all Herpesvirus subfamilies. Four of those proteins (pUL46, pUL47, pUL48 and pUL49, the homologue of VZV ORF9p) are present only in Alphaherpesviruses [309].

The pUL36 protein is the largest protein encoded by the *Herpesviridae*, with a mass of approximately 330 kDa in HSV-1 [4]. It is a key protein during secondary envelopment and in its absence, secondary envelopment and egress of both HSV-1 and PRV are blocked, resulting in the accumulation of naked capsids in the cytoplasm [120, 80]. pUL36 is a component of the CVSC where it is present as a dimer (Figure 1.14) [104, 70]. In PRV, two different forms of pUL36 were detected: a N-terminal-truncated form is associated with nuclear capsids and, after capsid arrival in the cytoplasm, it is replaced by the full-length pUL36, which is required for secondary envelopment [229]. Still in PRV, it was shown that pUL25 is required for association of pUL36 with capsids and these two proteins have been shown to co-immunoprecipitate when transiently expressed both in HSV-1 and PRV [64]. In PRV as well as in HSV-1, pUL36 interacts via its N-terminal region with another conserved tegument protein, pUL37, and this interaction is essential for secondary envelopment in HSV-1 [211, 419, 197]. The structure of the N-terminal domain of pUL37 is similar to cellular multisubunit tethering complexes (MTCs), which control vesicular trafficking by

docking transport vesicles to their destination membranes [326]. Furthermore, in HSV-1, Wild-type capsids have been shown to accumulate at the *trans*-Golgi network, whereas upon deletion of pUL37, capsids were distributed throughout the cytoplasm [317]. These data suggest that pUL37 is implicated in the targeting of capsids to the site of secondary envelopment.

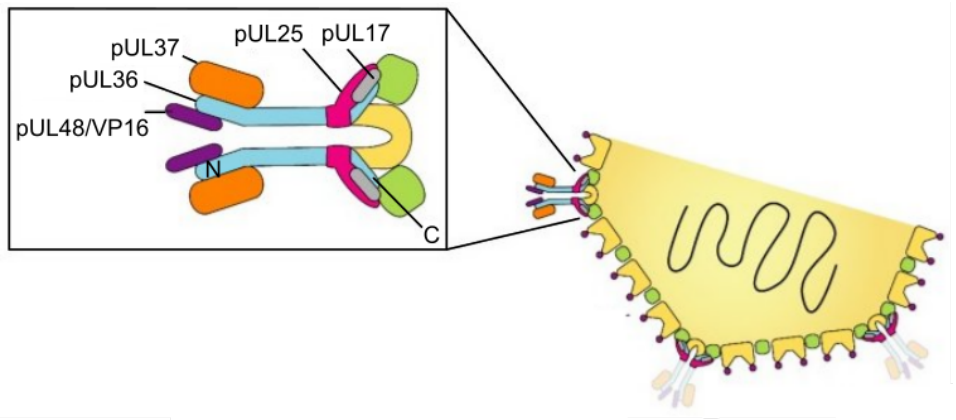

Figure 1.14: **Structure of HSV-1 CVSC.** CVSC is an essential complex for capsid tegumentation and secondary envelopment. Two of its components, pUL36 and pUL37, have been shown to be required to direct the capsid to the envelopment site. Figure modified from [309].

Once the inner tegument is attached to the capsid, both pUL36 and pUL37 direct the nascent virion to the site of secondary envelopment by microtubule-directed anterograde transport [4, 335]. Indeed, *in vitro* studies using purified non-enveloped HSV-1 capsids showed that kinesin-1 and kinesin-2 could bind capsids only if pUL36 and pUL37 were present and not masked by the outer tegument [335]. In HSV-1, pUL36 possesses two tryptophan-acidic motifs, ^{1766}WD^{1767} and ^{1862}WE^{1863}, that are conserved in all HSV-1 and HSV-2 isolates. Mutation of these motifs severely impairs secondary envelopment even if pUL36 and pUL37 are still incorporated onto capsids [177]. These tryptophan-acidic motifs are similar to the motifs that cargo proteins use to bind the kinesin light chains [4, 322]. Thus, pUL36 could mediate microtubule-directed anterograde transport by recruiting kinesin motors. On the other hand, HSV-1 pUL37 has been shown to interact with dystonin/BPAG1 in a yeast two-hybrid assay [315]. Dystonin is a protein with numerous isoforms. The three major isoforms are the neuronal isoform (dystonin-a), the muscle isoform (dystonin-b), and the epithelial isoform (BPAG1) [112]. Dystonins are cytoskeletal cross-linking proteins that interact with a great variety of proteins [112]. They have been shown to interact with the actin cytoskeleton and with clathrin, and to play a role

in regulating organelles structure and microtubules stability [4, 112, 356]. Thus, pUL36 and pUL37 may direct capsids towards the site of secondary envelopment by their interaction with kinesins and dystonins.

While it is widely accepted that Alphaherpesviruses secondary envelopment occurs at post-Golgi membranes, the precise identity of these membranes is yet to be unraveled. Currently available data point to two compartments, the TGN and the endosomes. The most universally accepted site of secondary envelopment is the TGN (Figure 1.15). Indeed, HSV-1, PRV, and VZV have been observed to undergo secondary envelopment at membranes resembling the TGN and stained with TGN markers [137, 161, 150]. In addition, analysis of the phospholipid composition of extracellular HSV particles revealed that viral membranes have high concentrations of sphingomyelin and phosphatidylserine. These lipids are typically enriched in the Golgi apparatus [416]. Moreover, pUL37, which is necessary for secondary envelopment, has been shown to be localized in the Golgi complex during infection [79]. Finally, blocking TGN export by incubating infected cells at 20°C showed that, under these conditions, HSV-1 capsids colocalize with TGN markers, and viral glycoproteins were often found adjacent to the capsids. These studies, however, also showed limited colocalization between capsids and EEA1, an early endosome marker, suggesting that endosomes could serve as a secondary envelopment site [413]. The latter hypothesis is further supported by ultrastructural studies of HSV-1-infected cells. In these studies, horseradish peroxidase (HRP) was used as a fluid phase marker and capsids were shown to envelope in endocytic tubules labelled with HRP as early as two minutes after HRP addition. The capsids did not colocalize with TGN or late endosomal markers, but colocalized with the transferrin receptor, which is known to be recycled to the cell surface after endocytosis. Furthermore, depletion of both Rab5 and Rab11, respectively markers of early and recycling endosomes, almost completely blocked virions envelopment, resulting in aberrant localization of capsids. The authors thus concluded that endocytic tubules originating from the plasma membrane were the main source of HSV-1 envelope (Figure 1.16) [168]. More recent studies conducted by the same team on BoHV-1 showed that capsids were also wrapped in endocytic tubules [354]. In addition, it was shown that inhibitors of dynamin or clathrin, which prevent endocytosis, decreased the transport of viral glycoproteins to assembly sites, and deletion of dynamin or the clathrin adaptor AP180 significantly decreased virus yield, highlighting the importance of the endocytic pathway in HSV-1 assembly [7].
Importantly, the endocytic and secretory pathways are highly dynamic and interconnected networks and the TGN has been shown to be an important compartment for both pathways [246, 124]. Moreover, HSV-1 is well known to induce cytoskeleton reorganization and remodeling of the endocytic and

secretory pathways upon infection [17, 45]. The two models presented above are thus not necessarily contradictory but further investigations are needed to unravel the specific involvement of each of these pathways in Alphaherpesviruses secondary envelopment.

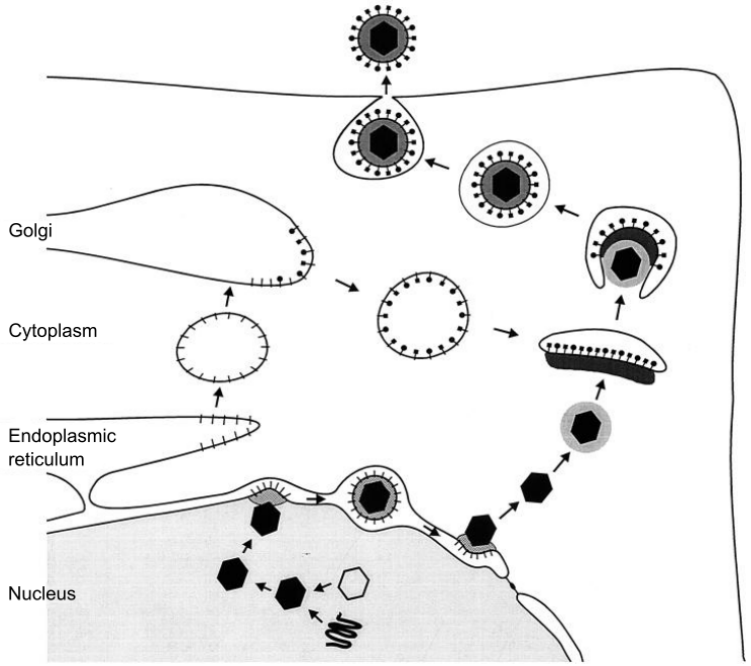

Figure 1.15: **Common model of Alphaherpesviruses envelopment.** Capsids acquire a primary envelope while budding at the INM. This envelope is then lost by fusion with the ONM and the capsids are released in the cytoplasm. In parallel, viral glycoproteins are synthesized in the endoplasmic reticulum and maturate in the Golgi apparatus. The mature glycoproteins are then packed in Golgi-derived vesicles. Tegument proteins accumulate on the surface of these vesicles by interacting with the cytoplasmic tails of glycoproteins. The secondary envelopment takes place when the capsids covered with the inner tegument interact with the membrane-associated outer tegument. Figure from [262].

Whatever the precise cellular compartment where the secondary envelopment takes place, all the viral glycoproteins need to be delivered there. HSV-1 encodes 16 membrane proteins that are thought to be incorporated into virions [309]. Some of these proteins possess trafficking motifs in their cytoplasmic domains, which mediate their subcellular localization upon interaction with the cellular protein sorting machinery [309]. In particular, gB and gE from HSV-1 as well as PRV have been shown to possess tyrosine-based motifs in their intracellular domain [288, 417, 10, 29]. These motifs allow interaction with clathrin adaptors and are important for endocytosis

and intracellular trafficking [410]. These motifs will be described in detail further in this manuscript. Some essential HSV-1 glycoproteins such as gD and gH/gL lack such sorting motifs and thus rely on other viral proteins for their correct localization [4, 309]. gM, although considered non-essential, has been shown to mediate the internalization of gD and gH/gL from the plasma membrane in both HSV-1 and PRV [68, 340]. Furthermore, gM as well as gK/pUL20, have been shown to be needed for the incorporation of gD and gH/gL into HSV-1 virions [340, 225]. The exact details regarding how the different viral membrane proteins reach the site of secondary envelopment are still unclear. Hopefully, studies to decipher the protein-protein interactions networks linking viral glycoproteins with each other and with the tegument will shed light on how the different viral proteins are concentrated at the site of envelopment and how membrane acquisition occurs.

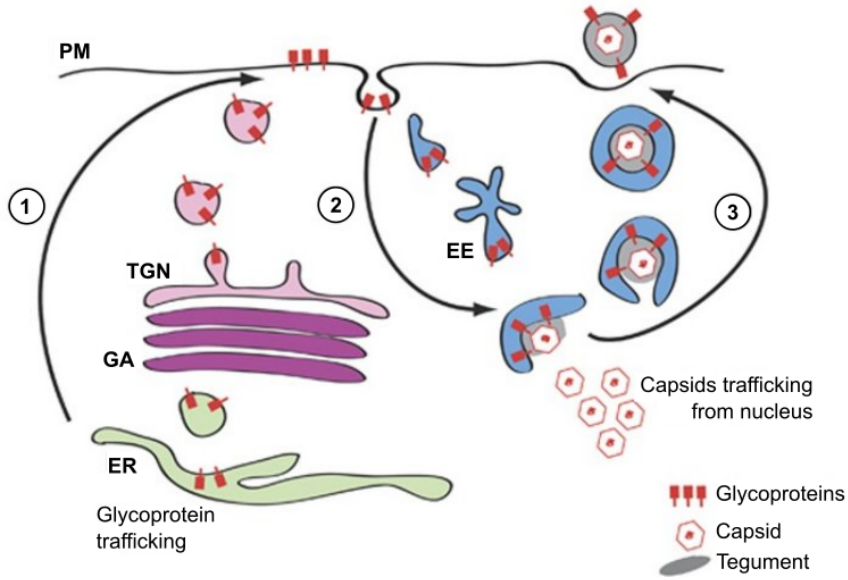

Figure 1.16: **Alternative model with endocytic membranes as source of final envelope.** The capsids escape the nucleus the same way as in the first model. In the cytoplasm: 1) the glycoproteins are synthesized in the endoplasmic reticulum (ER) and processed in the Golgi/TGN. 2) The glycoproteins are endocytosed from the plasma membrane (PM) and transported to the early endosomes (EE). 3) Glycoproteins-containing endocytic tubules wrap cytoplasmic capsids forming virions with a double membrane. The virions-containing vesicles are then transported to the cell surface where they fuse with the cell membrane to release single-enveloped virions. Figure adapted from [168].

Once the viral membrane proteins have been concentrated into the envelopment site, the capsid must dock at the surface of this cellular compartment. This step is possibly mediated by pUL37 via its interaction with the gK/pUL20 complex [181]. This interaction relies on tyrosine residues in pUL37 that are conserved in all Alphaherpesviruses and hence, might highlight a crucial interaction for assembly of virions from this subfamily [57]. Another viral complex formed by pUL11, pUL16, and pUL21 could help tether the viral capsid to the soon-to-be envelope. Myristylation and palmitoylation of pUL11 serve to anchor this complex to the TGN membrane [244]. In HSV-1, pUL16 has been shown to transiently associate with cytoplasmic capsids under mildly acidic conditions like the ones found in the TGN [260]. This capsid association of pUL16 is independent of the presence of pUL36, pUL37 or gE [261]. Studies on PRV revealed that pUL21 is associated with capsids but little is known about this protein [429]. The pUL11/pUL16/pUL21 heterotrimer has been shown to interact with gE (Figure 1.17). This interaction is important for the incorporation of both gE and the heterotrimer in viral particles as well as for the correct processing, transport, and biological activity of gE [151]. It is thus possible that two different complexes (pUL36/pUL37 and pUL11/pUL16/pUL21) act together to attach the viral capsids to the glycoproteins at the site of secondary envelopment.

Once the capsid has docked at the envelopment membrane, several protein-protein interaction networks are established (Figure 1.18). The four most abundant proteins found in HSV-1 tegument, pUL46, pUL47, pUL48, and pUL49 (homologue of VZV ORF9p) are required for this set up [309, 245]. Among these four proteins, only pUL48 is thought to be essential for HSV-1 replication in culture [452, 98, 272, 426, 451, 329]. On the contrary, simultaneous deletion of all four proteins in PRV does not prevent virion assembly in culture albeit viral replication is strongly impacted [119]. In HSV-1, pUL48 acts as a key stone for secondary envelopment. Indeed, pUL48 has been shown to interact with the inner tegument protein pUL36 [419, 395, 214], with the outer tegument proteins pUL41, pUL46, and pUL49 [419, 101, 194, 375] as well as with glycoproteins such as gH and possibly gB and gD (Figure 1.18) [458, 192, 144].
pUL49 has long been thought to be a non-essential HSV-1 protein. Although it is not strictly required for viral assembly [98, 329], its deletion has been shown to cause mutations in pUL41, a tegument protein with RNAse activity regulating cellular and viral protein production [366, 257, 95]. The pUL49 protein forms extensive interactions with glycoproteins as well as with other tegument proteins and so, it plays an important role during secondary envelopment [4, 309]. In HSV-1, pUL49 has been shown to bridge a complex between gE and gM (Figure 1.18) [251, 389]. The

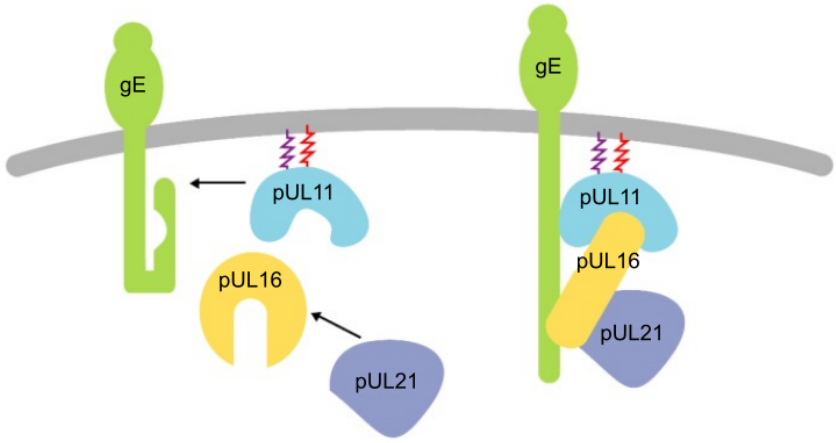

Figure 1.17: **A pUL11/pUL16/pUL21 complex as a link between capsids and envelope.** pUL11, with its myristylated and palmitoylated residues, anchors the complex to the envelopment membrane. pUL16 has been shown to transiently associate with capsids under conditions resembling the ones found in the TGN. pUL21 has also been shown to associate with capsids. The complex also interacts with gE and this interaction allows incorporation of gE and the complex in viral particles. Figure from [309].

gE/pUL49 complex is important for the correct localization of pUL49 at the TGN and for its incorporation into viral particles [389]. pUL49 has also been shown to interact with pUL48 and ICP0 and its deletion leads to reduced amounts of ICP0, ICP4 and gE in extracellular virions [98, 251, 389, 90]. Finally, co-transfection studies revealed an interaction between pUL49 and pUL16, which plays an important role in the incorporation of pUL49 into virions [383]. Altogether, these data point at pUL49 as an important player during secondary envelopment by its capacity to interact with a great number of glycoproteins and tegument proteins.
Yeast two-hybrid assays have identified numerous potential interactions between pUL47 and tegument proteins as well as between pUL46 and capsid, tegument, or membrane proteins, suggesting that pUL46 could be important to bridge the capsid to its envelope [419, 228, 117]. However, only a few of these interactions have been validated by other techniques [309]. Further studies are therefore needed to decipher the exact role of both proteins in secondary envelopment.

Beside the pUL11/pUL16/pUL21, another membrane bound complex formed by pUL51 and pUL7 is involved in cytoplasmic envelopment. Palmitoylation of pUL51 provides an anchor that, in transfected cells, ensures

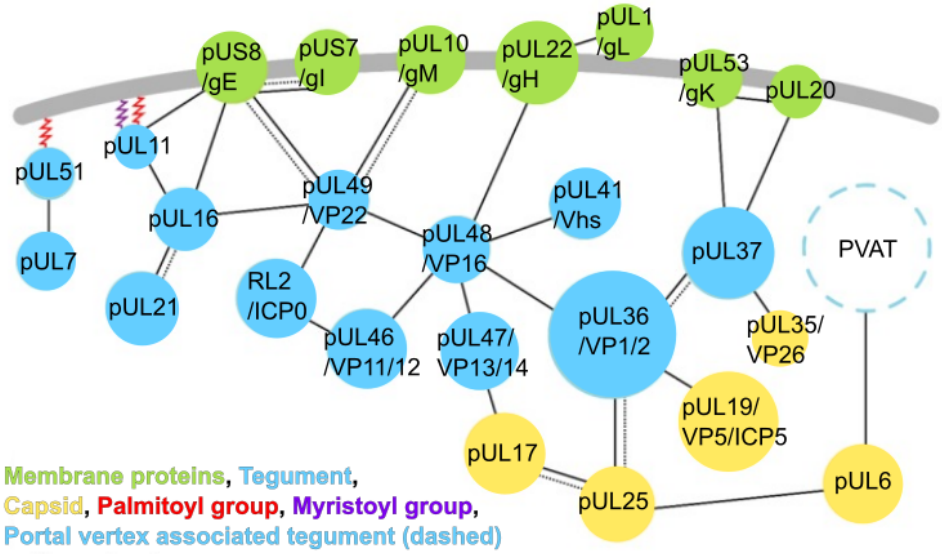

Figure 1.18: **Conserved protein-protein interactions network found in Alphaherpesviruses.** Tegument proteins (blue) link capsid proteins (yellow) to the viral glycoproteins and envelope proteins (green). Solid lines indicate interactions found in HSV and dashed lines show interactions found in PRV. Figure modified from [309].

its localization to the TGN [290]. In both HSV-1 and PRV, mutations in pUL51 lead to the accumulation of non-enveloped capsids in the cytoplasm associated with a reduction in viral titer [208, 289]. pUL51 has been shown to interact with gE and pUL7 [349, 351]. Deletion of pUL7 in HSV-1 also leads to an envelopment defect [400]. This complex has recently been shown to localize at focal adhesions at the plasma membrane, both in the absence of other viral proteins or in infected cells. There, it stabilizes focal adhesions to maintain the morphology of infected cells [6]. Interestingly, deletion of pUL7 or mutation in the C-terminal domain of pUL51 results in a defect in cell-to-cell spread of the virus. This defect is associated with a failure of gE to accumulate at cell junctions [113].

The recent finding of the crystal structure of the pUL51/ pUL7 complex reveals that the conformation of pUL51 resembles CHMP4B, a component of the cellular endosomal complex required for transport (ESCRT)-III complex [42]. Moreover, pUL51 can self-assemble to form ESCRT-III-like filaments *in vitro*. Interaction of pUL7 with pUL51 inhibits this self-assembly of pUL51. Altogether, these data suggest a direct role for pUL51 in promoting membrane scission during viral assembly that may be regulated by pUL7 [42].

After envelopment, viral particles are accumulated into large vesicles that need to be transported toward the cell surface for viral release. Whatever the cell type, the gE/gI complex seems to mediate HSV-1 particles sorting [4]. In cultured polarized epithelial cells, gE/gI direct HSV-1 virions towards cell-cell junctions on the lateral surfaces to promote cell-to-cell spread [4, 187, 83]. HSV-1 lacking gE or just its cytoplasmic domain is not transported to cell junctions, but rather to apical surfaces where it is released into the medium [187]. In PRV-infected cells, the μ1B subunit of the AP-1 clathrin adaptor complex has been shown to be involved in targeting of viral particles to the lateral surfaces [187]. Interactions with the AP-1 complex are mediated by tyrosine-based or dileucine motifs [314]. Such motifs are found in the cytoplasmic domain of gE in HSV-1, PRV and VZV [187]. It is thus possible that gE/gI serve to concentrate viral particles in subdomains of the TGN specialized for sorting towards lateral surfaces [4, 187]. The presence of gE/gI at the cell junctions possibly serves to facilitate transfer of viral particles from an infected cell to its neighboring non-infected cell by promoting movement across the junction or localized fusion between the cells by interaction with extracellular ligands [4]. This hypothesis is supported by studies on human HaCaT keratinocytes where mutations in the extracellular domain of gE led to reduction in HSV-1 spread comparable to what is observed with a gE-null mutant [4, 187, 327].
In neurons, gE/gI work in cooperation with pUS9, a small non-glycosylated membrane protein, to modulate virions trafficking [4]. While simultaneous deletion of pUS9 and gE/gI almost completely blocks delivery of virions to the axon, deletion of pUS9 alone only reduces it by 50% [91, 170, 376]. This indicates that in neurons, gE/gI and pUS9 function in a redundant manner [4].

Finally, HSV-1, PRV, and BoHV-1 have been shown to induce the formation of tunneling nanotubes (TNTs) that facilitate viral transmission to surrounding cells [85, 231, 111, 182, 311, 218, 183]. TNTs are long membranous tubes interconnecting cells and serve in intercellular communication [16, 355]. Two different types of TNTs have been described depending on their diameter, length, and cytoskeletal composition: while all TNTs backbone contains F-actin filaments, thick TNTs (diameter >0.7 μm) often contain microtubules as well [182, 16, 308]. In addition, both types of TNTs may contain nonconventional actin-based myosin motors such as myosin Va and/or myosin X and thick TNTs may also contain kinesin-1 and dynein motors [182, 355, 147]. The conserved Alphaherpesvirus serine/threonine kinase pUS3 is necessary and sufficient to induce the formation of TNTs [4, 111, 182, 114, 41, 220]. While most TNTs are stable for a relatively short time, TNTs induced by pUS3 are very stable and can exist for up to 24h [111, 182, 183]. This increased stability is probably due to pUS3-induced microtubules

acetylation and the marked enrichment in adherens junction components such as beta-catenin and E-cadherin at the contact sites between TNTs and adjacent cells [182, 183, 276].
Studies on PRV suggest that viral transmission by TNTs occurs via the release of enveloped virions into the extracellular space followed by fusion of the viral envelope with the membrane of the uninfected cell, rather than by direct transfer through TNTs and direct cytoplasmic connection [4, 183]. Indeed, PRV particles transported through TNTs are enveloped and transported in vesicles. Furthermore, virions are released from the entire length of the TNT and not only from the contact areas [183].
The use of TNTs for viral spread may be useful because the increased contacts between cells allow viral transmission without being exposed to the immune system. TNTs may also be required for invasion of tissues from the epithelium through the basal membrane: in PRV infection of *ex vivo* porcine mucosa explants, the TNT-inducing pUS3 is important for mucosal invasion through the basal membrane [182, 224].

1.4 VZV glycoproteins involved in cell fusion

VZV encodes ten glycoproteins: gB, gC, gE, gH, gI, gK, gL, gM, gN, and ORFS/L. Three of these glycoproteins, namely gB, gH, and gL, form the core fusion machinery used by the virus during cell entry. These three glycoproteins are also necessary and sufficient to induce cell-cell fusion in *in vitro* transfection experiments, provided that the cytoplasmic tail of gH is truncated [390, 305]. This is in contrast with HSV, which requires the addition of a fourth glycoprotein, gD, to induce fusion [15, 414].

1.4.1 gB

VZV gB is a 931 amino acids glycoprotein and is the most conserved Herpesvirus glycoprotein [305, 96, 425]. Herpesviruses gBs are class III fusion proteins that trimerize to form the active fusogen (Figure 1.19) [21, 159, 305]. In VZV, each gB protomer is composed of 13 α-helices and 31 β-strands, which form five distinct domains (DI to DV) stabilized by five disulfide bonds [305]. The fusion loops are located in domain I, and long linker regions near domains I and II possibly allow a large-scale rotation necessary to trigger fusion [65].

Mutagenesis studies on the cytoplasmic tail of VZV gB (gBcyt) revealed that it is important to regulate fusion. First, Heineman and Hall constructed a VZV gB mutant with a truncation of the last 36 amino acids of gBcyt. Cells infected with this mutant formed extensive syncytia, but very little viral particles were present on the surface of the cells compared to cells infected

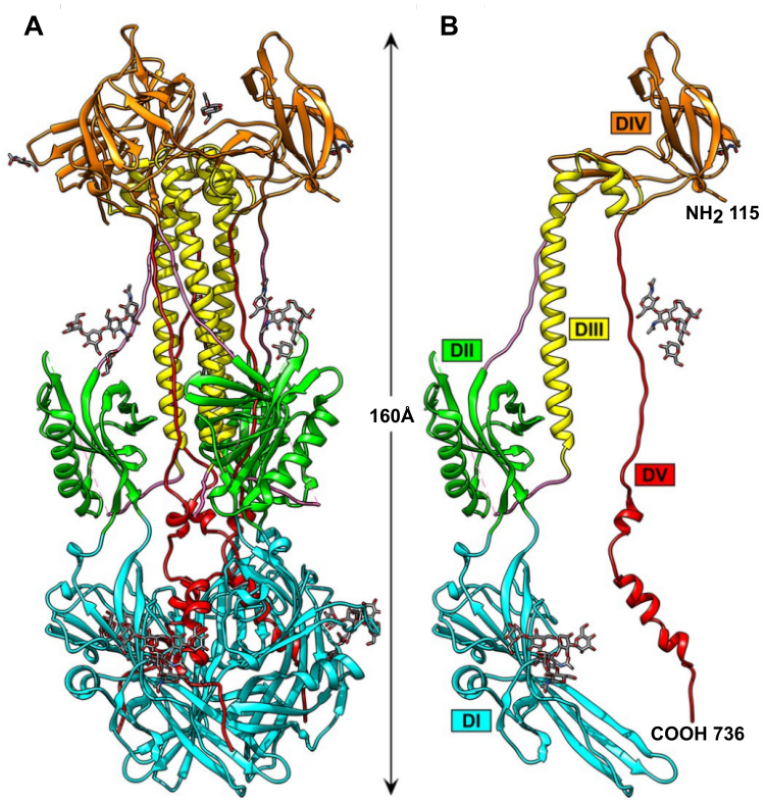

Figure 1.19: **Crystal structure of VZV gB ectodomain.** Ribbon diagram of the gB trimer (A) and monomer (B). The ectodomain of gB contains five domains (DI to DV). The fusion loops are located in DI. Figure adapted form [304].

with a Wild-type virus, which formed smaller syncytia and had numerous virions on their surface [156].
The cytoplasmic tail of gB contains two tyrosine-based motifs, ^{881}YMTL^{884} and ^{920}YSRV^{923}, that are important for its internalization from the plasma membrane and intracellular trafficking [158, 157]. Substitution of the tyrosine by aspartic or glutamic acid, or of the leucine by a glycine in the YMTL motif disrupted the trafficking of gB, and significantly reduced its expression on the cell surface, hence preventing cell fusion in a cell fusion assay [302]. Interestingly, mutation of the tyrosine residue by tryptophan or phenylalanine led to exaggerated cell fusion both in a cell fusion assay and in infection, without significant impact on the trafficking or internalization of gB, suggesting that the hydroxyl group of the tyrosine residue is crucial for the regulation of cell fusion [302]. The same study revealed that the YMTL motif is part of a canonical immunoreceptor tyrosine-based inhibition

motif (ITIM; consensus sequence [ILV]xYxx[LV]), ^{879}IKYMTL^{884} [302]. ITIM must be tyrosine phosphorylated to be functional. They usually function in cells of the immune system to inhibit intracellular signaling cascades, but may also play a role in signaling cascades affecting cell motility [305, 302]. The residue Y881 was indeed shown to be phosphorylated during infection. These data clearly demonstrate that the ITIM in gBcyt is important for the regulation of cell fusion [302]. Replacement of the tyrosine in the second tyrosine-based motif (YSRV) by phenylalanine had no significant impact on the surface expression or endocytosis of gB, but led to a decrease in cell-cell fusion in a cell fusion assay compared to the Wild-type [302].
Mutation of both YMTL and YSRV motifs (Y881/920F mutant) had no impact on the surface expression or endocytosis of gB, but cell-cell fusion was significantly enhanced both in a cell fusion assay and in infection. Interestingly, accentuated cell fusion with the Y881F and Y881/920F mutants was associated with lower viral titers and reduced plaque size [302].

In addition to the two tyrosine-based motifs, a conserved lysine cluster (K894, K897, K898, and K900) downstream of the ITIM has been shown to be important for fusion regulation [441]. Substitution of the four lysine residues of the cluster by arginine residues (to preserve the positive charge of the motif) had no impact on fusion in a cell fusion assay despite lower levels of gB at the surface. However, when the mutation was inserted into the VZV genome, the gB[4R] mutant was hyper-fusogenic and plaque size was slightly increased [441]. Lysine to alanine substitution on the gB lysine cluster (gB[4A] mutant) led to a 440% increase in fusion in the cell fusion assay despite a 16% decrease in gB surface expression. A VZV gB[4A] mutant exhibited extensively exaggerated syncytia and markedly reduced plaque size [441].

As already mentioned above, gB is the most conserved Herpesvirus glycoprotein. It is thus not a surprise that the two tyrosine-based motifs and the lysine cluster found in VZV gBcyt are also found in the other alphaherpesviruses (Figure 1.20). Although syncytia formation is unusual during HSV infections, studies on HSV-1 and HSV-2 gB showed that the tyrosine-based motifs also serve to regulate syncytia formation in these viruses. First, valine to alanine substitution in HSV-2 gB (YMALV -> YMALA) just after the ITIM enhanced cell-cell fusion in a cell fusion assay [353]. Then, substitution of the tyrosine residue by an alanine in the HSV-1 gB ^{889}YTQV^{892} (corresponding to VZV ^{920}YSRV^{923} motif) was shown to prevent gB internalization and to abolish syncytia formation [29]. Finally, the same study showed that an unconventional dileucine motif (^{871}LL^{872} present in HSV-1 gB was important for its targeting to the Golgi after endocytosis. Substitution of the two leucine residues by alanines promoted gB recycling to the

cell surface and enhanced cell-cell fusion [29].

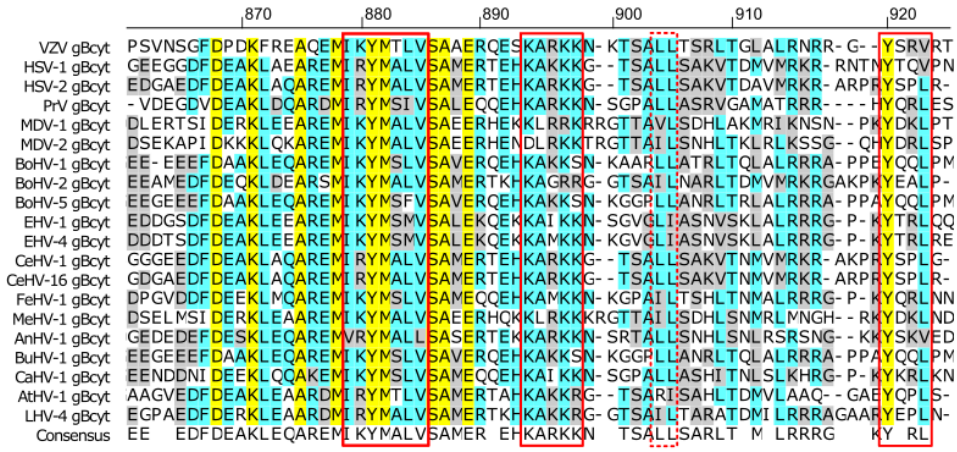

Figure 1.20: **Protein sequence alignment of the gBcyt region including the two tyrosine-based motifs.** The two tyrosine-based motifs and the lysine cluster important for VZV gBcyt-mediated cell fusion regulation are conserved among Alphaherpesviruses (solid box). The unconventional dileucine motif important for HSV-1 gB trafficking is also conserved (dashed box). Identical amino acids are highlighted in yellow, conserved amino acids are in blue and similar amino acids in grey.

1.4.2 gH/gL

The gH/gL complex is another part of the core fusion machinery. VZV gH is an 841 amino acids protein that forms a dimer with the 160 amino acids gL. The latter acts as a chaperone for the correct processing and trafficking of gH [93, 92]. The structure of the gH/gL complex is similar in Herpesvirus orthologs (Figure 1.21): gH is composed of three distinct domains (DI to DIII). The N-terminus of gH forms DI, which is composed of β-sheets that cofold with gL, the central domain (DII) contains 16 α-helices, and the C-terminal domain (DIII) forms a highly conserved β-sandwich [301, 420, 255, 22, 59].

VZV gH has a short cytoplasmic domain consisting of only 18 amino acids. Despite being extremely short, it is crucial for fusion regulation. Indeed, in a cell fusion assay, expressing gB, gH[WT], and gL induced fusion similar to the vector alone. However, shortening of the cytoplasmic domain of gH by introducing a stop codon at E834 (gH[TL] mutant) or by deletion of the seven last residues (gH[834-841] mutant) induced extensive fusion (Figure 1.22) [440]. Substitution of the 834-841 residues by V5, cMyc, and hydrophobic or hydrophilic sequences had no impact on fusion compared

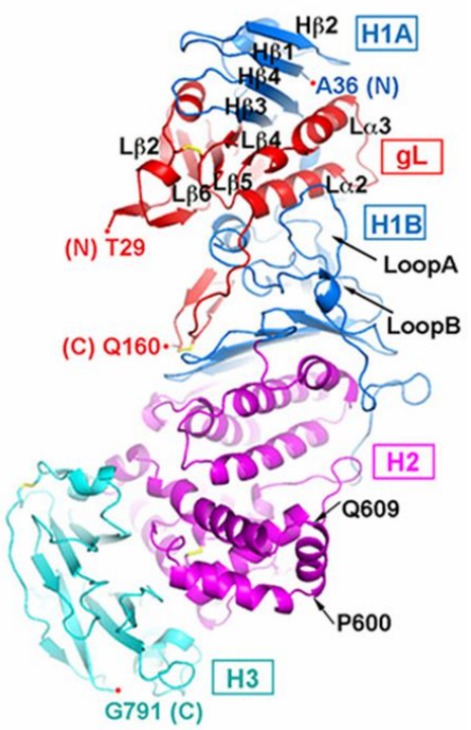

Figure 1.21: **Structure of the VZV gH/gL complex.** The ectodomain of gH forms three distinct domains (H1 to H3). Domain I of gH (in blue) is composed of β-sheets that cofold with the chaperone gL (in red). Domain II (in magenta) is formed by 16 α-helices, and domain III (in cyan) forms a highly conserved β-sandwich. Figure adapted from [437].

to gH[WT], suggesting that the length of gHcyt rather than specific motifs or biochemical properties is important for fusion regulation (Figure 1.22). This was further supported by stepwise deletions of amino acids 834-841 causing incremental increases in cell fusion [440]. Introduction of the gH[TL] or gH[934-841] mutations in VZV genome led to exaggerated syncytia formation and lower viral titer [440].

Importantly, expression of gB[Y881F], gH[TL], and gL in the cell fusion assay led to increased fusion compared to the expression of gB[WT], gH[TL], and gL, whereas gB[Y881F] did not induce fusion when expressed with gH[WT] and gL. These results suggest that the function of gHcyt in fusion regulation is independent of the ITIM domain of gB [440]. Introduction of both gB[Y881F] and gH[834-841] in VZV genome was lethal for the virus as no infectious virions were produced and no capsid assembly was observed in the nucleus [440].

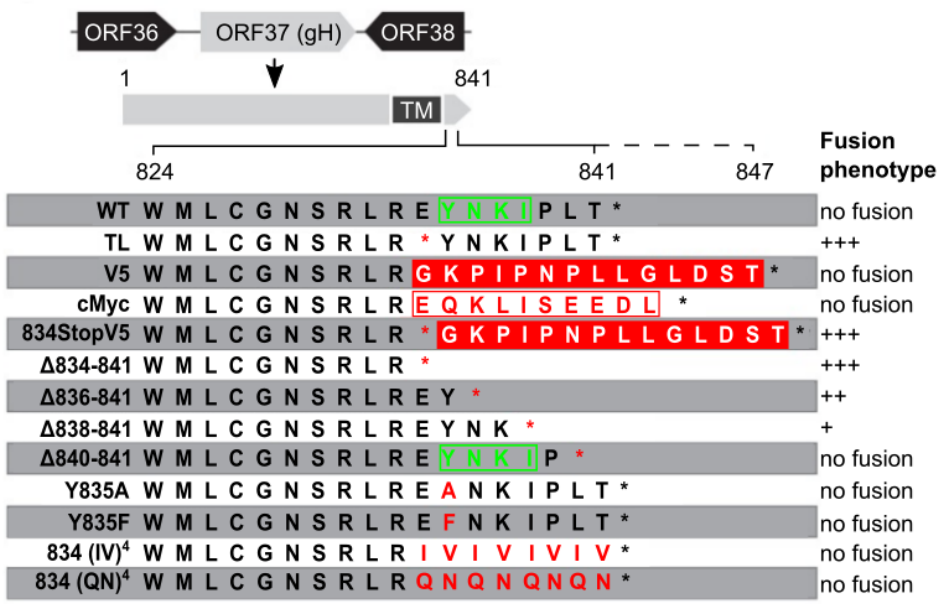

Figure 1.22: **Construction of VZV gHcyt mutants and their fusion phenotype in a cell fusion assay.** The solid black line represents the length of the WT gHcyt (824-841) while the dotted line represents extension of the gHcyt in the V5 and cMyc constructs. The V5 sequence is boxed in red and the cMyc sequence is boxed in white. The predicted endocytic Yxxϕ motif is boxed in green. Mutations made in gHcyt are in red and stop codons are represented by asterisks. TM indicates the transmembrane domain. Figure adapted from [440].

The fact that mutations of both gB and/or gH enhancing cell-cell fusion are associated with reduced plaque size and with a lack of infectious viral particles production is contrasting with the long-thought idea that cell-cell fusion helps VZV spread and suggests that syncytia formation must be tightly regulated to ensure optimal VZV spread [305].

A model has been proposed to explain how the cytoplasmic domains of VZV gB and gH/gL may regulate cell fusion: The cytoplasmic domain of VZV gB is predicted to contain three α-helices, one harboring the ITIM domain. This α-helix is positively charged (pI 9.4) and is suspected to bind to the cell membrane. Phosphorylation of serine residues near the ITIM is thought to destabilize membrane association and to allow exposure of Y881 [302]. The gHcyt is proposed to act as a gate keeper using its physical length to regulate the phosphorylation of gB Y881 by controlling kinase or phosphatase access to the ITIM [440].

Although gB and gH/gL are described as necessary and sufficient to induce

fusion in VZV, the fact that the cell fusion assay requires a truncated form of gH (gH[TL]) suggests that other viral proteins may be required to initiate the fusion reaction *in vivo.*

1.4.3 Other glycoproteins implicated in cell fusion

VZV gE is the most abundant glycoprotein in infected cells and is known to form heterodimers with gI [12]. These two proteins have homologs in all Alphaherpesviruses, but VZV gE has a unique N-terminal domain of 188 amino acids that is not present in its homologs. Furthermore, VZV gE is essential for replication while its homologs are not [12]. Neither gE, gI nor the gE/gI heterodimer are required for fusion in the cell fusion assay [305]. Nonetheless, two VZV strains harboring a D150N mutation in gE have been isolated in 1998 and 2002 in North America. These two mutants were respectively called VZV-MSP and VZV-BC [359, 405]. Both mutants exhibit an enhanced cell-to-cell spread [360, 143]. VZV-MSP was also shown to induce extensive syncytia formation in human epidermal cells compared to VZV-WT, but it did not enhance fusion in human fibroblasts compared to WT [63]. Furthermore, coexpression of gB and gE alone has been shown to induce syncytia formation *in vitro* [249]. This result and the existence of VZV-MSP suggest that VZV gE plays a role in virus-induced cell-cell fusion and that this fusion is regulated in a cell-type dependent manner.

In HSV-1 or PRV, other glycoproteins have been shown to modulate cell fusion. In HSV-1, the gK/pUL20 complex has been shown to interact with gB and gH and mutation of either gK or pUL20 caused extensive syncytia formation [58]. Furthermore, expression of gK in addition to gB, gH, gL and gD in the cell fusion assay inhibited cell-cell fusion [19]. Co-expression of gK and pUL20 in the cell fusion assay drastically reduced fusion and this anti-fusion activity was correlated with a downregulation of the surface expression of gB, gH, gL, and gD [18].
PRV gM has been shown to inhibit membrane fusion when cotransfected with gB, gH, gL, and gD [210]. It was also shown to inhibit fusion mediated by HSV-1 gB, gH, gL, and gD in a cell fusion assay, and HSV-1 gM/pUL49A (homolog of VZV gN) complex also prevented HSV-1-mediated fusion. In both cases, fusion inhibition was correlated with a relocalization of HSV glycoproteins from the plasma membrane to a juxtanuclear compartment [68]. Thus, even if non-essential for fusion *in vitro*, other VZV glycoproteins may be required to regulate syncytia formation possibly by altering the trafficking of the core fusion glycoproteins.

1.5 The Alphaherpesvirus tegument protein VP22

VP22 is the homologue of VZV ORF9p and is conserved in all Alphaherpesviruses [434]. The sections below will refer mostly to HSV-1 VP22 as it is the model Alphaherpesvirus. Some differences exist between HSV-1 VP22 and VZV ORF9p and will be detailed in a later section dedicated to VZV ORF9p.

1.5.1 General features

VP22 is one of the most expressed proteins of HSV-1 and is estimated to be present in more than 2 000 copies in the tegument of viral particles [434, 155, 245]. It is conserved only in Alphaherpesviruses where it is most frequently encoded by the *ul49* gene [434, 196].
Surprisingly, deletion of the *ul49* gene has two different outcomes depending on the virus considered: in MDV and EHV-1, deletion of VP22 is lethal for the virus in cultured cells [298, 87], while in HSV, PRV and BoHV-1, VP22 is dispensable in cell culture [90, 343, 240]. However, deletion of VP22 impedes the fitness of both BoHV-1 and HSV in their natural hosts or animal models by altering the composition of the newly formed virions as well as viral replication [329, 98].

The length of the *ul49* gene differs among the Alphaherpesviruses, ranging from about 600 bp to about 1 000 bp [434]. Sequence comparison and secondary structure predictions have demonstrated that VP22 possesses a conserved core domain in its C-terminal region, while its N-terminal region is not conserved [292]. The core domain comprises approximately 80 amino acids and is differentially located in VP22 homologs [409]. In VZV ORF9p and VP22 of PRV, MDV and the avian infectious laryngotracheitis virus (ILTV), it forms three alpha helices and one beta strand [434, 409]. HSV-1 VP22 has been shown to oligomerize by association of the beta strands to form a beta sheet (Figure 1.23) [165]. Interestingly, the core domain of VP22 shares structural homology with the tegument protein ORF52 from Murid herpesvirus 68 (Gammaherpesvirus) despite any obvious sequence similarity. This suggests a functional conservation between the two subfamilies [165].

VP22 is a phosphoprotein that, in HSV-1, is phosphorylated by the cellular CKII and the viral protein kinase pUL13 [100, 14]. Moreover, in BoHV-1, the second viral kinase, pUS3, has been shown to phosphorylate VP22 [219]. Studies on HSV-1 showed that VP22 exists in both phosphorylated and non-phosphorylated forms in infected cells, and the phosphorylation state of VP22 correlates with its subcellular distribution: at early stages of viral

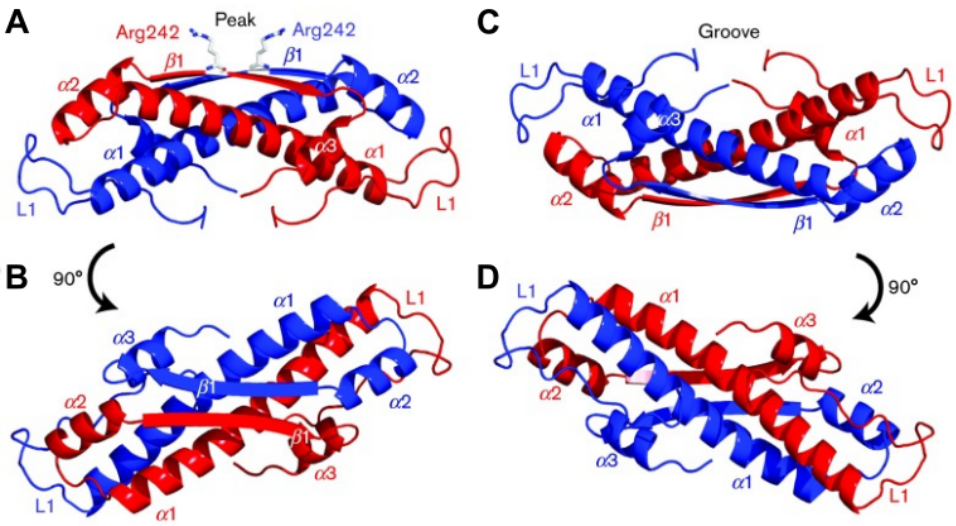

Figure 1.23: **Crystal structure of HSV-1 VP22 core domain.** Each monomer (in red and blue) is formed by three alpha helices (α1-3) and one beta strand (β1). VP22 can oligomerize by interaction of the beta strands to form a beta sheet. Figure from [165].

infection, VP22 is mainly present in the cytoplasm, but at later stages, it migrates to the nucleus where highly phosphorylated VP22 accumulates [328, 394]. Finally, only hypo-phosphorylated VP22 is incorporated into newly formed HSV-1 virions [125].

HSV-1 and BoHV-1 VP22 have been shown to be able to reach the nucleus of infected cells independently from other viral proteins [152]. However, amino acid sequence analysis of VP22 in BoHV-1 did not predict the presence of classical or non-classical nuclear localization signal (NLS) [454]. It was postulated that VP22 could interact with cellular proteins to mediate its nuclear targeting [409]. The C-terminal domain of BoHV-1 VP22 and the N-terminal domain of MDV VP22 both have been demonstrated to be essential for the nuclear localization of the protein. Interestingly, these domains are also important for histone association, which could be responsible for the nuclear localization of VP22 [409, 454, 338, 456].

Surprisingly, in HSV-1, VP22 has been demonstrated to have intercellular transport properties. This phenomenon is so efficient that following expression in a cell population, VP22 spreads to every cell in the monolayer. This intercellular transport capacity was observed both in transfection and infection studies [97]. Furthermore, VP22 has been shown to bind RNA and to transport it in an adjacent uninfected cell where it is expressed. It was

thus postulated that VP22 transports RNA in uninfected cells to create an environment facilitating effective initiation of infection [365]. This interesting transport capacity of VP22 has been under many investigations for its potential application in gene therapy [447, 265, 438, 334, 140].

1.5.2 Effects on gene transcription and protein synthesis

Several studies have shown that HSV-1 VP22 plays a role in viral gene transcription, mainly by affecting the action of the virion host shutoff (VHS) protein, a viral endoribonuclease that degrades mRNA during early stages of infection [434]. Initially, Taddeo *et al.* showed that VP22 could bind VHS, but only in the presence of pUL48, to form a VP22/pUL48/VHS complex that promotes viral mRNA translation. Furthermore, expression of both pUL48 and VP22 was required for the translation of VHS in transfected cells. The authors proposed a model in which VHS functions by sequestrating mRNAs in compartments inaccessible to the cellular translation machinery and that pUL48 and VP22 rescue the mRNAs by interacting with VHS [396]. More recent studies have demonstrated that translation of VHS only requires the expression of VP22 and not the pUL48/VP22 complex [99]. Other studies by the same group showed that in a Wild-type infection, immediate-early and early transcripts were retained in the nucleus in a VHS-dependent manner while late transcripts were cytoplasmic. On the contrary, deletion of VP22 leads to nuclear retention of late transcripts as well. The rescue of this VHS-induced nuclear retention was enhanced when VP22 interacted with pUL48, but this interaction is not fundamental [325]. These data suggest that VHS affects both cellular and viral transcription by nuclear retention rather than degradation of the mRNAs, and VP22 acts as a co-factor to mediate the spatiotemporal regulation of the infected cell transcriptome [325].

Besides its activity on VHS, VP22 has been shown to coprecipitate with TATA box binding protein associated factor (TAF-I) protein [232]. TAF-I plays a role in chromatin remodeling and promotes the deposition of histones on naked DNA [232, 300, 267]. The interaction of VP22 with TAF-I has two effects *in vitro*: first, it inhibits TAF-I-mediated nucleosome deposition on DNA, and it abolishes the non-specific binding of VP22 with DNA. It was proposed that the TAF-I/VP22 interaction may be important to prevent association of the incoming viral genome with nucleosomes early after viral entry, which would prevent IE genes transcription. In this model, VP22 could inhibit nucleosome deposition in two possible mechanisms: the VP22/TAF-I interaction would directly block TAF-I-mediated nucleosome deposition, or VP22 binding to viral DNA blocks nucleosome deposition. TAF-I would interact with VP22 to remove it from viral DNA and to allow nucleosomes to access DNA [232]. Thus, VP22 may be important early in

infection to regulate viral DNA organization through its interaction with TAF-I. Consistent with this, overexpression of TAF-I in infected cells affects the progression of HSV-1 infection [232].

1.5.3 Effects on immune evasion

In HSV-1, VP22 has been shown to act as an antagonist of interferon (IFN) signaling by interacting with and inhibiting the enzymatic activity of cyclic GMP-AMP synthase (cGAS) (Figure 1.24). cGAS normally senses intracellular DNA and initiates the innate immune response by activating type I interferon production. Huang *et al.* showed that ectopic expression of VP22 decreased cGAS/STING-mediated activation of IFN-beta promoter and production of IFN-beta. Deletion of VP22 from HSV-1 genome prevented the inhibition of the IFN signaling pathway and stable knock-down of cGAS improved the replication of a VP22-deleted virus but had no effect on the Wild-type virus [434, 171].

VP22 also mediates immune evasion by affecting the AIM2 inflammasome (Figure 1.24). This inflammasome is usually activated by cytoplasmic DNA, leading to caspase-1 activation and release of interleukin (IL) 1-beta and IL-18, inflammatory cytokines mediating the innate immune response against pathogens. Maruzuru *et al.* have recently shown that VP22 can bind to AIM2 and prevent its oligomerization, which is normally required for activation of the inflammasome. Furthermore, replication of a VP22-deleted virus is restored in AIM2-deficient mice [434, 254].

1.5.4 Effects on viral assembly

In addition to its role in DNA transcription, protein synthesis, and immune evasion, VP22 plays a role in viral assembly. First, VP22 or its homologs have been shown to interact with various tegument proteins (Figure 1.25). In HSV-1, it has been demonstrated to interact with pUL48 and ICP0 [101, 446], this latter interaction being important for the incorporation of ICP0 into virions [98]. Moreover, HSV-1 VP22 is required for the correct subcellular localization of pUL48, pUL35, ICP0, ICP4, and pUL54, and mutations in VP22 affecting the subcellular localization of these proteins also decreased viral replication and neurovirulence in an experimental murine model [399].

VP22 not only interacts with tegument proteins, but also with viral membrane proteins (Figure 1.25). In HSV-1, it has been shown to interact with at least pUS9, pUL56, gE and gM [292, 107, 117, 228]. Conflicting evidence have been found concerning the interaction between VP22 and gD in HSV. Two studies found an interaction between VP22 and the C-terminal domain of gD [108, 56], while another study could not confirm this interaction [251].

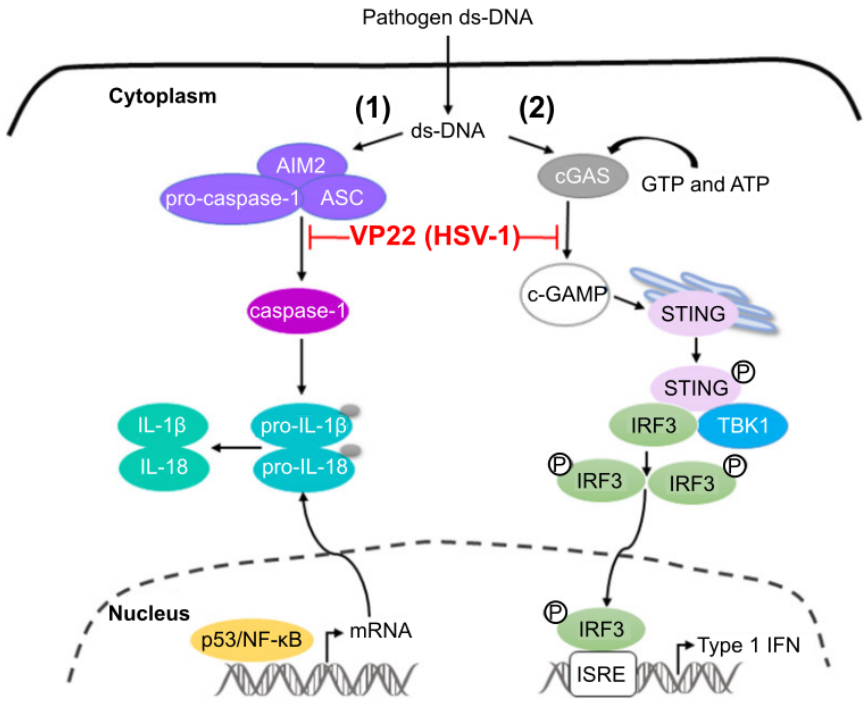

Figure 1.24: **VP22 mediates immune evasion via two pathways.** 1) AIM2 recognizes specific patterns in dsDNA and then binds to the linker protein ASC and pro-caspase-1 to form the AIM2 inflammasome. The latter activates caspase-1, which can cleave pro-IL-1β and pro-IL-18. Once cleaved and activated, these inflammatory factors are secreted to fight the infection. 2) cGAS is usually activated upon binding of dsDNA. cGAS uses GTP and ATP to generate cGAMP which activates STING. Phosphorylated STING recruits TBK1 to activate IRF3 which enters the nucleus after phosphorylation. In the nucleus, phosphoIRF3 activates the interferon-stimulated response element (ISRE), producing type I interferon to fight pathogens. Figure modified from [434].

Studies using a HSV VP22-null virus further proved the importance of VP22 in viral assembly. Indeed, the composition of the virion is affected by the absence of VP22, with ICP0, gE and gD being less incorporated in viral particles in the VP22-null virus compared to WT or VP22-repaired virus [90].
In PRV, the interaction between VP22 and the cytoplasmic domains of gE and gM is conserved, and deletion of both glycoproteins prevents the incorporation of VP22 into virions [121]. It has recently been shown that BoHV-1 VP22 may interact with gN without the need for gM [312]. Altogether, these data suggest that VP22 is important for viral assembly by forming interconnected protein-protein interaction networks between the capsid,

tegument, and envelope proteins.

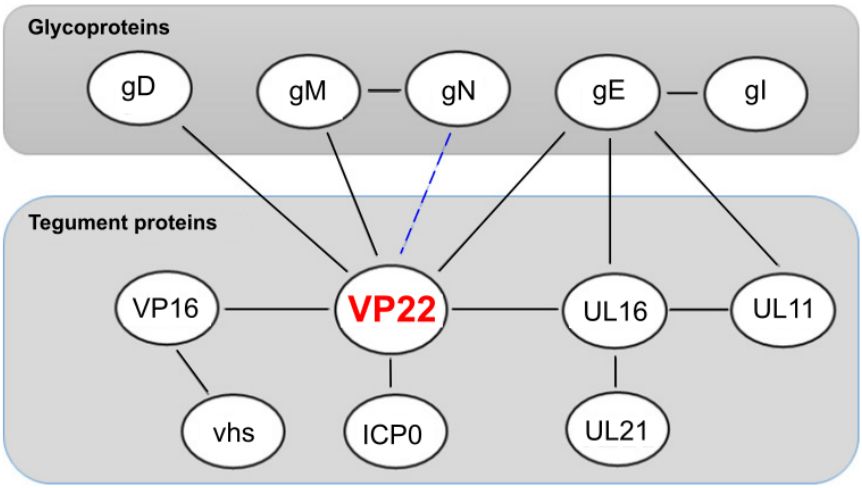

Figure 1.25: **Network of protein-protein interaction around the tegument protein VP22.** VP22 of several alphaherpesviruses has been shown to interact with a great number of viral glycoproteins and tegument proteins, suggesting its importance in viral assembly. Figure from [434].

1.5.5 Effects on cell-to-cell spread

Several studies on MDV and BoHV-1 have identified VP22 as important for cell-to-cell spread of these viruses [409, 312, 35, 191]. One of the studies showed that the core region of MDV VP22, associated with the N-terminal part of the protein, is necessary for cell-to-cell spread, whereas the C-terminal part is dispensable, but favors cell-to-cell spread [409]. Furthermore, this study showed that PRV VP22 could complement MDV spread at 32%, while the protein from VZV or ILTV could not [409]. In BoHV-1, deletion of VP22 leads to smaller plaques. This size reduction is even more important if gE or gN are deleted in combination with VP22 [312, 191]. Studies on HSV-1 using a VP22-deleted virus showed that the VP22-null virus produced smaller plaques in cultured cells, but these analyses revealed that this defect is primarily due to decreased viral release rather than a decrease in viral assembly or cell-to-cell spread [90].

1.6 VZV ORF9p

In VZV, the homologue of VP22 is ORF9p, a 302 amino acids tegument protein with a molecular weight of 32 846 Daltons. The *orf9* is the most

transcribed gene during the VZV lytic cycle [200, 62] and is essential for VZV replication in cultured cells [52]. ORF9p is also extremely well conserved between the different VZV strains identified worldwide, with 99.7% identity between the different protein sequences. Indeed, only strains derived from the pOka strain identified in Japan (and strain VZV-8 identified in Canada) differ from all other by one threonine to alanine substitution at the end of the protein (Figure1.26).

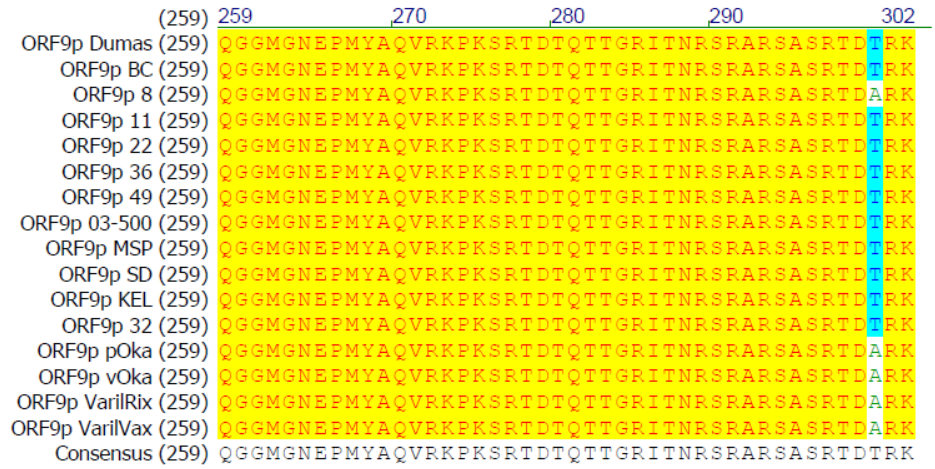

Figure 1.26: **Partial protein sequence alignment of VZV ORF9p in the different strains identified.** ORF9p is extremely well conserved between the different VZV strains, with 99.7% identity. Only strains derived from the Japanese pOka strain and strain VZV-8 present one point mutation at the end of the protein. Sequence alignment was performed using the VectorNTi program (Invitrogen) with sequenced coming from VZV strains identified in [324] and obtained from NCBI. Identical amino acids are highlighted in yellow, conserved amino acids in blue.

Although homologues, sequence alignment between HSV-1 VP22 and VZV ORF9p revealed a poor sequence conservation between the two proteins. Indeed, there are only 25% identity and 34% similarity between the two sequences. These percentages increase to 43% identity and 56% similarity when considering only the core domain of both proteins. Thus, HSV-1 VP22 and VZV ORF9p could share some similar functions without acting exactly the same [60].

In silico analysis of VZV ORF9p revealed the possible presence of two nuclear localization signals (NLS) and two nuclear export signals (NES). The N-terminal bipartite NLS mapped to amino acids 16-32 and the NES

found at amino acids 103-117 were shown to be active in transiently transfected COS-7 cells (Figure 1.27) [44]. Immunolabelling in combination with transmission electron microscopy studies confirmed the presence of small amounts of ORF9p in the nucleus and showed that it is also located in the *trans*-Golgi network [52].

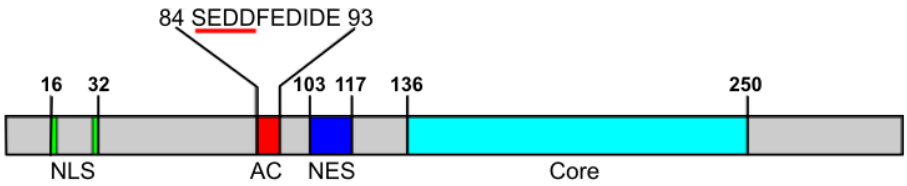

Figure 1.27: **Schematic representation of ORF9p.** The Alphaherpesvirus core domain is located in the second half of the protein (Core, light blue). ORF9p has been shown to have a functional bipartite Nuclear Localization Signal (NLS, green) as well as a functional Nuclear Export Signal (NES, dark blue). An acidic region (AC, red) overlapping ORF47p consensus site (SEDD, red underline) is also present in ORF9p.

Like VP22, ORF9p has recently been shown to bind to cGAS to reduce type I IFN response [164]. ORF9p could also be the key stone of a large protein-protein interaction network. Yeast-two-hybrid studies have identified the glycoproteins gI, and gN, the envelope proteins ORF15p, the tegument protein ORF38p, and the small capsid protein ORF23p as potential ORF9p interacting partners [384, 415]. Furthermore, co-immunoprecipitation analyses revealed an interaction with microtubules, gE, the major viral transactivator IE62, and the RNA binding protein ORF11p [60, 52, 53].

Previous studies from our laboratory showed that during infection, the viral kinase ORF47p, homologue to HSV-1 pUL13, interacts with, and heavily phosphorylates ORF9p [345]. Interestingly, a point mutation in ORF9p abolishing its phosphorylation by ORF47p (E85R mutation) without impacting their association leads to accumulation of unenveloped capsids near the Golgi apparatus, suggesting that the phosphorylation of ORF9p by ORF47p is important for viral assembly [345]. Other studies from our laboratory also showed the presence of an acidic cluster in ORF9p overlapping the consensus ORF47p phosphorylation site (Figure 1.27). Deletion of this acidic cluster abolished the interaction with ORF47p and resulted in a nuclear accumulation of both proteins as well as accumulation of primary enveloped capsids in the perinuclear space, directly suggesting a role for ORF9p in nuclear egress of VZV capsids [344].

1.7 Adaptor Protein complexes

Cargo proteins trafficking in the endocytic and secretory pathways are packed into vesicles to be delivered to their target sites. Vesicle formation and targeting to the correct organelle is mediated by adaptor protein (AP) complexes. AP complexes bind to sorting signals present in the cytoplasmic tail of the cargo proteins, recruit clathrin and/or other accessory proteins, and concentrate cargo proteins into vesicles, which then travel to their target organelle [314].

To date, five AP complexes have been identified. AP-1, AP-2, and AP-3 all have clathrin-binding motifs, but it is not clear if AP-3 uses a clathrin scaffold to form vesicles. On the contrary, both AP-4 and AP-5 do not bind clathrin [314]. Each complex performs its function at distinct intracellular organelles (Figure 1.28). AP-1 is localized on the TGN and endosomes, where it regulates the bidirectional transport between these two organelles. It is also implicated in the basolateral sorting of proteins in polarized cells. AP-2 is found on the cytosolic face of the plasma membrane where it regulates clathrin-mediated endocytosis. AP-3 is mostly found on tubular endosomes and mediates cargo transport towards late endosomes. It is also involved in the biogenesis of lysosome-related organelles (LRO). AP-4 is preferentially found on the TGN where it regulates the transport from the TGN to endosomes in a clathrin-independent manner. AP-4 has also been shown to mediate polarized sorting in epithelial cells and neurons. Finally, AP-5 is found on late endosomes and multivesicular bodies (MVB), but its precise function is still unknown [314].

1.7.1 Structure

AP complexes are heterotetramers composed of two large (one each of $\gamma/\alpha/\delta/\epsilon/\zeta$ and β 1-5, respectively), one medium (μ 1-5), and one small subunit (σ 1-5) (Figure 1.29). Some of these subunits have multiple isoforms encoded by different genes: AP-1 has two γ (1 and 2), two μ (1A and 1B) and three σ (1A, 1B, and 1C) isoforms; AP-2 has two α isoforms (A and C); and AP-3 has two β (3A and 3B), two μ (3A and 3B), and two σ (3A and 3B) isoforms [314]. The N-terminal part of the two large subunits and the full-length μ and σ subunits form the core domain of the AP complex (Figure 1.29). The core recognizes sorting signals and meditates membrane association of the complex. The C-terminal domains of the two large subunits form the ears domains, which interact with accessory/regulatory proteins. The ears domains are linked to the core domain by two mostly unstructured hinge domains (Figure 1.29). In AP-1, AP-2, and AP-3, the hinge domains

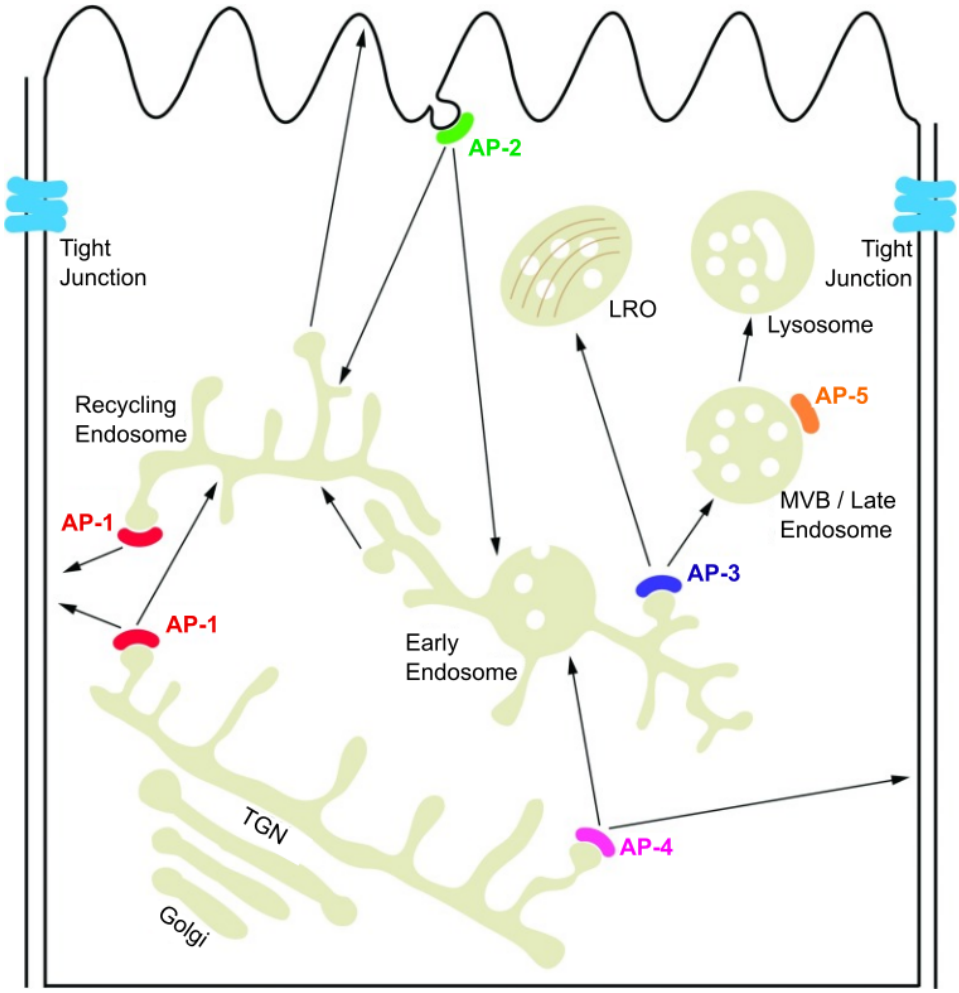

Figure 1.28: **Cellular localization of the AP complexes.** AP-1 is located on the TGN and recycling endosomes and regulates the bidirectional transport between these organelles. AP-2 mediates clathrin-dependent endocytosis from the plasma membrane. AP-3 is located on endosomes and participates in LRO biogenesis. AP-4 mediates transport from the TGN to endosomes or the basolateral plasma membrane. AP-5 is localized to late endosomes, but its function is unknown. Figure from [314].

contain the clathrin-binding sites, which allows the interaction with the clathrin heavy chain to form the clathrin-coated vesicle [314].

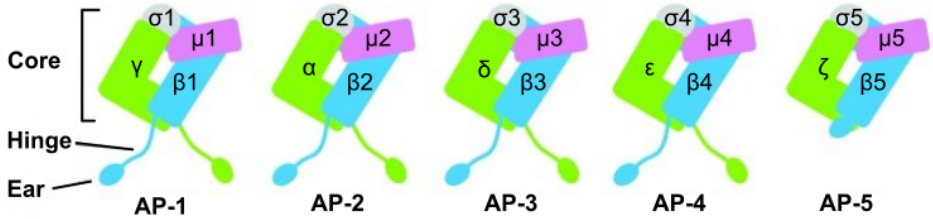

Figure 1.29: **Structure of the five AP complexes.** AP complexes are heterotetramers composed of two large, one medium and one small subunits. The AP complexes are composed of three domains: the core is responsible for association with the membrane and recognition of the sorting signals, the ears interact with accessory/regulatory proteins, and the hinges are mostly unstructured domains linking the ears to the core. Figure adapted from [314].

1.7.2 Interaction motifs

Different types of motifs are recognized by the adaptor protein complexes. The best characterized motifs are tyrosine-based motifs, dileucine motifs, and acidic clusters [39]. More recently, a basic motif in the cytoplasmic tail of L-selectin has been shown to allow interaction with AP-1 [81]. The importance of these motifs in protein sorting will be discussed hereafter.

1.7.2.1 Tyrosine-based motifs

Tyrosine-based motifs are found in various types of proteins and are important for endocytosis, intracellular sorting, and lysosome targeting among others [39].

This type of motif has a Yxxϕ consensus sequence, where the tyrosine residue is essential for function and cannot be substituted by other aromatic residues such as phenylalanine, suggesting that the hydroxyl group is essential. The ϕ position can accommodate residues with a bulky hydrophobic side chain [39]. The identity of this residue can modify the specificity of the signal for the different AP complexes [39, 352, 296]. The identity of the x residues is variable but tends to be hydrophilic. The residues at position Y -1 as well as the identity of the x residues have a strong impact on lysosomal targeting. Most proteins directed to lysosomes have a glycine residue immediately prior to the tyrosine. Furthermore, acidic residues at the x positions tend to be present in lysosomal-sorting Yxxϕ motifs [153, 39, 352].

The amino acid sequence of the motif is not the only important prerequisite for protein sorting; the position of the motif in the cytosolic domain also has an influence. Tyrosine-based motifs involved in endocytosis are mostly

found at 10-40 residues from the transmembrane domains, but not at the C-termini of proteins. On the contrary, tyrosine-based motifs responsible for lysosomal targeting are mostly found either near the transmembrane domain (at 6-9 residues) or at the C-terminus of the cargo protein [39, 295].

Yxxϕ motifs on the cargo proteins are recognized by the μ subunit of the AP complexes [294]. The first crystal structure of an AP μ subunit was obtained with the AP-2 complex, but significant sequence homology exists between the μ subunits of the different complexes. Their structure and mechanism of binding are thus thought to be similar to what is observed with AP-2 [38]. The C-terminal domain of μ2 has an elongated, banana-shaped structure composed of a 16-strands β-sheet that is organized into two β-sandwich subdomains (A and B) (Figure 1.30). The Yxxϕ signal peptide binds to strands β1 and β16 of the A subdomain and forms a β-strand paired with β16 of μ2. Both the tyrosine and the ϕ residue bind into two hydrophobic pockets on the surface of μ2. The aromatic group of the tyrosine residue forms hydrophobic interactions with tryptophan and phenylalanine residues on the inside of the pocket and the hydroxyl group forms hydrogen bonds with aspartic acid, lysine, and arginine residues. The latter properties might explain why tyrosine to phenylalanine mutation only gives a poor binding of the motif with the μ subunit. The hydrophobic residue binding site is a pocket lined with aliphatic amino acids giving flexibility to the pocket to accommodate the residues at this position [39, 310].

Several Alphaherpesviruses glycoproteins have been shown to be endocytosed via tyrosine-based motifs in their cytoplasmic tails [109]. In VZV, gE, gB, and gH have been shown to have functional tyrosine-based motifs [109, 156, 158, 9, 307, 318]. The same has been found for HSV-1 and PRV gE [109, 10, 406], as well as for HSV-1, HSV-2 and PRV gB [109, 110, 105, 29].

1.7.2.2 Dileucine motifs

As it is the case for tyrosine-based motifs, dileucine motifs are found in a great variety of transmembrane proteins and play different functions, among which internalization as well as targeting to the endo-lysosomal compartments [39]. The consensus sequence of these motifs is [DE]xxxL[LI]. The first leucine is invariant, but the second can be replaced by an isoleucine or methionine [39, 358, 234]. The presence of an aspartic acid or glutamic acid residue at position -4 from the first leucine seems important for targeting to the late endosomes or lysosomes but is not required for internalization of the protein [39, 358, 331]. Interestingly, some dileucine motifs have arginine residues instead of acidic residues as it is the case for GLUT4 (RTPSLL sequence). It is thus possible that distinct motifs interact with different AP

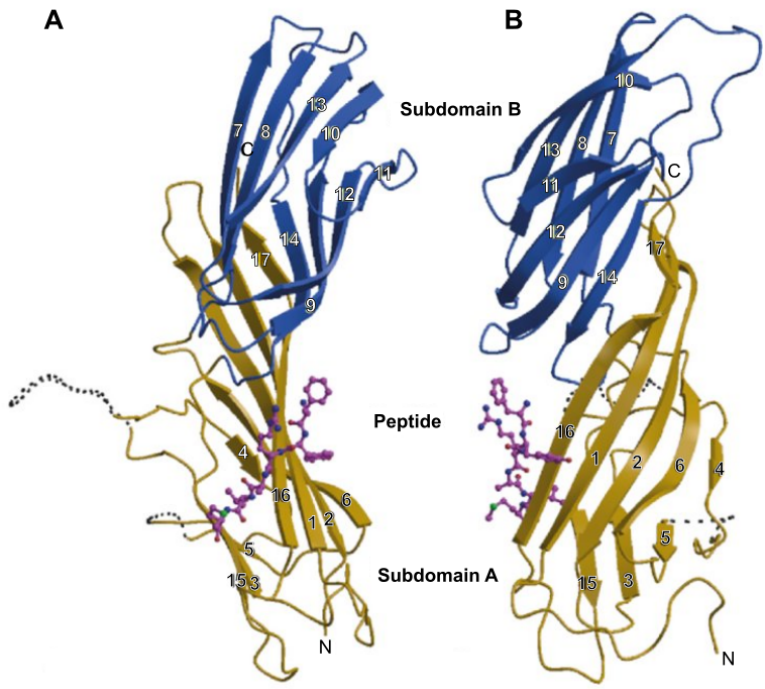

Figure 1.30: **Structure of the μ subunit from AP-2.** A and B, orthogonal views of μ2. The C-terminal domain of μ2 is composed of a 16-strands β-sheet forming two subdomains (subdomain A in gold, and subdomain B in blue). The bound peptide is shown in magenta. Figure from [310].

complexes at different sites [39, 358]. As for tyrosine-based motifs, the position of the dileucine motifs is important. Indeed, these motifs must be close to the transmembrane domain or near the carboxy terminus of a protein to be recognized for targeting towards late endosomes or lysosomes [39].

GST-pull down assays with hemi-complexes of AP-1 and AP-2 showed that dileucine motifs interact with the γ/σ1 hemi-complex of AP-1 and with the α/σ2 hemi-complex of AP-2 (Figure 1.31). Interestingly, the presence of an aspartate residue at position -4 from the first leucine in the motif compromised binding with the AP-1 hemi-complex while it had minimal impact in AP-2 hemi-complex binding. This confirms that distinct motifs can interact with different AP complexes [88]. Mutational and binding analyses showed that the dileucine recognition sites of AP-1, AP-2, and AP-3 were similar [256]. The resolution of the crystal structure of the AP-2 complex revealed how the binding with dileucine motifs occurs: the side chains of the two leucine residues bind in hydrophobic pockets on the surface of the σ2 subunit, whereas the acidic residues of the motif interact with basic

amino acids in the N-terminal regions of the $\sigma 2$ and α subunits [48, 198].

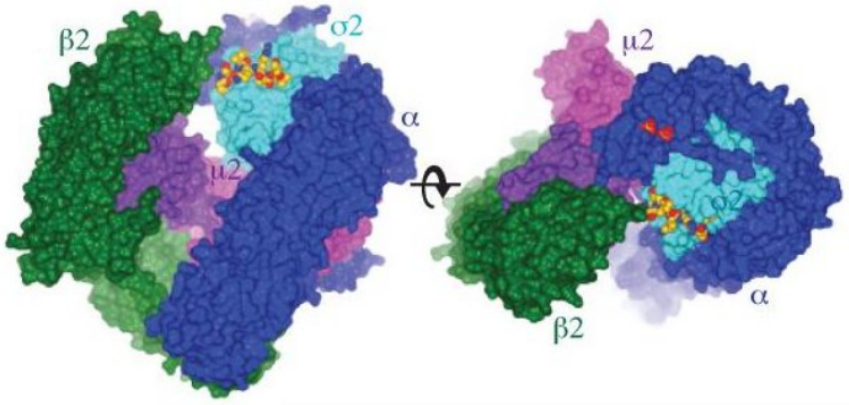

Figure 1.31: **Structure of the core domain of AP-2 in complex with the dileucine peptide from CD4.** The dileucine motif binding site is located in the $\alpha/\sigma 2$ hemicomplex of AP-2. The dileucine motif peptide is shown as spheres with carbons colored gold. Figure adapted from [198].

1.7.2.3 Acidic cluster motifs

Another common sorting motif consists of a cluster of acidic amino acids containing CKII phosphorylation sites. These motifs are usually found in proteins cycling between the TGN and endosomes [39]. The acidic cluster and the phosphorylation of the CKII sites are important for retrieval of the proteins from endosomes to the TGN [39, 189]. Initial studies indicated that a connector protein, PACS-1 (phosphofurin acidic cluster sorting protein 1), was required for protein sorting by interacting with the phosphorylated acidic cluster of the cargo protein, and connecting it to the AP-1 or AP-3 complex [39, 422, 69]. However, more recent studies identified the μ subunit of both AP-1 and AP-2 as contributing directly to the binding of phosphoserine acidic cluster. This binding is mediated by basic patches on the surface of the μ subunit of the AP complexes [374, 278].
It is possible that direct binding to the μ subunit of the AP complex or interaction with the connector PACS-1 play different roles in protein trafficking. It is also possible that binding to the μ subunit serves to strengthen the interaction with another trafficking motif (tyrosine-based or dileucine motif). Nonetheless, in both cases, the AP complex is required to insure the correct trafficking of the cargo protein.

1.7.2.4 Non-canonical motifs

Recently, a non-canonical motif was found in the cytoplasmic tail of L-selectin. It is formed by a triplet of di-basic amino acids (RRxKKxKK). This motif has been shown to allow interaction with the μ subunit of AP-1 by interaction with aspartate and glutamate residues on the surface of μ1, and formation of hydrogen bonds with asparagine and glutamine residues in μ1 [81].

1.7.3 AP-1 complex

1.7.3.1 Functions in post-Golgi and basolateral sorting

The two best characterized AP-1 isoforms are μ1A and μ1B, forming two distinct AP-1 complexes (AP-1A and AP-1B). In contrast with AP-1A, which is expressed ubiquitously, AP-1B is expressed in a subset of polarized cells [293, 146, 398]. Fölsch *et al.* showed in the early 2000s that AP-1A is localized at the TGN while AP-1B is localized at the recycling endosomes and so, they hypothesized that AP-1A functions in biosynthetic sorting at the TGN whereas AP-1B regulates the recycling of basolateral proteins from the endosomes [398, 116, 115]. However, more recent high-resolution microscopy studies revealed that both μ1A and μ1B colocalize to similar extent with TGN and recycling endosomes in polarized epithelial cells [146]. Moreover, knockdown studies revealed that single knockdown of AP-1A or AP-1B did not dramatically reduce the delivery of newly synthesized proteins from the TGN to the basolateral membrane, but double knockdown did, suggesting that AP-1A and AP-1B can compensate for each other to regulate the traffic of cargo proteins from the TGN [398, 139]. However, AP-1A knockdown increased the traffic of the transferrin receptor and LDLR from the TGN to the recycling endosomes, and knockdown of AP-1B significantly decreased the steady-state basolateral polarity of the transferrin receptor and LDLR. This suggests that AP-1A regulates the biosynthetic trafficking to the plasma membrane independently of the recycling endosomes, and AP-1B mediates the maintenance of basolateral polarity in epithelial cells [398, 139]. Interestingly, yeast two-hybrid studies revealed that some cargos interacted preferentially with μ1A or μ1B. Indeed, LDLR was shown to interact preferentially with AP-1B, and this interaction was mediated by a non-canonical tyrosine-based motif and an acidic cluster [146]. Thus, AP-1A and AP-1B have complementary but non-overlapping roles in protein sorting and maintaining basolateral polarity [398].

Apart from its role in epithelial polarized cells, AP-1 has also been shown to be important to regulate somatodendritic sorting and polarity in neurons [398, 145, 106, 94, 250, 236]. The importance of the AP-1 complex in

neurons is further supported by the existence of genetic disorders caused by mutations of the AP-1 σ subunit. The first mutation was identified in four families displaying a unique syndrome characterized by mental retardation, enteropathy, deafness, peripheral neuropathy, ichthyosis, and keratodermia (MEDNIK syndrome). This syndrome is due to a splice mutation in the *ap1s1* gene, coding the σ1A subunit, leading to a premature stop codon [270]. In addition, sequencing of the X chromosome of patients presenting mental retardation identified a mutation in the *ap1s2* gene, coding the σ1B subunit of AP-1. This syndrome is known as the Fried/Pettigrew syndrome [145, 401, 43]. These two syndromes probably result from a mislocalization of neuronal cargos that require the σ1A or σ1B subunit of AP-1 for their trafficking. It is yet unknown if the specific requirement for one or the other subunit results from a different signal-recognition specificity or the expression of the σ1 subunits in different neuronal populations [145].

1.7.3.2 Activation

AP-1 exists in two conformations: a closed conformation, representing a soluble, cytosolic form preventing premature association with the cargo protein and with clathrin, and an open conformation representing the membrane-associated AP-1 capable of cargo binding and clathrin association [27]. Activation of AP-1 is mediated by the small GTPase ADP ribosylation factor 1 (Arf1) (Figure 1.32) [339]. Recruitment of AP-1 to the TGN or endosome membrane is thought to be mediated by both Arf1 and phosphatidylinositol 4-phosphate (PI4P), which is enriched in TGN membranes [398]. Structural studies showed that AP-1 has three Arf1 binding sites: two of these sites are located in the N-terminus of each large subunit of AP-1 and are necessary for membrane association, while the third site is located in the back of the γ subunit [398]. The current model for the activation of AP-1 proposes that AP-1, in the closed conformation, is initially recruited to the TGN by two copies of Arf1. Once on the membrane, the presence of the cargo is thought to shift AP-1 to the opened state (Figure 1.32A). The high local concentration of AP-1 complexes then promotes dimerization via the formation of an Arf1 back-side contact, stabilizing the open form (Figure 1.32B) [339].

1.7.3.3 AP-1 complex and viruses

The AP-1 complex has been shown to be important for several viruses: in HIV, Vpu and Nef were shown to interact with AP-1 [185, 184, 431]. Nef has been shown to form a complex with MHC-I and AP-1 to disrupt MHC-I trafficking [431], while Vpu downregulates BST2/tetherin, an antiviral restriction factor inhibiting the release of enveloped viruses from the cell surface, to promote viral release [185]. AP-1 is also crucial for hepatitis C

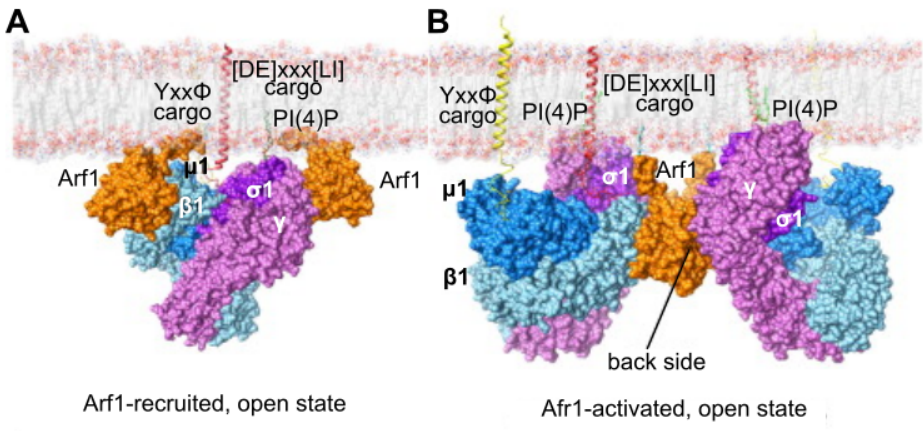

Figure 1.32: **Activation of AP-1 by Arf1.** A) A model of AP-1 recruited by two Arf1 molecules in cooperation with PI(4)P on a membrane. Cargo binding further stabilizes AP-1. B) Two AP-1 complexes dimerize via an Arf1 back-side contact stabilizing the open state. Figure adapted from [339].

virus (HCV) infections [30, 239, 436]. HCV nonstructural 2 (NS2) protein can interact with AP-1 via two dileucine motifs and this interaction mediates viral release [436]. Furthermore, the structural E2 protein of HCV also interacts with AP-1 and this interaction is required to protect E2 from proteasomal degradation [239]. In addition, AP-1 plays a role in African swine fever virus (ASFV) infections where the viral CD2v protein, involved in virulence enhancement, viral hemadsorption, and pathogenesis, has been shown to interact with AP-1. Unfortunately, the exact role of this interactions in ASFV infection is not known [321]. AP-1 has also been shown to be important for Dengue virus replication: siRNA knock-down of AP-1A reduced significantly viral RNA level and virion production compared with control siRNA. The authors of this study hypothesized that AP-1A may partly control DENV-induced membrane rearrangement required for viral replication [444]. Finally, in HHV-7-infected cells, both AP-1 and AP-3 have been shown to be required by the HHV-7 immunoevasin U21 to induce MHC Class I lysosomal degradation [202].

Part II

ORF9p and AP-1

2 Aim of the work

As described in section 1.6, ORF9p has been shown to interact with several other viral proteins and to play a role in viral envelopment and egress. To know if ORF9p may interact with cellular proteins that could be involved in viral envelopment, a yeast-two hybrid screen was performed by our laboratory before the start of this thesis. Thirty one cellular proteins were found as potential ORF9p interacting partners, among which the AP1M1 protein forming the μ subunit of the AP-1 complex.

The aim of this first part of the thesis was to confirm the ORF9p/AP-1 interaction and to identify the domain of ORF9p required for this interaction. First, we performed co-immunoprecipitation experiments in three different cell types to confirm the interaction in an infection context and to know whether or not it was cell type dependent. Then, we identified and mutated different potential interaction motifs within the sequence of ORF9p to identify which one was responsible for the ORF9p/AP-1 interaction. We also investigated if this interaction could be conserved within the *Alphaherpesviridae* via GST-pulldown comparing ORF9p to HSV-2 and MDV VP22. Finally, the impact of the loss of ORF9p/AP-1 interaction on viral replication was assessed *in vitro* as well as in a 3D skin model.

3 Results

3.1 ORF9p interacts with AP-1 in infected cells

A yeast-two hybrid screen previously performed in our laboratory found the cellular AP-1 complex as a potential interaction partner for ORF9p. This interaction was confirmed by GST-pull down before the start of this thesis. To confirm the interaction in an infectious context, we performed co-immunoprecipitation experiments from infected cells extracts using three cell lines frequently used for VZV production (MeWo, MRC-5, and ARPE-19). AT 48 h.p.i., cells were lyzed and the γ subunit of AP-1 was immunorpecipitated. Western blotting on the immunoprecipitated complex revealed the presence of both ORF9p and AP-1μ1 in the three cell lines (Figure 3.1).

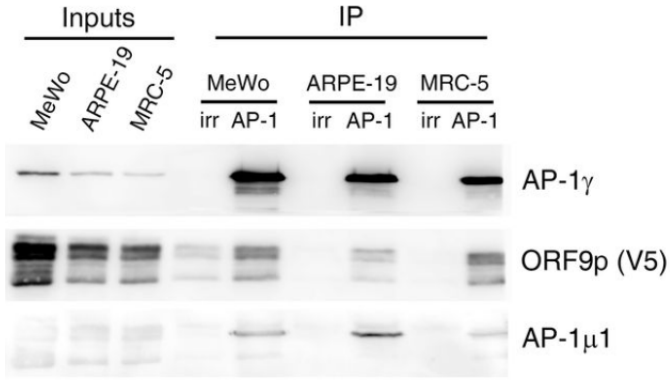

Figure 3.1: **ORF9p interacts with AP-1.** Co-immunoprecipitation of the ORF9p/AP-1 complex from VZV-ORF9-V5-infected MeWo, ARPE-19 and MRC-5 cells at 48 h.p.i. An antibody against AP-1γ was used for immunoprecipitation (IP), and the presence of ORF9p-V5, AP-1γ, and AP-1μ was verified by Western blotting. Normal mouse IgG was used as the IP control (irr).

3.2 ORF9p colocalizes with AP-1 in infected cells

Next, we studied the subcellular localization of ORF9p and AP-1 in MRC-5 and ARPE-19 cells. These cell lines were selected for immunofluorescence studies because, contrarily to MeWo cells, MRC-5 cells do not form syncytia and ARPE-19 cells fuse moderately upon VZV infection, thus facilitating colocalization analysis. Cells were infected with VZV-ORF9-V5 and fixed at 48 h.p.i. As seen in figure 3.2, a large amount of ORF9p colocalized with the

AP-1 complex in cytoplasmic structures close to the nucleus. This result is consistent with the ORF9p binding to AP-1 observed above.

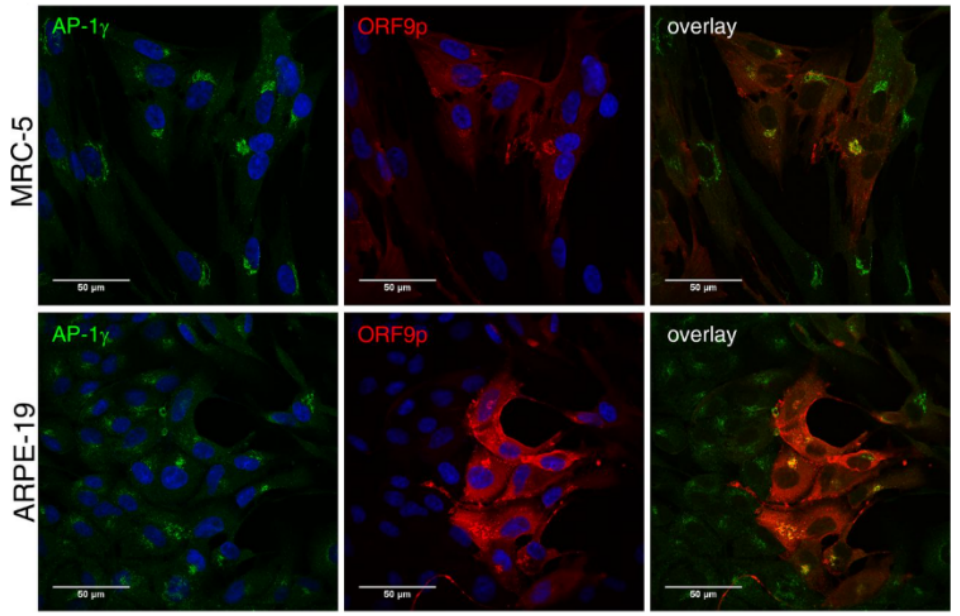

Figure 3.2: **ORF9p colocalizes with AP-1.** MRC-5 and ARPE-19 cells were infected with VZV-ORF9-V5 for 48h before fixation. Cells were then permeabilized and stained with mouse anti-V5 and rabbit anti-AP-1γ antibodies. Appropriate secondary antibodies were used, and nuclei were counterstained with TO-PRO-3. Images were recorded with a 63x oil objective. Scale bar represents 50 μm.

3.3 ORF9p residue leucine 231 is required for AP-1 interaction

As described in section 1.7.2 of the introduction, three main types of motifs are known to mediate the binding of cargo proteins to the AP-1 complex: tyrosine-based motifs, dileucine motifs, or acidic clusters. Analysis of the primary sequence of ORF9p revealed an acidic cluster (^{85}EDDFEDIDE^{93}), two tyrosine-based motifs (^{61}YADL^{64} and ^{268}YAQV^{271}), and two dileucine motifs (^{211}ELDRLL^{216} and ^{227}EGLNLI^{231}) (Figure 3.3A). We generated four VZV mutants in which the tyrosine-based or dileucine motifs were independently mutated. The VZV-ORF9p-ΔAC-V5 mutant, in which the acidic cluster is deleted, was already available [344]. We then tested the ORF9p/AP-1 interaction for each of these mutants. In the co-IP experiment, neither the deletion of the acidic region, nor the Y61G, Y268A, or L215A substitutions

had an impact on the ORF9p/AP-1 interaction (Figure 3.3B and C), while the L231A mutation completely abolished this interaction (Figure 3.3D). In addition, this L231A also abolished the colocalization between ORF9p and AP-1 that was observed with the VZV-ORF9-V5 virus (compare Figure 3.3E with Figure 3.2).

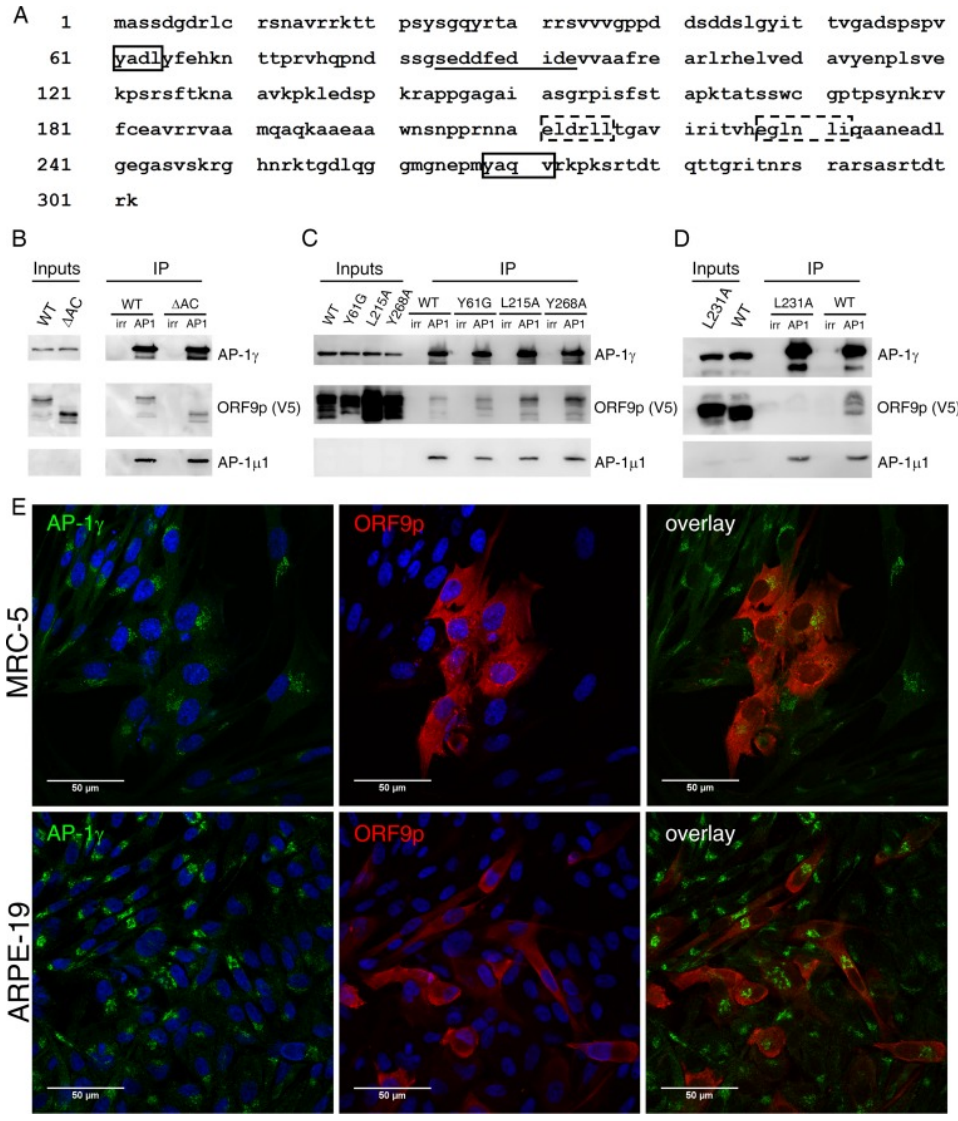

Figure 3.3: **ORF9p leucine 231 is important for the interaction between ORF9p and the AP-1 complex.** A) The primary sequence of ORF9p harbors several potential AP-1 interaction motifs: *(continued on next page)*

Figure 3.3 (previous page)*:* two tyrosine-based motifs (boxes with solid lines) and two dileucine motifs (boxed with dashed lines), as well as an acidic domain (underlined). B, C, D) The AP-1γ subunit was immunoprecipitated from total extracts of MeWo cells infected for 48h with VZV-ORF9-V5 (WT) (B, C and D), VZV-ORF9-ΔAC-V5 (B), VZV-ORF9-Y61G-V5, -L231A-V5, and -Y268A-V5 (C), and VZV-ORF9-L231A-V5 (D). A control immunoprecipitation with normal mouse IgG was performed in parallel (irr). The presence of ORF9p, AP-1γ, and AP-1μ in the immunoprecipitated complex was verified by Western blotting. AC, acidic region. E) MRC-5 and ARPE-19 cells were infected with VZV-ORF9-L231A-V5 for 48h and immunostained with a mouse anti-V5 and a rabbit anti-AP-1γ antibody. Appropriate secondary antibodies were used, and nuclei were counterstained with To-PRO-3. Images were recorded with a 63x oil objective. Scale bar represents 50 μm.

3.4 The dileucine motif important for ORF9p interaction with AP-1 is conserved among alphaherpesviruses

We then wanted to know if the ORF9p/AP-1 interaction identified with VZV could be conserved among Alphaherpesviruses. We first analyzed the primary sequences of ORF9p homologues to know if they also contained the interaction motifs found in ORF9p. Although the acidic domain of ORF9p, overlapping the ORF47p-binding site, is not strictly conserved among alphaherpesviruses, many VP22 homologs possess, in their N-terminal part, an acidic cluster downstream of serine residues (not shown). None of the above-described tyrosine-based motifs are conserved among alphaherpesviruses, even though HSV-1 harbors a motif that resembles the VZV ^{61}YADL^{64} motif, and a real tyrosine-based motif in an upstream region (^{18}YEDL^{22}) (not shown). However, both the ^{211}ELDRLL^{216} and ^{227}EGLNLI^{232} dileucine motifs were highly conserved among the 27 alphaherpesvirus genomes that we analyzed (Figure 3.4A). In particular, the glutamic acid as well as the first and second (iso)leucines of the ^{227}EGLNLI^{232} motif were conserved in almost all viruses (93%, 96%, and 78%, respectively) (Figure 3.4A). To verify whether the interaction with AP-1 is shared by other alphaherpesviruses, HSV-2 and MDV VP22 were cloned into pGEX 5.1. It is worth noting that while HSV-2 VP22 harbors a well-conserved dileucine motif (^{250}EGKNLL^{255}), the MDV VP22 motif (^{264}EGPNLM^{269}) is not perfectly conserved, with the second leucine being replaced by a methionine. The fusion proteins were purified on gluthathione agarose beads in parallel with GST alone as a control, and used in a GST pulldown assay in the presence of total cell extracts from uninfected MeWo cells. In both cases, the μ and γ subunits of AP-1 were detected, reflecting that ORF9p homologs can also

interact with this adaptor protein complex (Figure 3.4B).

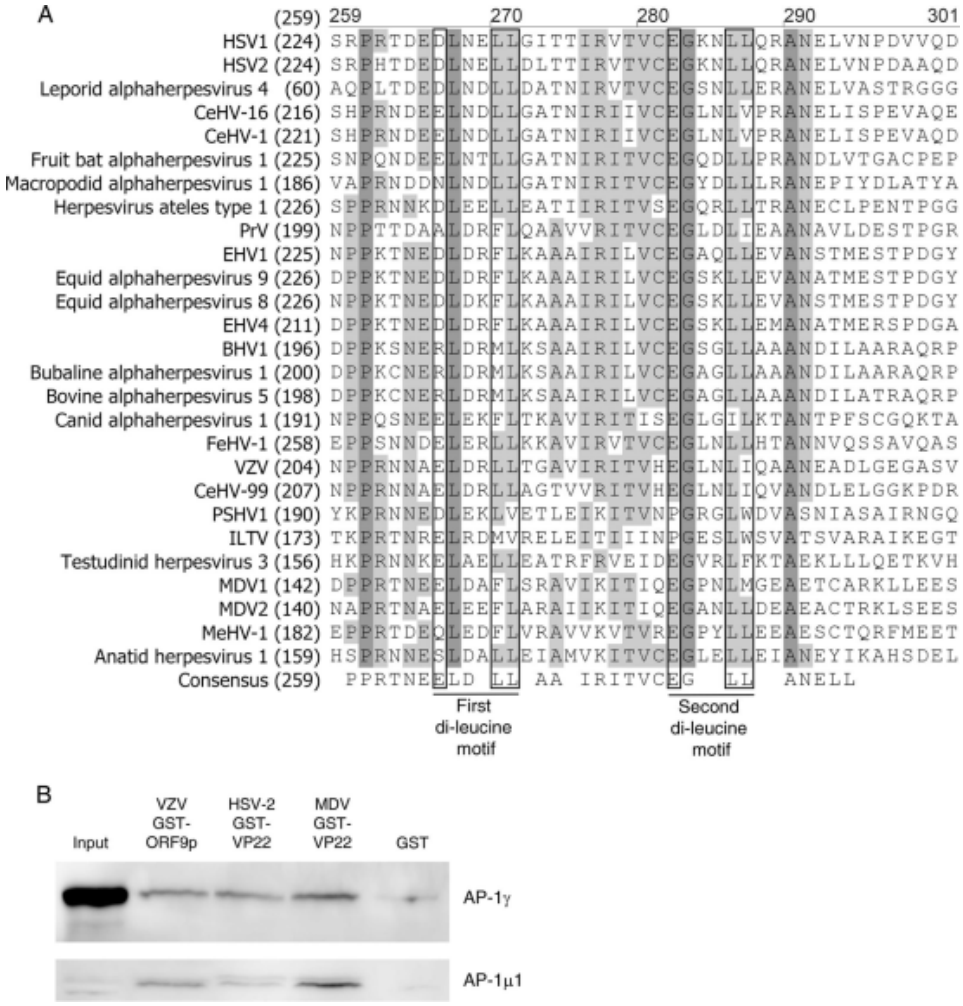

Figure 3.4: **The ORF9p (VP22) interaction with the AP-1 complex is conserved among alphaherpesviruses.** A) The primary sequences of 27 homologous VP22 proteins were aligned with the VectorNTi program (Invitrogen). Only the region containing the two dileucine motifs is shown. Dark gray, identical residues; light gray, similar residues. The first dileucine motif is relatively well conserved (present in 11 homologs); the second is highly conserved (present in 20 homologs). HSV-1, herpes simplex virus 1; CeHV-16, cercopithecine herpesvirus 16; PRV, pseudorabies virus; EHV1, equine herpesvirus 1; BHV1, bovine herpesvirus 1; FeHV-1, feline herpesvirus 1; PSHV1, psittacine herpesvirus 1; ILTV, infectious laryngotracheitis virus; MDV, Marek's disease herpesvirus 1; MeHV-1, meleagrid herpesvirus 1.

3.5 ORF9p leucine 231 is important for viral infectivity in culture

The infectivity of all mutants was determined in both MeWo (Figure 3.5A) and MRC-5 (Figure 3.5C) cells. The size of the infection foci in MeWo cells was assessed at 48 h.p.i. and showed that all mutants, except VZV-ORF9-Y268A-V5, present a slight to moderate defect in viral spread compared to the WT. However, the mutation of leucine 231 had the greatest impact on viral spread (Figure 3.5A). In MRC-5 cells, minor to moderate differences in the replication properties of VZV-ORF9-Y61G-V5, -L231A-V5, and -Y268A-V5 were observed, while the infectivity of VZV-ORF9-L231A-V5 was severely impaired, with the number of plaque forming units (PFU) at 72 h.p.i. being more than five times lower than the number of PFU obtained with the VZV-ORF9-V5 (Figure 3.5C). To confirm that the replication defect of the L231A mutant was solely due to the leucine mutation, a revertant virus (VZV-ORF9-L231A-rev-V5) was generated by reintroducing the Wild-type *orf9* instead of the mutant copy into VZV-ORF9-L231A-V5. The infectivity of the revertant in MeWo and MRC-5 cells was then compared to that of VZV-ORF9-V5. No major differences could be observed between the two viral strains, demonstrating that the replication defect of the VZV-ORF9-L231A-V5 is attributable only to the leucine 231 mutation (Figure 3.5B and D). In addition, the revertant virus restored the colocalization of ORF9p and AP-1 in both MRC-5 and ARPE-19 cells (not shown).

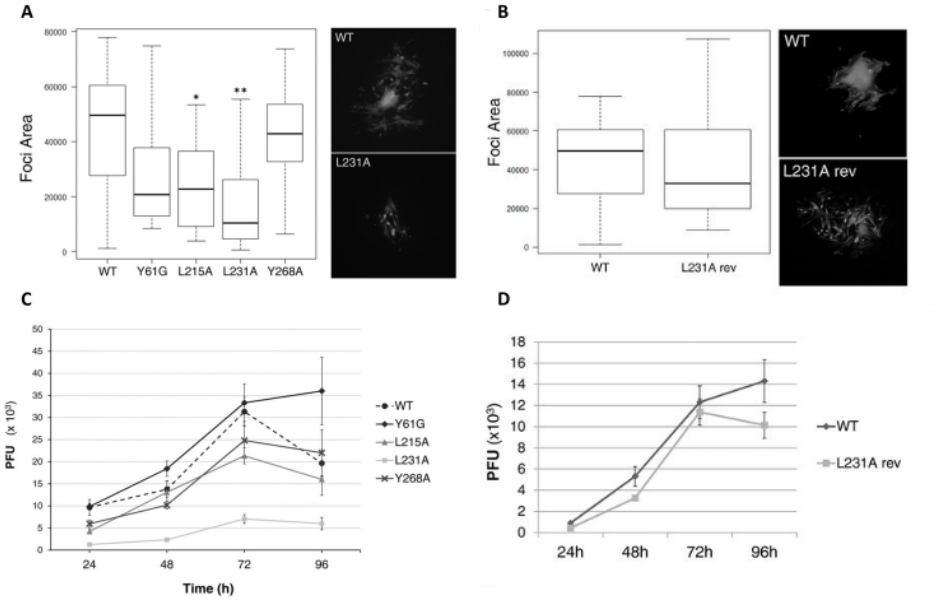

Figure 3.5: **The L231A mutation strongly impacts infectivity in MeWo and MRC-5 cells.** VZV-ORF9-V5 (WT) and mutant strain infectivity was assessed in MeWo (A and B) or MRC-5 (C and D) cells. A and B) Infection foci measurement at 48 h.p.i. MeWo cells were infected for 48h and size of the infection foci was determined using CellProfiler software and expressed as the number of pixels present in each infection focus. The box plot depicts the 1st and 3rd quantiles (the lower and upper limits of the boxes, respectively) and the median (heavy black lines). Error bars represent minimum and maximum values. A two-tailed *t* test was used to compare, at each time point, each mutant to the WT. *, P<0.05; **, P<0.01. C and D) Replication curves in MRC-5 cells. The graph shows the result of one representative experiment out of four; error bars represent the standard error of the mean (SEM).

These results are part of an article published in Journal of Virology in 2018.

AMERICAN SOCIETY FOR MICROBIOLOGY | Journal of Virology®

VIRUS-CELL INTERACTIONS

Varicella-Zoster Virus ORF9p Binding to Cellular Adaptor Protein Complex 1 Is Important for Viral Infectivity

Marielle Lebrun,[a] Julien Lambert,[a] Laura Riva,[a]* Nicolas Thelen,[b] Xavier Rambout,[c]* Caroline Blondeau,[a] Marc Thiry,[b] Robert Snoeck,[d] Jean-Claude Twizere,[c] Franck Dequiedt,[c] Graciela Andrei,[d] Catherine Sadzot-Delvaux[a]

[a]Virology and Immunology Unit, GIGA-Infection, Immunity and Inflammation, University of Liege, Liege, Belgium

[b]Cellular Biology Unit, GIGA-Neurosciences, University of Liege, Liege, Belgium

[c]Protein Signaling and Interactions Laboratory, GIGA-Molecular Biology of Diseases, University of Liege, Liege, Belgium

[d]Rega Institute, KUL, Leuven, Belgium

ABSTRACT ORF9p (homologous to herpes simplex virus 1 [HSV-1] VP22) is a varicella-zoster virus (VZV) tegument protein essential for viral replication. Even though its precise functions are far from being fully described, a role in the secondary envelopment of the virus has long been suggested. We performed a yeast two-hybrid screen to identify cellular proteins interacting with ORF9p that might be important for this function. We found 31 ORF9p interaction partners, among which was AP1M1, the μ subunit of the adaptor protein complex 1 (AP-1). AP-1 is a heterotetramer involved in intracellular vesicle-mediated transport and regulates the shuttling of cargo proteins between endosomes and the *trans*-Golgi network via clathrin-coated vesicles. We confirmed that AP-1 interacts with ORF9p in infected cells and mapped potential interaction motifs within ORF9p. We generated VZV mutants in which each of these motifs was individually impaired and identified leucine 231 in ORF9p to be critical for the interaction with AP-1. Disrupting ORF9p binding to AP-1 by mutating leucine 231 to alanine in ORF9p strongly impaired viral growth, most likely by preventing efficient secondary envelopment of the virus. Leucine 231 is part of a dileucine motif conserved among alphaherpesviruses, and we showed that VP22 of Marek's disease virus and HSV-2 also interacts with AP-1. This indicates that the function of this interaction in secondary envelopment might be conserved as well.

IMPORTANCE Herpesviruses are responsible for infections that, especially in immunocompromised patients, can lead to severe complications, including neurological symptoms and strokes. The constant emergence of viral strains resistant to classical antivirals (mainly acyclovir and its derivatives) pleads for the identification of new targets for future antiviral treatments. Cellular adaptor protein (AP) complexes have been implicated in the correct addressing of herpesvirus glycoproteins in infected cells, and the discovery that a major constituent of the varicella-zoster virus tegument interacts with AP-1 reveals a previously unsuspected role of this tegument protein. Unraveling the complex mechanisms leading to virion production will certainly be an important step in the discovery of future therapeutic targets.

KEYWORDS adaptin, ORF9p, VP22, adaptor proteins, dileucine, herpesviruses, secondary envelopment, tegument, varicella-zoster virus, viral assembly

All viruses are cellular parasites and subvert the host machinery to replicate and/or to interfere with cellular pathways. Herpesviruses, with their complex infectious cycle, do not escape this rule and use subcellular trafficking pathways to assemble and generate new virions.

Received 22 February 2018 **Accepted** 14 May 2018

Accepted manuscript posted online 23 May 2018

Citation Lebrun M, Lambert J, Riva L, Thelen N, Rambout X, Blondeau C, Thiry M, Snoeck R, Twizere J-C, Dequiedt F, Andrei G, Sadzot-Delvaux C. 2018. Varicella-zoster virus ORF9p binding to cellular adaptor protein complex 1 is important for viral infectivity. J Virol 92:e00295-18. https://doi.org/10.1128/JVI.00295-18.

Editor Rozanne M. Sandri-Goldin, University of California, Irvine

Address correspondence to Catherine Sadzot-Delvaux, csadzot@ulg.ac.be.

* Present address: Laura Riva, Immunity and Pathogenesis Program, Infectious and Inflammatory Diseases Center, Sanford Burnham Prebys Medical Discovery Institute, La Jolla, California, USA; Xavier Rambout, Center for RNA Biology, Department of Biochemistry and Biophysics, School of Medicine and Dentistry, University of Rochester, Rochester, New York, USA.

M.L., J.L., and L.R. contributed equally to this article.

Varicella-zoster virus (VZV) is a human alphaherpesvirus responsible for two pathologies. Primary infection generally occurs during childhood and leads to varicella, whose symptomatic phase is characterized by a generalized cutaneous rash during which the virus establishes a latent infection in sensory ganglia. When the host immune response is impaired or decreased, the virus may reactivate and reach back to the skin, where it causes a localized cutaneous rash usually associated with pain, known as zoster.

Herpesvirus particles are made of a nucleocapsid containing the DNA genome, surrounded by the tegument, a complex protein layer. The tegument is contained in a lipid envelope, in which is inserted a series of viral glycoproteins mediating viral entry into the host cell. Capsids are assembled in the nucleus, where they acquire a viral genome copy before crossing the nuclear envelope to reach the cytoplasm, where a secondary envelopment takes place. Therefore, the definitive envelope results from a very complex process of acquisition of a primary envelope at the inner nuclear membrane, deenvelopment at the outer nuclear membrane, and reenvelopment in association with intracellular membranes (1). While *trans*-Golgi network (TGN)-derived vesicles were long thought to be the site of the secondary envelopment, more recent data have challenged this old dogma (2, 3). The labeling of endocytic tubules freshly retrieved from the cell surface has shown many herpes simplex virus 1 (HSV-1) capsids budding through these labeled vesicles and demonstrated that endocytosis from the plasma membrane into endocytic tubules could actually provide the viral envelope (4). This idea is further strengthened by some old but also new data demonstrating the importance of endocytosis for the correct cellular targeting and virion incorporation of some herpesvirus glycoproteins (5–8).

VZV ORF9p, homologous to HSV-1 VP22, is a major tegument phosphoprotein conserved among the alphaherpesviruses. It is one of the most abundant tegument proteins, with a high number of copies being embedded in each virion (9, 10). HSV VP22 has been shown to shuttle between the nucleus and the cytoplasm and to play various roles in infected cells. In particular, it is required for the cytoplasmic redistribution of some proteins, among which are VP16, ICP4, ICP27, and ICP0 (11), and has been shown to directly interact with VP16, ICP0, gE, gM, and gD (12). Thanks to its interaction with gE, VP22 can be recruited to the Golgi apparatus/*trans*-Golgi network. The deletion of the C-terminal part of VP22, which is responsible for its interaction with gE, impairs its recruitment into the complexes described above and its packaging into virions, leading to poor growth in epithelial cells. These observations suggest a role in viral assembly (13). The deletion of *UL49*, coding for VP22 in pseudorabies virus (PRV), has only a minor impact on viral growth (14, 15), whereas in HSV-1, the lack of VP22 is rapidly compensated for by mutations in *UL41* (16–18). However, HSV-1 null mutants replicate less efficiently and do not accumulate at the cell surface, and the absence of VP22 affects the virion composition and indirectly modulates viral fitness (19–21).

VZV ORF9p has been less characterized, but contrary to HSV-1 or PRV VP22, it has been shown to be essential (22, 23). In transfected cells, it shuttles between the nucleus and the cytoplasm, and in infected cells, it partially localizes to the endomembrane network, including the TGN (22, 24). In infected cells, ORF9p interacts with the major glycoprotein gE and the major transactivator IE62, and mutation of the ORF9p interaction motif in IE62 has a strong impact on viral growth (25–27). In yeast two-hybrid (Y2H) experiments, ORF9p has been shown to interact with many other viral proteins, including glycoproteins, tegument proteins, and capsid proteins (28, 29). Recently, we have also shown that ORF9p interacts with and is phosphorylated by ORF47p, one of the two VZV protein kinases, and that this phosphorylation is crucial for both nuclear egress and secondary envelopment (30, 31). All these observations suggest that ORF9p, like VP22, could be central in viral assembly and particularly in orchestrating the secondary envelopment process.

Cellular adaptor protein (adaptin or AP) complexes are heterotetramers important for the intracellular trafficking of membrane-bound proteins. Five AP complexes have been described so far (32, 33). Both AP-1 and AP-2 bind to clathrin and are involved in clathrin-dependent transport, whereas AP-3, even though it is able to interact with

clathrin, together with AP-4 and AP-5, mediates clathrin-independent transport (34, 35). The AP-1 complex is specifically implicated in the vesicular transport between endosomes and the TGN (36). Like all AP family members, it is composed of two large subunits (γ and β1), one medium subunit (μ1), and one small subunit (σ1). It is recruited from the cytosol by its cargo and allows subsequent binding to clathrin, followed by membrane curvature and vesicle formation (33, 37).

To dissect more precisely the role of ORF9p in the VZV infectious cycle, we searched for new cellular partners through a Y2H screen and identified 31 distinct candidates, among which was AP1M1, the μ subunit of the adaptor protein complex 1 (AP-1μ1), known to play a role in protein trafficking. The interaction between AP-1μ1 and VZV ORF9p was confirmed *in vitro* by glutathione *S*-transferase (GST) pulldown as well as by coimmunoprecipitation (co-IP) using infected cell extracts. We identified five potential interaction motifs (one acidic region, two tyrosine-based motifs, and two dileucine motifs) within the ORF9p primary sequence. Viruses were generated by mutation of these potential interaction motifs within the *orf9* coding sequence in the pOka genome. The characterization of these mutants revealed that the mutation of leucine 231, which is conserved among alphaherpesviruses, completely abolishes the interaction between ORF9p and the AP-1 complex and strongly impairs the infectivity of the virus. In cells infected with this mutant strain, only a limited number of viral particles were found at the cell surface, transport vesicles containing complete virions or light particles were very rare compared to their occurrence in wild-type (WT) VZV-infected cells, and abnormal features were observed by electron microscopy. This suggests that, in the absence of an ORF9p/AP-1 interaction, the viral components are not properly addressed within the cell and/or that virions could be somehow retargeted for degradation by either the lysosomal or the autophagy pathway, or by both pathways.

To our knowledge, this is the first time that an interaction between a herpesvirus tegument protein and the AP-1 complex has been described, and altogether, our results suggest that this interaction is important for the formation of infectious viral particles and, thus, VZV pathogenicity.

RESULTS

ORF9p interacts with the adaptor protein complex 1. In order to identify cellular partners for ORF9p, we performed a yeast two-hybrid (Y2H) screen against the human ORFeome version 5.1 (hORFeome 5.1). Thirty-one distinct candidates were identified by sequencing clones growing on the selection medium. These interactions were then verified in a pairwise retest. For this experiment, not only the full-length ORF9p but also N-terminal ORF9p deletion mutants (ORF9p amino acids [aa] 50 to 302, 100 to 302, and 150 to 302) and C-terminal deletion mutants (ORF9p aa 1 to 250, 1 to 200, and 1 to 150) were used as baits. Based on the literature, four additional proteins interacting with HSV-1 VP22, namely, SET, ANP32B, HIST1H4I, and HIST1H3E, were included as positive controls. All 31 candidates and the four controls were found to be positive in the Y2H pairwise retest. Fifteen were found to be positive in both orientations (Gal4-activation domain ORF9p [AD-ORF9p] with the Gal4 DNA binding domain candidate [DB-candidate] and DB-ORF9p with the AD-candidate) and are highlighted in bold in Fig. 1A. All interactions were maintained when the 50 first amino acids (aa 50 to 302 construct) or the 50 last amino acids (aa 1 to 250 construct) of ORF9p were deleted but lost with larger deletions (aa 100 to 302, 150 to 302, 1 to 200, and 1 to 150), suggesting that the region of interaction is likely located between amino acids 50 and 250 of ORF9p (data not shown).

We performed gene ontology enrichment analyses using both the DAVID (38) and TOPPGENE (39) platforms to classify the Y2H-identified interaction partners based on their cellular functions (Fig. 1A and B). Interestingly, 12 interaction partners were involved in organelle organization, a process that is certainly required for the infectious cycle and, more precisely, for viral assembly. Among them, we focused on AP1M1, the μ subunit of adaptor protein complex 1 (AP-1), which mediates the bidirectional transport between TGN and endosomes (32). The interaction between ORF9p and AP-1

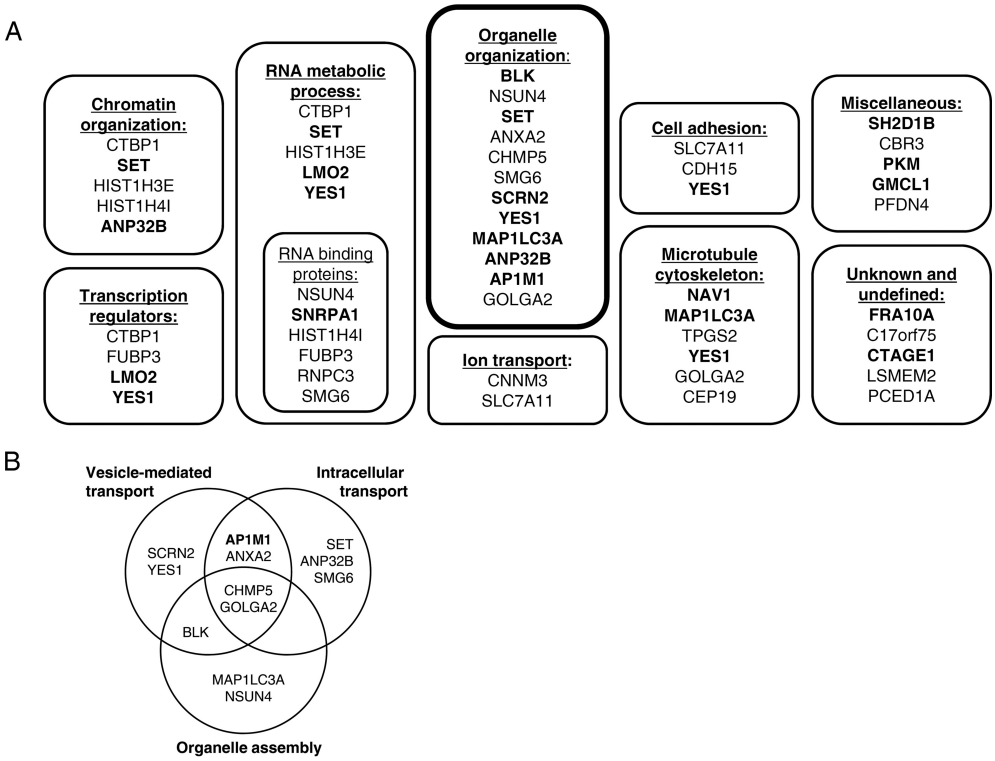

FIG 1 ORF9p interacts with cellular proteins involved in various processes. A yeast two-hybrid screen against human ORFeome 5.1 was performed and identified 31 potential cellular partners of ORF9p. The 31 candidates, along with 4 controls (SET, ANP32N, HIST1H4I, HIST1H3E) known to interact with VP22, were then confirmed in a pairwise retest and classified based on a Gene Ontology analysis. (A) Interactions confirmed in both directions in the retest are highlighted in bold. (B) Twelve out of the 35 interacting proteins are involved in the organelle organization category, which can be subdivided into several subclasses.

was first confirmed by a GST pulldown assay in which an ORF9p-GST fusion protein or GST alone was incubated with total cell extracts from uninfected or pOka VZV-infected MeWo cells. Both AP-1 subunits were pulled down from uninfected and infected cell extracts (Fig. 2A). To confirm the ORF9p/AP-1 interaction in an infectious context, we performed coimmunoprecipitation (co-IP) experiments from infected cell extracts. Because there was no antibody against the μ subunit suitable for immunoprecipitation (IP), the AP-1 complex was immunoprecipitated via the γ subunit from infected MeWo, ARPE-19, and MRC-5 cells (at 48 h postinfection [hpi]), three cell lines frequently used for VZV production. VZV-ORF9-V5 (pOka genomic background), expressing ORF9p fused to a V5 epitope, was used as the wild-type (WT) strain. This virus has been previously characterized and replicates with the same efficacy as the wild-type pOka control (30). Western blotting on the immunoprecipitated complex revealed the presence of both ORF9p and AP-1μ1 in the three cell lines (Fig. 2B). We next studied the subcellular localization of ORF9p and AP-1 in MRC-5 and ARPE-19 cells. Contrary to MeWo cells, MRC-5 cells do not form syncytia and ARPE-19 cells fuse moderately upon VZV infection, facilitating immunofluorescence colocalization analyses. MRC-5 and ARPE-19 cells were infected with VZV-ORF9-V5 and fixed at 48 hpi. Consistent with ORF9p binding to AP-1, a substantial amount of ORF9p colocalized with the AP-1 complex in cytoplasmic structures close to the nucleus (Fig. 2C).

ORF9p leucine 231 is important for ORF9p interaction with the AP-1 complex. Three types of motifs are known to mediate the binding of cargo proteins to the AP-1

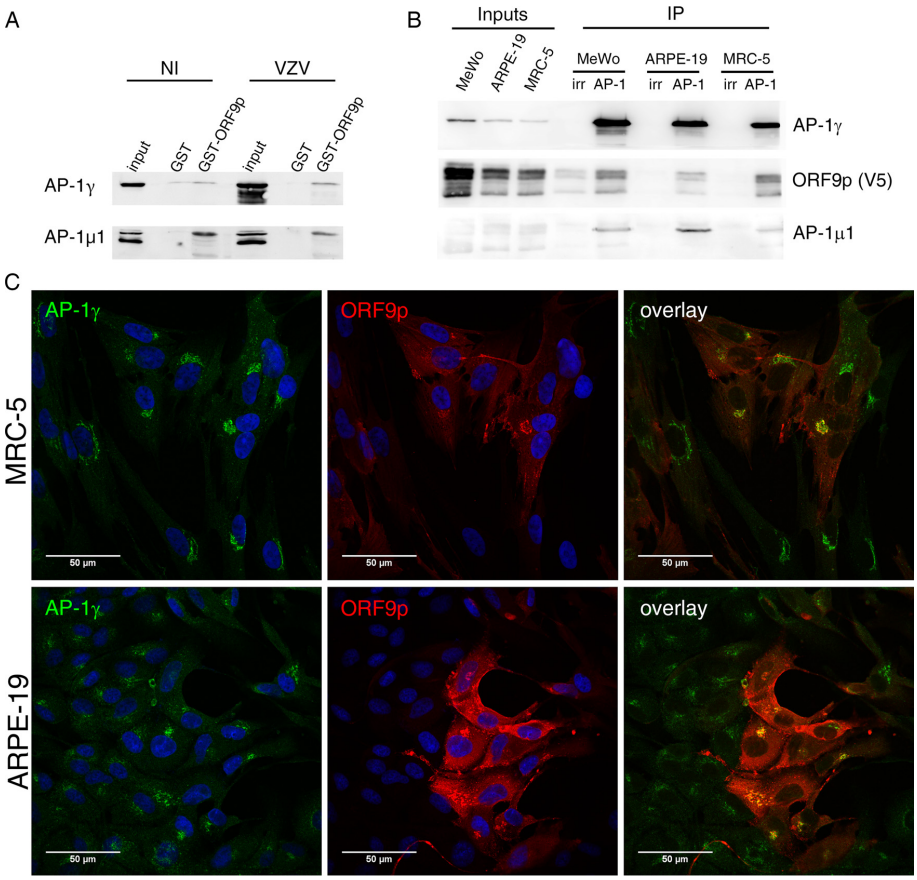

FIG 2 ORF9p interacts and colocalizes with the AP-1 complex. (A) The interaction of ORF9p and the AP-1 complex was verified by GST pulldown using ORF9p-GST and total extracts of MeWo cells infected or not infected by pOka VZV. NI, noninfected. (B) Coimmunoprecipitation of the ORF9p/AP-1 complex from VZV-ORF9-V5 (WT)-infected MeWo, ARPE-19, and MRC-5 cells (48 hpi). An antibody against AP-1γ was used for immunoprecipitation, and the presence of ORF9p-V5, AP-1γ, and AP-1μ1 was verified by Western blotting. Normal mouse IgG was used as the IP control (irr). (C) MRC-5 and ARPE-19 cells were infected with VZV-ORF9-V5 for 48 h and immunostained with a mouse anti-V5 and a rabbit anti-AP-1γ. Appropriate secondary antibodies were used, and nuclei were counterstained with TO-PRO-3. Images were recorded with a 63× oil objective.

complex: acidic clusters, tyrosine-based motifs (NPXY or YXXΦ), and dileucine motifs [(D/E)XXXL(L/I)] (40). ORF9p primary sequence analysis revealed an acidic cluster (^{85}EDDFEDIDE^{93}), two tyrosine-based motifs (^{61}YADL^{64} and ^{268}YAQV^{271}), and two dileucine motifs (^{211}ELDRLL^{216} and ^{227}EGLNLI^{232}) (Fig. 3A), all of which were found between amino acids 50 and 250, a region that we showed to be required for binding to AP-1μ1. The VZV-ORF9p-ΔAC-V5 strain, in which the acidic region is deleted, was already available (31). We generated four additional VZV mutants in which the tyrosine-based or the dileucine motifs were independently mutated.

In the co-IP experiment, neither the deletion of the acidic region nor the mutation of tyrosine 61 to glycine or tyrosine 268 and leucine 215 to alanine had an impact on the interaction between ORF9p and the AP-1 complex (Fig. 3B and C), while the mutation of leucine 231 to alanine completely abolished this interaction (Fig. 3D). In addition, ORF9p did not colocalize with AP-1 in MRC-5 or ARPE-19 cells infected with VZV-ORF9-L231A-V5 (compare Fig. 3E to Fig. 2C).

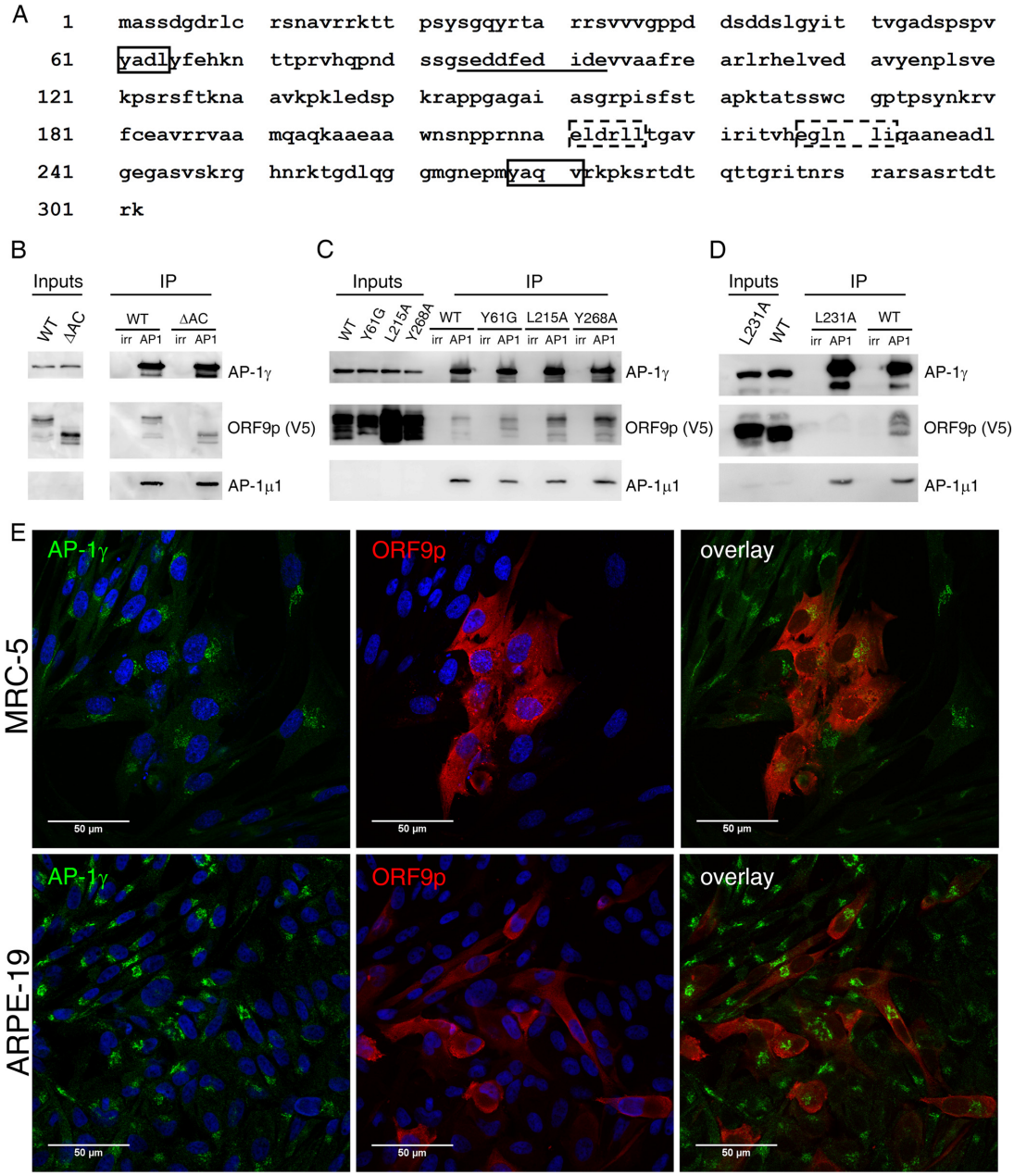

FIG 3 ORF9p leucine 231 is important for ORF9p interaction with the AP-1 complex. (A) The ORF9p primary sequence harbors several potential AP-1 interaction motifs, two tyrosine-based motifs (boxes with solid lines) and two dileucine motifs (boxes with dashed lines), as well as an acidic domain (underlined). (B, C, D) The AP-1γ subunit was immunoprecipitated from total extracts of MeWo cells infected for 48 h by VZV-ORF9-V5 (WT) (B, C and D), VZV-ORF9-ΔAC-V5 (B), VZV-ORF9-Y61G-V5, -L215A-V5, and-Y268A-V5 (C), and VZV-ORF9-L231A-V5 (D). A control immunoprecipitation with normal mouse IgG was performed in parallel (irr). The presence of ORF9p, AP-1γ, and AP-1μ1 in the immunoprecipitated complex was verified by Western blotting. AC, acidic region. (E) MRC-5 and ARPE-19 cells were infected with VZV-ORF9-L231A-V5 for 48 h and immunostained with a mouse anti-V5 and a rabbit anti-AP-1γ. Appropriate secondary antibodies were used, and nuclei were counterstained with TO-PRO-3. Images were recorded with a 63× oil objective.

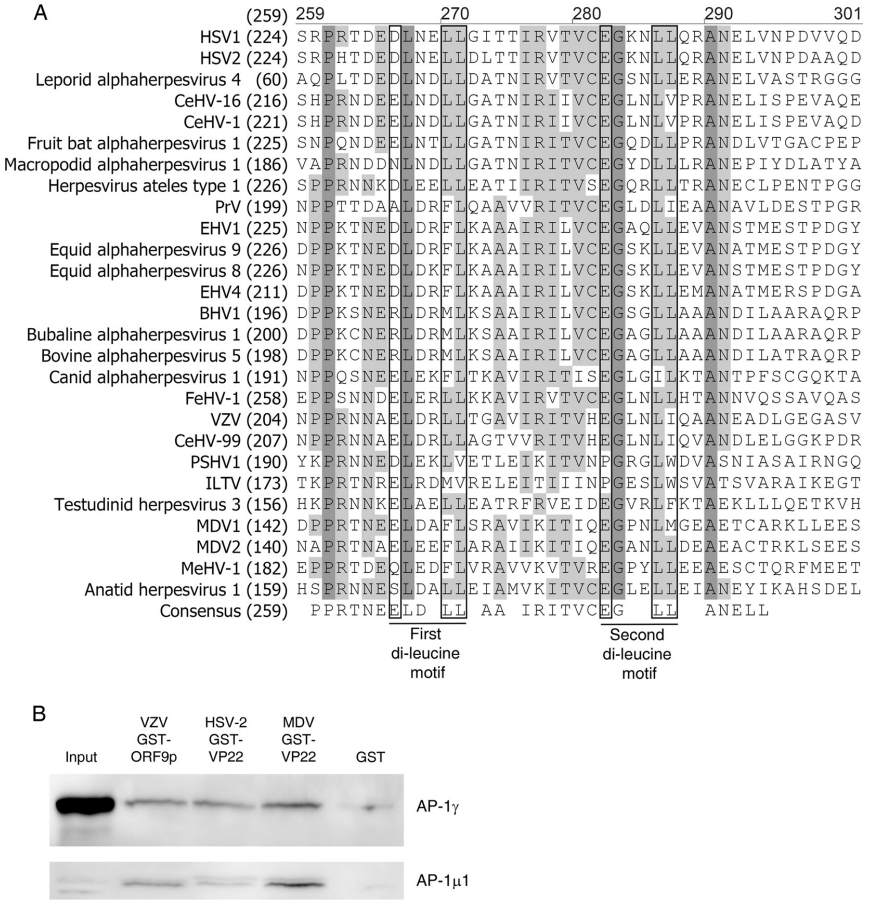

FIG 4 The ORF9p (VP22) interaction with the AP-1 complex is conserved among alphaherpesviruses. (A) The primary sequences of 27 homologous VP22 proteins were aligned with the Vector NTi program (Invitrogen). Only the region containing the two dileucine motifs is shown. Dark gray, identical residues; light gray, similar residues. The first dileucine motif is relatively well conserved (present in 11 homologs); the second is highly conserved (present in 20 homologs). HSV-1, herpes simplex virus 1; CeHV-16, cercopithecine herpesvirus 16; PrV, pseudorabies virus; EHV1, equine herpesvirus 1; BHV1, bovine herpesvirus 1; FeHV-1, feline herpesvirus 1; PSHV1, psittacine herpesvirus 1; ILTV, infectious laryngotracheitis virus; MDV1, Marek's disease herpesvirus 1; MeHV-1, meleagrid herpesvirus 1. (B) The VZV ORF9p homolog (HSV-2 or MDV VP22) interaction with the AP-1γ and μ1 subunits was analyzed by GST pulldown using the GST-ORF9p or GST-VP22 fusion protein and MeWo cell total cell extracts.

The dileucine motif important for ORF9p interaction with AP-1 is conserved among alphaherpesviruses. Although the ORF9p acidic region, which overlaps the ORF47p-binding site, is not strictly conserved among alphaherpesviruses, many VP22 homologs possess, in their N-terminal part, an acidic cluster downstream of serine residues. None of the above-described tyrosine-based motifs are conserved among alphaherpesviruses, even though HSV-1 harbors a motif that resembles the VZV ^{61}YADL^{64} motif and a real tyrosine-based motif in an upstream region (^{18}YEDL^{22}). However, both the ^{211}ELDRLL^{216} and ^{227}EGLNLI^{232} dileucine motifs were highly conserved among the 27 alphaherpesvirus genomes that we analyzed (Fig. 4A). In particular, the glutamic acid as well as the first and second (iso)leucines of the ^{227}EGLNLI^{232} motif were conserved in almost all viruses (93%, 96%, and 78%, respectively) (Fig. 4A). To verify whether the interaction with AP-1 is shared by other alphaherpesviruses,

HSV-2 and Marek's disease herpesvirus (MDV) VP22 was cloned into pGEX 5.1. It is worth noting that while HSV-2 VP22 harbors a well-conserved dileucine motif (^{250}EGKNLL^{255}), the MDV VP22 motif (^{264}EGPNLM^{269}) is not perfectly conserved, with the second leucine being replaced by a methionine. The fusion proteins were purified on glutathione agarose beads in parallel with GST alone as a control and used in a GST pulldown assay in the presence of total cell extracts from uninfected MeWo cells. In both cases, the μ1 and γ subunits of the AP-1 complex were detected, reflecting that ORF9p homologs can also interact with this adaptor protein complex (Fig. 4B).

ORF9p leucine 231 is important for viral infectivity in both MeWo and MRC-5 cells. The infectivity of all mutants was determined in both MeWo cells (Fig. 5A and B) and MRC-5 cells (Fig. 5C to E). The size of the infection foci in MeWo cells was assessed at 48 hpi and showed that all mutants, except VZV-ORF9-Y268A-V5, present a slight to moderate growth defect compared to the WT strain. However, the mutation of leucine 231 had the greatest impact on viral growth (Fig. 5A). In parallel, a known number of individual infected cells was used to infect MeWo cells seeded in a 24-well plate, and the number of infection foci was determined at 72 hpi. The number of infection foci present in the well corresponds to the number of infectious cells present in the inoculum. The mean ratio of infectious cells/infected cells was significantly reduced for VZV-ORF9-L231A-V5 compared to the wild type or the other mutant strains (less than 10% compared to 30 to 40% in Fig. 5B). This suggests that the entry and maybe the expression of viral genes are not affected by the L231A mutation, while the production and/or egress of the progeny virion might be affected.

In MRC-5 cells, minor to moderate differences in the growth properties of VZV-ORF9-Y61G-V5, -L215A-V5, and -Y286A-V5 were observed, while the infectivity of VZV-ORF9-L231A-V5 was severely impaired, with the number of PFU at 72 hpi being more than five times lower than the number of VZV-ORF9-V5 PFU (Fig. 5C). To get additional information regarding the different steps of the infectious cycle that may be impacted by the mutation, MRC-5 cell RNA and genomic DNA were extracted at each time point to determine the expression level of the three classes of viral genes, i.e., immediate early (IE; *orf4*), early (E; *orf47*), and late (L; *orf40*) genes, and the amount of viral genomic DNA. The amount of viral genomes was expressed per nanogram of total DNA (Fig. 5D), and RNA levels were normalized to the 18S rRNA level and expressed as a fold induction relative to that in the VZV-ORF9-V5-infected cells at 24 hpi (Fig. 5E). Both analyses confirmed a global growth defect of the VZV-ORF9-L231A-V5 mutant, although a slight decrease in IE, E, and L gene expression was also observed for VZV-ORF9-Y61G-V5, -Y268A-V5, and -L215-V5 (Fig. 5E).

To confirm that the growth defect of the L231A mutant was solely due to the leucine mutation, a revertant virus (VZV-ORF9-L231A-rev-V5) was generated by reintroducing the wild-type *orf9* instead of the mutant copy into VZV-ORF9-L231A-V5. The infectivity of VZV-ORF9-L231A-rev-V5 in MeWo and MRC-5 cells was then compared to that of VZV-ORF9-V5. No major differences could be observed between the two viral strains, demonstrating that the growth defect of VZV-ORF9-L231A-V5 is attributable only to the leucine 231 mutation (Fig. 6A to E). In addition, immunofluorescence on infected MRC-5 and ARPE-19 cells shows that the colocalization of ORF9p and AP-1 is restored when the L231 mutation is repaired (Fig. 6F).

ORF9p leucine 231 is important for viral infectivity in a 3D skin model. VZV-ORF9-L231A-V5 infectivity was then evaluated in a previously described human three-dimensional (3D) skin model (41). Five thousand VZV-ORF9-V5-, -L231A-V5-, and -L231A-rev-V5-infected MRC-5 cells were layered on skin rafts and maintained in culture for 6 days. Immunohistochemistry with an anti-V5 antibody to detect ORF9p-V5 was performed on five series of 6 sections (Fig. 7A). Large infection foci were present in all series for VZV-ORF9-V5 and -L231A-rev-V5, whereas very small foci were observed only in one set of VZV-ORF9-L231A-V5 sections. In addition, VZV-ORF9-L231A-V5 foci remained limited to the upper layers of keratinocytes, in contrast to the spreading throughout the thickness of the skin rafts observed with VZV-ORF9-V5 and -L231-rev-V5 (Fig. 7A). It is worth noting that a similar result was obtained by labeling the sections

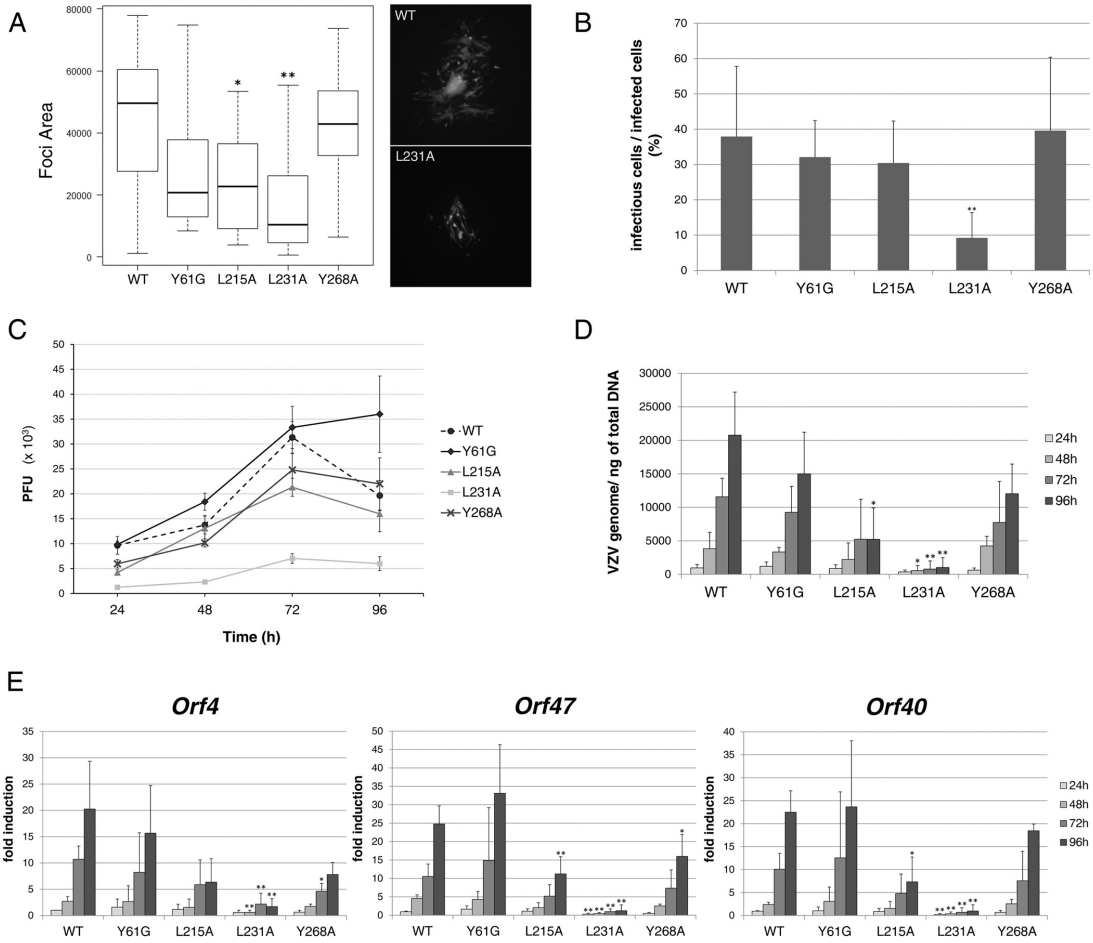

FIG 5 The L231A mutation strongly impacts infectivity in MeWo and MRC-5 cells. VZV-ORF9-V5 (WT) and mutant strain infectivity was assessed in MeWo cells (A and B) or MRC-5 cells (C to E). (A) Infection focus measurement at 48 hpi. MeWo cells were infected for 48 h, and the size of the infection foci was determined using CellProfiler software and expressed as the number of pixels present in each infection focus. The box plot depicts the 1st and 3rd quantiles (the lower and upper limits of the boxes, respectively) and the median (heavy black lines). Error bars represent minimum and maximum values. (B) Infectivity of infected cells. A known number of infected cells was used to infect MeWo cells seeded in a 24-well plate, and the number of infectious foci was determined in each well 3 days later. The graph shows the mean ratio of infectious cells/infected cells; error bars represent the standard deviation (SD). (C) Growth curves in MRC-5 cells. The graph shows the results of one representative experiment out of four; error bars represent the standard error of the mean (SEM). (D) The amount of the VZV genome over time was quantified by qPCR on DNA extracts. Primers in the human *p21* promoter were used for normalization. Serial dilutions of a BAC-VZV of a known concentration were used to build a standard curve. Results are expressed as the absolute number of VZV genomes per nanogram of total DNA. Means from three independent experiments are depicted; error bars represent the SD. (E) In parallel, qRT-PCR was performed on RNA extracts to quantify the expression of IE (*orf4*), E (*orf47*), and L (*orf40*) genes. The expression of 18S rRNA was used to calculate the change in the threshold cycle number, and for each gene, relative expression levels were calculated, with the expression level for the WT at 24 hpi being used as a control. Means from three independent experiments are depicted; error bars represent the SD. (A, B, D, and E) A two-tailed *t* test was used to compare, at each time point, each mutant to the WT strain. *, $P < 0.05$; **, $P < 0.01$.

with an antibody against IE63, reflecting a global growth defect rather than a particular issue with the expression or detection of L231A-V5 (data not shown). The massive reduction of infectivity was also observed when the viral genome copy number and viral gene expression were measured, respectively, by quantitative PCR (qPCR) or quantitative reverse transcription-PCR (qRT-PCR) (Fig. 7B and C).

The L231A mutant exhibits assembly and egress defects. MeWo cells were analyzed at the ultrastructural level using a transmission electron microscope (TEM) to

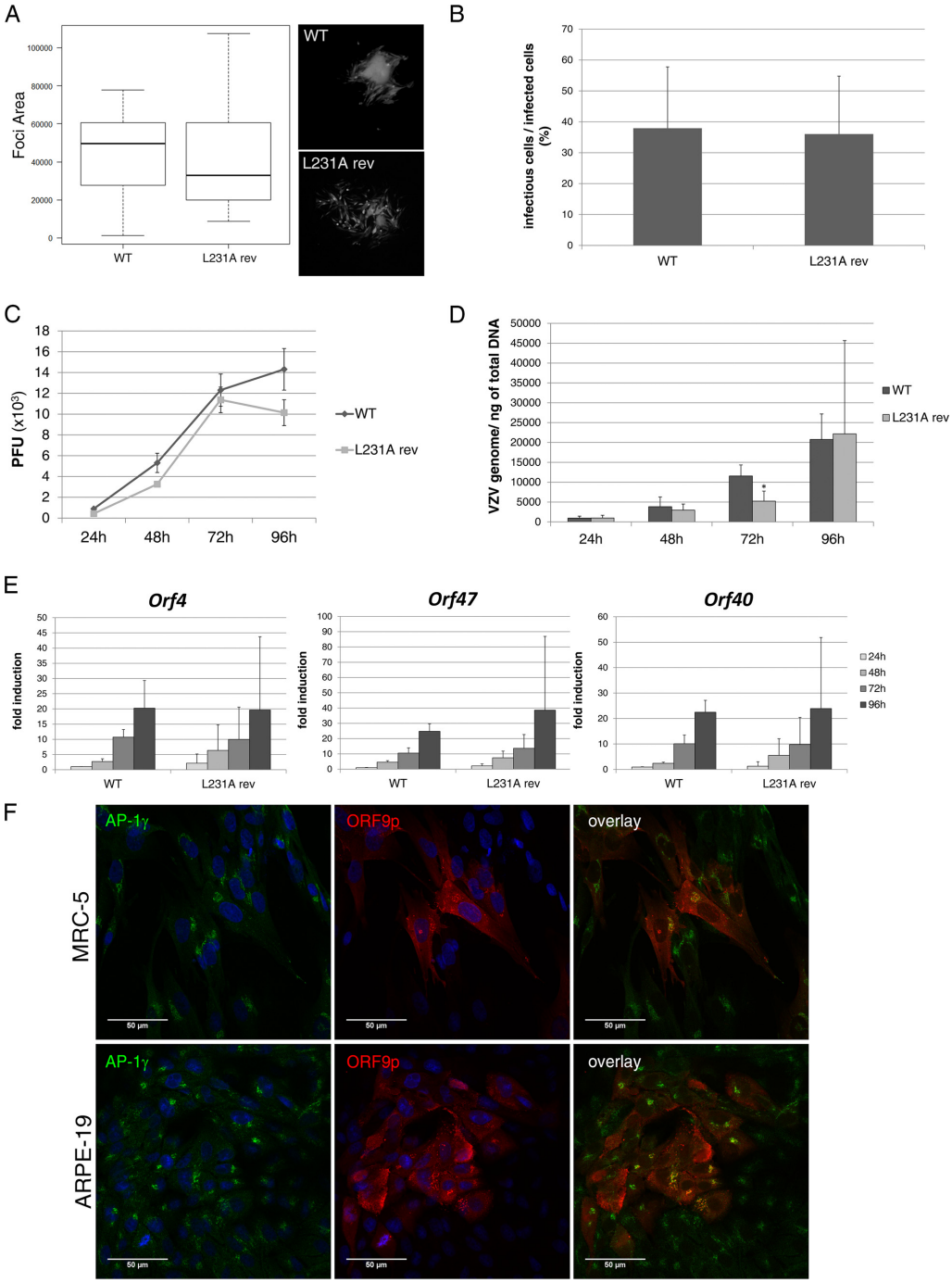

FIG 6 The replacement of ORF9-L231A-V5 by a WT ORF9-V5 copy restores the infectivity and the colocalization with AP-1. (A to E) VZV-ORF9-V5 (WT) and VZV-ORF9-L231A-rev-V5 (L231A rev) infectivity was assessed in MeWo cells (A and B) or MRC-5 cells (C to E). (A) Infection focus measurement at

(Continued on next page)

search for abnormal phenotypes. About 20 VZV-ORF9-V5-infected cells and 20 VZV-ORF9-L231A-V5-infected cells were carefully analyzed. While many complete virions or light particles were observed at the periphery of VZV-ORF9-V5-infected cells (Fig. 8A), they were scarce in VZV-ORF9-L231A-V5-infected cells (Fig. 8B). Transport vesicles containing enveloped virions and light particles were abundant and large in VZV-ORF9-V5-infected cells (Fig. 8A, middle) but extremely rare in VZV-ORF9-L231A-V5-infected cells, and when present, they were small and contained only a few viral particles (Fig. 8B). Interestingly, we noticed that while the particles of the ORF9-V5 virus (complete virions and light particles) seemed to be tightly bound to the membrane of the transport vesicles and to the cell membrane (Fig. 8A, right), this association appeared to be much looser for the L231A-V5 strain (Fig. 8B, right). In addition, L231A-V5-infected cells frequently showed dense material, likely the viral tegument, in association with curved membranes (endoplasmic reticulum, Golgi cisternae, and/or endocytic tubules) without being associated with viral particles or light particles (Fig. 8C). Surprisingly, vesicles resembling lysosomes and autophagosomes, some of them in the close vicinity of transport vesicles, were frequently observed in VZV-ORF9-L231A-V5-infected cells (Fig. 9A). Such figures were only rarely observed in WT-infected cells, and when observed, they were usually not in the vicinity of transport vesicles (Fig. 9B).

DISCUSSION

Although it is admitted that the tegument proteins, in general, and ORF9p or its homologs, in particular, play a role in envelopment, the molecular mechanisms and the interactions supporting these crucial steps are still poorly understood. The Y2H experiment described in this paper is the first attempt to identify putative cellular partners of ORF9p. The screening of hORFeome 5.1 with ORF9p, used as bait, together with a pairwise retest identified 35 cellular proteins directly interacting with ORF9p. Interestingly, the ORF9p region mapping to amino acids (aa) 50 to 250 containing the homology region (HR; aa 136 to 250) conserved in all alphaherpesviruses is important for these interactions. A gene ontology analysis to classify the partners based on their cellular functions highlighted several cellular processes, among which were microtubule cytoskeleton, chromatin organization, RNA metabolic processes, and transcription, suggesting that ORF9p could play various roles in infected cells. This is in agreement with the fact that both ORF9p and VP22 have been reported to interact with the cytoskeleton (26, 42), while HSV VP22 is also known to bind to the chromatin in dividing cells and to mRNA, enhancing thereby the accumulation of mRNA at early times of infection and protein synthesis at late times of infection (42–44).

Remarkably, 12 candidates out of the 35 were related to organelle organization. Among these proteins, four, namely, ANXA2, GOLGA2, CHMP5, and AP1M1, were associated with both intracellular transport and vesicle-mediated transport. ANXA2 (annexin A2) is a calcium-dependent, anionic phospholipid-binding protein that has pleiotropic functions, among which is the capacity to interact with endosomes following organelle destabilization (45). GOLGA2 (golgin A2) is a *cis*-Golgi matrix

FIG 6 Legend (Continued)
48 hpi. MeWo cells were infected for 48 h, and the size of the infection foci was determined using CellProfiler software and expressed as the number of pixels present in each infection focus. The box plot depicts the 1st and 3rd quantiles (the lower and upper limits of the boxes, respectively) and the median (heavy black lines). Error bars represent minimum and maximum values. (B) Infectivity of infected cells. A known number of infected cells was used to infect MeWo cells seeded in a 24-well plate, and the number of infectious foci was determined in each well 3 days later. The graph shows the mean ratio of infectious cells/infected cells; error bars represent the standard deviation (SD). (C) Growth curves in MRC-5 cells. The graph shows the results of one representative experiment out of four; error bars represent the standard error of the mean (SEM). (D) The amount of the VZV genome over time was quantified by qPCR on DNA extracts. Primers in the human *p21* promoter were used for normalization. Serial dilutions of a BAC-VZV of a known concentration were used to build a standard curve. Results are expressed as the absolute number of VZV genomes per nanogram of total DNA. Means from three independent experiments are depicted; error bars represent the SD. (E) In parallel, qRT-PCR was performed on RNA extracts to quantify the expression of IE (*orf4*), E (*orf47*), and L (*orf40*) genes. The expression of 18S rRNA was used to calculate the change in the threshold cycle number, and for each gene, relative expression levels were calculated, with the expression level for the WT at 24 hpi being used as a control. Means from three independent experiments are depicted; error bars represent the SD. (A, B, D, and E) A two-tailed *t* test was used to compare, at each time point, each mutant to the WT strain. *, $P < 0.05$. (F) MRC-5 and ARPE-19 cells were infected with VZV-ORF9-L231A-rev-V5 for 48 h and immunostained with both a mouse anti-V5 and a rabbit anti-AP-1γ. Appropriate secondary antibodies were used, and nuclei were counterstained with TO-PRO-3. Images were recorded with a 63× oil objective.

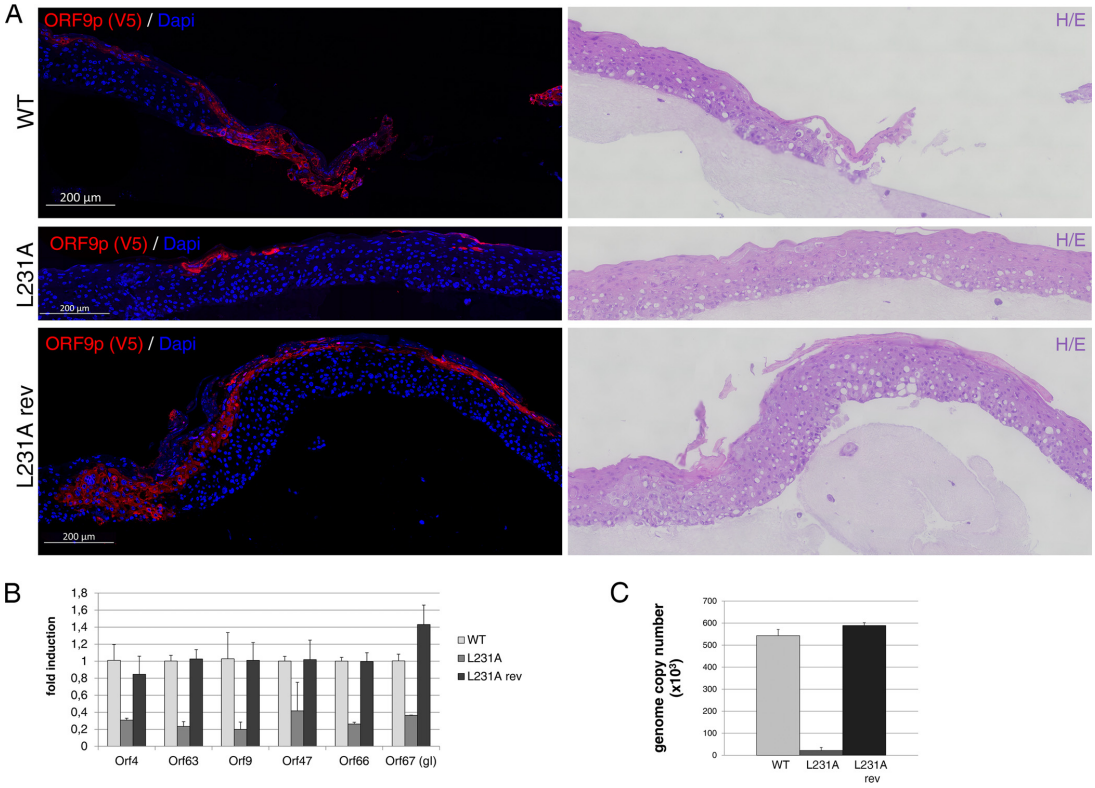

FIG 7 ORF9p leucine 231 is important for viral infectivity in a 3D skin model. Human primary keratinocytes were allowed to divide and differentiate at the air-liquid interface on top of a collagen matrix for 4 days. VZV-ORF9-V5 (WT)-, VZV-L213A-V5-, and VZV-L231A-rev-V5-infected MRC-5 cells were then layered on the epithelial cells and skin rafts were processed 6 days later. Three skin rafts were prepared for each infection. (A) For each infection, one raft was embedded in paraffin and a series of successive sections was prepared. (Left) Immunostaining against ORF9p (anti-V5 primary antibody). Nuclei were counterstained with DAPI. (Right) Control hematoxylin-eosin (H/E) staining. (B) Total RNA was extracted from a second skin raft, and the expression of IE (*orf4* and *orf63*), E (*orf9*, *orf47* and *orf66*), and L (*orf67*) genes was analyzed by qRT-PCR. The expression of 18S rRNA was used to calculate the change in the threshold cycle value, and for each gene, relative expression levels were calculated, with the VZV-ORF9-V5-infected raft being used as a control. Means for internal replicates are shown, and error bars represent the SD. (C) Genomic DNA was extracted from a third raft, and qPCR was performed to evaluate the number of VZV genome copies per microgram of total DNA. Primers in the human *p21* promoter were used for normalization. Serial dilutions of a BAC-VZV of a known concentration were used to build a standard curve. Means for internal replicates are shown, and error bars represent the SD.

protein that plays a major role in the stacking of Golgi cisternae and maintenance of the Golgi apparatus structure and participates in the glycosylation and transport of proteins and lipids in the secretory pathway (46, 47). CHMP5 (charged multivesicular body protein 5) is a component of ESCRT-III (endosomal sorting complex required for transport III), a complex involved in both the degradation of surface receptor proteins and the formation of endocytic multivesicular bodies (MVBs) (48). Knowing the potential implication of MVBs in the secondary envelopment process of herpesviruses, this could be of a particular interest (49, 50). Finally, AP1M1 is the μ subunit of the adaptor protein complex 1 (AP-1), which mediates the bidirectional clathrin-dependent trafficking of cargo proteins between the TGN and the endosomal network. The interaction with the cargo protein is mediated by the μ subunit or by the junction between the γ and σ subunits, while the clathrin and accessory molecules interact with the β and γ subunits (34).

The interaction of the most abundant tegument protein with the AP-1 complex appears to be highly relevant in the context of viral egress. Indeed, the site of secondary

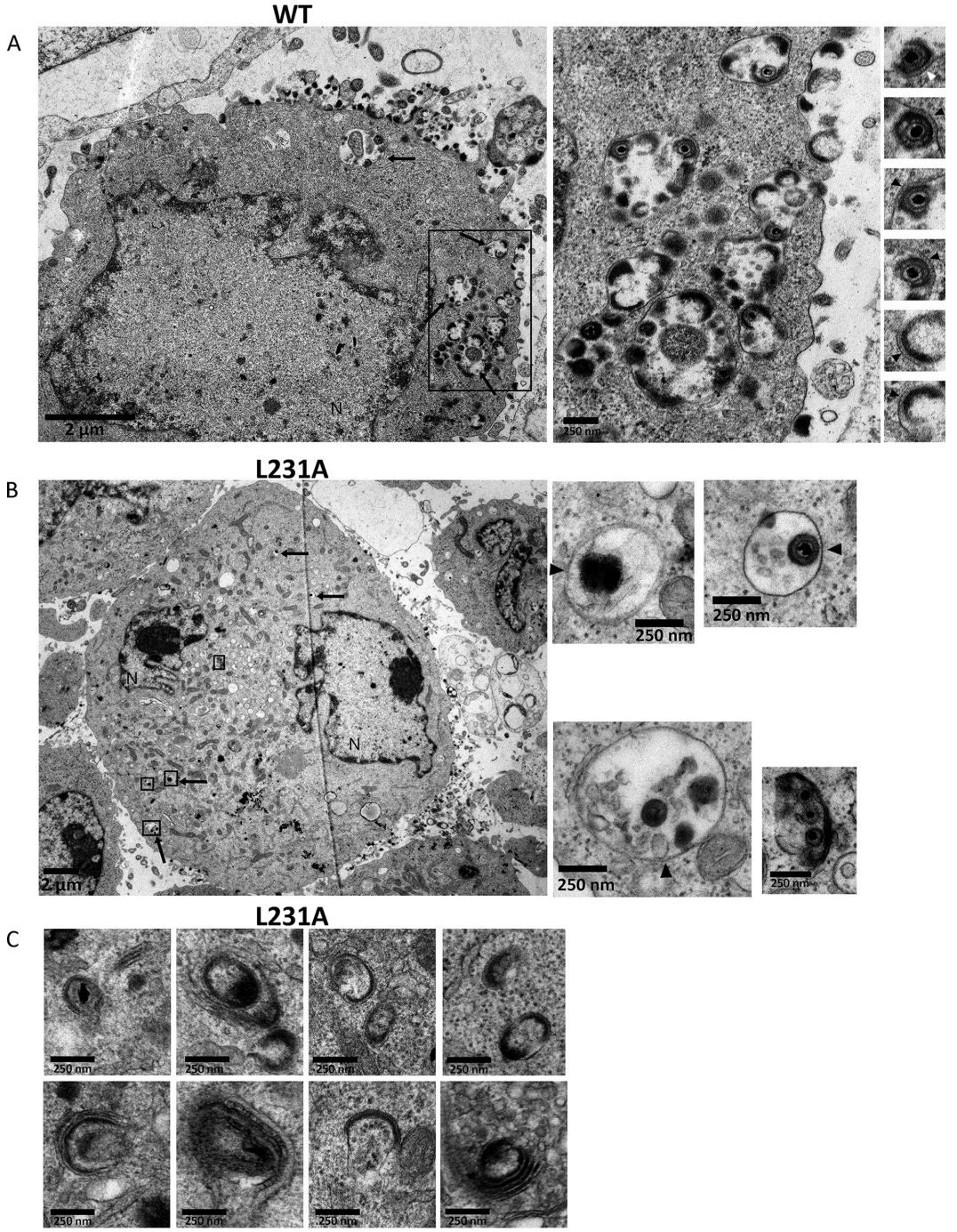

FIG 8 The VZV-ORF9-L231A-V5 mutant exhibits assembly and egress defects. Transmission electron microscopy was used to compare VZV-ORF9-V5-infected cells to VZV-ORF9-L231A-V5-infected cells. (A) VZV-ORF9-V5-infected MeWo cells are characterized by many particles at the cell surface as well as many

(Continued on next page)

envelopment and the precise nature of the transport vesicles are still debated. The importance of the TGN in the secondary envelopment process was widely recognized not only because most tegument proteins and glycoproteins present in extracellular particles accumulate in this cellular compartment before being incorporated into the final particles but also because of the lipid composition of the viral envelope (2, 3). Additionally, ultrastructural studies have identified capsids budding through vesicles positively stained for TGN markers (51–54). More recent work on HSV-1 has brought the idea that endocytic tubules instead might be the major site of secondary envelopment (4). In addition, some glycoproteins are first transported to the plasma membrane and secondarily endocytosed and transported to the TGN, supposedly the site of final envelopment, suggesting that endocytosis might represent an essential step in viral assembly (5, 55). We confirmed the interaction between ORF9p and AP-1 in a GST pulldown assay and by coimmunoprecipitation from infected MeWo, MRC-5, or ARPE-19 cell lysates. This was further supported by the colocalization of the ORF9p and AP-1γ proteins in the infectious context. The mutation of ORF9p leucine 231 led to a complete loss of interaction between ORF9p and AP-1, which was confirmed by a lack of colocalization, indicating that ^{227}EGLNLI^{232} is crucial for this interaction. The infectivity of the VZV-ORF9-L231A-V5 mutant was dramatically impaired in both MeWo and MRC-5 cells as well as in a human 3D skin model. The interaction between AP members and viral components has been shown to be important for the infectivity of various viruses. For example, AP-1 interacts with HIV Nef (56) and with African swine fever virus CD2v (57), while AP-2 interacts with the hepatitis B virus large envelope protein (58).

Interactions with AP-1 generally require cargo proteins to be inserted in the membrane in the vicinity of AP-1, usually thanks to lipid modifications. A bioinformatic analysis of ORF9p reveals that glycine 6 and cysteine 10 might be myristoylated or palmitoylated, respectively. We are currently investigating this hypothesis. Nevertheless, some cytoplasmic proteins are known to bind adaptor protein complexes in order to bring cargo to the sorting machinery. For example, PACS-1, a cytoplasmic protein, is required to mediate the interaction between furin and AP-1 for the subsequent addressing to the TGN (59). PACS-1 is also described to bind the mannose 6-phosphate receptor (MPR) or VZV gE (59) and to mediate the interaction between HIV Nef, AP-1, and the major histocompatibility complex (MHC) (60). It is thus possible that, even in the absence of a lipid modification, ORF9p, like PACS-1, ensures the proper localization of viral components necessary for assembly. Any mutation of ORF9p impairing its interaction with AP-1 would then affect the localization of other viral components and, consequently, viral assembly. Mass spectrometry analyses on the immunoprecipitated AP-1 complex are ongoing and will allow characterization, more broadly, of this complex in VZV-ORF9-V5- or VZV-ORF9-L231A-V5-infected cells.

Of note, the mutation of the conserved dileucine motifs in HSV-1 VP22 has demonstrated their importance for the expression or proper redistribution of VP22 itself and of ICP0, ICP4, ICP27, and VP26 and their importance for neurovirulence (11). In addition, the mutation of either dileucine motif in HSV-1 VP22 impedes its interaction with VP16, while the mutation of the first dileucine motif impairs its interaction with gE and, consequently, the incorporation of VP22 into the virion (61). Immunostaining and Western blotting experiments to detect possible modifications of the expression and/or localization of several VZV proteins, among which were some of the homologs of the HSV proteins described above, revealed only a minor nuclear retention of the kinase ORF47p (data not shown). Besides, preliminary results suggest that ORF9p interaction with gE, ORF10p (VP16 homolog), or IE62, the major VZV transactivator (which is an

FIG 8 Legend (Continued)
transport vesicles (arrows and middle). Enveloped virions or light particles were tightly associated with membranes (right, arrowheads). The boxed region in the left panel is shown as an enlargement in the middle panel. (B) VZV-ORF9-L231A-V5-infected MeWo cells are characterized by very few particles at the cell surface and very few transport vesicles (arrows). When present, viral particles are not tightly associated with the membranes (arrowheads). Specific regions of the left panel are boxed and enlarged in the right panels. N, nucleus. (C) A dense material bound to cisternae from the Golgi apparatus or the endoplasmic reticulum is frequently observed in VZV-ORF9-L231A-V5-infected MeWo cells.

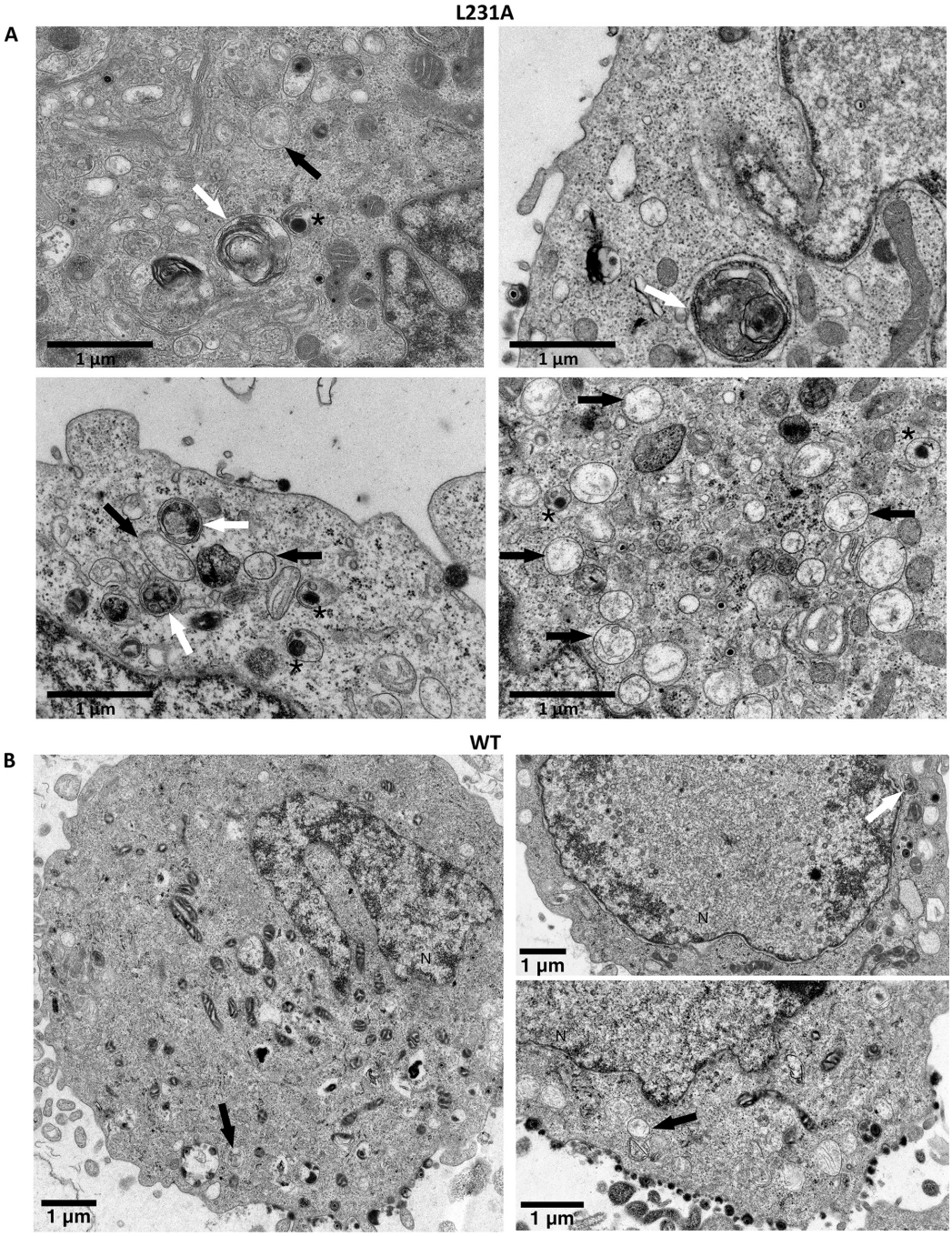

FIG 9 VZV-ORF9-L231A-V5-infected MeWo cells present peculiar features. (A) TEM micrographs of VZV-ORF9-L231A-V5-infected (48 hpi) MeWo cells showing the presence of many lysosomes (black arrows) and autophagosomes (white arrows). VZV particles in transport vesicles are present in close vicinity (asterisks). (B) TEM micrographs of VZV-ORF9-V5 infected MeWo cells (48 hpi) display few lysosomes (black arrows) and autophagosomes (white arrows). N, nucleus.

HSV-1 ICP4 homolog but which shares some functional properties with VP16) (27), is maintained despite the L231A mutation (data not shown). Additional experiments would be required to verify whether some other viral proteins are mislocalized or incorrectly expressed in VZV-ORF9-L231-V5-infected cells and whether the final composition of the released virions is affected. A very elegant flow virometry analysis of the extracellular HSV-1 particles indicates that the particles sorted for their high VP22 content show a modest but reproducible increase in infectivity compared to the particles containing smaller amounts of VP22, although the authors concluded that the VP22 level acts only indirectly on viral fitness (20). Although technically difficult due to the small amount of particles produced, a mass spectrometry analysis of VZV-ORF9-L231A-V5 particles would certainly be informative. Alternatively, immunostaining on ultrathin sections with antibodies against the main glycoproteins might give some clue to provide an understanding of why the infectivity of this virus is so low.

Electron microscopy analyses clearly reflected the growth defect of VZV-ORF9-L231A-V5: (i) VZV-ORF9-L231A-V5-infected cells showed very few enveloped virions or light particles at the cell surface and sparse small transport vesicles containing only a few particles, (ii) the particles seemed not to be tightly bound to the cell membrane or transport vesicle membrane, contrary to what is observed with the wild-type strain, and (iii) a dense material resembling the viral tegument associated with curved vesicles most likely belonging to the Golgi apparatus, the endoplasmic reticulum, and/or the endocytic tubule network was often observed. These observations suggest that ORF9p/AP-1 interaction might be necessary to recruit and/or stabilize other viral components at the appropriate localization to ensure the final assembly.

On the other hand, TEM analyses did not reveal any accumulation of capsids in the cytoplasm of VZV-ORF9-L231-V5-infected cells, which would be expected with a defect only at a secondary egress step. Moreover, in VZV-ORF9-L231A-V5-infected MRC-5 cells sorted by flow cytometry according to their expression of green fluorescent protein (GFP), TEM analyses revealed the presence of capsids only in a low percentage of cells (data not shown). This might reflect either a nucleocapsid assembly default or a targeting of newly produced virions for degradation. In the cell culture systems used to produce and study VZV, the majority of particles reaching the cell surface are actually noninfectious and aberrant at the ultrastructural level (62, 63). It was postulated that after secondary envelopment, VZV particles are redirected to the late secretory pathway, where they are partially degraded before reaching the cell surface (52). More recently, the transport vesicles containing VZV virions were shown to be single walled and positive for both Rab11 (endocytic pathway) and LC3B (autophagic pathway), and exocytosis of VZV particles was shown to rely, at least partially, on a convergence between the autophagy and endosomal pathways (64, 65). Interestingly, vesicles resembling lysosomes and autophagosomes, some of them being in the close vicinity of transport vesicles, were frequently observed in VZV-ORF9-L231A-V5-infected cells, while they were rarer in WT-infected cells. Immunostaining on ultrathin sections is required to draw conclusions on the precise nature of these vesicles. Nevertheless, it is tempting to speculate that it might reflect that the diversion of the autophagic pathways to the virus's own benefit is impaired in the mutant virus, leading to virion degradation. It is interesting to note that among the ORF9p interaction partners identified in the Y2H experiment, we found MAP1LC3A, also known as LC3.

In conclusion, we have shown that ORF9p, the major tegument protein, interacts with the AP-1 complex through the ^{227}EGLNLI^{232} dileucine motif and that the mutation of this motif dramatically impairs the infectious cycle. Like all viruses, VZV exploits the cellular machinery to its own profit, including the mechanisms allowing the transport of cargo to the appropriate localization. The fact that this interaction is conserved in HSV-2 and MDV and that the dileucine motif is conserved in almost all alphaherpesviruses suggests that the interaction with AP-1 is important for the infectious cycle.

More broadly, it is possible that this interaction perturbs the cell physiology by

interfering with the transport of cellular proteins, as it has been described for Nef of HIV, which leads to a decrease of MHC class I or CD4 at the cell surface (66). This possibility is under investigation.

MATERIALS AND METHODS

Cell culture. MeWo (a human melanoma cell line; ATCC HTB-65), MRC-5 (human primary embryonic lung fibroblasts), and ARPE-19 (human retinal pigmented epithelium; ATCC CRL-2302) cells were cultured in Eagle minimal essential medium (MeWo and MRC-5 cells) or Dulbecco's modified Eagle's medium–Ham's F-12 medium (ARPE-19 cells) supplemented with 1% nonessential amino acids, 1% L-glutamine, 1% antibiotic mix (penicillin-streptomycin), and 10% fetal bovine serum (Fisher Scientific, Gibco).

Recombinant virus production. To reconstitute recombinant viruses, MeWo cells were transfected with bacterial artificial chromosomes (BACs) containing the entire WT or mutated pOka genome (3 μg per well of 6-well plates) using 4.5 μl of the JetPEI transfection reagent (Polyplus transfection). All BACs contained a gene coding for GFP under the control of the cytomegalovirus promoter, allowing the detection of infected cells by confocal microscopy or flow cytometry. At 3 days after transfection, the cells were transferred into a 25-cm^2 flask and passaged every 2 to 3 days until typical infection foci appeared. MRC-5 or ARPE-19 cells were infected by coculture with infected MeWo cells at a 24/1 ratio.

Antibodies. The following commercial antibodies were used: mouse anti-V5 (catalog number R960-25; Life Technologies), mouse anti-γ-adaptin (catalog number A4200; Sigma), and rabbit anti-γ-adaptin (catalog number ab220251; Abcam). Antibody against AP-1μ1 was a kind gift of L. Traub (67). VZV anti-IE63 (9D12) was previously described (68). Alexa Fluor 405- and Alexa Fluor 568-conjugated secondary antibodies were obtained from Invitrogen.

High-throughput yeast two-hybrid assay. *orf9* was amplified by PCR with the 9WT_gateFw and 9WT_gateRv primers (Table 1) and cloned by Gateway cloning (Invitrogen) in pAD-dest-CYH and pDB-dest, which were transformed, respectively, into *MAT***a** Y8800 and *MAT*α Y8930 *Saccharomyces cerevisiae* strains (as previously described [69, 70]). The AD-ORF9p Y8800 was mated to each of the 15,483 DB ORFs Y8930 of the human ORFeome 5.1 (CCSB; Dana-Farber Cancer Institute; described in reference 71), the 165 pools of 94 AD ORFs of the hORFeome 5.1 were mated to DB ORF9 Y8930, and interactions were identified strictly as described in reference 72. Colonies positive for the GAL1::HIS3 and GAL1::ADE2 selective markers but negative for autoactivation were selected for PCR amplification (with Zymolyase 20T [Seikagaku Biobusiness] and Platinum *Taq* DNA polymerase [Invitrogen]). Interacting proteins were identified by sequencing of the respective AD and DB ORFs. The interaction of partners of interest with WT and six *orf9* truncated constructs (expressing aa 50 to 302, 100 to 302, 150 to 302, 1 to 250, 1 to 200, and 1 to 150) was validated/tested similarly using isolated AD and DB clones.

GST pulldown. pGex-ORF9 has been described previously (30). The MDV and HSV-2 *UL49* genes were amplified by PCR, using pcDNA3-UL49 (a kind gift from C. Denesvre [73]) or genomic DNA purified from HSV-2-infected cells as the template and the primers described in Table 1. Amplified sequences were inserted into pGEX-5X-1, which had previously been digested with SmaI. pOka VZV-infected and noninfected MeWo cells were lysed with GST buffer (50 mM Tris-HCl [pH 8], 5 mM EDTA, 150 mM NaCl, 10 mM $MgCl_2$, 1% Triton X-100, cOmplete protease inhibitor cocktail [1:50; Roche]) and centrifuged for 3 min at maximum speed. Cleared lysates were incubated for 2 h at 4°C with GST-, GST-ORF9p-, or GST-VP22-coated agarose beads (GE Healthcare). After three washes, the pulled-down proteins were eluted and subjected to Western blotting.

Immunofluorescence. MRC-5 or ARPE-19 cells were seeded on glass coverslips and infected by coculture with infected MeWo cells. At 48 h postinfection (hpi), cells were washed with phosphate-buffered saline (PBS), fixed for 10 min in 4% paraformaldehyde–PBS, permeabilized for 10 min in 0.3% Triton X-100–PBS, and blocked with 10% bovine serum albumin (BSA)–PBS for 45 min. The coverslips were then incubated overnight at 4°C with the primary antibodies diluted in 5% BSA–PBS (anti-V5, 1/250; anti-AP-1γ, 1/250). After 3 washes in 5% BSA–PBS, the coverslips were incubated for 1 h with the appropriate Alexa Fluor 405- or Alexa Fluor 568-conjugated secondary antibody (1/400 in 5% BSA–PBS at room temperature). Nuclei were stained with TO-PRO-3 (1/2,000), and images were recorded with an Olympus FV1000 confocal microscope using a 63× oil objective.

Site-directed mutagenesis. pcDNA-3.1-ORF9p-Y61G, -ORF9p-L215A, -ORF9p-L231A, and -ORF9p-Y268A were generated by directional mutagenesis using TurboPFU polymerase (Stratagene), the appropriate primers (Table 1), and pcDNA-3.1-ORF9-V5 as a template (30).

Construction of BAC-VZV carrying the ORF9p mutation. All constructs were created by modification of the BAC-VZV-pOka WT (a kind gift from H. Zhu [74]) using the GalK positive/negative selection technique described by Warming et al. (75) and materials (pGalK plasmid and SW102 bacterial strain) obtained from the Biology Research Branch (BRB) at NCI, Bethesda, MD.

BAC-VZV-ORF9-V5 and VZV-ORF9-ΔAC-V5 (ΔAC-V5) were already described (30, 31). BAC-VZV-ORF9-Y61G-V5, -L215A-V5, -L231A-V5, and -Y268A-V5 were generated by replacing the *orf9* coding sequence by the *galK*-expressing cassette, which was subsequently replaced by the mutated copy of *orf9*. The primers listed in Table 1 and the four mutated pcDNA-3.1 vectors were used to obtain the recombination cassettes. To create the L231A revertant BAC, the ΔORF9 GalK cassette was reintroduced into BAC-VZV-ORF9-L231A-V5 and subsequently replaced by a WT ORF9-V5 copy.

Coimmunoprecipitation. Infected MeWo cells (48 hpi) were lysed, and the immunoprecipitation step was performed as described by Iijima et al. (66), except that protein A/G magnetic beads (Pierce) were used and a phosphatase inhibitor cocktail (25 mM β-glycine, 1 mM Na_3VO_4, 1.5 mM NaF) was added in the lysis buffer. After four washes of the beads (1% Triton X-100, 150 mM NaCl, 50 mM Tris-HCl [pH

TABLE 1 Primers used in this study

Primer purpose and primer	Sequence
Gateway cloning	
9WT_gateFw	5′-GGGGACAACTTTGTACAAAAAAGTTGGCATGGCATCTTCCGACGGTGACAGA-3′
50-302_gateFw	5′-GGGGACAACTTTGTACAAAAAAGTTGGC ATGACCACAGTTGGGGCCGATTCTC-3′
100-302_gateFw	5′-GGGGACAACTTTGTACAAAAAAGTTGGCATGGAGGCCCGTTTGAGACATGAAC-3′
150-302_gate Fw	5′-GGGGACAACTTTGTACAAAAAAGTTGGCATTGCCAGCGGGAGACCAATTTCC-3′
9WT_gateRv	5′-GGGGACAACTTTGTACAAGAAAGTTGATTATTTTCGCGCATCAGTTCTTGATG-3′
1-250_gateRv	5′-GGGGACAACTTTGTACAAGAAAGTTGATCCACGTTTGGATACCGATGCTCC-3′
1-200_gateRv	5′-GGGACAACTTTGTACAAGAAAGTTGAAGCCGCTTCGGCAGCCTTTTGTGC-3′
1-150_gateRv	5′-GGGGACAACTTTGTACAAGAAAGTTGAAATTGCGCCTGCTCCCGGGGGAGC-3′
Site-directed mutagenesis	
ORF9_Y61G_Fw	5′-CCGATTCTCCTTCTCCAGTGGGCGCGGATCTTTAT-3′
ORF9_Y61G_Rv	5′-GTTCAAAATAAAGATCCGCGCCCACTGGAGAAGGA-3′
ORF9L215A_Fw	5′-ATTAGACCGTGCGTTAACCGGAGCCGTTATTCGTA-3′
ORF9L215A_Rv	5′-CTCCGGTTAACGCACGGTCTAATTCGGCGTTATTC-3′
ORF9L231A_Fw	5′-GGGTTTAAATGCAATACAAGCCGCTAATGAAGCAG-3′
ORF9L231A_Rv	5′-CGGCTTGTATTGCATTTAAACCCTCATGCACCGTA-3′
ORF9Y268A_Fw	5′-TGAACCTATGGCCGCACAAGTTCGTAAGCCAAAAA-3′
ORF9Y268A_Rv	5′-TTTTTGGCTTACGAACTTGTGCGGCCATAGGTTCA-3′
BAC recombineering	
ORF9galKN_Fw	5′-CGCGGTCTGCCGTGTTTGGATATTTCACGACCCTATCGTTTATTTACGTACCTGTTGACAATTAATCATCGGCA-3′
ORF9GalKC_Rv	5′-TTATTTATTATACATAATACCGGGTAAACCGTTACTGCGTAATTATATCCTCAGCACTGTCCTGCTCCTT-3′
WT9_Fw	5′-CGCGGTCTGCCGTGTTTGGATATTTCACGACCCTATCGTTTATTTACGTAATGGCATCTTCCGACGGTGACAGA-3′
WT9_Rv	5′-TTATTTATTATACATAATACCGGGTAAACCGTTACTGCGTAATTATATCCTCAATGGTGATGGTGATGATGACCG-3′
GST constructs	
VP22-HSV2-Fw	5′-ATGACCTCTCGCCGCTCCGTCAAGTCGTGTCCGC-3′
VP22-HSV2-Rv	5′-CTCGAGGGGGCGGCGGGGACGGGAAGCCGAGCGG-3′
VP22-MDV-Fw	5′-ATGGGGGATTCTGAAAGGCGGAAATCGGAACGGC-3′
VP22-MDV-Rv	5′-TTCGCTATCACTGCTACGATATCCGCGGGCGGATG-3′
qRT-PCR and genomic PCR	
18S_FW	5′-AACTTTCGATGGTAGTCGCCG-3′
18S_Rv	5′-CCTTGGATGTGGTAGCCGTTT-3′
qRT_IE4_Fw	5′-CTTCAATTCCAACCGACCCAG-3′
qRT_IE4_Rv	5′-ATCGGTGACTTCCAATGCAAAG-3′
qRT_IE63_Fw	5′-TACAGCTTCAACCCACCCAGAC-3′
qRT_IE63_Rv	5′-ATTCGGCGCCTCAATGAAC-3′
qRT_ORF9_Fw	5′-AAAAATGCGGCGGTTAAACC-3′
qRT_ORF9_Rv	5′-GCAGTGCTGAAGGAAATTGGTC-3′
qRT_ORF47_Fw	5′-CCCGTATTTCCCGGAATTCTT-3′
qRT_ORF47_Rv	5′-TAATGAGGCCGGAATGCGT-3′
qRT_ORF66_Fw	5′-GTTTTGCGTTTGCGTGTATGG-3′
qRT_ORF66_Rv	5′-AACGCTCTTAACACGGTTGCC-3′
qRT_ORF40_Fw	5′-CGATGAAACCATTGCAACG-3′
qRT_ORF40_Rv	5′-CCGCCTAGCATTTGTCATTC-3′
qRT_ORF67_Fw	5′-GGCTCGCATCACAACATTCA-3′
qRT_ORF67_Rv	5′-GTCGCGGGTAAATCACACAA-3′
ORF10prom_Fw	5′-GACAGTCGTGGTTTGTGTTTATT-3′
ORF10prom_Rv	5′-AATGGGGTTTGTTTGGTAGC-3′
P21prom_Fw	5′-GTGGCTCTGATTGGCTTTCTG-3′
P21prom_Rv	5′-CTGAAAACAGGCAGCCCAAG-3′

7.0], 1 mM $CaCl_2$, 1 mM $MgCl_2$), proteins were eluted with 2% SDS at 37°C for 10 min, followed by the addition of an equal volume of SDS loading buffer and another incubation at 37°C for 10 min.

Viral growth curve. To assess the growth properties of the ORF9p mutant in MeWo cells, infected cells were first filtered through a cell strainer to remove syncytia and obtain a single-cell suspension. The proportion of GFP-positive cells in the suspension, corresponding to infected cells, was assessed using a FACSCanto II flow cytometer, and a known number of infected cells was then used to infect MeWo cells. At 48 hpi, pictures of the infection foci were recorded (range, 16 to 92) using an inverted fluorescence microscope (Olympus FSX-100). To determine the size of the infection foci, the pictures were processed with CellProfiler software (www.cellprofiler.org) (76). In parallel, at 48 and 72 hpi, the number of infection foci was determined in each well ($n = 8$) and divided by the number of infected cells used to infect the cells at day 0, to obtain the ratio of infectious cells/infected cells.

For the growth curve in MRC-5 cells, infected MeWo cells were trypsinized on day 1 and the proportion of GFP-positive cells, corresponding to infected cells, was assessed using a FACSCanto II flow

cytometer. The cells in four 25-cm² flasks of MRC-5 cells for each viral strain were then infected with 500 infected MeWo cells. On days 1 to 4, a 25-cm² flask for each virus was trypsinized and an aliquot was serially diluted (range, 1/62.5 to 1/2,000) and used to infect MRC-5 cells in 24-well plates. Each 24-well plate was analyzed twice (48 hpi and 72 hpi) with an inverted fluorescence microscope to determine the number of infection foci. The cells that were not used for the serial dilution were divided into three tubes, two of which were frozen for subsequent DNA and RNA extraction, while the third was centrifuged; the cells were fixed in 4% platelet-activating factor for 20 min; and the proportion of infected cells was determined by fluorescence-activated cell sorting (FACS).

qPCR and qRT-PCR. RNA was extracted from infected cells with the TriPure reagent (Roche) and treated with RNase-free DNase for an hour at 37°C. One microgram of RNA was used to produce cDNA with a RevertAid H Minus First Strand cDNA synthesis kit (Thermo Scientific). Twenty nanograms of cDNA was used for the subsequent PCR, except for 18S rRNA primers, for which 20 pg was used. The expression of 18S rRNA was used for normalization.

For genomic DNA extraction, cells were resuspended in Tris-SDS buffer (10 mM Tris, pH 7.4, 10 mM EDTA, 150 mM NaCl, 0.4% SDS) containing 0.2 mg/ml of proteinase K and incubated for 3 h at 50°C. Genomic DNA was subsequently isolated via a classical phenol-chloroform extraction. For viral genome quantification, 10 ng of DNA was used for the subsequent PCR. Primers in the VZV *orf10* promoter were used for viral genome detection, and normalization was performed with primers against the human *p21* promoter. In order to obtain the absolute number of VZV genomes present in the samples, a standard curve was built in parallel via serial dilution of a BAC-VZV WT DNA preparation of a known concentration.

Quantitative PCR or RT-PCR were performed with a Roche LightCycler 480 apparatus in 384-well plates, in which triplicates of 2 μl of genomic DNA or cDNA were mixed with 8 μl of a mix containing FastStart Universal Sybr green master mix (Roche) and specific primers (Table 1).

3D skin model. For the preparation of epidermal equivalents, a collagen matrix solution was made with collagen mixed on ice with 10-fold-concentrated Ham's F-12 medium, 10-fold reconstitution buffer, and Swiss 3T3 J2 fibroblasts. One milliliter of the collagen matrix solution was poured into 24-well plates. After gel equilibration with 1 ml of growth medium overnight at 37°C, 2.5×10^5 PHK cells were seeded on top of the gels and maintained submerged for 24 to 48 h. The collagen rafts were raised and placed onto stainless steel grids at the interface between the air and the liquid culture medium. The growth medium was a mixture of Ham's F-12 medium and Dulbecco's modified Eagle's medium (1:2) supplemented with 0.5 μg/ml hydrocortisone, 10 ng/ml epidermal growth factor, 10% fetal calf serum, 2 mM L-glutamine, 10 mM HEPES, 1 mM sodium pyruvate, 10^{-10} mM cholera toxin, 5 μg/ml insulin, 5 μg/ml transferrin, and 15×10^{-4} mg/ml 3,3′,5′-triiodo-L-thyronine. Epithelial cells were allowed to stratify for 4 days, with the medium being replaced every other day. Five thousand infected MRC-5 cells were then placed on top of the epithelium, which was maintained in culture for 6 additional days. The cultures were then harvested and either fixed in 10% buffered formalin and embedded in paraffin for subsequent immunohistohemistry or frozen for further RNA or DNA extraction.

Immunohistochemistry. Skin raft sections (5 μm) were incubated for an hour with the primary antibodies (anti-V5 [1/500] and anti-IE63 [1/250] in a Dako Real detection system), washed three times with PBS, and incubated for 30 min with the secondary antibody (Alexa Fluor 568-conjugated anti-mouse immunoglobulin [1/500] in a Dako Real detection system). A DAPI (4′,6-diamidino-2-phenylindole)-containing mounting medium (catalog number S3023; Dako) was used for nuclear staining and sample fixation.

Alternatively, sections were washed, incubated in hematoxylin-eosin, washed again, and mounted with Leica CV Mount mounting medium. Observations were made with a Zeiss LSM880 Airy scan confocal microscope with a 40× oil objective or with an Olympus FSX-100 microscope with a 40× dry objective.

Transmission electron microscopy. MeWo cells infected with VZV-ORF9-V5 or VZV-L231A-V5 were sorted by FACS, fixed for 90 min at 4°C with 2.5% glutaraldehyde in Sörensen 0.1 M phosphate buffer (pH 7.4), and postfixed for 30 min with 2% osmium tetroxide. After dehydration in graded ethanol, samples were embedded in Epon. Ultrathin sections obtained with a Reichert Ultracut S ultramicrotome were contrasted with uranyl acetate and lead citrate. Observations were made with a JEOL JEM-1400 transmission electron microscope at 80 kV.

ACKNOWLEDGMENTS

This work was supported by the University of Liege, Fonds National pour la Recherche Scientifique (F.R.S.-FNRS, Belgium), and by the Fonds Leon Fredericq. J.L. and L.R. were supported by the Fonds pour la Recherche dans l'Industrie et l'Agriculture (FRIA, Brussels, Belgium). C.B. was supported by the FP7-People-COFUND 2013-2019 program.

We are grateful to L. Traub for the generous gift of anti-AP-1μ1 antibodies and S. Jonjic for anti-ORF10p antibodies. We also thank H. Zhu for the BAC-VZV-pOka WT, C. Denesvre for pcDNA3-UL49, and the Biology Research Branch (BRB) at NCI, Bethesda, MD, for the GalK plasmid and for the SW102 bacterial strain. Finally, we thank C. Lassence for technical assistance; P. Piscicelli for TEM preparation; S. Ormenese, J. J. Goval, and S. Freeman for technical support with confocal microscopy (Imaging Technological Platform, GIGA-R); T. DiSalvo, A. Marquet, and C.

Humblet for immunohistochemistry; R. Stephan for cell sorting; and E. De Waegeneare for organotypic assays.

REFERENCES

1. Mettenleiter TC, Klupp BG, Granzow H. 2009. Herpesvirus assembly: an update. Virus Res 143:222–234. https://doi.org/10.1016/j.virusres.2009.03.018.
2. Hambleton S, Gershon MD, Gershon AA. 2004. The role of the trans-Golgi network in varicella zoster virus biology. Cell Mol Life Sci 61:3047–3056. https://doi.org/10.1007/s00018-004-4269-7.
3. Johnson DC, Baines JD. 2011. Herpesviruses remodel host membranes for virus egress. Nat Rev Microbiol 9:382–394. https://doi.org/10.1038/nrmicro2559.
4. Hollinshead M, Johns HL, Sayers CL, Gonzalez-Lopez C, Smith GL, Elliott G. 2012. Endocytic tubules regulated by Rab GTPases 5 and 11 are used for envelopment of herpes simplex virus. EMBO J 31:4204–4220. https://doi.org/10.1038/emboj.2012.262.
5. Maresova L, Pasieka TJ, Homan E, Gerday E, Grose C. 2005. Incorporation of three endocytosed varicella-zoster virus glycoproteins, gE, gH, and gB, into the virion envelope. J Virol 79:997–1007. https://doi.org/10.1128/JVI.79.2.997-1007.2005.
6. Beitia Ortiz de Zarate I, Cantero-Aguilar L, Longo M, Berlioz-Torrent C, Rozenberg F. 2007. Contribution of endocytic motifs in the cytoplasmic tail of herpes simplex virus type 1 glycoprotein B to virus replication and cell-cell fusion. J Virol 81:13889–13903. https://doi.org/10.1128/JVI.01231-07.
7. Albecka A, Laine RF, Janssen AFJ, Kaminski CF, Crump CM. 2016. HSV-1 glycoproteins are delivered to virus assembly sites through dynamin-dependent endocytosis. Traffic 17:21–39. https://doi.org/10.1111/tra.12340.
8. Nixdorf R, Mettenleiter TC, Klupp BG. 2001. Role of the cytoplasmic tails of pseudorabies virus glycoproteins B, E and M in intracellular localization and virion incorporation. J Gen Virol 82:215–226. https://doi.org/10.1099/0022-1317-82-1-215.
9. Elliott GD, Meredith DM. 1992. The herpes simplex virus type 1 tegument protein VP22 is encoded by gene UL49. J Gen Virol 73:723–726. https://doi.org/10.1099/0022-1317-73-3-723.
10. Spengler M, Niesen N, Grose C, Ruyechan WT, Hay J. 2001. Interactions among structural proteins of varicella zoster virus. Arch Virol Suppl 2001:71–79.
11. Tanaka M, Kato A, Satoh Y, Ide T, Sagou K, Kimura K, Hasegawa H, Kawaguchi Y. 2012. Herpes simplex virus 1 VP22 regulates translocation of multiple viral and cellular proteins and promotes neurovirulence. J Virol 86:5264–5277. https://doi.org/10.1128/JVI.06913-11.
12. Maringer K, Stylianou J, Elliott G. 2012. A network of protein interactions around the herpes simplex virus tegument protein VP22. J Virol 86:12971–12982. https://doi.org/10.1128/JVI.01913-12.
13. Stylianou J, Maringer K, Cook R, Bernard E, Elliott G. 2009. Virion incorporation of the herpes simplex virus type 1 tegument protein VP22 occurs via glycoprotein E-specific recruitment to the late secretory pathway. J Virol 83:5204–5218. https://doi.org/10.1128/JVI.00069-09.
14. del Rio T, Werner HC, Enquist LW. 2002. The pseudorabies virus VP22 homologue (UL49) is dispensable for virus growth in vitro and has no effect on virulence and neuronal spread in rodents. J Virol 76:774–782. https://doi.org/10.1128/JVI.76.2.774-782.2002.
15. Fuchs W, Klupp BG, Granzow H, Hengartner C, Brack A, Mundt A, Enquist LW, Mettenleiter TC. 2002. Physical interaction between envelope glycoproteins E and M of pseudorabies virus and the major tegument protein UL49. J Virol 76:8208–8217. https://doi.org/10.1128/JVI.76.16.8208-8217.2002.
16. Sciortino MT, Taddeo B, Giuffrè-Cuculletto M, Medici MA, Mastino A, Roizman B. 2007. Replication-competent herpes simplex virus 1 isolates selected from cells transfected with a bacterial artificial chromosome DNA lacking only the UL49 gene vary with respect to the defect in the UL41 gene encoding host shutoff RNase. J Virol 81:10924–10932. https://doi.org/10.1128/JVI.01239-07.
17. Ebert K, Depledge DP, Breuer J, Harman L, Elliott G. 2013. Mode of virus rescue determines the acquisition of VHS mutations in VP22-negative herpes simplex virus 1. J Virol 87:10389–10393. https://doi.org/10.1128/JVI.01654-13.
18. Mbong EF, Woodley L, Dunkerley E, Schrimpf JE, Morrison LA, Duffy C. 2012. Deletion of the herpes simplex virus 1 UL49 gene results in mRNA and protein translation defects that are complemented by secondary mutations in UL41. J Virol 86:12351–12361. https://doi.org/10.1128/JVI.01975-12.
19. Duffy C, Lavail JH, Tauscher AN, Wills EG, Blaho JA, Baines JD. 2006. Characterization of a UL49-null mutant: VP22 of herpes simplex virus type 1 facilitates viral spread in cultured cells and the mouse cornea. J Virol 80:8664–8675. https://doi.org/10.1128/JVI.00498-06.
20. El Bilali N, Duron J, Gingras D, Lippé R. 2017. Quantitative evaluation of protein heterogeneity within herpes simplex virus 1 particles. J Virol 91:e00320-17. https://doi.org/10.1128/JVI.00320-17.
21. Elliott G, Hafezi W, Whiteley A, Bernard E. 2005. Deletion of the herpes simplex virus VP22-encoding gene (UL49) alters the expression, localization, and virion incorporation of ICP0. J Virol 79:9735–9745. https://doi.org/10.1128/JVI.79.15.9735-9745.2005.
22. Che X, Reichelt M, Sommer MH, Rajamani J, Zerboni L, Arvin AM. 2008. Functions of the ORF9-to-ORF12 gene cluster in varicella-zoster virus replication and in the pathogenesis of skin infection. J Virol 82:5825–5834. https://doi.org/10.1128/JVI.00303-08.
23. Tischer BK, Kaufer BB, Sommer M, Wussow F, Arvin AM, Osterrieder N. 2007. A self-excisable infectious bacterial artificial chromosome clone of varicella-zoster virus allows analysis of the essential tegument protein encoded by ORF9. J Virol 81:13200–13208. https://doi.org/10.1128/JVI.01148-07.
24. Cai M, Wang S, Xing J, Zheng C. 2011. Characterization of the nuclear import and export signals, and subcellular transport mechanism of varicella-zoster virus ORF9. J Gen Virol 92(Pt 3):621–626. https://doi.org/10.1099/vir.0.027029-0.
25. Che X, Oliver SL, Reichelt M, Sommer MH, Haas J, Rovis TL, Arvin AM. 2013. ORF11 protein interacts with the ORF9 essential tegument protein in varicella-zoster virus infection. J Virol 87:5106–5117. https://doi.org/10.1128/JVI.00102-13.
26. Cilloniz C, Jackson W, Grose C, Czechowski D, Hay J, Ruyechan WT. 2007. The varicella-zoster virus (VZV) ORF9 protein interacts with the IE62 major VZV transactivator. J Virol 81:761–774. https://doi.org/10.1128/JVI.01274-06.
27. Sato B, Ito H, Hinchliffe S, Sommer MH, Zerboni L, Arvin AM. 2003. Mutational analysis of open reading frames 62 and 71, encoding the varicella-zoster virus immediate-early transactivating protein, IE62, and effects on replication in vitro and in skin xenografts in the SCID-hu mouse in vivo. J Virol 77:5607–5620. https://doi.org/10.1128/JVI.77.10.5607-5620.2003.
28. Stellberger T, Hauser R, Baiker A, Pothineni VR, Haas J, Uetz P. 2010. Improving the yeast two-hybrid system with permutated fusions proteins: the varicella zoster virus interactome. Proteome Sci 8:8. https://doi.org/10.1186/1477-5956-8-8.
29. Uetz P. 2006. Herpesviral protein networks and their interaction with the human proteome. Science 311:239–242. https://doi.org/10.1126/science.1116804.
30. Riva L, Thiry M, Bontems S, Joris A, Piette J, Lebrun M, Sadzot-Delvaux C. 2013. ORF9p phosphorylation by ORF47p is crucial for the formation and egress of varicella-zoster virus viral particles. J Virol 87:2868–2881. https://doi.org/10.1128/JVI.02757-12.
31. Riva L, Thiry M, Lebrun M, L'homme L, Piette J, Sadzot-Delvaux C. 2015. Deletion of the ORF9p acidic cluster impairs the nuclear egress of varicella-zoster virus capsids. J Virol 89:2436–2441. https://doi.org/10.1128/JVI.03215-14.
32. Hirst J, Barlow LD, Francisco GC, Sahlender DA, Seaman MN, Dacks JB, Robinson MS. 2011. The fifth adaptor protein complex. PLoS Biol 9:e1001170. https://doi.org/10.1371/journal.pbio.1001170.
33. Robinson MS, Bonifacino JS. 2001. Adaptor-related proteins. Curr Opin Cell Biol 13:444–453. https://doi.org/10.1016/S0955-0674(00)00235-0.
34. Traub LM. 2005. Common principles in clathrin-mediated sorting at the Golgi and the plasma membrane. Biochim Biophys Acta 1744:415–437. https://doi.org/10.1016/j.bbamcr.2005.04.005.
35. Boehm M, Bonifacino JS. 2001. Adaptins: the final recount. Mol Biol Cell 12:2907–2920. https://doi.org/10.1091/mbc.12.10.2907.

36. Klumperman J, Hille A, Veenendaal T, Oorschot V, Stoorvogel W, von Figura K, Geuze HJ. 1993. Differences in the endosomal distributions of the two mannose 6-phosphate receptors. J Cell Biol 121:997–1010. https://doi.org/10.1083/jcb.121.5.997.
37. Traub LM, Ostrom JA, Kornfeld S. 1993. Biochemical dissection of AP-1 recruitment onto Golgi membranes. J Cell Biol 123:561–573. https://doi.org/10.1083/jcb.123.3.561.
38. Huang DW, Sherman BT, Lempicki RA. 2009. Systematic and integrative analysis of large gene lists using DAVID bioinformatics resources. Nat Protoc 4:44–57. https://doi.org/10.1038/nprot.2008.211.
39. Chen J, Bardes EE, Aronow BJ, Jegga AG. 2009. ToppGene suite for gene list enrichment analysis and candidate gene prioritization. Nucleic Acids Res 37:W305–W311. https://doi.org/10.1093/nar/gkp427.
40. Park SY, Guo X. 2014. Adaptor protein complexes and intracellular transport. Biosci Rep 34:e00123. https://doi.org/10.1042/BSR20140069.
41. Andrei G, van den Oord J, Fiten P, Opdenakker G, De Wolf-Peeters C, De Clercq E, Snoeck R. 2005. Organotypic epithelial raft cultures as a model for evaluating compounds against alphaherpesviruses. Antimicrob Agents Chemother 49:4671–4680. https://doi.org/10.1128/AAC.49.11.4671-4680.2005.
42. Elliott G, O'Hare P. 2000. Cytoplasm-to-nucleus translocation of a herpesvirus tegument protein during cell division. J Virol 74:2131–2141. https://doi.org/10.1128/JVI.74.5.2131-2141.2000.
43. Duffy C, Mbong EF, Baines JD. 2009. VP22 of herpes simplex virus 1 promotes protein synthesis at late times in infection and accumulation of a subset of viral mRNAs at early times in infection. J Virol 83:1009–1017. https://doi.org/10.1128/JVI.02245-07.
44. Sciortino MT, Taddeo B, Poon AP, Mastino A, Roizman B. 2002. Of the three tegument proteins that package mRNA in herpes simplex virions, one (VP22) transports the mRNA to uninfected cells for expression prior to viral infection. Proc Natl Acad Sci U S A 99:8318–8323. https://doi.org/10.1073/pnas.122231699.
45. Scharf B, Clement CC, Wu X-X, Morozova K, Zanolini D, Follenzi A, Larocca JN, Levon K, Sutterwala FS, Rand J, Cobelli N, Purdue E, Hajjar KA, Santambrogio L. 2012. Annexin A2 binds to endosomes following organelle destabilization by particulate wear debris. Nat Commun 3:755. https://doi.org/10.1038/ncomms1754.
46. Nakamura N, Rabouille C, Watson R, Nilsson T, Hui N, Slusarewicz P, Kreis TE, Warren G. 1995. Characterization of a cis-Golgi matrix protein, GM130. J Cell Biol 131:1715–1726. https://doi.org/10.1083/jcb.131.6.1715.
47. Nakamura N. 2010. Emerging new roles of GM130, a cis-Golgi matrix protein, in higher order cell functions. J Pharmacol Sci 112:255–264. https://doi.org/10.1254/jphs.09R03CR.
48. Ward DM, Vaughn MB, Shiflett SL, White PL, Pollock AL, Hill J, Schnegelberger R, Sundquist WI, Kaplan J. 2005. The role of LIP5 and CHMP5 in multivesicular body formation and HIV-1 budding in mammalian cells. J Biol Chem 280:10548–10555. https://doi.org/10.1074/jbc.M413734200.
49. Calistri A, Sette P, Salata C, Cancellotti E, Forghieri C, Comin A, Gottlinger H, Campadelli-Fiume G, Palu G, Parolin C. 2007. Intracellular trafficking and maturation of herpes simplex virus type 1 gB and virus egress require functional biogenesis of multivesicular bodies. J Virol 81:11468–11478. https://doi.org/10.1128/JVI.01364-07.
50. Pawliczek T, Crump CM. 2009. Herpes simplex virus type 1 production requires a functional ESCRT-III complex but is independent of TSG101 and ALIX expression. J Virol 83:11254–11264. https://doi.org/10.1128/JVI.00574-09.
51. Komuro M, Tajima M, Kato K. 1989. Transformation of Golgi membrane into the envelope of herpes simplex virus in rat anterior pituitary cells. Eur J Cell Biol 50:398–406.
52. Gershon AA, Sherman DL, Zhu Z, Gabel CA, Ambron RT, Gershon MD. 1994. Intracellular transport of newly synthesized varicella-zoster virus: final envelopment in the trans-Golgi network. J Virol 68:6372–6390.
53. Granzow H, Weiland F, Jöns A, Klupp BG, Karger A, Mettenleiter TC. 1997. Ultrastructural analysis of the replication cycle of pseudorabies virus in cell culture: a reassessment. J Virol 71:2072–2082.
54. Granzow H, Klupp BG, Fuchs W, Veits J, Osterrieder N, Mettenleiter TC. 2001. Egress of alphaherpesviruses: comparative ultrastructural study. J Virol 75:3675–3684. https://doi.org/10.1128/JVI.75.8.3675-3684.2001.
55. Olson JK, Grose C. 1997. Endocytosis and recycling of varicella-zoster virus Fc receptor glycoprotein gE: internalization mediated by a YXXL motif in the cytoplasmic tail. J Virol 71:4042–4054.
56. Bresnahan PA, Yonemoto W, Ferrell S, Williams-Herman D, Geleziunas R, Greene WC. 1998. A dileucine motif in HIV-1 Nef acts as an internalization signal for CD4 downregulation and binds the AP-1 clathrin adaptor. Curr Biol 8:1235–1238. https://doi.org/10.1016/S0960-9822(07)00517-9.
57. Pérez-Núñez D, García-Urdiales E, Martínez-Bonet M, Nogal ML, Barroso S, Revilla Y, Madrid R. 2015. CD2v interacts with adaptor protein AP-1 during African swine fever infection. PLoS One 10:e0123714. https://doi.org/10.1371/journal.pone.0123714.
58. Hartmann-Stühler C, Prange R. 2001. Hepatitis B virus large envelope protein interacts with gamma2-adaptin, a clathrin adaptor-related protein. J Virol 75:5343–5351. https://doi.org/10.1128/JVI.75.11.5343-5351.2001.
59. Wan L, Molloy S, Thomas L, Liu G, Xiang Y, Rybak SL, Thomas G. 1998. PACS-1 defines a novel gene family of cytosolic sorting proteins required for trans-Golgi network localization. Cell 94:205–216. https://doi.org/10.1016/S0092-8674(00)81420-8.
60. Piguet V, Wan L, Borel C, Mangasarian A, Demaurex N, Thomas G, Trono D. 2000. HIV-1 Nef protein binds to the cellular protein PACS-1 to downregulate class I major histocompatibility complexes. Nat Cell Biol 2:163–167. https://doi.org/10.1038/35004038.
61. O'Regan KJ, Murphy MA, Bucks MA, Wills JW, Courtney RJ. 2007. Incorporation of the herpes simplex virus type 1 tegument protein VP22 into the virus particle is independent of interaction with VP16. Virology 369:263–280. https://doi.org/10.1016/j.virol.2007.07.020.
62. Padilla JA, Nii S, Grose C. 2003. Imaging of the varicella zoster virion in the viral highways: comparison with herpes simplex viruses 1 and 2, cytomegalovirus, pseudorabies virus, and human herpes viruses 6 and 7. J Med Virol 70:S103–S110. https://doi.org/10.1002/jmv.10330.
63. Carpenter JE, Henderson EP, Grose C. 2009. Enumeration of an extremely high particle-to-PFU ratio for varicella-zoster virus. J Virol 83:6917–6921. https://doi.org/10.1128/JVI.00081-09.
64. Buckingham EM, Jarosinski KW, Jackson W, Carpenter JE, Grose C. 2016. Exocytosis of varicella-zoster virus virions involves a convergence of endosomal and autophagy pathways. J Virol 90:8673–8685. https://doi.org/10.1128/JVI.00915-16.
65. Grose C, Buckingham E, Carpenter J, Kunkel J. 2016. Varicella-zoster virus infectious cycle: ER stress, autophagic flux, and amphisome-mediated trafficking. Pathogens 5:67. https://doi.org/10.3390/pathogens5040067.
66. Iijima S, Lee Y-J, Ode H, Arold ST, Kimura N, Yokoyama M, Sato H, Tanaka Y, Strebel K, Akari H. 2012. A noncanonical mu-1A-binding motif in the N terminus of HIV-1 Nef determines its ability to downregulate major histocompatibility complex class I in T lymphocytes. J Virol 86:3944–3951. https://doi.org/10.1128/JVI.06257-11.
67. Traub LM, Bannykh SI, Rodel JE, Aridor M, Balch WE, Kornfeld S. 1996. AP-2-containing clathrin coats assemble on mature lysosomes. J Cell Biol 135:1801–1814. https://doi.org/10.1083/jcb.135.6.1801.
68. Debrus S, Sadzot-Delvaux C, Nikkels AF, Piette J, Rentier B. 1995. Varicella-zoster virus gene 63 encodes an immediate-early protein that is abundantly expressed during latency. J Virol 69:3240–3245.
69. James P, Halladay J, Craig EA. 1996. Genomic libraries and a host strain designed for highly efficient two-hybrid selection in yeast. Genetics 144:1425–1436.
70. Walhout AJ, Vidal M. 2001. High-throughput yeast two-hybrid assays for large-scale protein interaction mapping. Methods 24:297–306. https://doi.org/10.1006/meth.2001.1190.
71. Rolland T, Tasan M, Charloteaux B, Pevzner SJ, Zhong Q, Sahni N, Yi S, Lemmens I, Fontanillo C, Mosca R, Kamburov A, Ghiassian SD, Yang X, Ghamsari L, Balcha D, Begg BE, Braun P, Brehme M, Broly MP, Carvunis AR, Convery-Zupan D, Corominas R, Coulombe-Huntington J, Dann E, Dreze M, Dricot A, Fan C, Franzosa E, Gebreab F, Gutierrez BJ, Hardy MF, Jin M, Kang S, Kiros R, Lin GN, Luck K, MacWilliams A, Menche J, Murray RR, Palagi A, Poulin MM, Rambout X, Rasla J, Reichert P, Romero V, Ruyssinck E, Sahalie JM, Scholz A, Shah AA, Sharma A, et al. 2014. A proteome-scale map of the human interactome network. Cell 159:1212–1226. https://doi.org/10.1016/j.cell.2014.10.050.
72. Rual JF, Venkatesan K, Hao T, Hirozane-Kishikawa T, Dricot A, Li N, Berriz GF, Gibbons FD, Dreze M, Ayivi-Guedehoussou N, Klitgord N, Simon C, Boxem M, Milstein S, Rosenberg J, Goldberg DS, Zhang LV, Wong SL, Franklin G, Li S, Albala JS, Lim J, Fraughton C, Llamosas E, Cevik S, Bex C, Lamesch P, Sikorski RS, Vandenhaute J, Zoghbi HY, Smolyar A, Bosak S, Sequerra R, Doucette-Stamm L, Cusick ME, Hill DE, Roth FP, Vidal M. 2005. Towards a proteome-scale map of the human protein-protein interaction network. Nature 437:1173–1178. https://doi.org/10.1038/nature04209.
73. Trapp-Fragnet L, Bencherit D, Chabanne-Vautherot D, Le Vern Y, Remy S,

Boutet-Robinet E, Mirey G, Vautherot JF, Denesvre C. 2014. Cell cycle modulation by Marek's disease virus: the tegument protein VP22 triggers S-phase arrest and DNA damage in proliferating cells. PLoS One 9:e100004. https://doi.org/10.1371/journal.pone.0100004.

74. Zhang Z, Huang Y, Zhu H. 2008. A highly efficient protocol of generating and analyzing VZV ORF deletion mutants based on a newly developed luciferase VZV BAC system. J Virol Methods 148:197–204. https://doi.org/10.1016/j.jviromet.2007.11.012.

75. Warming S, Costantino N, Court DL, Jenkins NA, Copeland NG. 2005. Simple and highly efficient BAC recombineering using galK selection. Nucleic Acids Res 33:e36. https://doi.org/10.1093/nar/gni035.

76. Carpenter AE, Jones TR, Lamprecht MR, Clarke C, Kang I, Friman O, Guertin DA, Chang J, Lindquist RA, Moffat J, Golland P, Sabatini DM. 2006. CellProfiler: image analysis software for identifying and quantifying cell phenotypes. Genome Biol 7:R100. https://doi.org/10.1186/gb-2006-7-10-r100.

Part III

ORF9p and cell-cell fusion

4 Aim of the work

As already described before, VZV is commonly known to form gigantic syncytia upon infection of MeWo cells. Surprisingly, we noticed that the ORF9p-L231A mutant did not induce syncytia formation in cell culture. Even more surprising, the fusion phenotype is restored after 10 to 15 passages of the ORF9p-L231A mutant in cell culture.

The aim of the second part of this thesis was to decipher the role of ORF9p in cell-cell fusion. First, we sequenced ten naturally occurring ORF9-L231A-Revertants to know if additional mutations in the genome of VZV were responsible for the reappearance of syncytia in infected MeWo cells. The impact of the additional mutations on foci growth and syncytia formation was then evaluated *in vitro*. Moreover, we investigated whether or not ORF9p could increase cell fusion when expressed with the core fusion machinery in a cell fusion assay. We also investigated the interaction between ORF9p and some glycoproteins in an ORF9p-WT or ORF9p-L231A context. Finally, the distribution of the glycoproteins at the surface of infected cells was assessed in an ORF9p-WT or ORF9p-L231A context.

5 Results

5.1 L231A substitution in ORF9p impedes cell-cell fusion

As previously reported, L231A substitution in VZV ORF9p leads to an important replication defect *in vitro* [227]. Interestingly, this replication defect is associated with a lack of cell-cell fusion in MeWo cells (Figure 5.1). After 24h of infection, approximately one third of MeWo cells infected with VZV-ORF9-V5 (hereafter called 9WT) showed evident signs of cell-cell fusion (not shown). At 48 h.p.i, almost all foci formed extensive syncytia. On the contrary, cells infected with VZV-ORF9-L231A-V5 (hereafter called 9L231A) showed no apparent cell-cell fusion, even after 72h post-infection. More importantly, after ten to fifteen passages in culture, this phenotype is reverted and syncytia are observed again (Figure 5.1). The foci formed by the revertant were similar to those formed by the 9WT virus, with roughly 90% of the foci forming large syncytia at 48 h.p.i. These results suggest an important role for VZV ORF9p in MeWo cell-cell fusion.

5.2 Compensatory mutations on gH and/or gE restore 9L231A fusion phenotype

To understand if the reversion of the fusion phenotype observed after several passages of the 9L231A mutant was due to compensatory mutations in the VZV genome, we sequenced the entire genome of ten different spontaneous 9L231A revertants that appeared after several successive passages of the 9L231A mutant in cell culture (Figure 5.2). Eight of these spontaneous revertants had mutations in the gH coding sequence and four in the gE coding sequence (Figure 5.2A). Interestingly, 80% of the mutations in gH led to the apparition of an early stop codon in its cytoplasmic tail, truncating the last eight or nine amino acids of gHcyt (Figure 5.2B). In addition, two spontaneous revertants harbored a double mutation on gE (D436H and D620Y), without additional mutations on gH (Rev-2 and Rev-6, Figure 5.2A). The first gE mutation (D436H) appears in its extracellular domain, close to a N-glycosylation site and between two cysteine residues forming a disulfide bond (Figure 5.2B). The second mutation (D620Y) touches the intracellular domain of gE, close to the end of the protein. Bioinformatics analysis using the eukaryotic linear motif (ELM) prediction tool showed that these mutations are unlikely to impact the existence of functional motifs within gE.

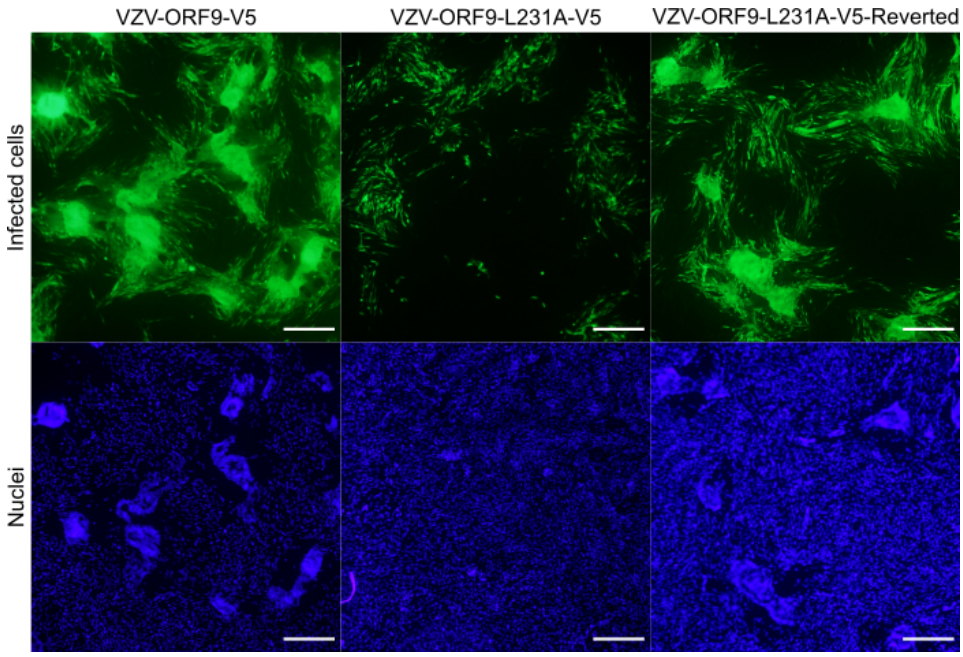

Figure 5.1: **ORF9-L231A mutation leads to a fusion defect that is reverted after a few passages.** MeWo cells were infected with VZV-9WT, VZV-9L231A or VZV-9L231A-Reverted, fixed with 4% PFA, and nuclei were labelled with Hoechst. Infected cells express GFP and are shown in green. Images were taken using an Olympus FSX-100 microscope with 40X magnification. Scale bar represents 250 μm. Figure shows representative foci at 48 h.p.i.

5.3 Spontaneous mutations in gH or gE partially restore VZV-9L231A spread *in vitro*

To evaluate the impact of the gH or gE mutations on VZV-9L231A spread, gH-E834STOP (hereafter called gHΔcyt) or gE-D436H/D620Y (hereafter called gE-Dble) mutations were introduced in a BAC containing the complete VZV genome in an ORF9-L231A-V5 background. Transfection of MeWo cells with these BACs rapidly gave rise to infections. The impact of the different mutations on viral spread and cell-cell fusion was evaluated by measuring foci or syncytia area and percentage of syncytia among the foci. A total of 300 foci and 150 syncytia from three independent experiments were analyzed for each virus (Figure 5.3).

The mutation of either gH or gE partially restored 9L231A spread compared to 9WT (91% and 82% of 9WT foci size, respectively) (Figure 5.3A). To assess the impact of gH or gE mutations on cell-cell fusion, we first calculated the

A

	ORF37 (gH)					ORF68 (gE)	
ORF9-L231A-V5	Promotor	A168V	D686Y	Y804D	STOP codon	D436H	D620Y
Rev-1					E834STOP (31 %)		42%
Rev-2						96%	85%
Rev-3	A->G (33%)				E834STOP (71 %)		
Rev-4		21%			E834STOP (34 %)		52%
Rev-5					R833STOP (36 %)		
Rev-6						85%	89%
Rev-7				16%	E834STOP (78 %)		
Rev-8			13%		E834STOP (72 %)		
Rev-9					R833STOP (30 %)		
Rev-10					R833STOP (41 %)		

B

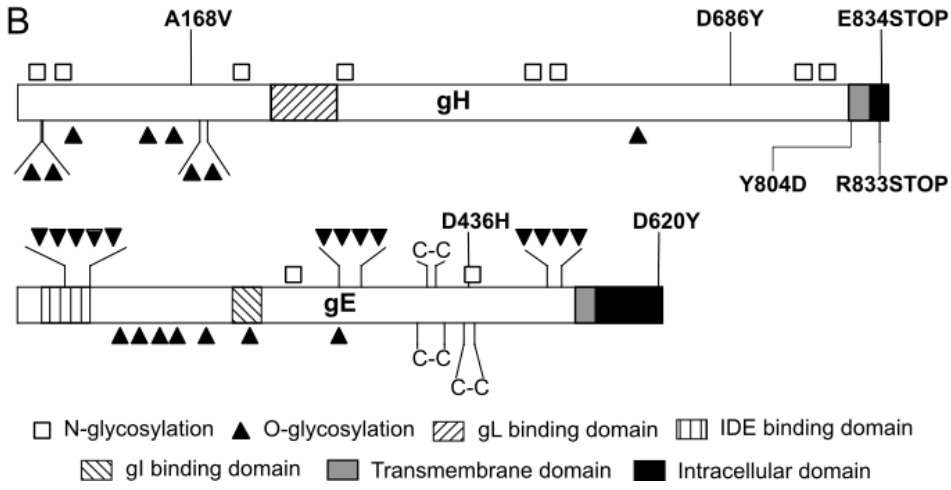

Figure 5.2: **Reversion of 9L231A fusion phenotype is associated with mutations in VZV gH and/or gE.** The complete genomes of 10 different spontaneous revertants from 9L231A mutant were sequenced to assess if the reversion of the fusion phenotype was associated with compensatory mutations. A) Percentages on the table represent the number of reads in the DNA sample presenting the mutation. B) Schematic representation of VZV gH and gE and their respective mutations. Information regarding the modifications on gH and gE were obtained from Uniprot and [23].

percentage of syncytia among the foci present in our samples (Figure 5.3B). At 48 h.p.i. almost all VZV-9WT foci (96%) had formed syncytia. On the contrary, only 4% of VZV-9L231A foci showed signs of cell-cell fusion. The introduction of gH or gE mutations in VZV-9L231A completely restored the percentage of infectious foci presenting syncytia in these samples (Figure 5.3B).

To further analyze the impact of gH or gE mutations on cell-cell fusion, we measured the ratio of the syncytia area compared to the foci area (Figure 5.3C). This allowed us to evaluate the fusion capacity of each virus without taking into account the differences in syncytia or foci size between the different viruses. As the number of syncytia formed by VZV-9L231A mutant was too low to obtain sufficient measures, this mutant was removed from the analysis. The mean ratios calculated from 150 infection foci show that mutations on either gE or gH not only restore the fusion capacity, but actually lead to an hyperfusion phenotype compared to the WT (Figure 5.3C).

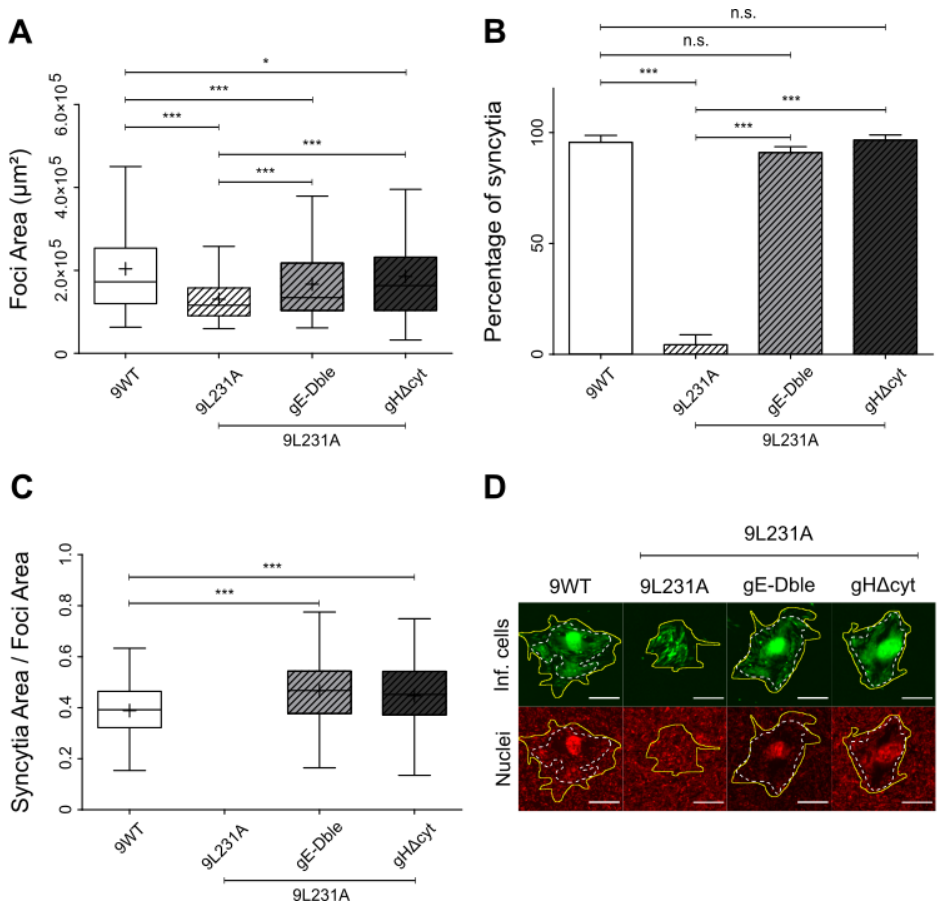

Figure 5.3: **Mutations on gH or gE partially restore VZV-9L231A spread and restore cell-cell fusion.** MeWo cells were seeded in 6-well plates and infected with VZV-9WT or VZV-9L231A with or without additional mutations on gH (gH-WT or gHΔcyt) or gE (gE-WT or gE-Dble). At 48 h.p.i. cells were fixed with 4% PFA and Nuclei were stained using Nuclear-ID Red DNA stain. *(continued on next page).*

Figure 5.3 (previous page)*:* Picture of the whole well were taken with a 4X objective using an Incucyte S3. For each virus, a total of 300 foci from three independent experiments were randomly selected for analysis. Among those 300 foci, 150 were randomly selected for syncytia analysis, except for 9L231A mutant which presented too few syncytia. A) Foci area was measured manually using ImageJ. B) For each mutant, the percentage of syncytia was calculated manually. C) The fusogenic capacity of each mutant was calculated by dividing the syncytia area by the foci area. D) Pictures of representative foci for each mutant. The yellow line shows the foci limits, while the white dotted line shows the syncytia limits. Scale bar represents 250 μm. A and C, a Kruskal-Wallis test was performed to compare the variance of the samples, then a Dunn's multiple comparison test was performed to compare the represented pairs of viruses. The boxplot depicts the 1st and 3rd quantiles, the horizontal bar shows the median and the cross shows the mean. The upper error bar represents Q3 + 1.5 x IQR, while the lower error bar represents Q1 1.5 x IQR. B, a one-way ANOVA was performed to compare the variance of the samples, then a Bonferoni's multiple comparison test was performed to compare the represented pairs of viruses. The graph shows the mean percentage of syncytia. Error bars represent standard deviation. *, P<0.05. **, P<0.01. ***, P<0.001.

5.4 gE or gH mutations further increase fusion in a 9WT infection

In order to study the impact of gH or gE mutations on cell-cell fusion in a 9WT context, VZV mutants were constructed as described above and their spread and fusion capacity was analyzed.

In a 9WT context, addition of the gH mutation decreased viral spread by 21% (Figure 5.4A). On the other hand, gE mutations had no impact on foci size as compared to 9WT. Neither mutation on gH nor gE impacted the percentage of syncytia at 48h.p.i. (Figure 5.4B), but both increased cell-cell fusion compared to WT (Figure 5.4C).
Interestingly, no statistically significant difference was found when comparing the foci size or the syncytia/foci area ratio of 9WT-gHΔcyt and 9L231A-gHΔcyt or 9WT-gE-Dble and 9L231A-gE-Dble, suggesting that mutations on gH or gE act independently of the ORF9p/AP-1 interaction (Supplemental Figure 6.1).

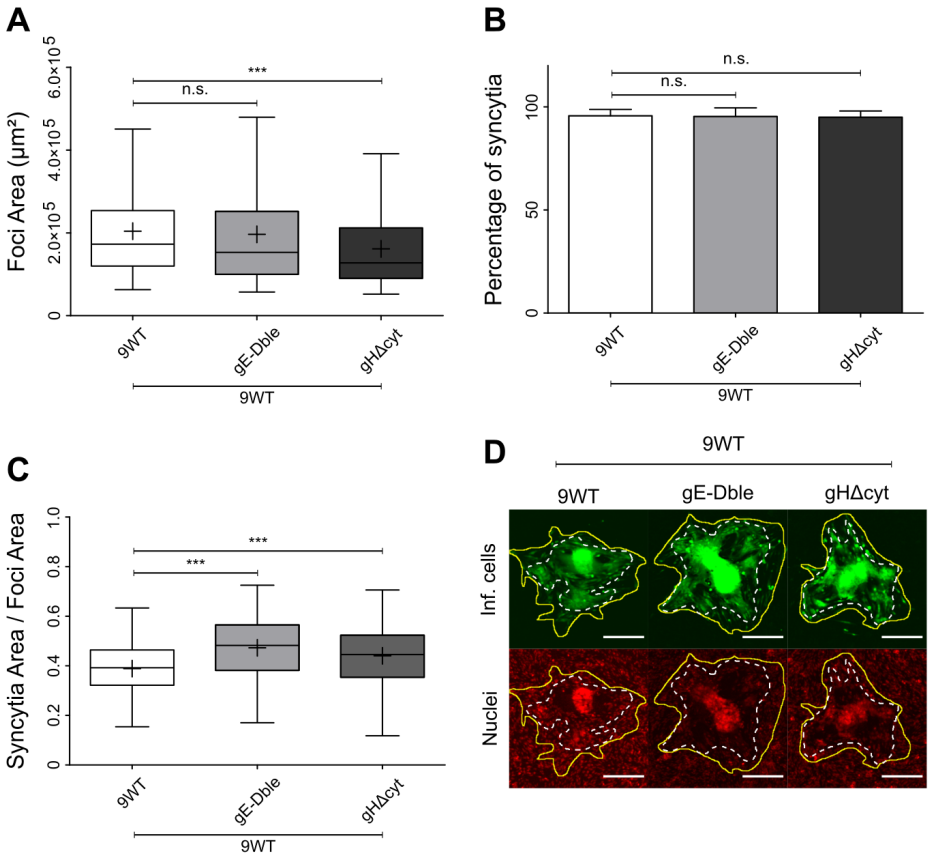

Figure 5.4: **Mutations on gH or gE increase the fusogenicity of VZV-9WT.** MeWo cells were seeded in 6-well plates and infected with VZV-9WT with or without additional mutations on gH (gH-WT or gHΔcyt) or gE (gE-WT or gE-Dble). At 48 h.p.i. cells were fixed with 4% PFA and Nuclei were stained using Nuclear-ID Red DNA stain. Pictures of the whole well were taken with a 4X objective using an Incucyte S3. For each virus, a total of 300 foci from three independent experiments were randomly selected for analysis. Among those 300 foci, 150 were randomly selected for syncytia analysis. A) Foci area was measured manually using ImageJ. B) For each mutant, the percentage of syncytia was calculated manually. C) The fusogenic capacity of each mutant was calculated by dividing the syncytia area by the foci area. D) Pictures of representative foci for each mutant. The yellow line shows the foci limits, while the white dotted line shows the syncytia limits. Scale bar represents 250 μm. A and C, a Kruskal-Wallis test was performed to compare the variance of the samples, then a Dunn's multiple comparison test was performed to compare each mutant to the WT. The boxplot depicts the 1st and 3rd quantiles, the horizontal bar shows the median and the cross shows the mean. The upper error bar represents Q3 + 1.5 x IQR, while the lower error bar represents Q1 1.5 x IQR. *(continued on next page)*.

Figure 5.4 (previous page)*:* B, a one-way ANOVA was performed to compare the variance of the samples, then a Dunnett's multiple comparison test was performed to compare each mutant to the WT. The graph shows the mean percentage of syncytia. Error bars represent standard deviation. *, P<0.05. **, P<0.01. ***, P<0.001.

5.5 ORF9p increases cell fusion when expressed with the core fusion machinery *in vitro*

To know if ORF9p could impact cell fusion without other viral proteins (except the core fusion machinery), we performed a cell fusion assay. This assay was initially developed by Ishikawa *et al.* using a dual split protein (DSP) reporter [176]. This assay was then adapted to VZV by Yang *et al.* [439]. Briefly, CHO cells expressing the DSP1 half of a GFP-luciferase construct were transfected to express gB or gB/gH-gL with or without ORF9p or ORF9p-L231A. These cells were then mixed with MeWo cells expressing the DSP2 half of the GFP-luciferase. When cell fusion occurs, the two halves of the GFP-luciferase construct can self-associate and luminescence signal can be detected.

As expected, when only gB was present (with or without ORF9p or ORF9p-L231A), no fusion occurred, but when gB was expressed with gH-gL, CHO and MeWo cells started to fuse (Figure 5.5). Interestingly, expression of ORF9p in combination with gB/gH-gL significantly enhanced cell fusion, regardless of the presence of the ORF9p-L231A mutation, suggesting that ORF9p may impact cell fusion without any other viral proteins but the gB/gH-gL complex (Figure 5.5).

5.6 The 9L231A mutation diminishes the ORF9p/gH as well as the ORF9p/gE interaction

To evaluate if ORF9p played a role in cell fusion directly by acting on the glycoproteins interactions network, we performed co-immunoprecipitations studies. We focused our attention on both gH and gE because gH is known to be mandatory to induce cell fusion and because mutations on both proteins increased the fusion capacity of the virus. Two separate immunoprecipitations were done in parallel using the same pre-cleared cell extracts and magnetic beads coupled with an anti-gE or anti-gH antibody. After stringent washes of the beads, the bound proteins were eluted and separated on a SDS-PAGE gel. After the transfer step, the membranes were

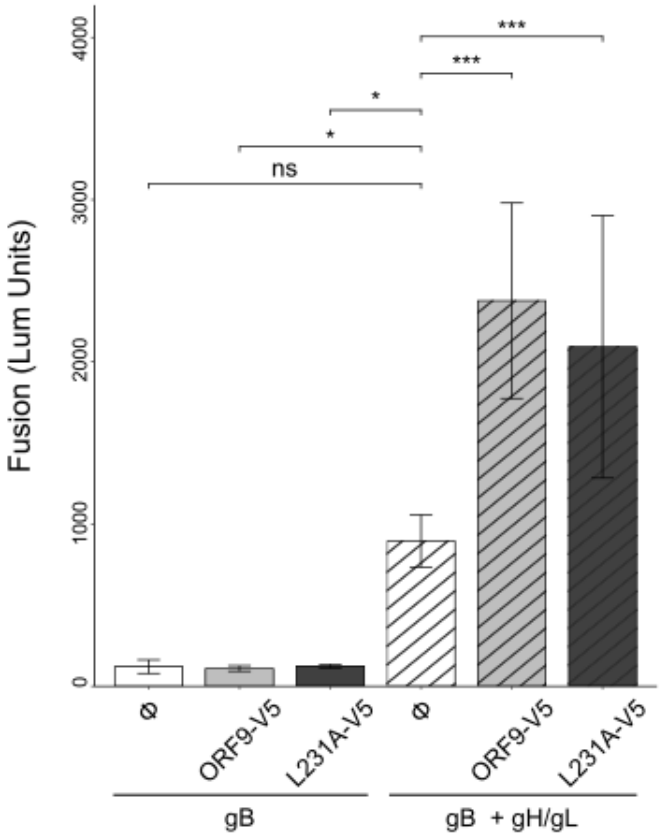

Figure 5.5: **Effect of ORF9p on VZV gB/gH-gL-mediated cell-cell fusion.** CHO-DSP1 cells were transfected to express gB or gB/gH-gL without (Φ) or with ORF9-V5 or ORF9-L231A-V5 and were then mixed with MeWo-DSP2 cells. Fusion efficiency was measured by *Renilla* luminescence at 48h post transfection and is presented as raw Lum units. The experiment was repeated twice with two clones/condition in each experiment. The graph represents the mean fusion and error bars represent standard deviation. Statistical differences are compared to gB/gH-gL without ORF9p by a one-way ANOVA test followed by a Dunnett's multiple comparison test. *, P<0.05. **, P<0.01. ***, P<0.001. Experiment performed by Dr. Momei Zhou from Stanford university.

cut in two to perform Western blots against gE, gH and V5 (ORF9p) in parallel.

As expected from previous results and from the literature, ORF9p interacts with gE in a wild-type context (Figure 5.6A). The 9L231A mutation strongly decreases this interaction (Figure 5.6A, compare lane 10 with lane 9). The interaction is restored by the gE-Dble mutations but not by the gHΔcyt

mutation. After the first Western blot, the membrane pieces were stripped to remove the bound antibodies and subsequently incubated with an anti-gB antibody. As shown in the input in Figure 5.6A, gB is present in infected cells in a premature, uncleaved form of about 120 kD and in a mature, cleaved form around 55 kD. Interestingly, the mature form of gB is also found to precipitate with gE, but only when ORF9p also interacts with gE. The membranes were then stripped a second time before incubation with an anti-gI antibody which showed that the gE/gI interaction is present regardless of the ORF9p/gE interaction.

On the other hand, ORF9p also interacts with gH in a wild-type context (Figure 5.6B). This interaction is also strongly impacted by the 9L231A mutation. Neither the gE-Dble mutations, nor the gHΔcyt mutation were able to restore the ORF9p/gH interaction. The membrane pieces were also stripped then incubated with an anti-gB antibody. The mature form of gB is, again, co-immunoprecipitating with the anti-gH coupled beads only when ORF9p is present in the complex. This seems to prove that the immunoprecipitation of gH is indeed working even though no signal is seen on the anti-gH Western blot (Figure 5.6B, upper panel). The membranes were stripped a second time to perform the anti-gI Western blot, which gave no signal, showing that the complexes immunoprecipitated with either the anti-gE or the anti-gH are most likely different.

We struggled to understand why we could not detect gH by Western blot in these co-immunoprecipitation experiments. Our hypothesis is that the antibody was unable to detect the denaturated form of gH. To overcome this problem and also to know whether we could recapitulate and study the glycoprotein networks outside the infection context, we generated transient transfection vectors for ORF9p (WT and L231A), gE (WT and D436H/D620Y), gI, gB, gH (WT and Δcyt), and gL. We cloned V5-tagged versions of ORF9p and for gH, we inserted a FLAG tag right after the signal peptide. These constructs were then transfected in HEK293 cells and the immunoprecipitation experiments were repeated using the same conditions as described above.
By cotransfection of ORF9p-V5, gE, and gI expressing vectors, we first confirmed that the 9L231A mutation reduces the ORF9p/gE interaction, but, this time, the additional mutations on gE could not restore the interaction with the 9L231A mutant (Figure 5.6C).
By cotransfection of ORF9p-V5, Flag-gH, gB, and gL, we then confirmed that ORF9p interacts with gH in a 9WT context. This ineracton is reduced when ORF9p is mutated, and the mutation on gH does not restore the interaction (Figure 5.6D). In this experiment, gB is found to interact with gH independently of the ORF9p/gH interaction. It is however important

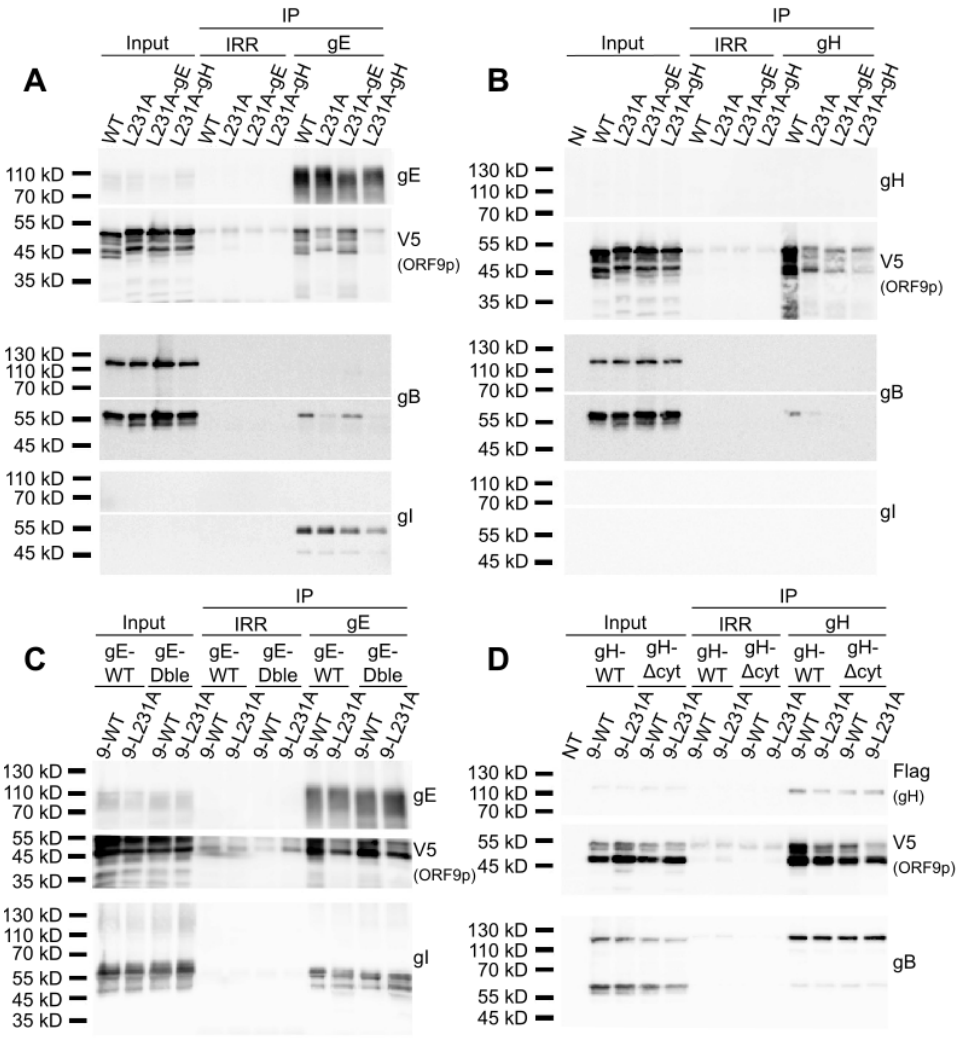

Figure 5.6: **Effect of the L231A, gE and gH mutations on the ORF9p/gE and ORF9p/gH interactions.** MeWo cells were infected (A and B) or transfected (C and D) for 48h before lysis. The samples were then precleared and separated in two to have the gE or gH immunoprecipitations performed in parallel.A) gE immunoprecipitation in infection. B) gH immunoprecipitation in infection. C) gE immunoprecipitation in transfection. D) gH immunoprecipitation in transfection. Immunoprecipitations in infection and transfection were repeated at least three times, representative pictures are shown.

to note that this time, it is the premature form of gB that interacts with gH. This is in accordance with results previously obtained by Oliver *et al.* [301]. It is also noteworthy that, in transfection, the main ORF9p band

observed (around 45 kD) is different than the one observed in infection (around 55 kD). Thus, even if the transfection experiments are useful to study the protein-protein interactions, it does not entirely recapitulate what happens in the course of an infection.

5.7 The 9L231A mutation impacts the cell surface distribution of the glycoproteins

As described above, ORF9p-WT interacts with gE and gH (and gB) in infected cells, but not the 9L231A mutant. To know if this lack of interaction had an impact on glycoproteins expression and distribution at the cell surface, we performed an immunofluorescence experiment (Figure 5.7).

First, we studied the expression of the glycoproteins in 9WT- or 9L231A-infected permeabilized cells. No major difference was observed between both infections, which showed glycoproteins heavily present in the perinuclear region. This suggests that the lack of fusion observed with the 9L231A mutant does not result from a lack of glycoprotein production (see Supplemental Figure 6.2).

Then, we studied the expression and localization of the glycoproteins at the surface of non-permeabilized cells. As shown on Figure 5.7A, gB, gH and gE all are heavily present at the surface of the syncytia. Interestingly, the glycoproteins are not evenly distributed at the cell surface, but seem to cluster in restricted area of the surface. This is not only the case in fused cells, but also in cells at an earlier stage of infection (Figure 5.7B). On the contrary, in 9L231A-infected cells, whereas the glycoproteins are also strongly expressed at the surface, they seem to be more evenly distributed. In both 9WT- and 9L231A-infected cells, no obvious difference in gB/gE or gB/gH colocalization was observed. Altogether, these results suggest that the interaction between ORF9p and the glycoproteins is important for their correct targeting towards specific regions of the cell surface.

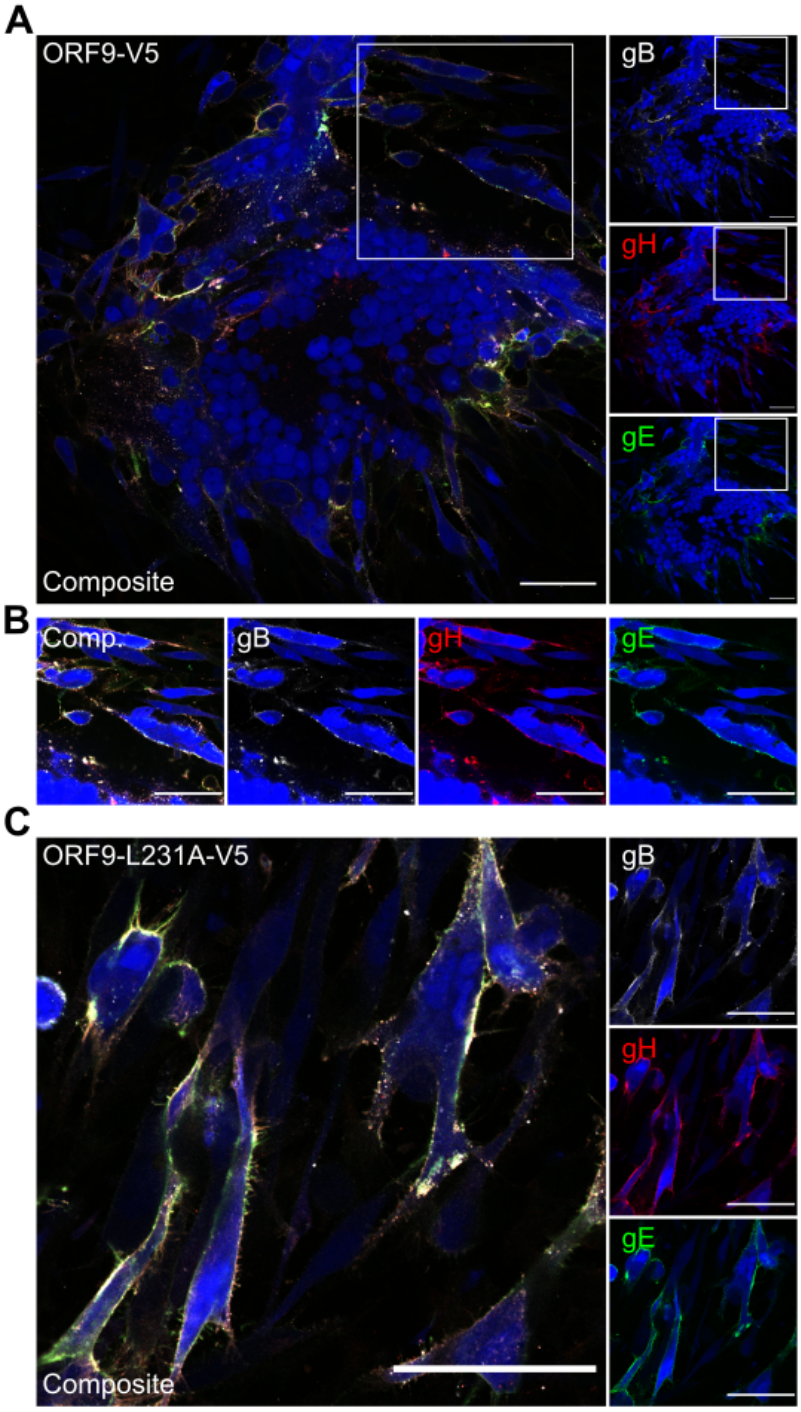

Figure 5.7: **ORF9p L231A mutation impacts the glycoproteins distribution at the surface of infected cells.** *(continued on next page).*

Figure 5.7 (previous page)*:* MeWo cells were seeded on coverslips and infected for 48h. The coversilps were then washed with PBS and fixed with 4% PFA. Cells were labeled with the different antibodies without permeabilization. Images were taken with a Zeiss LSM 980 microscope with a 60x objective. A) 9WT-infected cells. B) Magnification of the squared area in A. C) 9L231A-infected cells. gB is shown in white, gH in red, gE in green, and infected cells are shown in blue. Scale bar represents 50 μm. Experiments were repeated three times and representative pictures are shown.

6 Supplemental Figures

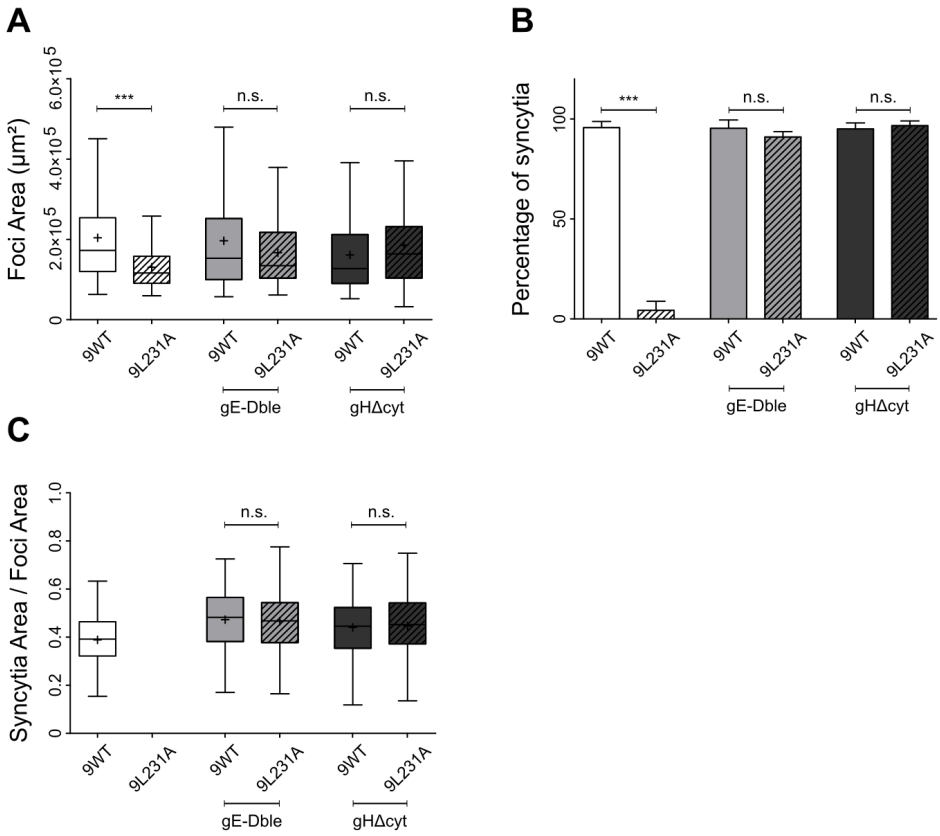

Figure 6.1: **gH or gE mutations increase cell-cell fusion regardless of ORF9p.** MeWo cells were seeded in 6-well plates and infected with VZV-9WT or VZV-9L231A with or without additional mutations on gH (gH-WT or gHΔcyt) or gE (gE-WT or gE-Dble). At 48 h.p.i. cells were fixed with 4% PFA and Nuclei were stained using Nuclear-ID Red DNA stain. Pictures of the whole well were taken with a 4X objective using an Incucyte S3. For each virus, a total of 300 foci from three independent experiments were randomly selected for analysis. Among those 300 foci, 150 were randomly selected for syncytia analysis, except for 9L231A mutant which presented too few syncytia. A) Foci area was measured manually using ImageJ. B) For each mutant, the percentage of syncytia was calculated manually. C) The fusogenic capacity of each mutant was calculated by dividing the syncytia area by the foci area. A and C, a Mann Whitney test was performed to compare the represented pairs of viruses. The boxplot depicts the 1st and 3rd quantiles, the horizontal bar shows the median and the cross shows the mean.*(continued on next page)*.

Figure 6.1 (previous page)*:* The upper error bar represents Q3 + 1.5 x IQR, while the lower error bar represents Q1 1.5 x IQR. B, a two-tailed t test was performed to compare the represented pairs of viruses. The graph shows the mean percentage of syncytia. Error bars represent standard deviation. *, P<0.05. **, P<0.01. ***, P<0.001.

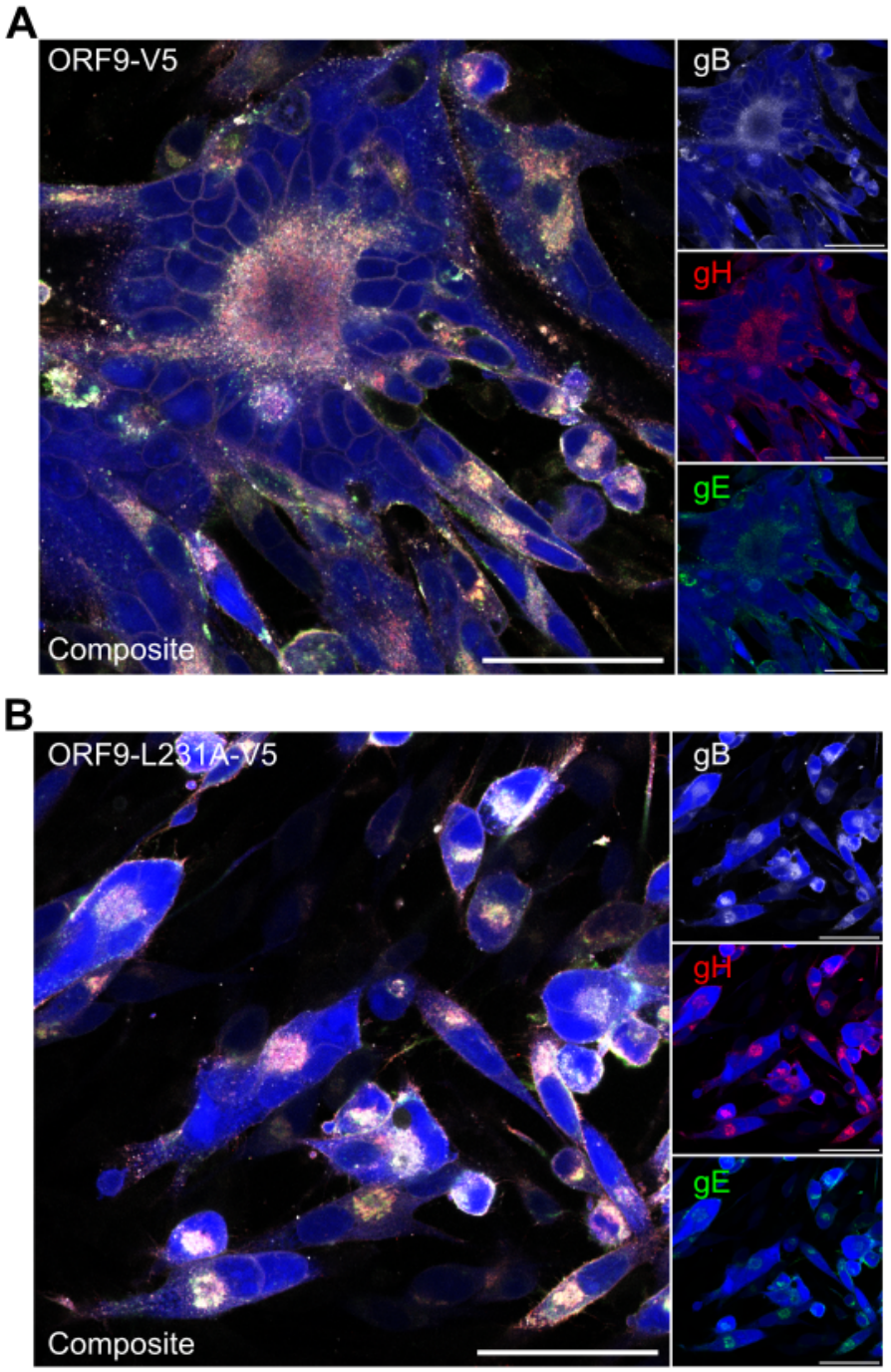

Figure 6.2: **Glycoproteins expression in 9WT- and 9L231A-infected cells.**
(continued on next page).

Figure 6.2 (previous page)*:* MeWo cells were seeded on coverslips and infected for 48h. The coverslips were then washed with PBS and fixed with 4% PFA. Cells were permeabilized with 0.1% Triton-X100 then labeled with the different antibodies. Images were taken using a Zeiss LSM 980 microscope with a 60X objective. A) 9WT-infected cells. B) 9L231A-infected cells. gB is shown in white, gH in red, gE in green, and infected cells are shown in blue. Scale bar represents 50 μm. Experiment was repeated thrice and representative pictures are shown.

Part IV

Materials and methods

7 Materials and methods

Cell Culture

MeWo (human melanoma cell line; ATCC HTB-65) cells were cultured in Eagle minimal essential medium supplemented with 1% nonessential amino acids, 1% L-glutamine, 1% antibiotic mix (penicillin-streptomycin), and 10% fetal bovine serum (Fisher Scientific).

Recombinant virus production

To reconstitute recombinant viruses, MeWo cells were transfected with bacterial artificial chromosomes (BACs) containing the entire WT or mutated pOka genome (3 μg per well of 6-well plates) using 4.5 μL of JetPEI transfection reagent. All BACs contained a gene coding for GFP under the control of the Cytomegalovirus promoter, allowing the detection of infected cells by confocal microscopy. At 3 days post transfection, the cells were transferred into a 25 cm^2 flask and passaged every 2 to 3 days until typical infection foci appeared.

Antibodies

Monoclonal mouse anti-gH (HR-VZV-22) and anti-gB (HR-VZV-15) used in immunoprecipitation or western-blot were purchase at CAPRI. Anti-gH and anti-gB used in immunofluorescence were from Meridian Life Sciences and were directly coupled to CF568 and CF633 respectively, using a coupling kit from Sigma-Aldrich (Mix-n-stain, MX568S100 and MX633S100). Mouse anti-gE was produced and characterized in our laboratory some years ago [287]. Mouse anti-V5 (R960-25) was purchased from Thermofisher.

Construction of BAC-VZV carrying the gH or gE mutations

All constructs were generated by modification of the BAC-VZV-pOka WT (a kind gift from H. Zhu [453]) using the "en passant" technique described by Tischer *et al.* [407].

First, the recombination cassette was generated by PCR using the primers listed in table 7.1 and the pEPkan-S plasmid as a template. Then, 100 ng of

the purified PCR product where electroporated in electro-competent GS1783 bacteria containing the VZV BAC with the following settings: 17.5 kV/cm, 25 μF, and 200 Ω. The bacteria were then placed in a shaking incubator for 1h at 32°C in 1 mL of LB medium. The bacteria were diluted 8X in LB + 12.5 μg/mL chloramphenicol + 25 μg/mL kanamycin and plated on chloramphenicol + kanamycin plates and incubated at 32°C for 24h. Candidate colonies were checked by PCR before proceeding to the second recombination.
For the second Red recombination, an overnight culture was grown in LB with chloramphenicol and kanamycin at 32°C. Five milliliters of warm LB with chloramphenicol were inoculated with 250 μL of the overnight culture and then placed in a shaking incubator at 32°C until OD reached 0.4 (1h30-2h). Two milliliters of the culture were diluted with 2 mL of warm LB containing chloramphenicol and 1% arabinose and put back in the incubator for 50 min. The induction of the Red recombination system was done by placing the culture in a shaking waterbath at 42°C for exactly 15 min. The culture was then returned in the incubator for another 3h. Finally, two dilutions (100 μL of 10^{-5} and 100 μL of 10^{-6}) were plated on agar plates containing chloramphenicol and 1% arabinose. The plates were incubated at 32°C for 48h and candidates colonies were checked by PCR and sequencing.

The BAC-VZV-ORF9-V5 and BAC-VZV-ORF9-L231A-V5 were already described before [345, 227].

Primers used for recombinant viruses creation and plasmid transfections

Table 7.1: List of primers used.

Primer name	Primer sequence
BAC recombineering	
gHcyt_kana_FW	5′-TATTATCGGATGGATGTTATGTGGAAAT TCCCGCCTTCGATAATATAATAAAATACCT CTGAAGGATGACGACGATAAGTAGGG-3′
gHcyt_kana_RV	5′-ATTATACATGTTTTTTATGTCAGAGGTAT TTTATTATATTATCGAAGGCGGGAATTTCC ACCCAGTGTTACAACCAATTAACC-3′
gH_middle_FW	5′-CCGATCCATCGCAGCTTCATG-3′

gH_RV	5′-TATAACGGCGCTGTGCGTCTA-3′
gED436HKanaF	5′-GCGTGTTGCAAGCACAGTGTATCAAAA TTGTGAACATGCACATAACTACACCGCAT ATTGAGGATGACGACGATAAGTAGGG-3′
gED436HKanaR	5′-TCCATATGAGATATTCCCAGACAATATG CGGTGTAGTTATGTGCATGTTCACAATTTT GAGCCAGTGTTACAACCAATTAACC-3′
gED620YKanaF	5′-TGGAGGGAGTCACGGGGGTTCGAGTT ACACGGTGTATATATATAAGACCCGGTGA TCACCAGGATGACGACGATAAGTAGGG-3′
gED620YKanaR	5′-CGCTCGACGTTGCCCCGGTTCGGTGAT CACCGGGTCTTATATATACACCGTGTAAC TCGCCAGTGTTACAACCAATTAACC-3′
gE_mid_FW	5′-TCCGATGGTACGTCTACCTACGCC-3′
gE_RV	5′-AACCCACGAGAGATCCTGACACC-3′
plasmid creation for transfections	
pCAGGS_ORF9_FW	5′-TCACTATAGGGCTCGAGATCGATATGGC ATCTTCCGACGGTGACAGAC-3′
pCAGGS_ORF9_RV	5′-CATGCCATGTGTAATCCCAGCAGTCAAT GGTGATGGTGATGATGACCG-3′
pCAGGS_gE_FW	5′-TCACTATAGGGCTCGAGATCGATATGGG GACAGTTAATAAACCTGTGG-3′
pCAGGS_gE_RV	5′-CATGCCATGTGTAATCCCAGCAGTCAC CGGGTCTTATCTATATACACC-3′
pCAGGS_gI_FW	5′-TCACTATAGGGCTCGAGATCGATATGTT TTTAATCCAATGTTTGATATCGGCC-3′
pCAGGS_gI_RV	5′-CATGCCATGTGTAATCCCAGCAGCTATT TAACAAACGGGTTTACAACGG-3′
pCAGGS_gH_FW	5′-TCACTATAGGGCTCGAGATCGATATGTT TGCGCTAGTTTTAGCGGTGG-3′
pCAGGS_gH_RV	5′-CATGCCATGTGTAATCCCAGCAGTTATG TCAGAGGTATTTTATTATATTCTCG-3′

pCAGGS_gL_FW	5′-TCACTATAGGGCTCGAGATCGATATGGC ATCACATAAATGGTTACTGC-3′
pCAGGS_gL_RV	5′-CATGCCATGTGTAATCCCAGCAGCATTG GCATACGCGTTGGAACAAA-3′
pCAGGS_gB_FW	5′-TCACTATAGGGCTCGAGATCGATATGTC CCCTTGTGGCTATTATTCAAAG-3′
pCAGGS_gB_RV	5′-CATGCCATGTGTAATCCCAGCAGTTACA CCCCCGTTACATTCTCGGTG-3′
pCAGGS-gH-Flag-FW	5′-TCACTATAGGGCTCGAGATCGATATGTT TGCGCTAGTTTTAGCGGTGGTAATTCTTCC TCTTTGGACCACGGCTGATTACAAGGATG ACGATGACAAAAATAAATCTTACGTAACA CCAACCCCTGC-3′

Construction of the vectors used in transient transfections

WT or mutated versions of *orf9*, *orf31* (gB), *orf37* (gH), *orf60* (gL), *orf67* (gI),or *orf68* (gE) were amplified by PCR using the primers listed in table 7.1 and the BAC-VZV WT or mutated on *orf9*, *orf37*, or *orf68* as DNA template. The PCR products were cloned in a pCAGGS vector (kind gift of DR. Delcroix), using the NEBuilder HIFI DNA assembly kit from NEB (E2621L). The cloning mix were transformed into homemade electrocompetent DH10B *E. coli* and selected on ampicillin. All constructs were subsequently verified by Sanger sequencing.

Foci and Syncytia area measurements

Non-infected MeWo cells were seeded 3 days before infection at 50% confluency in 6-well plates. On the day of infection, MeWo cells infected with either VZV-ORF9-V5, VZV-ORF9-L231A-V5, VZV-ORF9-L231A-V5/gE-D436H-D620Y or VZV-ORF9-L231A-V5/gHΔcyt were trypsinised and the inoculum was passed through a strainer to remove pre-existing syncytia before infection of the 6-well plates. At 48 h.p.i., cells were washed with PBS and fixed with 4% PFA for 30 minutes at room temperature. Nuclei were stained with Nuclear-ID (Enzo Lifesciences) for 15 minutes at room temperature (dilution 1/10 000 in PBS). Cells were then washed three times

with PBS before taking pictures. Whole well pictures were taken using an Incucyte S3 (Sartorius) at 4X magnification. Foci and syncytium areas were measured using ImageJ in three independent experiments (100 foci and 50 syncytia were randomly selected and measured for each virus in each experiment). For syncytia percentage calculation, every foci present in the 6-well plates were taken into account.

Co-immunoprecipitation

Infected cells were seeded on 75 cm^2 dishes (one dish/IP) and incubated for 48h at 37°C. At 48 h.p.i., cells were washed with ice-cold PBS and then collected in lysis buffer (50 mM Tris-HCl pH 7.00, 1 mM $MgCl_2$, 1 mM $CaCl_2$, 150 mM NaCl and 1% Triton X-100). Cells were kept in lysis buffer on ice for 30 minutes then centrifuged at 3300 G for 1 minute. The supernatant was kept and incubated during 2h at 4°C with protein A-G magnetic beads (Thermofisher Scientific) previously coupled with either gE or gH antibody. After incubation, the beads were washed once with the lysis buffer and then thrice with a washing buffer (50 mM Tris-HCl pH 7.00, 1 mM $CaCl_2$, 300 mM NaCl and 1% Triton X-100). Finally, proteins were eluted with 30 μL of elution buffer (mix 1/1 of 2% SDS and TR2X) for 15 minutes at 37°C and then separated on a SDS PAGE gel.

Complete genome sequencing

Viral particles concentration

For each virus to be sequenced, two 500 cm^2 culture plates were seeded with non-infected MeWo cells at 50% confluency and then kept in the incubator for 72h with EMEM medium. At 72h, the cells were infected by co-culture with infected cells then put back in the incubator for 48h. At 48 h.p.i., the cells were washed with ice-cold PBS (25 mL/plate). Cells were then scrapped in 15 mL of stabilization solution (PBS + 5% sucrose). Cells were lysed on ice by 20 passages in a Dounce homogenizer followed by sonication (amplitude 70%, 10 cycles with 1 second on and 2 seconds off). The samples were treated with 250 μL of DNAse (20 U/mL) and 20 mM $MgCl_2$ for 1h at 10°C. Cell debris were removed by centrifugation at 2 500 G at 4°C for 10 minutes. The supernatant was collected and centrifugated at 100 000 G on a 30% sucrose (weight/volume) cushion (3 mL/tube) at 4°C for 1h using a pre-cooled rotor. After centrifugation, the supernatant was discarded and the pellet was resuspended in 500 μL of MNT buffer (30 mM MES, 100 mM NaCl, 20 mM Tris pH 7.5). The concentrated virus sample was separated on a 60% (weight/volume) potassium tartrate in SET buffer (0.1 M NaCl,

1 mM EDTA, 50 mM Tris pH 7.5) and 30% (volume/volume) glycerol in SET buffer gradient during 16h at 115 000 G and 4°C. After the gradient, the infectious virus band was harvested with a needle and diluted in SET buffer then concentrated by a subsequent centrifugation for 1h at 200 000 G at 4°C.

VZV genome extraction

The concentrated particles were resuspended in 2.5 mL of nuclear extraction buffer (10 mM Tris pH 7.5, 10% sucrose and 2 mM $MgCl_2$). Leftover cellular DNA was digested by incubating the extract with benzonase and RNAse for 1h at 37°C. Benzonase was then inactivated by adding 62.5 μL of 0.5 mM EDTA then the capsid proteins were digested by adding 2.5 mL of proteinase K digesting buffer (EDTA 40 mM, NaCl 200 mM, SDS 0.8%, 50 μL of 20 mg/mL proteinase K) and incubating the sample for 3h at 50°C. The sample was then transferred to a 15 mL tube and 5 mL of phenol-chloro-isoamyl alcool were added before gently shaking for 20 minutes. The sample was centrifugated at 6 000 G for 10 minutes. The upper phase was transferred to a new 15 mL tube and 5 mL of chloroform were added. The tube was inverted 50 times before centrifugation for 10 minutes at 6 000 G. The upper phase was again transferred to a new 15 mL tube and 450 μL of 3 M sodium acetate were added together with 4.5 mL of isopropanol. The tube was inverted several times then left overnight at room temperature. The next day, the sample was centrifugated for 15 minutes at 6 000 G at 4°C. The supernatant was discarded and the pellet was dried for 20 minutes. The DNA was finally resuspended in 50 μL of 10 mM Tris pH 8.0.

Sequencing

Whole genome library were carried out using Nextera XT Illumina kit according to manufacturer's guidelines. The quality control of DNA library was performed using Kapa Quant kit (Illumina). The libraries were then sequenced on a MiSeq System (Illumina) using the MiSeq v3 kit, 9.5 pM were charged and 300 cycles performed.
The reads obtained from the GIGA sequencing platform were aligned on the BAC-VZV-WT sequence using Burrows-Wheeler Aligner (BWA) MEM algorithm. The alignments were then sorted and indexed with SAM tools and further analyzed with IGV viewer.

Immunofluorescence

Uninfected and infected MeWo cells previously strained on 70 μm mesh to remove all syncytia were mixed at a 90:1 ratio and plated on 24-wells

plates containing glass coverslides. At 24h or 48h post infection, cells were washed with PBS and then fixed with 2% PFA-PBS for 30 minutes. Cells were permeabilized or not with 0.1% triton-PBS and then blocked with 3% BSA-PBS for 30 minutes. The coverslides were then incubated for 1h30 with anti-gE mouse antibody diluted in 3% BSA-PBS. After two washes in 3% BSA-PBS, cells were incubated with CF405 coupled anti-mouse antibody for 1h30, washed again twice, then incubated overnight with CF568-anti-gH and CF633-anti-gB antibodies diluted in 3% BSA-PBS. After three washes in PBS, coverslides were mounted on glass slides with Mowiol.

Cell fusion assay

Quantification of fusion events was performed using the quantitative Cre reporter assay as previously described [439]. Briefly, CHO-DSP1 cells were transfected with equimolar amounts of pcDNA3.1-gL, pME18s-gH, pCAGGS-gB, and either pCAGGS-ORF9-V5 or pCAGSS-ORF9L231A-V5 using Lipofectamine 2000 (Invitrogen). Transfected cells were harvested at 6h posttransfection and cocultured with MeWo-DSP2 cells. The cocultures were harvested after an additionnal 36h, and frequency of GFP-positive cells, indicating fusion events, was quantified using a FACSCalibur controlled by CellQuest Pro (BD Bioscience) and analyzed with FlowJo (TreeStar). A negative control was performed with pME18s- and pcDNA-empty vectors to establish background levels of GFP expression, which were then substracted from the fusion frequency data obtained with the test constructs. Experiments were performed in duplicate with two clones used for each construction.

Part V

Discussion and perspectives

8 Discussion and perspectives

In the first part of this thesis, we have shown that ORF9p interacts with the AP-1 complex and that mutation of the L231 residue of ORF9p abolishes this interaction. Importantly, this mutation on ORF9p led to a strong replication defect *in vitro* as well as an assembly defect of viral particles.

In the second part of the thesis, we have shown that the ORF9p-L231A mutation was also associated with a complete lack of syncytia formation in infected MeWo cells, known to usually form gigantic syncytia upon VZV infection. Surprisingly, additional mutations on gH (E834STOP or R833STOP) and/or gE (D436H and/or D620Y) reverted this phenotype, and even enhanced cell-cell fusion as compared to a Wild-type infection. While the gH mutation has already been described before [440], to our knowledge, it is the first time that it naturally occurs. On the other hand, two natural VZV mutants were already reported in the past to induce extensive syncytia formation [359, 405]. However, both mutants had the same D150N mutation in the extracellular part of gE, whereas the mutant we describe here shows mutations on both the extracellular (D436H) and intracellular (D620Y) domains. Single gE mutants (either D436H or D620Y) were generated and are under investigation to understand the impact of each mutation on VZV replication and syncytia formation. Interestingly, we showed that ORF9p was able to increase cell fusion when expressed with gB and gH-gL *in vitro*, without addition of any other viral protein, suggesting that ORF9p directly acts on the core fusion machinery to promote cell fusion. Additionally, we showed by co-immunoprecipitation that two glycoproteins networks exist around ORF9p: one forming the gE-gI/ORF9p/gB cluster, and the other one the gH-gL/ORF9p/gB cluster. It is however not clear whether these two complexes are linked together to form a supercomplex, as in our experiments no gH could be shown to coprecipitate with gE, nor gE could be shown to coprecipitate with gH. Formation of these glycoproteins clusters was prevented by the 9L231A mutation but formation of the gE-gI/ORF9p/gB cluster was restored by additional mutations on gE, whereas mutation on gH could no restore formation of the gH-gL/ORF9p/gB cluster, suggesting that mutations on gE or gH act in two separate ways to restore syncytia formation. Finally, our immunofluorescence experiments seem to indicate that, during a wild-type infection, gB, gE and gH may be targeted to specific regions of the plasma membrane where they form clusters. On the contrary, upon infection with the 9L231A mutant, the glycoproteins seem to be more homogeneously distributed at the cell surface. Further studies are still needed to know the impact of the gE or gH mutations on

the glycoproteins localization and distribution at the cell surface.
Altogether, these data allow us to propose a model explaining how VZV ORF9p participates in cell-cell fusion and in viral assembly: during a wild-type infection, upon interaction with AP-1, ORF9p is targeted towards the TGN. Once there, ORF9p promotes the formation of an AP-1/ORF9p/gE-gI/gB complex or a AP-1/ORF9p/gH-gL/gB complex by interacting with gE and gB, or gH and gB, respectively (Figure 8.1). In this model, ORF9p would serve to link glycoproteins together and the interaction between ORF9p and AP-1 would serve to target these glycoproteins clusters to the plasma membrane where they can mediate cell fusion.

Figure 8.1: **Model of glycoproteins clusters around ORF9p/AP-1.** We hypothesize that ORF9p is targeted to the TGN via its interaction with AP-1. Once there, it promotes the formation of two glycoproteins complexes by interacting either with gE and gB, or gH and gB.

Interestingly, only infected cells seem to be able to fuse with one another as only the center of the infection foci show signs of fusion. This suggests that interaction of glycoproteins on two facing membranes may be required to trigger cell-cell fusion. Additionally, VZV-induced cell-cell fusion leads to different outcomes with regard to the infected cell type. Indeed, while VZV is widely known to form huge syncytia upon infection of MeWo cells, infection of MRC-5 cells leads to syncytia containing a limited number of fused cells, typically less than a dozen (not shown). It thus seems that cell-specific mechanisms regulate cell-cell fusion.
In HSV-1, gE has been shown to colocalize with the adherens junctions protein β-catenin [84] and to be essential to target virions to the lateral surfaces, which include extensive cell junctions [187]. Targeting of the glycoproteins to the cell junction probably favors cell-cell fusion because the membranes of the adjacent cells are already in close proximity, facilitating the interaction between the glycoproteins on each of the facing membranes. Interestingly, gE from HSV and PRV is required for efficient spread of viruses between polarized cells with extensive cells junctions (*e.g.* epithelial

cells and neurons), but is not needed for spread between highly transformed, non-polarized cells, forming less junctions [187]. This may explain why infection of MeWo cells leads to formation of huge syncytia while infection of MRC-5 cells leads to limited fusion. The same study by Johnson *et al.* showed that the μ1B subunit of the AP-1 complex enhanced cell-to cell spread of PRV [187].

In our model, ORF9p serves to send the glycoproteins clusters to the cell surface by interacting with AP-1 (Figure 8.2). When a polarized cell is infected, the AP-1/ORF9p/gE-gI/gB complex would be targeted towards the cell junctions via interaction of gE with AP-1B while the AP-1/ORF9p/gH-gL/gB complex would be targeted more randomly to the cell surface via interaction with AP-1A. Once on the surface, gB would interact with glycoproteins on the opposite membrane to trigger cell-cell fusion. On the other hand, when a non-polarized cell is infected, AP-1B is not present to send the AP-1/ORF9p/gE-gI/gB complex towards cell junctions. Both complexes would then be randomly targeted towards the surface via interaction with AP-1A. To be able to fuse, gB would need to be close to the opposing membrane, which would also need to harbour glycoproteins. These conditions being less likely to happen at the same time, this may explain why non-polarized cells form limited syncytia in culture.
During an infection by the 9L231A mutant, ORF9p is unable to interact with AP-1 and thus, unable to form glycoproteins clusters at the TGN. The glycoproteins would then be targeted to the cell surface independently from one another and therefore, formation of the core fusion machinery is less likely to happen, and all conditions for cell-cell fusion triggering are unlikely to be met.

Our co-immunoprecipitation experiments show that the gE-D436H/D620Y mutations restore the formation of an ORF9p/gE-gI/gB complex. We propose that this complex, via interaction between gE and AP-1B, can be targeted towards the cell junctions to mediate cell fusion. At the cell junctions, both gE and gB may be sufficient to trigger cell-cell fusion. Indeed, the coexpression of both gE and gB has been shown to lead to abundant syncytia formation in a cell fusion assay [249]. This further supports the idea that gE-gI and gH-gL regulate syncytia formation via two independent pathways. It is also possible that the gE-D436H mutation, occurring near a N-glycosylation site and between two cysteines forming a disulfide bond (see Figure 5.2), modifies the conformation of gE, increasing its ability to promote cell fusion. This is supported by our observation that the gE double mutants have a higher fusion capacity compared to gE-WT. Further studies are however needed to consolidate this hypothesis. First, high-resolution immunofluorescence studies are needed to see whether or not

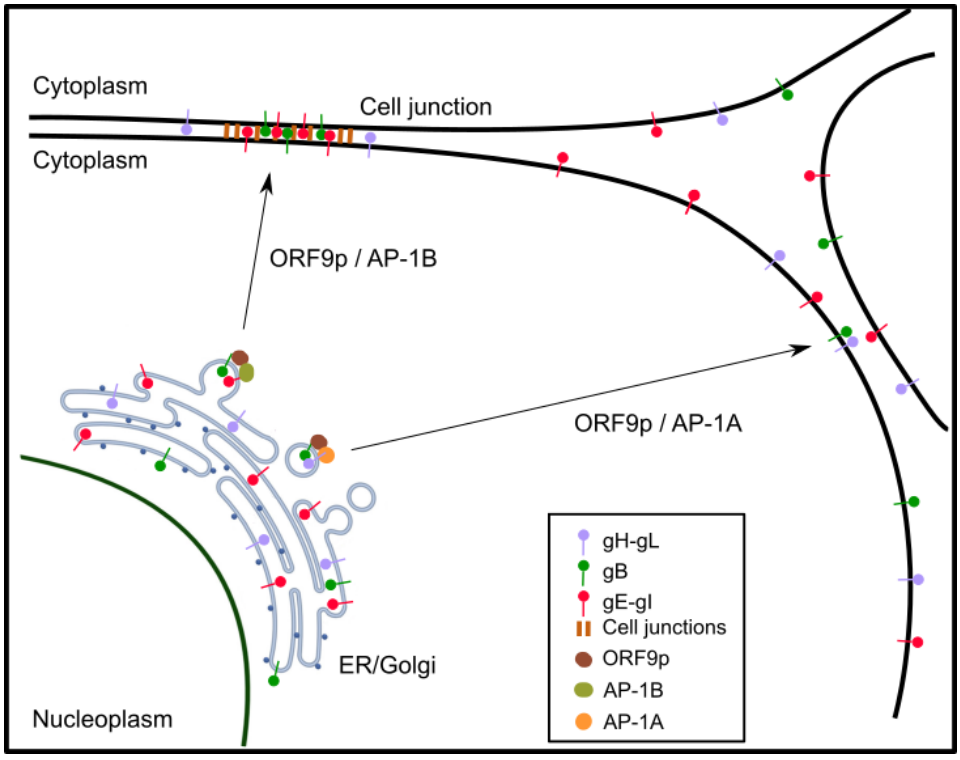

Figure 8.2: **Model of ORF9p/AP-1 mediated glycoprotein transport.** In polarized cells, gE-gI/gB are targeted towards the cell junction via interaction of gE with AP-1B, while gH-gL/gB are targeted randomly towards the surface via the ORF9p/AP-1A interaction. In non-polarized cell lines, the glycoproteins are targeted towards the surface randomly via AP-1A.

the ORF9p/gE-gI/gB complex is indeed targeted towards the cell junctions in MeWo cells, and to see if gH is necessary to induce cell-cell fusion at the cell junctions. It would also be interesting to see if the gE-D436H/D620Y mutant is able to induce the formation of bigger syncytia in MRC-5 cells. Finally, analysis of gE-D436H and gE-D620Y single mutants should help us understand how each of these mutations affect cell-cell fusion.
Regarding the gHΔcyt mutation, Yang *et al.* hypothesized that the cytoplasmic tail of gH could act as a gate keeper, regulating phosphorylation of the ITIM of gB by controlling either kinases or phosphates access to the Y881 residue. Therefore, in a mutant lacking this gate keeper, gB would be in a dysregulated state and enhance fusion [440]. In 2017, Oliver *et al.* showed that the exaggerated syncytia formation phenotype of the gB[Y881F] mutant was caused by fusion of infected cells with many uninfected cells [303]. Thus, when gB is in a dysregulated phase, the presence of glycoproteins

on the surface of both cells does not seem to be required to induce cell-cell fusion. However, the precise mechanisms used by the gHΔcyt mutant to induce an enhanced cell-cell fusion are unclear. Indeed, gB is known to be unable to induce cell fusion on its own, and to require the presence of gH-gL to trigger fusion. In our co-immunoprecipitation experiments, we were unable to show the restoration of the gH/gB interaction by the gHΔcyt mutant. The fact that our gH antibody does not recognize gH in Western blot in denaturing conditions makes it difficult to know if this is due to a lack of interaction or inadequate gH precipitation. Further studies are thus needed to confirm our immunoprecipitations results, possibly by tagging gH to facilitate its detection. Yang *et al.* showed that, in transfection, gHΔcyt was 12% more present at the cell surface as compared to gH-WT. This over-expression of gH at the surface combined with the loss of gH-mediated gB regulation may in part explain the enhanced fusion, but additional studies are needed to know if gHΔcyt is more expressed at the surface in the course of an infection and to understand if and how gH and gB interact at the surface.
Finally, most cell fusion experiments are done by transfecting a cell population then co-culturing it with a non-transfected population and therefore, these experiments are more suited to study viral entry in an uninfected cell than cell-cell fusion in which viral glycoproteins are expressed on both cells that fuse. It would be interesting to try different combinations of glycoproteins transfections in both cell populations before co-culturing them to better understand the proteins required for syncytia formation and the differences that exist between the fusion of the viral envelope and the cell membrane, and cell-cell fusion.

In 1968, Darlington and Moss showed that enveloped Herpesviral particles cluster in both small and large vacuoles in the cytoplasm [71]. More recently, Girsch *et al.* proposed a model with two different envelopment pathways leading to these two types of vacuoles (Figure 8.3) [132]. According to the authors, both pathways can be distinguished by the presence or absence of the M6PR: the pathway leading to large vacuoles filed with viruses, most commonly found in VZV-infected cells, is associated with the M6PR, while the pathway leading to small vacuoles, found in HSV-1 and PRV, is not. The authors propose that the large vacuoles pathway results from the hijacking of the autophagy pathway by the virus. Indeed, the large vacuoles would be derived from late endosomes, known to form large vacuoles because they can fuse with one another or with other organelles, and because most M6PR resides in late endosomes [132, 215, 385]. In the model proposed by Girsch *et al.*, the viral glycoproteins can travel directly to the viral assembly compartment (VAC), presumably derived from the TGN, or they could travel to the plasma membrane, where they undergo endocytosis and are

then directed to the VAC (Figure 8.3). Likewise, the M6PR could attach to the glycoproteins either in the TGN or on the cell surface. After envelopment in the VAC, enveloped virions without the M6PR would travel directly to the plasma membrane in small vacuoles (Figure 8.3, pathway A), whereas viral particles with M6P residues in their glycoproteins would be transported in the M6PR pathway to a late endosome (Figure 8.3, pathway B). The late endosome containing several particles still attached to M6PRs would be transported to the cell surface without undergoing xenophagy [132]. Finally, the authors hypothesize that the M6PR pathway is most utilized during VZV infection, while the small vacuole pathway is most used in HSV or PRV infections. The presence or absence of gD could be responsible for pathway selection as VZV lacks a gD, while HSV and PRV do not [132].

Unexpectedly, the presence of the M6PR pathway seems to correlate with the capacity of the cells to form syncytia. Indeed, our TEM results showed that WT particles were transported in large vacuoles in MeWo cells, and the virions seemed to be attached to the membrane of the transport vacuole. On the contrary, only a few vacuoles containing a limited number of viral particles were found upon infection with the 9L231A mutant. This idea is further supported by the fact that Wild-type HSV and PRV rarely form syncytia in cell culture as compared to VZV [323, 330].

As discussed above, our hypothesis is that ORF9p forms glycoproteins clusters that could be directed towards the adherens junctions thanks to gE-gI/AP-1B. The adherence junctions are dynamic structures that are regularly formed, broken and rearranged due to cadherin endocytosis, degradation or recycling [216]. E-cadherin, expressed in epithelial cells, has been shown to undergo clathrin-mediated endocytosis, and its cytoplasmic tail interacts with the AP-2 complex [216, 362]. Moreover, it has been shown that the higher rate of cadherin endocytosis, the higher the proportion of endocytosed cadherin selected for degradation rather than recycling [216]. Thus, we hypothesize that the presence of large amounts of viral glycoproteins at the cell junction would increase the rate of endocytosis, and that viral particles would envelope in the endosomes containing the endocytosed glycoproteins. ORF9p could once again intervene in the process by interacting with capsid, tegument and envelope proteins [384, 415, 60, 52, 53]. The enveloped particles would then be targeted to the late endosome where they would form large vesicles. The vesicles would finally be targeted for recycling to the cell surface instead of following the degradation pathway. How the vesicles are selected for recycling instead of degradation is however unknown.

ORF9p was already known to be essential for VZV replication [52] and to

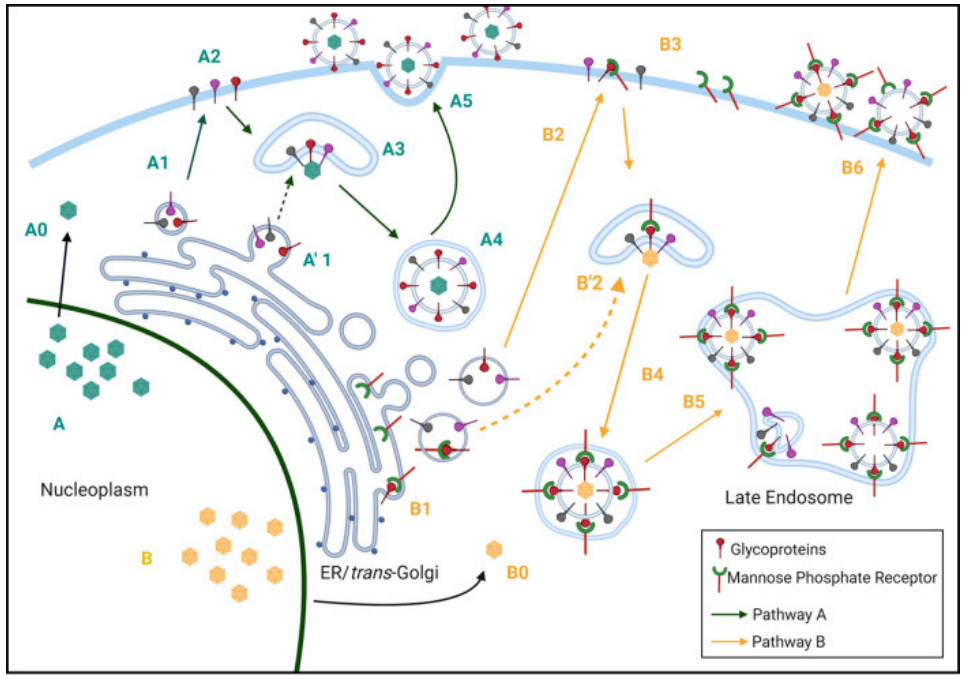

Figure 8.3: **VZV egress pathways.** Two different pathways, called the large vacuole and the small vacuole pathways, are proposed to serve in VZV egress. A) The small vacuole pathway. In this pathway, the glycoproteins are transported to the plasma membrane and internalized (A1, A2) or small glycoprotein-containing vacuoles (A'1) serve as the enveloping compartment. Once enveloped, virions are transported in small vacuoles (A4) lacking M6PR, directly to the cell surface. B) In the large vacuole pathway, the viral glycoproteins are transported to the plasma membrane (B1, B2), where they interact with the M6PR and are internalized as a complex (B3). Alternatively, the glycoproteins can attach to the M6PR in the TGN (B1) and this complex evolves into the assembly compartment (B'2). After exciting the assembly compartment (B4), virions associated to the M6PR are transported to the late endosome (B5). Fusion of the transport vesicles with endosomes leads to a large M6PR-positive vacuole with multiple viral particles. Signals present in the M6PR cytoplasmic tail then facilitate the transport of the large vesicle towards the surface. Figure form [132].

play a role in viral envelopment [345, 344]. The results presented in this thesis show for the first time that it is also important for VZV-mediated cell-cell fusion *in vitro*. The model proposed above tries to explain how ORF9p plays a role in viral envelopment and cell-cell fusion by forming multiprotein complexes and delivering them to the site of viral envelopment, thus making it essential for the virus. Several studies are still needed to support and

improve this model. Purification of viral particles followed by mass spectrometry analysis would be interesting to know if adhesion molecules are incorporated in the virions. Such experiments were performed during this thesis, but unfortunately, the extreme cell-associated nature of VZV makes it difficult to have sufficiently pure viral particles for MS analysis. One way to bypass this problem would be to perform immunogold labelling of cadherins followed by TEM analysis to know if cadherins are incorporated in viral particles or in the vacuole membranes. It would also be interesting to analyze MeWo cells infected with the gE-Dble and gHΔcyt mutants, to know if these mutations restore the large vacuole pathways in infected cells. This may be useful to determinate if these mutations act on different pathways or not. Such experiments have already been performed by Yang *et al.* with the gHΔcyt mutant. The authors showed that the particles formed by the gHΔcyt mutant were also found in cytoplasmic vesicles. However, the size of the vesicles and the number of virions inside was not further described [440]. Finally, it would be interesting to know if incorporation of the L231A mutation in the ORF9p homologs impacts the fusion and cell-to-cell spread of the other Alphaherpesviruses.

Part VI

Appendix

A VZV proteins and their HSV-1 homologs

VZV proteins	Characteristics	HSV-1 homologs
ORF0 (ORF S/L)	membrane protein	UL56
ORF1	membrane protein	/
ORF2	myristoylated tegument protein	/
ORF3	nuclear protein	UL55
ORF4 (IE4)	transactivator tegument protein	UL54 (ICP27)
ORF5	envelope glycoprotein K (gK)	UL53
ORF6	helicase/primase, primase subunit	UL52
ORF7	tegument protein	UL51
ORF8	dUTPase	UL50
ORF9	major tegument protein	UL49 (VP22)
ORF9A	envelope glycoprotein N (gN)	UL49A
ORF10	transactivating tegument protein	UL48 (VP16)
ORF11	RNA binding protein	UL47 (VP13-14)
ORF12	cell cycle regulator	UL46
ORF13	thymidylate synthetase	/
ORF14	envelope glycoprotein C (gC)	UL44
ORF15	envelope protein	UL43
ORF16	DNA polymerase, processivity subunit	UL42
ORF17	tegument protein	UL41 (VHS)
ORF18	ribonucleotide reductase, small subunit	UL40 (RR2)

ORF19	ribonucleotide reductase, large subunit	UL39 (RR1)
ORF20	ribonucleotide reductase, small subunit	UL38 (ICP32)
ORF21	minor inner tegument protein	UL37 (VP7)
ORF22	major inner tegument protein	UL36 (VP1-2)
ORF23	small capsid protein	UL35 (VP26)
ORF24	nuclear envelopment complex	UL34
ORF25	DNA cleavage/packaging complex	UL33
ORF26	DNA packaging protein	UL32
ORF27	nuclear envelopment complex	UL31
ORF28	DNA polymerase, catalytic subunit	UL30
ORF29	ssDNA binding protein	UL29 (ICP8)
ORF30	cleavage/packaging complex, terminase core	UL28
ORF31	envelope glycoprotein B (gB)	UL27
ORF32	phosphoprotein	/
ORF33	capsid maturation protease	UL26 (VP24)
ORF33.5	capsid scaffold protein	UL26.5 (VP22a)
ORF34	capsid capping tegument protein	UL25
ORF35	nuclear protein	UL24
ORF36	thymidine kinase	UL23
ORF37	envelope glycoprotein H (gH)	UL22
ORF38	tegument protein	UL21
ORF39	envelope protein	UL20
ORF40	major capsid protein	UL19 (VP5)
ORF41	capsid scaffolding protein	UL18 (VP23)

ORF42/45	cleavage/packaging complex, terminase core	UL15
ORF43	DNA packaging tegument protein	UL17
ORF44	tegument protein	UL16
ORF46	tegument protein	UL14
ORF47	tegument Ser/Thr kinase	UL13 (VP18.8)
ORF48	deoxyribonuclease	UL12
ORF49	myristoylated tegument protein	UL11
ORF50	envelope glycoprotein M (gM)	UL10
ORF51	DNA replication origin-binding protein	UL9
ORF52	helicase/primase subunit	UL8
ORF53	tegument protein	UL7
ORF54	capsid portal protein	UL6 (VP11-12)
ORF55	helicase/primase, helicase subunit	UL5
ORF56	nuclear protein	UL4
ORF57	cytosolic protein	/
ORF58	nuclear protein	UL3
ORF59	uracil-DNA glycosylase	UL2
ORF60	envelope glycoprotein L (gL)	UL1
ORF61	transactivator, transrepressor	ICP0
ORF62/71 (IE62)	transcriptional regulator	ICP4
ORF63/70 (IE63)	regulatory protein	US1 (ICP22)
ORF64/69	virion protein	US10
ORF65	membrane protein	US9
ORF66	Ser/Thr kinase	US3
ORF67	envelope glycoprotein I (gI)	US7
ORF68	envelope glycoprotein E (gE)	US8

Part VII

References

References

[1] A. Abendroth et al. *Varicella-zoster Virus*. Ed. by A. Abendroth et al. Vol. 342. Current Topics in Microbiology and Immunology. Berlin, Heidelberg: Springer Berlin Heidelberg, 2010.
DOI: 10.1007/978-3-642-12728-1.

[2] K. Adelman et al. "Herpes simplex virus DNA packaging sequences adopt novel structures that are specifically recognized by a component of the cleavage and packaging machinery". *Proceedings of the National Academy of Sciences of the United States of America* 98.6 (2001).
DOI: 10.1073/pnas.061555698.

[3] A. Aggarwal et al. "Ultrastructural Visualization of Individual Tegument Protein Dissociation during Entry of Herpes Simplex Virus 1 into Human and Rat Dorsal Root Ganglion Neurons". *Journal Of Virology* 86.11 (2012).
DOI: 10.1128/jvi.07016-11.

[4] I. Ahmad and D. W. Wilson. "Hsv-1 cytoplasmic envelopment and egress". *International Journal of Molecular Sciences* 21.17 (2020).
DOI: 10.3390/ijms21175969.

[5] K. H. Ahn et al. *Congenital varicella syndrome: A systematic review*. 2016.
DOI: 10.3109/01443615.2015.1127905.

[6] A. Albecka et al. "Dual Function of the pUL7-pUL51 Tegument Protein Complex in Herpes Simplex Virus 1 Infection". *Journal of Virology* 91.2 (2017).
DOI: 10.1128/jvi.02196-16.

[7] A. Albecka et al. "HSV-1 Glycoproteins Are Delivered to Virus Assembly Sites Through Dynamin Dependent Endocytosis". *Traffic* 17.1 (2016).
DOI: 10.1111/tra.12340.

[8] B. S. Albright et al. "The Putative Herpes Simplex Virus 1 Chaperone Protein UL32 Modulates Disulfide Bond Formation during Infection". *Journal of Virology* 89.1 (2015).
DOI: 10.1128/jvi.01913-14.

[9] A. Alconada et al. "A tyrosine-based motif and a casein kinase II phosphorylation site regulate the intracellular trafficking of the varicella-zoster virus glycoprotein I, a protein localized in the trans-Golgi network." *The EMBO journal* 15.22 (1996).

[10] A. A. Alconada et al. "Intracellular Traffic of Herpes Simplex Virus Glycoprotein gE: Characterization of the Sorting Signals Required for Its trans-Golgi Network Localization". *Journal of Virology* 73.1

(1999).
DOI: 10.1128/jvi.73.1.377-387.1999.

[11] A. M. Arvin. "Varicella-zoster virus." *Clinical Microbiology Reviews* 9.3 (1996).
DOI: 10.1074/jbc.M110.210575.

[12] A. M. Arvin et al. "Analysis of the Functions of Glycoproteins E and I and Their Promoters During VZV Replication In Vitro and in Skin and T-Cell Xenografts in the SCID Mouse Model of VZV Pathogenesis". In: *Current topics in microbiology and immunology*. Vol. 342. Curr Top Microbiol Immunol, 2010.
DOI: 10.1007/82_2009_1.

[13] A. M. Arvin et al. "Varicella-zoster virus T cell tropism and the pathogenesis of skin infection". *Current topics in microbiology and immunology* 342 (2010).
DOI: 10.1007/82_2010_29.

[14] R. Asai et al. "Identification of proteins directly phosphorylated by UL13 protein kinase from herpes simplex virus 1". *Microbes and Infection* 9.12-13 (2007).
DOI: 10.1016/j.micinf.2007.07.008.

[15] D. Atanasiu et al. "Bimolecular Complementation Defines Functional Regions of Herpes Simplex Virus gB That Are Involved with gH/gL as a Necessary Step Leading to Cell Fusion". *Journal of Virology* 84.8 (2010).
DOI: 10.1128/jvi.02687-09.

[16] M. W. Austefjord et al. "Tunneling nanotubes: Diversity in morphology and structure". *Communicative and Integrative Biology* 7.2 (2014).
DOI: 10.4161/cib.27934.

[17] E. Avitabile et al. "Redistribution of microtubules and Golgi apparatus in herpes simplex virus-infected cells and their role in viral exocytosis". *Journal of Virology* 69.12 (1995).
DOI: 10.1128/jvi.69.12.7472-7482.1995.

[18] E. Avitabile et al. "Coexpression of UL20p and gK Inhibits Cell-Cell Fusion Mediated by Herpes Simplex Virus Glycoproteins gD, gH-gL, and Wild-Type gB or an Endocytosis-Defective gB Mutant and Downmodulates Their Cell Surface Expression". *Journal of Virology* 78.15 (2004).
DOI: 10.1128/jvi.78.15.8015-8025.2004.

[19] E. Avitabile et al. "Herpes Simplex Virus Glycoprotein K, but Not Its Syncytial Allele, Inhibits Cell-Cell Fusion Mediated by the Four Fusogenic Glycoproteins, gD, gB, gH, and gL". *Journal of Virology* 77.12 (2003).
DOI: 10.1128/jvi.77.12.6836-6844.2003.

[20] W. Azab and K. Osterrieder. "Initial contact: The first steps in herpesvirus entry". In: *Advances in Anatomy Embryology and Cell Biology*. Vol. 223. Springer Verlag, 2017.
DOI: 10.1007/978-3-319-53168-7_1.

[21] M. Backovic and T. S. Jardetzky. *Class III viral membrane fusion proteins*. 2009.
DOI: 10.1016/j.sbi.2009.02.012.

[22] M. Backovic et al. "Structure of a core fragment of glycoprotein H from pseudorabies virus in complex with antibody". *Proceedings of the National Academy of Sciences of the United States of America* 107.52 (2010).
DOI: 10.1073/pnas.1011507107.

[23] I. Bagdonaite et al. "Global mapping of o-glycosylation of varicella zoster virus, human cytomegalovirus, and Epstein-Barr virus". *Journal of Biological Chemistry* 291.23 (2016).
DOI: 10.1074/jbc.M116.721746.

[24] J. D. Baines. "Herpes simplex virus capsid assembly and DNA packaging: A present and future antiviral drug target". *Trends in Microbiology* 19.12 (2011).
DOI: 10.1016/j.tim.2011.09.001.

[25] J. D. Baines and P. E. Pellett. "Genetic comparison of human alphaherpesvirus genomes". In: *Human Herpesviruses: Biology, Therapy, and Immunoprophylaxis*. Cambridge University Press, 2007.
DOI: 10.1017/CBO9780511545313.006.

[26] J. D. Baines et al. "Glycoprotein M of Herpes Simplex Virus 1 Is Incorporated into Virions during Budding at the Inner Nuclear Membrane". *Journal of Virology* 81.2 (2007).
DOI: 10.1128/jvi.01756-06.

[27] G. M. Beacham et al. "Conformational regulation of AP1 and AP2 clathrin adaptor complexes". *Traffic* 20.10 (2019).
DOI: 10.1111/tra.12677.

[28] P. M. Beard and J. D. Baines. "The DNA cleavage and packaging protein encoded by the UL33 gene of herpes simplex virus 1 associates with capsids". *Virology* 324.2 (2004).
DOI: 10.1016/j.virol.2004.03.044.

[29] I. Beitia Ortiz de Zarate et al. "Contribution of Endocytic Motifs in the Cytoplasmic Tail of Herpes Simplex Virus Type 1 Glycoprotein B to Virus Replication and Cell-Cell Fusion". *Journal of Virology* 81.24 (2007).
DOI: 10.1128/jvi.01231-07.

[30] I. Benedicto et al. "Clathrin Mediates Infectious Hepatitis C Virus Particle Egress". *Journal of Virology* 89.8 (2015).
DOI: 10.1128/JVI.03620-14.

[31] O. Bermek and R. S. Williams. "The three-component helicase/primase complex of herpes simplex virus-1". *Open Biology* 11.6 (2021).
DOI: 10.1098/rsob.210011.

[32] J. M. Bigalke and E. E. Heldwein. "Structural basis of membrane budding by the nuclear egress complex of herpesviruses". *The EMBO Journal* 34.23 (2015).
DOI: 10.15252/embj.201592359.

[33] J. M. Bigalke et al. "Membrane deformation and scission by the HSV-1 nuclear egress complex". *Nature Communications* 5 (2014).
DOI: 10.1038/ncomms5131.

[34] S. L. Bjerke and R. J. Roller. "Roles for herpes simplex virus type 1 UL34 and US3 proteins in disrupting the nuclear lamina during herpes simplex virus type 1 egress". *Virology* 347.2 (2006).
DOI: 10.1016/j.virol.2005.11.053.

[35] C. Blondeau et al. "Functional Homologies between Avian and Human Alphaherpesvirus VP22 Proteins in Cell-to-Cell Spreading as Revealed by a New cis-Complementation Assay". *Journal of Virology* 82.18 (2008).
DOI: 10.1128/jvi.00598-08.

[36] P. E. Boehmer and I. R. Lehman. "Herpes simplex virus DNA replication". *Annual Review of Biochemistry* 66.1 (1997).
DOI: 10.1146/annurev.biochem.66.1.347.

[37] P. E. Boehmer et al. "The herpes simplex virus type-1 origin binding protein. DNA helicase activity". *Journal of Biological Chemistry* 268.2 (1993).
DOI: 10.1016/s0021-9258(18)54063-1.

[38] J. S. Bonifacino and E. C. Dell'Angelica. "Molecular bases for the recognition of tyrosine-based sorting signals". *Journal of Cell Biology* 145.5 (1999).
DOI: 10.1083/jcb.145.5.923.

[39] J. S. Bonifacino and L. M. Traub. "Signals for sorting of transmembrane proteins to endosomes and lysosomes." *Annual review of biochemistry* 72 (2003).
DOI: 10.1146/annurev.biochem.72.121801.161800.

[40] C. R. Brunetti et al. "Role of Mannose-6-Phosphate Receptors in Herpes Simplex Virus Entry into Cells and Cell-to-Cell Transmission". *JOURNAL OF VIROLOGY* 69 (6 1995).

[41] A. Brzozowska et al. "Point mutations in BHV-1 Us3 gene abolish its ability to induce cytoskeletal changes in various cell types". *Veterinary Microbiology* 143.1 (2010).
DOI: 10.1016/j.vetmic.2010.02.008.

[42] B. G. Butt et al. "Insights into herpesvirus assembly from the structure of the pUL7:PUL51 complex". *eLife* 9 (2020).
DOI: 10.7554/eLife.53789.

[43] P. Cacciagli et al. "AP1S2 is mutated in X-linked Dandy Walker malformation with intellectual disability, basal ganglia disease and seizures (Pettigrew syndrome)". *European Journal of Human Genetics* 22.3 (2014).
DOI: 10.1038/ejhg.2013.135.

[44] M. Cai et al. "Characterization of the nuclear import and export signals, and subcellular transport mechanism of varicella-zoster virus ORF9". *Journal of General Virology* 92.3 (2011).
DOI: 10.1099/vir.0.027029-0.

[45] G. Campadelli et al. "Fragmentation and dispersal of Golgi proteins and redistribution of glycoproteins and glycolipids processed through the Golgi apparatus after infection with herpes simplex virus 1". *Proceedings of the National Academy of Sciences of the United States of America* 90.7 (1993).
DOI: 10.1073/pnas.90.7.2798.

[46] G. Campadelli-Fiume and L. Menotti. *Entry of alphaherpesviruses into the cell*. Cambridge University Press, 2007.

[47] G. Campadelli-Fiume et al. "The novel receptors that mediate the entry of herpes simplex viruses and animal alphaherpesviruses into cells". *Reviews in Medical Virology* 10.5 (2000).
DOI: 10.1002/1099-1654(200009/10)10:5<305::AID-RMV286>3.0.CO;2-T.

[48] B. J. Canagarajah et al. "The clathrin adaptor complexes as a paradigm for membrane-associated allostery". *Protein Science* 22.5 (2013).
DOI: 10.1002/pro.02235.

[49] G. L. Cano-Monreal et al. "Herpes simplex virus 2 UL13 protein kinase disrupts nuclear lamins". *Virology* 392.1 (2009).
DOI: 10.1016/j.virol.2009.06.051.

[50] G. Cardone et al. "The UL36 Tegument Protein of Herpes Simplex Virus 1 Has a Composite Binding Site at the Capsid Vertices". *Journal of Virology* 86.8 (2012).
DOI: 10.1128/jvi.00012-12.

[51] Centers for Disease Control and Prevention. *Chickenpox About Varicella*. 2016.

[52] X. Che et al. "Functions of the ORF9-to-ORF12 gene cluster in varicella-zoster virus replication and in the pathogenesis of skin infection." *Journal of virology* 82.12 (2008).
DOI: 10.1128/JVI.00303-08.

[53] X. Che et al. "ORF11 protein interacts with the ORF9 essential tegument protein in varicella-zoster virus infection." *Journal of virology* 87.9 (2013).
DOI: 10.1128/JVI.00102-13.

[54] J. J. Chen et al. "Mannose 6-phosphate receptor dependence of varicella zoster virus infection in vitro and in the epidermis during varicella and zoster". *Cell* 119.7 (2004).
DOI: 10.1016/j.cell.2004.11.007.

[55] Y. Chen et al. "Mutations in the Putative Zinc-Binding Motif of UL52 Demonstrate a Complex Interdependence between the UL5 and UL52 Subunits of the Human Herpes Simplex Virus Type 1 Helicase/Primase Complex". *Journal of Virology* 79.14 (2005).
DOI: 10.1128/jvi.79.14.9088-9096.2005.

[56] J. H. I. Chi et al. "The cytoplasmic tail of herpes simplex virus envelope glycoprotein D binds to the tegument protein VP22 and to capsids". *Journal of General Virology* 86.2 (2005).
DOI: 10.1099/vir.0.80444-0.

[57] D. V. Chouljenko et al. "Herpes Simplex Virus 1 UL37 Protein Tyrosine Residues Conserved among All Alphaherpesviruses Are Required for Interactions with Glycoprotein K, Cytoplasmic Virion Envelopment, and Infectious Virus Production". *Journal of Virology* 90.22 (2016).
DOI: 10.1128/jvi.01202-16.

[58] V. N. Chouljenko et al. "The Herpes Simplex Virus Type 1 UL20 Protein and the Amino Terminus of Glycoprotein K (gK) Physically Interact with gB". *Journal of Virology* 84.17 (2010).
DOI: 10.1128/jvi.00298-10.

[59] T. K. Chowdary et al. "Crystal structure of the conserved herpesvirus fusion regulator complex gH-gL". *Nature Structural and Molecular Biology* 17.7 (2010).
DOI: 10.1038/nsmb.1837.

[60] C. Cilloniz et al. "The Varicella-Zoster Virus (VZV) ORF9 Protein Interacts with the IE62 Major VZV Transactivator". 81.2 (2007).

[61] J. I. Cohen. "The Varicella-Zoster Virus Genome". In: *Current topics in microbiology and immunology*. Vol. 342. Curr Top Microbiol Immunol, 2010.
DOI: 10.1007/82_2010_10.

[62] R. J. Cohrs et al. "Array analysis of viral gene transcription during lytic infection of cells in tissue culture with Varicella-Zoster virus". *J Virol* 77.0022-538X (2003).
DOI: 10.1128/JVI.77.21.11718.

[63] N. L. Cole and C. Grose. "Membrane fusion mediated by herpesvirus glycoproteins: The paradigm of varicella-zoster virus". *Reviews in Medical Virology* 13.4 (2003).
DOI: 10.1002/rmv.377.

[64] K. E. Coller et al. "The Capsid and Tegument of the Alphaherpesviruses Are Linked by an Interaction between the UL25 and VP1/2 Proteins". *Journal of Virology* 81.21 (2007).
DOI: 10.1128/jvi.01113-07.

[65] S. A. Connolly et al. "Fusing structure and function: A structural view of the herpesvirus entry machinery". *Nature Reviews Microbiology* 9.5 (2011).
DOI: 10.1038/nrmicro2548.

[66] A. M. Copeland et al. "Herpes Simplex Virus Replication: Roles of Viral Proteins and Nucleoporins in Capsid-Nucleus Attachment". *Journal of Virology* 83.4 (2009).
DOI: 10.1128/jvi.01139-08.

[67] C. M. Crump. "Virus assembly and egress of HSV". In: *Advances in Experimental Medicine and Biology*. Vol. 1045. Springer New York LLC, 2018.
DOI: 10.1007/978-981-10-7230-7_2.

[68] C. M. Crump et al. "Alphaherpesvirus glycoprotein M causes the relocalization of plasma membrane proteins". *Journal of General Virology* 85.12 (2004).
DOI: 10.1099/vir.0.80361-0.

[69] C. M. Crump et al. "PACS-1 binding to adaptors is required for acidic cluster motif-mediated protein traffic". *EMBO Journal* 20.9 (2001).
DOI: 10.1093/emboj/20.9.2191.

[70] X. Dai and Z. Hong Zhou. "Structure of the herpes simplex virus 1 capsid with associated tegument protein complexes". *Science* 360.6384 (2018).
DOI: 10.1126/science.aao7298.

[71] R. W. Darlington and L. H. Moss. "Herpesvirus Envelopment". *Journal of Virology* 2.1 (1968).
DOI: 10.1128/jvi.2.1.48-55.1968.

[72] A. J. Davison. "Overview of classification". In: *Human Herpesviruses: Biology, Therapy, and Immunoprophylaxis*. Ed. by A. M. Arvin et al. Cambridge University Press, 2007. Chap. 1.
DOI: 10.1017/CBO9780511545313.002.

[73] A. J. Davison. "Structure of the genome termini of Varicella-Zoster Virus". *Journal of General Virology* 65 (1984).

[74] A. J. Davison and J. Scott. "The Complete DNA Sequence of Varicella-Zoster Virus". *Journal of General Virology* 67 (1986).

[75] S. Debrus et al. "Varicella-zoster virus gene 63 encodes an immediate-early protein that is abundantly expressed during latency." *Journal of virology* 69.5 (1995).
DOI: 10.1128/jvi.69.5.3240-3245.1995.

[76] P. Defechereux et al. "Varicella-zoster virus open reading frame 4 encodes an immediate-early protein with posttranscriptional regulatory properties." *Journal of virology* 71.9 (1997).
DOI: 10.1128/jvi.71.9.7073-7079.1997.

[77] M. J. Deruelle and H. W. Favoreel. "Keep it in the subfamily: The conserved alphaherpesvirus US3 protein kinase". *Journal of General Virology* 92.1 (2011).
DOI: 10.1099/vir.0.025593-0.

[78] P. J. Desai et al. "Reconstitution of the Kaposi's Sarcoma Associated Herpesvirus Nuclear Egress Complex and Formation of Nuclear Membrane Vesicles by Coexpression of ORF67 and ORF69 Gene Products". *Journal of Virology* 86.1 (2012).
DOI: 10.1128/jvi.05988-11.

[79] P. Desai et al. "Localization of Herpes Simplex Virus Type 1 UL37 in the Golgi Complex Requires UL36 but Not Capsid Structures". *Journal of Virology* 82.22 (2008).
DOI: 10.1128/jvi.00956-08.

[80] P. J. Desai. "A Null Mutation in the UL36 Gene of Herpes Simplex Virus Type 1 Results in Accumulation of Unenveloped DNA-Filled Capsids in the Cytoplasm of Infected Cells". *Journal of Virology* 74.24 (2000).
DOI: 10.1128/jvi.74.24.11608-11618.2000.

[81] K. Dib et al. "The cytoplasmic tail of L-selectin interacts with the adaptor-protein complex AP-1 subunit μ1A via a novel basic binding motif". *Journal of Biological Chemistry* 292.16 (2017).
DOI: 10.1074/jbc.M116.768598.

[82] B. Diewald et al. "Conformational dynamics of herpesviral NEC proteins in different oligomerization states". *International Journal of Molecular Sciences* 19.10 (2018).
DOI: 10.3390/ijms19102908.

[83] K. S. Dingwell et al. "Herpes simplex virus glycoproteins E and I facilitate cell-to-cell spread in vivo and across junctions of cultured cells." *Journal of Virology* 68.2 (1994).
DOI: 10.1128/jvi.68.2.834-845.1994.

[84] K. S. Dingwell and D. C. Johnson. "The Herpes Simplex Virus gE-gI Complex Facilitates Cell-to-Cell Spread and Binds to Components of Cell Junctions". *Journal of Virology* 72.11 (1998).
DOI: 10.1128/jvi.72.11.8933-8942.1998.

[85] R. Dixit et al. "Herpes simplex virus type 1 induces filopodia in differentiated P19 neural cells to facilitate viral spread". *Neuroscience Letters* 440.2 (2008).
DOI: 10.1016/j.neulet.2008.05.031.

[86] K. Döhner et al. "Function of dynein and dynactin in herpes simplex virus capsid transport". *Molecular Biology of the Cell* 13.8 (2002).
DOI: 10.1091/mbc.01-07-0348.

[87] F. Dorange et al. "Characterization of Marek's disease virus serotype 1 (MDV-1) deletion mutants that lack UL46 to UL49 genes: MDV-1 UL49, encoding VP22, is indispensable for virus growth." *Journal of virology* 76.4 (2002).
DOI: 10.1128/JVI.76.4.1959-1970.2002.

[88] B. Doray et al. "The $\gamma/\sigma 1$ and $\alpha/\sigma 2$ hemicomplexes of clathrin adaptors AP-1 and AP-2 Harbor the dileucine recognition site". *Mol. Biology of the Cell* 18.5 (2007).
DOI: 10.1091/mbc.E07-01-0012.

[89] E. B. Draganova et al. "Structural basis for capsid recruitment and coat formation during hsv-1 nuclear egress". *eLife* 9 (2020).
DOI: 10.7554/eLife.56627.

[90] C. Duffy et al. "Characterization of a U L 49-Null Mutant: VP22 of Herpes Simplex Virus Type 1 Facilitates Viral Spread in Cultured Cells and the Mouse Cornea". *Journal of Virology* 80.17 (2006).
DOI: 10.1128/jvi.00498-06.

[91] G. DuRaine et al. "Herpes Simplex Virus gE/gI and US9 Promote both Envelopment and Sorting of Virus Particles in the Cytoplasm of Neurons, Two Processes That Precede Anterograde Transport in Axons". *Journal of Virology* 91.11 (2017).
DOI: 10.1128/jvi.00050-17.

[92] K. M. Duus and C. Grose. "Multiple regulatory effects of varicella-zoster virus (VZV) gL on trafficking patterns and fusogenic properties of VZV gH." *Journal of virology* 70.12 (1996).
DOI: 10.1128/jvi.70.12.8961-8971.1996.

[93] K. M. Duus et al. "Cell surface expression and fusion by the varicella-zoster virus gH:gL glycoprotein complex: analysis by laser scanning confocal microscopy". *Virology* 210.2 (1995).
DOI: 10.1006/viro.1995.1359.

[94] N. D. Dwyer et al. "Polarized dendritic transport and the AP-1 $\mu 1$ clathrin adaptor UNC-101 localize odorant receptors to olfactory

cilia". *Neuron* 31.2 (2001).
DOI: 10.1016/S0896-6273(01)00361-0.

[95] K. Ebert et al. "Mode of Virus Rescue Determines the Acquisition of VHS Mutations in VP22-Negative Herpes Simplex Virus 1". *Journal of Virology* 87.18 (2013).
DOI: 10.1128/jvi.01654-13.

[96] R. J. Eisenberg et al. "Herpes virus fusion and entry: A story with many characters". *Viruses* 4.5 (2012).
DOI: 10.3390/v4050800.

[97] G. Elliott and P. O'Hare. "Intercellular trafficking and protein delivery by a herpesvirus structural protein". *Cell* 88.2 (1997).
DOI: 10.1016/S0092-8674(00)81843-7.

[98] G. Elliott et al. "Deletion of the Herpes Simplex Virus VP22-Encoding Gene (UL49) Alters the Expression, Localization, and Virion Incorporation of ICP0". *Journal of Virology* 79.15 (2005).
DOI: 10.1128/jvi.79.15.9735-9745.2005.

[99] G. Elliott et al. "Multiple Posttranscriptional Strategies To Regulate the Herpes Simplex Virus 1 vhs Endoribonuclease". *Journal of Virology* 92.17 (2018).
DOI: 10.1128/jvi.00818-18.

[100] G. Elliott et al. "Phosphorylation of the Herpes Simplex Virus Type 1 Tegument Protein VP22". *Virology* 226 (1996).

[101] G. Elliott et al. "VP16 interacts via its activation domain with VP22, a tegument protein of herpes simplex virus, and is relocated to a novel macromolecular assembly in coexpressing cells." *Journal of virology* 69.12 (1995).
DOI: 10.1128/jvi.69.12.7932-7941.1995.

[102] European Centre for Disease Prevention and Control. *ECDC Guidance - Varicella vaccination in the European Union*. Tech. rep. 2015.

[103] M. Falkenberg et al. "The UL8 subunit of the heterotrimeric herpes simplex virus type 1 helicase primase is required for the unwinding of single strand DNA-binding protein (ICP8)-coated DNA substrates". *Journal of Biological Chemistry* 272.36 (1997).
DOI: 10.1074/jbc.272.36.22766.

[104] W. H. Fan et al. "The Large Tegument Protein pUL36 Is Essential for Formation of the Capsid Vertex-Specific Component at the Capsid-Tegument Interface of Herpes Simplex Virus 1". *Journal of Virology* 89.3 (2015).
DOI: 10.1128/jvi.02887-14.

[105] Z. Fan et al. "Truncation of Herpes Simplex Virus Type 2 Glycoprotein B Increases Its Cell Surface Expression and Activity in Cell-Cell Fusion, but These Properties Are Unrelated". *Journal of Virology* 76.18

(2002).
DOI: 10.1128/jvi.76.18.9271-9283.2002.

[106] G. G. Farías et al. "Signal-Mediated, AP-1/Clathrin-Dependent Sorting of Transmembrane Receptors to the Somatodendritic Domain of Hippocampal Neurons". *Neuron* 75.5 (2012).
DOI: 10.1016/j.neuron.2012.07.007.

[107] A. Farnsworth et al. "Cytoplasmic residues of herpes simplex virus glycoprotein gE required for secondary envelopment and binding of tegument proteins VP22 and UL11 to gE and gD." *Journal of virology* 81.1 (2007).
DOI: 10.1128/JVI.01842-06.

[108] A. Farnsworth et al. "Herpes simplex virus glycoproteins gB and gH function in fusion between the virion envelope and the outer nuclear membrane." *Proceedings of the National Academy of Sciences of the United States of America* 104.24 (2007).
DOI: 10.1073/pnas.0703790104.

[109] H. W. Favoreel. "The why's of Y-based motifs in alphaherpesvirus envelope proteins". *Virus Research* 117.2 (2006).
DOI: 10.1016/j.virusres.2005.11.007.

[110] H. W. Favoreel et al. "A Tyrosine-Based Motif in the Cytoplasmic Tail of Pseudorabies Virus Glycoprotein B Is Important for both Antibody-Induced Internalization of Viral Glycoproteins and Efficient Cell-to-Cell Spread". *Journal of Virology* 76.13 (2002).
DOI: 10.1128/jvi.76.13.6845-6851.2002.

[111] H. W. Favoreel et al. "Cytoskeletal rearrangements and cell extensions induced by the US3 kinase of an alphaherpesvirus are associated with enhanced spread". *Proceedings of the National Academy of Sciences of the United States of America* 102.25 (2005).
DOI: 10.1073/pnas.0409099102.

[112] A. Ferrier et al. "Cellular and Molecular Biology of Neuronal Dystonin". In: *International Review of Cell and Molecular Biology*. Vol. 300. Elsevier Inc., 2013.
DOI: 10.1016/B978-0-12-405210-9.00003-5.

[113] E. Feutz et al. "Functional interactions between herpes simplex virus pUL51, pUL7 and gE reveal cell-specific mechanisms for epithelial cell-to-cell spread". *Virology* 537 (2019).
DOI: 10.1016/j.virol.2019.08.014.

[114] R. L. Finnen et al. "Analysis of filamentous process induction and nuclear localization properties of the HSV-2 serine/threonine kinase Us3". *Virology* 397.1 (2010).
DOI: 10.1016/j.virol.2009.11.012.

[115] H. Fölsch et al. "Distribution and function of AP-1 clathrin adaptor complexes in polarized epithelial cells". *Journal of Cell Biology* 153.3 (2001).
DOI: 10.1083/jcb.152.3.595.

[116] H. Fölsch et al. "The AP-1A and AP-1B clathrin adaptor complexes define biochemically and functionally distinct membrane domains". *Journal of Cell Biology* 163.2 (2003).
DOI: 10.1083/jcb.200309020.

[117] E. Fossum et al. "Evolutionarily conserved herpesviral protein interaction networks". *PLoS Pathogens* 5.9 (2009).
DOI: 10.1371/journal.ppat.1000570.

[118] G. Freer and M. Pistello. "Varicella-zoster virus infection: Natural history, clinical manifestations, immunity and current and future vaccination strategies". *New Microbiologica* 41.2 (2018).

[119] W. Fuchs et al. "A Pseudorabies Virus Recombinant Simultaneously Lacking the Major Tegument Proteins Encoded by the UL46, UL47, UL48, and UL49 Genes Is Viable in Cultured Cells". *Journal of Virology* 77.23 (2003).
DOI: 10.1128/jvi.77.23.12891-12900.2003.

[120] W. Fuchs et al. "Essential Function of the Pseudorabies Virus UL36 Gene Product Is Independent of Its Interaction with the UL37 Protein". *Journal of Virology* 78.21 (2004).
DOI: 10.1128/jvi.78.21.11879-11889.2004.

[121] W. Fuchs et al. "Physical interaction between envelope glycoproteins E and M of pseudorabies virus and the major tegument protein UL49." *Journal of virology* 76.16 (2002).
DOI: 10.1128/JVI.76.16.8208-8217.2002.

[122] W. Fuchs et al. "The Interacting UL31 and UL34 Gene Products of Pseudorabies Virus Are Involved in Egress from the Host-Cell Nucleus and Represent Components of Primary Enveloped but Not Mature Virions". *Journal of Virology* 76.1 (2002).
DOI: 10.1128/jvi.76.1.364-378.2002.

[123] A. O. Fuller et al. "Neutralizing antibodies specific for glycoprotein H of herpes simplex virus permit viral attachment to cells but prevent penetration". *Journal of virology* 63.8 (1989).
DOI: 10.1128/JVI.63.8.3435-3443.1989.

[124] M. Gallon and P. J. Cullen. "Retromer and sorting nexins in endosomal sorting". *Biochemical Society Transactions* 43.1 (2015).
DOI: 10.1042/BST20140290.

[125] B. J. Geiss et al. "Temporal Regulation of Herpes Simplex Virus Type 2 VP22 Expression and Phosphorylation". *Journal of Virology* 75.22

(2001).
DOI: 10.1128/jvi.75.22.10721-10729.2001.

[126] R. J. Geraghty et al. "Entry of alphaherpesviruses mediated by poliovirus receptor-related protein 1 and poliovirus receptor". *Science* 280.5369 (1998).
DOI: 10.1126/science.280.5369.1618.

[127] E. Gershburg and J. S. Pagano. "Conserved herpesvirus protein kinases". *Biochimica et Biophysica Acta - Proteins and Proteomics* 1784.1 (2008).
DOI: 10.1016/j.bbapap.2007.08.009.

[128] P. Ghosh et al. "Mannose 6-phosphate receptors: new twists in the tale". *Nature Reviews Molecular Cell Biology 2003 4:3* 4 (3 2003).
DOI: 10.1038/nrm1050.

[129] J. S. Gibbs et al. "Sequence and mapping analyses of the herpes simplex virus DNA polymerase gene predict a C-terminal substrate binding domain". *Proceedings of the National Academy of Sciences of the United States of America* 82.23 (1985).
DOI: 10.1073/pnas.82.23.7969.

[130] W. Gibson and B. Roizman. "Proteins Specified by Herpes Simplex Virus VIII. Characterization and Composition of Multiple Capsid Forms of Subtypes 1 and 2". *Journal of Virology* 10.5 (1972).
DOI: 10.1128/jvi.10.5.1044-1052.1972.

[131] D. H. Gilden et al. "Varicella-zoster". In: *Handbook of Clinical Neurology*. Vol. 123. Elsevier B.V., 2014.
DOI: 10.1016/B978-0-444-53488-0.00012-2.

[132] J. H. Girsch et al. "Exocytosis of Progeny Infectious Varicella-Zoster Virus Particles via a Mannose-6-Phosphate Receptor Pathway without Xenophagy following Secondary Envelopment". *Journal of Virology* 94.16 (2020).
DOI: 10.1128/jvi.00800-20.

[133] A. E. Gorbalenya and E. V. Koonin. "Helicases: amino acid sequence comparisons and structure-function relationships". *Current Opinion in Structural Biology* 3.3 (1993).
DOI: 10.1016/S0959-440X(05)80116-2.

[134] A. E. Gorbalenya and E. V. Koonin. "One more conserved sequence motif in helicases". *Nucleic Acids Research* 16.15 (1988).
DOI: 10.1093/nar/16.15.7734.

[135] A. E. Gorbalenya et al. "Two related superfamilies of putative helicases involved in replication, recombination, repair and expression of DNA and RNA genomes". *Nucleic Acids Research* 17.12 (1989).
DOI: 10.1093/nar/17.12.4713.

[136] J. Gottlieb et al. "The herpes simplex virus type 1 UL42 gene product: a subunit of DNA polymerase that functions to increase processivity." *Journal of Virology* 64.12 (1990).
DOI: 10.1128/jvi.64.12.5976-5987.1990.

[137] H. Granzow et al. "Egress of alphaherpesviruses: comparative ultrastructural study". *J Virol* 75.8 (2001).
DOI: 10.1128/jvi.75.8.3675-3684.2001.

[138] K. L. Graves-Woodward et al. "Biochemical analyses of mutations in the HSV-1 helicase-primase that alter ATP hydrolysis, DNA unwinding, and coupling between hydrolysis and unwinding". *Journal of Biological Chemistry* 272.7 (1997).
DOI: 10.1074/jbc.272.7.4623.

[139] D. Gravotta et al. "The Clathrin Adaptor AP-1A Mediates Basolateral Polarity". *Developmental Cell* 22.4 (2012).
DOI: 10.1016/j.devcel.2012.02.004.

[140] O. Greco et al. "VP22-mediated intercellular transport for suicide gene therapy under oxic and hypoxic conditions". *Gene Therapy* 12.12 (2005).
DOI: 10.1038/sj.gt.3302482.

[141] C. Grose. "Variation on a theme by Fenner: the pathogenesis of chickenpox." *Pediatrics* 68.5 (1981).

[142] C. Grose and T. I. Ng. "Intracellular Synthesis of Varicella Zoster Virus". *J. of Infectious Diseases* 166.Supplement 1 (1992).
DOI: 10.1093/infdis/166.Supplement_1.S7.

[143] C. Grose et al. "Complete DNA Sequence Analyses of the First Two Varicella-Zoster Virus Glycoprotein E (D150N) Mutant Viruses Found in North America: Evolution of Genotypes with an Accelerated Cell Spread Phenotype". *Journal of Virology* 78.13 (2004).
DOI: 10.1128/jvi.78.13.6799-6807.2004.

[144] S. T. Gross et al. "The cytoplasmic tail of Herpes simplex virus glycoprotein H binds to the tegument protein VP16 in vitro and in vivo". *Virology* 317.1 (2003).
DOI: 10.1016/j.virol.2003.08.023.

[145] C. M. Guardia et al. *Neuronal functions of adaptor complexes involved in protein sorting*. 2018.
DOI: 10.1016/j.conb.2018.02.021.

[146] X. Guo et al. "The Adaptor Protein-1μ1B Subunit Expands the Repertoire of Basolateral Sorting Signal Recognition in Epithelial Cells". *Developmental Cell* 27.3 (2013).
DOI: 10.1016/j.devcel.2013.10.006.

[147] S. Gurke et al. "Tunneling nanotube (TNT)-like structures facilitate a constitutive, actomyosin-dependent exchange of endocytic

organelles between normal rat kidney cells". *Experimental Cell Research* 314.20 (2008).
DOI: 10.1016/j.yexcr.2008.08.022.

[148] C. Hagen et al. "Structural Basis of Vesicle Formation at the Inner Nuclear Membrane". *Cell* 163.7 (2015).
DOI: 10.1016/j.cell.2015.11.029.

[149] S. Hambleton et al. "Cholesterol dependence of varicella zoster virion entry into target cells." *Journal of virology* 81.14 (2007).
DOI: 10.1128/jvi.00486-07.

[150] S. Hambleton et al. "The role of the trans-Golgi network in varicella zoster virus biology". *Cellular and Molecular Life Sciences* 61.24 (2004).
DOI: 10.1007/s00018-004-4269-7.

[151] J. Han et al. "Interaction and Interdependent Packaging of Tegument Protein UL11 and Glycoprotein E of Herpes Simplex Virus". *Journal of Virology* 85.18 (2011).
DOI: 10.1128/jvi.05207-11.

[152] J. S. Harms et al. "Distinctions between Bovine Herpesvirus 1 and Herpes Simplex Virus Type 1 VP22 Tegument Protein Subcellular Associations". *Journal of Virology* 74.7 (2000).
DOI: 10.1128/jvi.74.7.3301-3312.2000.

[153] C. Harter and I. Mellman. "Transport of the lysosomal membrane glycoprotein lgp120 (lgp-A) to lysosomes does not require appearance on the plasma membrane". *Journal of Cell Biology* 117.2 (1992).
DOI: 10.1083/jcb.117.2.311.

[154] J. Hay and W. T. Ruyechan. "Alphaherpesvirus DNA replication". In: *Human Herpesviruses: Biology, Therapy, and Immunoprophylaxis*. Cambridge University Press, 2007.
DOI: 10.1017/CBO9780511545313.011.

[155] J. W. Heine et al. "Proteins Specified by Herpes Simplex Virus XII. The Virion Polypeptides of Type 1 Strains". *Journal of Virology* 14.3 (1974).
DOI: 10.1128/jvi.14.3.640-651.1974.

[156] T. C. Heineman and S. L. Hall. "Role of the Varicella-Zoster Virus gB Cytoplasmic Domain in gB Transport and Viral Egress". *Journal of Virology* 76.2 (2002).
DOI: 10.1128/jvi.76.2.591-599.2002.

[157] T. C. Heineman and S. L. Hall. "VZV gB endocytosis and Golgi localization are mediated by YXXϕ motifs in its cytoplasmic domain". *Virology* 285.1 (2001).
DOI: 10.1006/viro.2001.0930.

[158] T. C. Heineman et al. "Cytoplasmic Domain Signal Sequences That Mediate Transport of Varicella-Zoster Virus gB from the Endoplasmic Reticulum to the Golgi". *Journal of Virology* 74.20 (2000).
DOI: 10.1128/jvi.74.20.9421-9430.2000.

[159] E. E. Heldwein et al. "Crystal structure of glycoprotein B from herpes simplex virus 1". *Science* 313.5784 (2006).
DOI: 10.1126/science.1126548.

[160] J. D. Heming et al. "Herpesvirus capsid assembly and DNA packaging". *Advances in Anatomy Embryology and Cell Biology* 223 (2017).
DOI: 10.1007/978-3-319-53168-7_6.

[161] D. Henaff et al. "Herpesviruses Exploit Several Host Compartments for Envelopment". *Traffic* 13.11 (2012).
DOI: 10.1111/j.1600-0854.2012.01399.x.

[162] B. C. Herold et al. "Glycoprotein C of herpes simplex virus type 1 plays a principal role in the adsorption of virus to cells and in infectivity." *Journal of Virology* 65.3 (1991).
DOI: 10.1128/jvi.65.3.1090-1098.1991.

[163] B. C. Herold et al. "Glycoprotein C-independent binding of herpes simplex virus to cells requires cell surface heparan sulphate and glycoprotein B". *Journal of General Virology* 75.6 (1994).
DOI: 10.1099/0022-1317-75-6-1211.

[164] J. Hertzog et al. "VaricellaZoster virus ORF9 is an antagonist of the DNA sensor cGAS". *The EMBO Journal* 41 (14 2022).
DOI: 10.15252/EMBJ.2021109217.

[165] K. Hew et al. "VP22 core domain from Herpes simplex virus 1 reveals a surprising structural conservation in both the Alpha- and Gammaherpesvirinae subfamilies". *Journal of General Virology* 96.Pt_6 (2015).
DOI: 10.1099/vir.0.000078.

[166] J. B. Heymann et al. "Dynamics of herpes simplex virus capsid maturation visualized by time-lapse cryo-electron microscopy". *Nature Structural Biology* 10.5 (2003).
DOI: 10.1038/nsb922.

[167] H. Hofemeister and P. O'Hare. "Nuclear Pore Composition and Gating in Herpes Simplex Virus-Infected Cells". *Journal of Virology* 82.17 (2008).
DOI: 10.1128/jvi.00951-08.

[168] M. Hollinshead et al. "Endocytic tubules regulated by Rab GTPases 5 and 11 are used for envelopment of herpes simplex virus." *The EMBO journal* 31.21 (2012).
DOI: 10.1038/emboj.2012.262.

[169] R. W. Honess and B. Roizman. "Regulation of Herpesvirus Macromolecular Synthesis I. Cascade Regulation of the Synthesis of Three Groups of Viral Proteins 1". *Journal of Virology* 14.1 (1974).
DOI: 10.1128/jvi.14.1.8-19.1974.

[170] P. W. Howard et al. "Herpes Simplex Virus Membrane Proteins gE/gI and US9 Act Cooperatively To Promote Transport of Capsids and Glycoproteins from Neuron Cell Bodies into Initial Axon Segments". *Journal of Virology* 87.1 (2013).
DOI: 10.1128/jvi.02465-12.

[171] J. Huang et al. "Herpes Simplex Virus 1 Tegument Protein VP22 Abrogates cGAS/STING-Mediated Antiviral Innate Immunity". *Journal of Virology* 92.15 (2018).
DOI: 10.1128/jvi.00841-18.

[172] A. Huet et al. "Role of the Herpes Simplex Virus CVSC Proteins at the Capsid Portal Vertex". *Journal of Virology* 94.24 (2020).
DOI: 10.1128/jvi.01534-20.

[173] L. Hutchinson and D. C. Johnson. "Herpes simplex virus glycoprotein K promotes egress of virus particles." *Journal of virology* 69.9 (1995).
DOI: 10.1128/jvi.69.9.5401-5413.1995.

[174] G. Inchauspe et al. "Mapping of two varicella-zoster virus-encoded genes that activate the expression of viral early and late genes". *Virology* 173.2 (1989).
DOI: 10.1016/0042-6822(89)90583-7.

[175] International Committee on Taxonomy of Viruses. *Herpesvirales*. 2011.

[176] H. Ishikawa et al. "Generation of a dual-functional split-reporter protein for monitoring membrane fusion using self-associating split GFP". *Protein Engineering, Design and Selection* 25 (12 2012).
DOI: 10.1093/PROTEIN/GZS051.

[177] L. Ivanova et al. "Conserved Tryptophan Motifs in the Large Tegument Protein pUL36 Are Required for Efficient Secondary Envelopment of Herpes Simplex Virus Capsids". *Journal of Virology* 90.11 (2016).
DOI: 10.1128/JVI.03167-15.

[178] P. Jackers et al. "Characterization of regulatory functions of the varicella-zoster virus gene 63-encoded protein." *Journal of Virology* 66.6 (1992).
DOI: 10.1128/jvi.66.6.3899-3903.1992.

[179] T. Jacob et al. "Viral Serine/Threonine Protein Kinases". *Journal of Virology* 85.3 (2011).
DOI: 10.1128/jvi.01369-10.

[180] A. Jacquet et al. “The varicella zoster virus glycoprotein B (gB) plays a role in virus binding to cell surface heparan sulfate proteoglycans”. *Virus Research* 53.2 (1998).
DOI: 10.1016/S0168-1702(97)00149-4.

[181] N. Jambunathan et al. “Herpes Simplex Virus 1 Protein UL37 Interacts with Viral Glycoprotein gK and Membrane Protein UL20 and Functions in Cytoplasmic Virion Envelopment”. *Journal of Virology* 88.11 (2014).
DOI: 10.1128/jvi.00278-14.

[182] R. J. J. Jansens et al. “Bridging the Gap: Virus Long-Distance Spread via Tunneling Nanotubes”. *Journal of Virology* 94.8 (2020).
DOI: 10.1128/jvi.02120-19.

[183] R. J. J. Jansens et al. “Pseudorabies Virus US3-Induced Tunneling Nanotubes Contain Stabilized Microtubules, Interact with Neighboring Cells via Cadherins, and Allow Intercellular Molecular Communication”. *Journal of Virology* 91.19 (2017).
DOI: 10.1128/jvi.00749-17.

[184] K. Janvier et al. “Recognition of dileucine-based sorting signals from HIV-1 Nef and LIMP-II by the AP-1 γ-σ1 and AP-3 δ-σ3 hemicomplexes”. *Journal of Cell Biology* 163.6 (2003).
DOI: 10.1083/jcb.200307157.

[185] X. Jia et al. “Structural basis of HIV-1 Vpu-mediated BST2 antagonism via hijacking of the clathrin adaptor protein complex 1”. *eLife* 2014.3 (2014).
DOI: 10.7554/eLife.02362.

[186] D. C. Johnson and J. D. Baines. “Herpesviruses remodel host membranes for virus egress”. *Nature Reviews Microbiology* 9.5 (2011).
DOI: 10.1038/nrmicro2559.

[187] D. C. Johnson et al. “Herpes Simplex Virus gE/gI Sorts Nascent Virions to Epithelial Cell Junctions, Promoting Virus Spread”. *Journal of Virology* 75.2 (2001).
DOI: 10.1128/JVI.75.2.821-833.2001.

[188] P. A. Johnson et al. “Isolation of a herpes simplex virus type 1 mutant deleted for the essential UL42 gene and characterization of its null phenotype.” *Journal of Virology* 65.2 (1991).
DOI: 10.1128/jvi.65.2.700-710.1991.

[189] B. G. Jones et al. “Intracellular trafficking of furin is modulated by the phosphorylation state of a casein kinase II site in its cytoplasmic tail”. *EMBO Journal* 14.23 (1995).
DOI: 10.1002/j.1460-2075.1995.tb00275.x.

[190] V. Jovasevic et al. “Proteolytic Cleavage of VP1-2 Is Required for Release of Herpes Simplex Virus 1 DNA into the Nucleus”. *Journal*

of Virology 82.7 (2008).
DOI: 10.1128/jvi.01919-07.

[191] D. Kalthoff et al. "The UL49 gene product of BoHV-1: A major factor in efficient cell-to-cell spread". *Journal of General Virology* 89.9 (2008).
DOI: 10.1099/vir.0.2008/000208-0.

[192] D. E. Kamen et al. "Structural Basis for the Physiological Temperature Dependence of the Association of VP16 with the Cytoplasmic Tail of Herpes Simplex Virus Glycoprotein H". *Journal of Virology* 79.10 (2005).
DOI: 10.1128/jvi.79.10.6134-6141.2005.

[193] A. Kato et al. "Herpes Simplex Virus 1-Encoded Protein Kinase UL13 Phosphorylates Viral Us3 Protein Kinase and Regulates Nuclear Localization of Viral Envelopment Factors UL34 and UL31". *Journal of Virology* 80.3 (2006).
DOI: 10.1128/jvi.80.3.1476-1486.2006.

[194] K. Kato et al. "Synthesis, subcellular localization and VP16 interaction of the herpes simplex virus type 2 UL46 gene product". *Archives of Virology* 145.10 (2000).
DOI: 10.1007/s007050070045.

[195] Y. Kawaguchi and K. Kato. "Protein kinases conserved in herpesviruses potentially share a function mimicking the cellular protein kinase cdc2". *Reviews in Medical Virology* 13.5 (2003).
DOI: 10.1002/rmv.402.

[196] B. J. Kelly et al. "Functional roles of the tegument proteins of herpes simplex virus type 1". *Virus Research* 145.2 (2009).
DOI: 10.1016/j.virusres.2009.07.007.

[197] B. J. Kelly et al. "The interaction of the HSV-1 tegument proteins pUL36 and pUL37 is essential for secondary envelopment during viral egress". *Virology* 454-455.1 (2014).
DOI: 10.1016/j.virol.2014.02.003.

[198] B. T. Kelly et al. "A structural explanation for the binding of endocytic dileucine motifs by the AP2 complex." *Nature* 456.7224 (2008).
DOI: 10.1038/nature07422.

[199] P. G. Kennedy et al. "Latent varicellazoster virus is located predominantly in neurons in human trigeminal ganglia". *Proceedings of the National Academy of Sciences of the United States of America* 95 (8 1998).
DOI: 10.1073/PNAS.95.8.4658.

[200] P. G. E. Kennedy et al. "Transcriptomal analysis of varicella-zoster virus infection using long oligonucleotide-based microarrays". *Journal of General Virology* 86.10 (2005).
DOI: 10.1099/vir.0.80946-0.

[201] M. I. Khalil et al. "Varicella-zoster virus (VZV) origin of DNA replication oriS influences origin-dependent DNA replication and flanking gene transcription". *Virology* 481 (2015).
DOI: 10.1016/j.virol.2015.02.049.

[202] L. A. Kimpler et al. "Adaptor protein complexes AP-1 and AP-3 are required by the HHV-7 immunoevasin U21 for rerouting of class I MHC molecules to the lysosomal compartment". *PLoS ONE* 9.6 (2014).
DOI: 10.1371/journal.pone.0099139.

[203] P. R. Kinchington et al. "The transcriptional regulatory proteins encoded by varicella zoster virus open reading frames (ORFs) 4 and 63, but not ORF 61, are associated with purified virus particles." *Journal of virology* 69.7 (1995).
DOI: 10.1128/jvi.69.7.4274-4282.1995.

[204] P. R. Kinchington et al. "The varicella-zoster virus immediate-early protein IE62 is a major component of virus particles." *Journal of Virology* 66.1 (1992).
DOI: 10.1128/jvi.66.1.359-366.1992.

[205] D. K. Klinedinst and M. D. Challberg. "Helicase primase complex of herpes simplex virus type 1: a mutation in the UL52 subunit abolishes primase activity." *Journal of Virology* 68.6 (1994).
DOI: 10.1128/jvi.68.6.3693-3701.1994.

[206] B. G. Klupp et al. "Effect of the pseudorabies virus US3 protein on nuclear membrane localization of the UL34 protein and virus egress from the nucleus". *Journal of General Virology* 82.10 (2001).
DOI: 10.1099/0022-1317-82-10-2363.

[207] B. G. Klupp et al. "Nuclear Envelope Breakdown Can Substitute for Primary Envelopment-Mediated Nuclear Egress of Herpesviruses". *Journal of Virology* 85.16 (2011).
DOI: 10.1128/jvi.00741-11.

[208] B. G. Klupp et al. "Functional Analysis of the Pseudorabies Virus UL51 Protein". *Journal of Virology* 79.6 (2005).
DOI: 10.1128/jvi.79.6.3831-3840.2005.

[209] B. G. Klupp et al. "Glycoproteins required for entry are not necessary for egress of pseudorabies virus". *Journal of Virology* 82.13 (2008).
DOI: 10.1128/JVI.00386-08.

[210] B. G. Klupp et al. "Pseudorabies Virus Glycoprotein M Inhibits Membrane Fusion". *Journal of Virology* 74.15 (2000).
DOI: 10.1128/jvi.74.15.6760-6768.2000.

[211] B. G. Klupp et al. "Pseudorabies Virus UL36 Tegument Protein Physically Interacts with the UL37 Protein". *Journal of Virology* 76.6 (2002).
DOI: 10.1128/jvi.76.6.3065-3071.2002.

[212] B. G. Klupp et al. "The Capsid-Associated UL25 Protein of the Alphaherpesvirus Pseudorabies Virus Is Nonessential for Cleavage and Encapsidation of Genomic DNA but Is Required for Nuclear Egress of Capsids". *Journal of Virology* 80.13 (2006).
DOI: 10.1128/jvi.02662-05.

[213] B. G. Klupp et al. "Vesicle formation from the nuclear membrane is induced by coexpression of two conserved herpesvirus proteins". *Proceedings of the National Academy of Sciences of the United States of America* 104.17 (2007).
DOI: 10.1073/pnas.0701757104.

[214] D. H. Ko et al. "The Major Determinant for Addition of Tegument Protein pUL48 (VP16) to Capsids in Herpes Simplex Virus Type 1 Is the Presence of the Major Tegument Protein pUL36 (VP1/2)". *Journal of Virology* 84.3 (2010).
DOI: 10.1128/jvi.01721-09.

[215] S. Kornfeld. "Structure and Function of the Mannose 6-Phosphate/ Insulin like Grrowth Factor II Receptors". *Annual Review of Biochemistry* 61 (1992).
DOI: 10.1146/ANNUREV.BI.61.070192.001515.

[216] A. P. Kowalczyk et al. "Adherens junction turnover: regulating adhesion through cadherin endocytosis, degradation, and recycling". *Sub-cellular biochemistry* 60 (2012).
DOI: 10.1007/978-94-007-4186-7_9.

[217] C. Krummenacher et al. "Comparative usage of herpesvirus entry mediator A and nectin-1 by laboratory strains and clinical isolates of herpes simplex virus". *Virology* 322.2 (2004).
DOI: 10.1016/j.virol.2004.02.005.

[218] S. La Boissière et al. "Compartmentalization of VP16 in Cells Infected with Recombinant Herpes Simplex Virus Expressing VP16-Green Fluorescent Protein Fusion Proteins". *Journal of Virology* 78.15 (2004).
DOI: 10.1128/jvi.78.15.8002-8014.2004.

[219] S. L. Labiuk et al. "Bovine herpesvirus-1 US3 protein kinase: Critical residues and involvement in the phosphorylation of VP22". *Journal of General Virology* 91.5 (2010).
DOI: 10.1099/vir.0.016600-0.

[220] M. F. Ladelfa et al. "Effect of the US3 protein of bovine herpesvirus 5 on the actin cytoskeleton and apoptosis". *Veterinary Microbiology* 153.3-4 (2011).
DOI: 10.1016/j.vetmic.2011.05.037.

[221] K. J. Laing et al. "Immunobiology of Varicella-Zoster Virus Infection". *The Journal of infectious diseases* 218.2 (2018).
DOI: 10.1093/infdis/jiy403.

[222] C. M. Lake and L. M. Hutt-Fletcher. "The Epstein-Barr virus BFRF1 and BFLF2 proteins interact and coexpression alters their cellular localization". *Virology* 320.1 (2004).
DOI: 10.1016/j.virol.2003.11.018.

[223] C. Lamberti and S. K. Weller. "The Herpes Simplex Virus Type 1 Cleavage/Packaging Protein, UL32, Is Involved in Efficient Localization of Capsids to Replication Compartments". *Journal of Virology* 72.3 (1998).
DOI: 10.1128/jvi.72.3.2463-2473.1998.

[224] J. A. S. Lamote et al. "The US3 Protein of Pseudorabies Virus Drives Viral Passage across the Basement Membrane in Porcine Respiratory Mucosa Explants". *Journal of Virology* 90.23 (2016).
DOI: 10.1128/jvi.01577-16.

[225] S. Y. K. Lau and C. M. Crump. "HSV-1 gm and the gK/pUL20 complex are important for the localization of gD and gH/L to viral assembly sites". *Viruses* 7.3 (2015).
DOI: 10.3390/v7030915.

[226] N. R. Leach and R. J. Roller. "Significance of host cell kinases in herpes simplex virus type 1 egress and lamin-associated protein disassembly from the nuclear lamina". *Virology* 406.1 (2010).
DOI: 10.1016/j.virol.2010.07.002.

[227] M. Lebrun et al. "Varicella-Zoster Virus ORF9p Binding to Cellular Adaptor Protein Complex 1 Is Important for Viral Infectivity". *Journal of Virology* 92.15 (2018). Ed. by R. M. Sandri-Goldin.
DOI: 10.1128/jvi.00295-18.

[228] C.-P. Lee et al. "Epstein-Barr Virus BGLF4 Kinase Induces Disassembly of the Nuclear Lamina To Facilitate Virion Production". *Journal of Virology* 82.23 (2008).
DOI: 10.1128/jvi.01100-08.

[229] M. Leelawong et al. "Nuclear Egress of Pseudorabies Virus Capsids Is Enhanced by a Subspecies of the Large Tegument Protein That Is Lost upon Cytoplasmic Maturation". *Journal of Virology* 86.11 (2012).
DOI: 10.1128/jvi.07051-11.

[230] R. de Leeuw et al. "Nuclear Lamins: Thin Filaments with Major Functions". *Trends in Cell Biology* 28.1 (2018).
DOI: 10.1016/j.tcb.2017.08.004.

[231] H. van Leeuwen et al. "Evidence of a Role for Nonmuscle Myosin II in Herpes Simplex Virus Type 1 Egress". *Society* 76.7 (2002).
DOI: 10.1128/JVI.76.7.3471.

[232] H. van Leeuwen et al. "Herpes simplex virus type 1 tegument protein VP22 interacts with TAF-I proteins and inhibits nucleosome

assembly but not regulation of histone acetylation by INHAT". *Journal of General Virology* 84.9 (2003).
DOI: 10.1099/vir.0.19326-0.

[233] I. R. Lehman and P. E. Boehmer. "Replication of herpes simplex virus DNA". *Journal of Biological Chemistry* 274.40 (1999).
DOI: 10.1074/jbc.274.40.28059.

[234] F. Letourneur and R. D. Klausner. "A novel di-leucine motif and a tyrosine-based motif independently mediate lysosomal targeting and endocytosis of CD3 chains". *Cell* 69.7 (1992).
DOI: 10.1016/0092-8674(92)90636-Q.

[235] H. Leuzinger et al. "Herpes Simplex Virus 1 Envelopment Follows Two Diverse Pathways". *Journal of Virology* 79.20 (2005).
DOI: 10.1128/jvi.79.20.13047-13059.2005.

[236] P. Li et al. "Two Clathrin Adaptor Protein Complexes Instruct Axon-Dendrite Polarity". *Neuron* 90.3 (2016).
DOI: 10.1016/j.neuron.2016.04.020.

[237] Q. Li et al. "Insulin degrading enzyme induces a conformational change in varicella-zoster virus gE, and enhances virus infectivity and stability". *PLoS ONE* 5.6 (2010). Ed. by S. Efstathiou.
DOI: 10.1371/journal.pone.0011327.

[238] Q. Li et al. "Insulin Degrading Enzyme Is a Cellular Receptor Mediating Varicella-Zoster Virus Infection and Cell-to-Cell Spread". *Cell* 127.2 (2006).
DOI: 10.1016/j.cell.2006.08.046.

[239] X. Li et al. "AP1S3 is required for hepatitis C virus infection by stabilizing E2 protein". *Antiviral Research* 131 (2016).
DOI: 10.1016/j.antiviral.2016.04.006.

[240] X. Liang et al. "Characterization of bovine herpesvirus 1 UL49 homolog gene and product: bovine herpesvirus 1 UL49 homolog is dispensable for virus growth". *Journal of Virology* 69.6 (1995).
DOI: 10.1128/jvi.69.6.3863-3867.1995.

[241] M. M. Linehan et al. "In Vivo Role of Nectin-1 in Entry of Herpes Simplex Virus Type 1 (HSV-1) and HSV-2 through the Vaginal Mucosa". *Journal of Virology* 78.5 (2004).
DOI: 10.1128/jvi.78.5.2530-2536.2004.

[242] F. Y. Liu and B. Roizman. "The herpes simplex virus 1 gene encoding a protease also contains within its coding domain the gene encoding the more abundant substrate." *Journal of Virology* 65.10 (1991).
DOI: 10.1128/jvi.65.10.5149-5156.1991.

[243] S. Liu et al. "Crystal structure of the herpes simplex virus 1 DNA polymerase". *Journal of Biological Chemistry* 281.26 (2006).
DOI: 10.1074/jbc.M602414200.

[244] J. S. Loomis et al. "Intracellular Trafficking of the UL11 Tegument Protein of Herpes Simplex Virus Type 1". *Journal of Virology* 75.24 (2001).
DOI: 10.1128/jvi.75.24.12209-12219.2001.

[245] S. Loret et al. "Comprehensive Characterization of Extracellular Herpes Simplex Virus Type 1 Virions". *Journal of Virology* 82.17 (2008).
DOI: 10.1128/jvi.00904-08.

[246] L. Lu and W. Hong. "From endosomes to the trans-Golgi network". *Seminars in Cell and Developmental Biology* 31 (2014).
DOI: 10.1016/j.semcdb.2014.04.024.

[247] J. M. Lynch et al. "Physical and functional interaction between the varicella zoster virus IE63 and IE62 proteins". *Virology* 302.1 (2002).
DOI: 10.1006/viro.2002.1555.

[248] T. Mallick-Searle et al. "Postherpetic neuralgia: epidemiology, pathophysiology, and pain management pharmacology" (2016).
DOI: 10.2147/JMDH.S106340.

[249] L. Maresova et al. "Varicella-Zoster Virus gB and gE Coexpression, but Not gB or gE Alone, Leads to Abundant Fusion and Syncytium Formation Equivalent to Those from gH and gL Coexpression". *Journal of Virology* 75.19 (2001).
DOI: 10.1128/jvi.75.19.9483-9492.2001.

[250] M. A. Margeta et al. "Clathrin adaptor AP-1 complex excludes multiple postsynaptic receptors from axons in C. elegans". *Proceedings of the National Academy of Sciences of the United States of America* 106.5 (2009).
DOI: 10.1073/pnas.0812078106.

[251] K. Maringer et al. "A Network of Protein Interactions around the Herpes Simplex Virus Tegument Protein VP22". *Journal of Virology* 86.23 (2012).
DOI: 10.1128/jvi.01913-12.

[252] M. Marschall et al. "Cellular p32 recruits cytomegalovirus kinase pUL97 to redistribute the nuclear lamina". *Journal of Biological Chemistry* 280.39 (2005).
DOI: 10.1074/jbc.M502672200.

[253] H. S. Marsden et al. "The catalytic subunit of the DNA polymerase of herpes simplex virus type 1 interacts specifically with the C terminus of the UL8 component of the viral helicase-primase complex." *Journal of virology* 71.9 (1997).
DOI: 10.1128/jvi.71.9.6390-6397.1997.

[254] Y. Maruzuru et al. "Herpes Simplex Virus 1 VP22 Inhibits AIM2-Dependent Inflammasome Activation to Enable Efficient Viral Replication". *Cell Host and Microbe* 23.2 (2018).
DOI: 10.1016/j.chom.2017.12.014.

[255] H. Matsuura et al. "Crystal structure of the Epstein-Barr virus (EBV) glycoprotein H/glycoprotein L (gHgL) complex". *Proceedings of the National Academy of Sciences of the United States of America* 107.52 (2010).
DOI: 10.1073/pnas.1011806108.

[256] R. Mattera et al. "Conservation and diversification of dileucine signal recognition by adaptor protein (AP) complex variants". *Journal of Biological Chemistry* 286.3 (2011).
DOI: 10.1074/jbc.M110.197178.

[257] E. F. Mbong et al. "Deletion of the Herpes Simplex Virus 1 UL49 Gene Results in mRNA and Protein Translation Defects That Are Complemented by Secondary Mutations in UL41". *Journal of Virology* 86.22 (2012).
DOI: 10.1128/jvi.01975-12.

[258] D. J. McGeoch et al. "Structures of herpes simplex virus type 1 genes required for replication of virus DNA." *Journal of Virology* 62.2 (1988).
DOI: 10.1128/jvi.62.2.444-453.1988.

[259] A. R. McNab et al. "The Product of the Herpes Simplex Virus Type 1 UL25 Gene Is Required for Encapsidation but Not for Cleavage of Replicated Viral DNA". *Journal of Virology* 72.2 (1998).
DOI: 10.1128/jvi.72.2.1060-1070.1998.

[260] D. G. Meckes and J. W. Wills. "Dynamic Interactions of the UL16 Tegument Protein with the Capsid of Herpes Simplex Virus". *Journal of Virology* 81.23 (2007).
DOI: 10.1128/jvi.01306-07.

[261] D. G. Meckes et al. "Complex mechanisms for the packaging of the UL16 tegument protein into herpes simplex virus". *Virology* 398.2 (2010).
DOI: 10.1016/j.virol.2009.12.004.

[262] T. C. Mettenleiter. "Herpesvirus Assembly and Egress". *Journal of Virology* 76.4 (2002).
DOI: 10.1128/JVI.76.4.1537.

[263] T. C. Mettenleiter et al. "Herpesvirus assembly: An update". *Virus Research* 143.2 (2009).
DOI: 10.1016/j.virusres.2009.03.018.

[264] T. C. Mettenleiter et al. "The way out: What we know and do not know about herpesvirus nuclear egress". *Cellular Microbiology* 15.2

(2013).
DOI: 10.1111/cmi.12044.

[265] R. Mi et al. "The enhanced efficacy of herpes simplex virus by lentivirus mediated VP22 and cytosine deaminase gene therapy against glioma". *Brain Research* 1743 (2020).
DOI: 10.1016/j.brainres.2020.146898.

[266] J. L. Miller et al. "Low-pH Endocytic Entry of the Porcine Alphaherpesvirus Pseudorabies Virus". *Journal of Virology* 93.2 (2018).
DOI: 10.1128/jvi.01849-18.

[267] M. Miyaji-Yamaguchi et al. "Coiled-coil structure-mediated dimerization of template activating factor-I is critical for its chromatin remodeling activity". *Journal of Molecular Biology* 290.2 (1999).
DOI: 10.1006/jmbi.1999.2898.

[268] J. F. Moffat et al. "The ORF47 and ORF66 putative protein kinases of varicella-zoster virus determine tropism for human T cells and skin in the SCID-hu mouse". *Proceedings of the National Academy of Sciences of the United States of America* 95.20 (1998).
DOI: 10.1073/pnas.95.20.11969.

[269] R. I. Montgomery et al. "Herpes simplex virus-1 entry into cells mediated by a novel member of the TNF/NGF receptor family". *Cell* 87.3 (1996).
DOI: 10.1016/S0092-8674(00)81363-X.

[270] A. Montpetit et al. "Disruption of AP1S1, causing a novel neurocutaneous syndrome, perturbs development of the skin and spinal cord". *PLoS Genetics* 4.12 (2008).
DOI: 10.1371/journal.pgen.1000296.

[271] H. Moriuchi et al. "Varicella-zoster virus (VZV) open reading frame 61 protein transactivates VZV gene promoters and enhances the infectivity of VZV DNA." *Journal of Virology* 67.7 (1993).
DOI: 10.1128/jvi.67.7.4290-4295.1993.

[272] K. L. Mossman et al. "Evidence that Herpes Simplex Virus VP16 Is Required for Viral Egress Downstream of the Initial Envelopment Event". *Journal of Virology* 74.14 (2000).
DOI: 10.1128/jvi.74.14.6287-6299.2000.

[273] F. Mou et al. "Phosphorylation of the U(L)31 protein of herpes simplex virus 1 by the U(S)3-encoded kinase regulates localization of the nuclear envelopment complex and egress of nucleocapsids." *Journal of virology* 83.10 (2009).
DOI: 10.1128/JVI.00090-09.

[274] I. Muylaert and P. Elias. "Knockdown of DNA ligase IV/XRCC4 by RNA interference inhibits herpes simplex virus type I DNA replication". *Journal of Biological Chemistry* 282.15 (2007).
DOI: 10.1074/jbc.M611834200.

[275] M. Nadal et al. "Structure and inhibition of herpesvirus DNA packaging terminase nuclease domain". *Proceedings of the National Academy of Sciences of the United States of America* 107.37 (2010).
DOI: 10.1073/pnas.1007144107.

[276] M. H. Naghavi et al. "Plus end tracking proteins, CLASPs, and a viral Akt mimic regulate herpesvirus-induced stable microtubule formation and virus spread". *Proceedings of the National Academy of Sciences of the United States of America* 110.45 (2013).
DOI: 10.1073/pnas.1310760110.

[277] S. Nagpal and J. M. Ostrove. "Characterization of a potent varicella-zoster virus-encoded trans-repressor." *Journal of Virology* 65.10 (1991).
DOI: 10.1128/jvi.65.10.5289-5296.1991.

[278] P. N. Negredo et al. "Contribution of the clathrin adaptor AP-1 subunit μ1 to acidic cluster protein sorting". *Journal of Cell Biology* 216.9 (2017).
DOI: 10.1083/jcb.201602058.

[279] W. W. Newcomb et al. "Assembly of the herpes simplex virus capsid: Characterization of intermediates observed during cell-free capsid formation". *Journal of Molecular Biology* 263.3 (1996).
DOI: 10.1006/jmbi.1996.0587.

[280] W. W. Newcomb et al. "Assembly of the Herpes Simplex Virus Capsid: Identification of Soluble Scaffold-Portal Complexes and Their Role in Formation of Portal-Containing Capsids". *Journal of Virology* 77.18 (2003).
DOI: 10.1128/jvi.77.18.9862-9871.2003.

[281] W. W. Newcomb et al. "Herpes Simplex Virus Capsid Structure: DNA Packaging Protein UL25 Is Located on the External Surface of the Capsid near the Vertices". *Journal of Virology* 80.13 (2006).
DOI: 10.1128/jvi.02648-05.

[282] W. W. Newcomb et al. "Involvement of the Portal at an Early Step in Herpes Simplex Virus Capsid Assembly". *Journal of Virology* 79.16 (2005).
DOI: 10.1128/jvi.79.16.10540-10546.2005.

[283] W. W. Newcomb et al. "Structure of the herpes simplex virus capsid: Molecular composition of the pentons and the triplexes". *Journal of Molecular Biology* 232.2 (1993).
DOI: 10.1006/jmbi.1993.1406.

[284] W. W. Newcomb et al. "The UL6 Gene Product Forms the Portal for Entry of DNA into the Herpes Simplex Virus Capsid". *Journal of Virology* 75.22 (2001).
DOI: 10.1128/jvi.75.22.10923-10932.2001.

[285] P. Nicholson et al. "Localization of the herpes simplex virus type 1 major capsid protein VP5 to the cell nucleus requires the abundant scaffolding protein VP22a". *Journal of General Virology* 75.5 (1994).
DOI: 10.1099/0022-1317-75-5-1091.

[286] A. V. Nicola et al. "Roles for Endocytosis and Low pH in Herpes Simplex Virus Entry into HeLa and Chinese Hamster Ovary Cells". *Journal of Virology* 77.9 (2003).
DOI: 10.1128/jvi.77.9.5324-5332.2003.

[287] A. F. Nikkels et al. "Comparative immunohistochemical study of herpes simplex and varicella-zoster infections". *Virchows Archiv. A, Pathological anatomy and histopathology* 422 (2 1993).
DOI: 10.1007/BF01607163.

[288] R. Nixdorf et al. "Role of the cytoplasmic tails of pseudorabies virus glycoproteins B, E and M intracellular localization and virion incorporation". *Journal of General Virology* 82.1 (2001).
DOI: 10.1099/0022-1317-82-1-215.

[289] N. Nozawa et al. "Herpes Simplex Virus Type 1 UL51 Protein Is Involved in Maturation and Egress of Virus Particles". *Journal of Virology* 79.11 (2005).
DOI: 10.1128/jvi.79.11.6947-6956.2005.

[290] N. Nozawa et al. "Subcellular localization of herpes simplex virus type 1 UL51 protein and role of palmitoylation in Golgi apparatus targeting." *Journal of virology* 77.5 (2003).
DOI: 10.1128/JVI.77.5.3204-3216.2003.

[291] M. O'Hara et al. "Mutational Analysis of the Herpes Simplex Virus Type 1 UL25 DNA Packaging Protein Reveals Regions That Are Important after the Viral DNA Has Been Packaged". *Journal of Virology* 84.9 (2010).
DOI: 10.1128/jvi.02442-09.

[292] K. J. O'Regan et al. "A conserved region of the herpes simplex virus type 1 tegument protein VP22 facilitates interaction with the cytoplasmic tail of glycoprotein E (gE)". *Virology* 358.1 (2007).
DOI: 10.1016/j.virol.2006.08.024.

[293] H. Ohno et al. "μ1B, a novel adaptor medium chain expressed in polarized epithelial cells". *FEBS Letters* 449.2-3 (1999).
DOI: 10.1016/S0014-5793(99)00432-9.

[294] H. Ohno et al. "Interaction of Tyrosine-Based Sorting Signals with Clathrin-Associated Proteins." *Science (New York, N.Y.)* 269.5232

(1995).
DOI: 10.1126/science.7569928.

[295] H. Ohno et al. "Structural determinants of interaction of tyrosine-based sorting signals with the adaptor medium chains". *Journal of Biological Chemistry* 271.46 (1996).
DOI: 10.1074/jbc.271.46.29009.

[296] H. Ohno et al. "The medium subunits of adaptor complexes recognize distinct but overlapping sets of tyrosine-based sorting signals". *Journal of Biological Chemistry* 273.40 (1998).
DOI: 10.1074/jbc.273.40.25915.

[297] P. M. Ojala et al. "Herpes Simplex Virus Type 1 Entry into Host Cells: Reconstitution of Capsid Binding and Uncoating at the Nuclear Pore Complex In Vitro". *Molecular and Cellular Biology* 20.13 (2000).
DOI: 10.1128/mcb.20.13.4922-4931.2000. arXiv: NIHMS150003.

[298] A. Okada et al. "Equine herpesvirus type 1 tegument protein VP22 is not essential for pathogenicity in a hamster model, but is required for efficient viral growth in cultured cells". *Journal of Veterinary Medical Science* 77.10 (2015).
DOI: 10.1292/jvms.14-0648.

[299] M. E. Okoye et al. "Functional Analysis of the Triplex Proteins (VP19C and VP23) of Herpes Simplex Virus Type 1". *Journal of Virology* 80.2 (2006).
DOI: 10.1128/jvi.80.2.929-940.2006.

[300] M. Okuwaki and K. Nagata. "Template activating factor-I remodels the chromatin structure and stimulates transcription from the chromatin template". *Journal of Biological Chemistry* 273.51 (1998).
DOI: 10.1074/jbc.273.51.34511.

[301] S. L. Oliver et al. "A glycoprotein B-neutralizing antibody structure at 2.8 Å uncovers a critical domain for herpesvirus fusion initiation". *Nature Communications* 11.1 (2020).
DOI: 10.1038/s41467-020-17911-0.

[302] S. L. Oliver et al. "An immunoreceptor tyrosine-based inhibition motif in varicella-zoster virus glycoprotein B regulates cell fusion and skin pathogenesis". *Proceedings of the National Academy of Sciences of the United States of America* 110.5 (2013).
DOI: 10.1073/pnas.1216985110.

[303] S. L. Oliver et al. "Dysregulated Glycoprotein B Mediated Cell-Cell Fusion Disrupts Varicella-Zoster Virus and Host Gene Transcription during Infection". *Journal of Virology* 91.1 (2017).
DOI: 10.1128/jvi.01613-16.

[304] S. L. Oliver et al. "The N-terminus of varicella-zoster virus glycoprotein B has a functional role in fusion". *PLoS Pathogens* 17.1 (2021). DOI: 10.1371/journal.ppat.1008961.

[305] S. L. Oliver et al. "Varicella-zoster virus: Molecular controls of cell fusion dependent pathogenesis". *Biochemical Society Transactions* 48.6 (2020). DOI: 10.1042/BST20190511.

[306] P. D. Olivo et al. "Herpes simplex virus DNA replication: The UL9 gene encodes an origin-binding protein". *Proceedings of the National Academy of Sciences of the United States of America* 85.15 (1988). DOI: 10.1073/pnas.85.15.5414.

[307] J. K. Olson and C. Grose. "Endocytosis and recycling of varicella-zoster virus Fc receptor glycoprotein gE: internalization mediated by a YXXL motif in the cytoplasmic tail." *Journal of virology* 71.5 (1997). DOI: 10.1128/jvi.71.5.4042-4054.1997.

[308] B. Önfelt et al. "Structurally Distinct Membrane Nanotubes between Human Macrophages Support Long-Distance Vesicular Traffic or Surfing of Bacteria". *The Journal of Immunology* 177.12 (2006). DOI: 10.4049/jimmunol.177.12.8476.

[309] D. J. Owen et al. "Tegument assembly and secondary envelopment of alphaherpesviruses". *Viruses* 7.9 (2015). DOI: 10.3390/v7092861.

[310] D. J. Owen and P. R. Evans. "A structural explanation for the recognition of tyrosine-based endocytotic signals". *Science* 282.5392 (1998). DOI: 10.1126/science.282.5392.1327.

[311] M. Panasiuk et al. "Tunneling Nanotubes as a Novel Route of Cell-to-Cell Spread of Herpesviruses". *Journal of Virology* 92.10 (2018). DOI: 10.1128/jvi.00090-18.

[312] K. Pannhorst et al. "Bovine Herpesvirus 1 U L 49.5 Interacts with gM and VP22 To Ensure Virus Cell-to-Cell Spread and Virion Incorporation: Novel Role for VP22 in gM-Independent U L 49.5 Virion Incorporation". *Journal of Virology* 92.13 (2018). DOI: 10.1128/jvi.00240-18.

[313] R. Park and J. D. Baines. "Herpes Simplex Virus Type 1 Infection Induces Activation and Recruitment of Protein Kinase C to the Nuclear Membrane and Increased Phosphorylation of Lamin B". *Journal of Virology* 80.1 (2006). DOI: 10.1128/jvi.80.1.494-504.2006.

[314] S. Y. Park and X. Guo. "Adaptor protein complexes and intracellular transport." *Bioscience Reports* 34.4 (2014). DOI: 10.1042/BSR20140069.

[315] D. Pasdeloup et al. "Herpesvirus Tegument Protein pUL37 Interacts with Dystonin/BPAG1 To Promote Capsid Transport on Microtubules during Egress". *Journal of Virology* 87.5 (2013).
DOI: 10.1128/jvi.02676-12.

[316] D. Pasdeloup et al. "Herpesvirus Capsid Association with the Nuclear Pore Complex and Viral DNA Release Involve the Nucleoporin CAN/Nup214 and the Capsid Protein pUL25". *Journal of Virology* 83.13 (2009).
DOI: 10.1128/jvi.02655-08.

[317] D. Pasdeloup et al. "Inner tegument protein pUL37 of herpes simplex virus type 1 is involved in directing capsids to the trans-Golgi network for envelopment". *Journal of General Virology* 91.9 (2010).
DOI: 10.1099/vir.0.022053-0.

[318] T. J. Pasieka et al. "A Functional YNKI Motif in the Short Cytoplasmic Tail of Varicella-Zoster Virus Glycoprotein gH Mediates Clathrin Dependent and Antibody Independent Endocytosis". *Journal of Virology* 77.7 (2003).
DOI: 10.1128/JVI.77.7.4191-4204.2003.

[319] P. E. Pellett and B. Roizman. *Herpesviridae | Basicmedical Key*.

[320] L. P. Perera et al. "The Varicella-Zoster virus immediate early protein, IE62, can positively regulate its cognate promoter". *Virology* 191.1 (1992).
DOI: 10.1016/0042-6822(92)90197-W.

[321] D. Pérez-Núñez et al. "CD2v interacts with Adaptor Protein AP-1 during African swine fever infection". *PLoS ONE* 10.4 (2015).
DOI: 10.1371/journal.pone.0123714.

[322] S. Pernigo et al. "Structural basis for kinesin-1:cargo recognition". *Science* 340.6130 (2013).
DOI: 10.1126/science.1234264.

[323] P. E. Pertel and P. G. Spear. "Modified entry and syncytium formation by herpes simplex virus type 1 mutants selected for resistance to heparin inhibition". *Virology* 226 (1 1996).
DOI: 10.1006/VIRO.1996.0624.

[324] G. A. Peters et al. "A Full-Genome Phylogenetic Analysis of Varicella-Zoster Virus Reveals a Novel Origin of Replication-Based Genotyping Scheme and Evidence of Recombination between Major Circulating Clades". *Journal of Virology* 80 (19 2006).
DOI: 10.1128/JVI.00715-06/SUPPL_FILE/SUPPLEMENTAL_VZV_SNP_DATA__FINAL_.DOC.

[325] K. Pheasant et al. "Nuclear-cytoplasmic compartmentalization of the herpes simplex virus 1 infected cell transcriptome is co-ordinated by the viral endoribonuclease vhs and cofactors to facilitate the

translation of late proteins". *PLoS Pathogens* 14.11 (2018). Ed. by E. A. Murphy.
DOI: 10.1371/journal.ppat.1007331.

[326] J. D. Pitts et al. "Crystal Structure of the Herpesvirus Inner Tegument Protein UL37 Supports Its Essential Role in Control of Viral Trafficking". *Journal of Virology* 88.10 (2014).
DOI: 10.1128/jvi.00163-14.

[327] K. Polcicova et al. "The Extracellular Domain of Herpes Simplex Virus gE Is Indispensable for Efficient Cell-to-Cell Spread: Evidence for gE/gI Receptors". *Journal of Virology* 79.18 (2005).
DOI: 10.1128/jvi.79.18.11990-12001.2005.

[328] L. E. Pomeranz and J. A. Blaho. "Modified VP22 localizes to the cell nucleus during synchronized herpes simplex virus type 1 infection." *Journal of virology* 73.8 (1999).

[329] L. E. Pomeranz and J. A. Blaho. "Assembly of Infectious Herpes Simplex Virus Type 1 Virions in the Absence of Full-Length VP22". *Journal of Virology* 74.21 (2000).
DOI: 10.1128/jvi.74.21.10041-10054.2000.

[330] L. E. Pomeranz et al. "Molecular Biology of Pseudorabies Virus: Impact on Neurovirology and Veterinary Medicine". *Microbiology and Molecular Biology Reviews* 69 (3 2005).
DOI: 10.1128/MMBR.69.3.462-500.2005.

[331] L. Pond et al. *A role for acidic residues in Di-leucine motif-based targeting to the endocytic pathway*. 1995.
DOI: 10.1074/jbc.270.34.19989.

[332] D. J. Purifoy et al. "Identification of the herpes simplex virus DNA polymerase gene". *Nature* 269.5629 (1977).
DOI: 10.1038/269621a0.

[333] F. C. Purves et al. "Herpes simplex virus 1 protein kinase is encoded by open reading frame US3 which is not essential for virus growth in cell culture." *Journal of Virology* 61.9 (1987).
DOI: 10.1128/jvi.61.9.2896-2901.1987.

[334] Z. Qiu et al. "Bovine Herpesvirus Tegument Protein VP22 Enhances Thymidine Kinase/Ganciclovir Suicide Gene Therapy for Neuroblastomas Compared to Herpes Simplex Virus VP22". *Journal of Virology* 78.8 (2004).
DOI: 10.1128/jvi.78.8.4224-4233.2004.

[335] K. Radtke et al. "Plus- and minus-end directed microtubule motors bind simultaneously to herpes simplex virus capsids using different inner tegument structures". *PLoS Pathogens* 6.7 (2010).
DOI: 10.1371/journal.ppat.1000991.

[336] J. C. Randell and D. M. Coen. "Linear diffusion on DNA despite high-affinity binding by a DNA polymerase processivity factor". *Molecular Cell* 8.4 (2001).
DOI: 10.1016/S1097-2765(01)00355-0.

[337] M. Reichelt et al. "The Replication Cycle of Varicella-Zoster Virus: Analysis of the Kinetics of Viral Protein Expression, Genome Synthesis, and Virion Assembly at the Single-Cell Level". *Journal of Virology* 83.8 (2009).
DOI: 10.1128/jvi.02137-08.

[338] X. Ren et al. "Tyrosine phosphorylation of bovine herpesvirus 1 tegument protein VP22 correlates with the incorporation of VP22 into virions." *Journal of virology* 75.19 (2001).
DOI: 10.1128/JVI.75.19.9010-9017.2001.

[339] X. Ren et al. "Structural basis for recruitment and activation of the AP-1 clathrin adaptor complex by Arf1". *Cell* 152.4 (2013).
DOI: 10.1016/j.cell.2012.12.042.

[340] Y. Ren et al. "Glycoprotein M is important for the efficient incorporation of glycoprotein H-L into herpes simplex virus type 1 particles". *Journal of General Virology* 93.2 (2012).
DOI: 10.1099/vir.0.035444-0.

[341] A. E. Reynolds et al. "UL31 and UL34 Proteins of Herpes Simplex Virus Type 1 Form a Complex That Accumulates at the Nuclear Rim and Is Required for Envelopment of Nucleocapsids". *Journal of Virology* 75.18 (2001).
DOI: 10.1128/jvi.75.18.8803-8817.2001.

[342] A. E. Reynolds et al. "Ultrastructural Localization of the Herpes Simplex Virus Type 1 UL31, UL34, and US3 Proteins Suggests Specific Roles in Primary Envelopment and Egress of Nucleocapsids". *Journal of Virology* 76.17 (2002).
DOI: 10.1128/jvi.76.17.8939-8952.2002.

[343] T. del Rio et al. "The Pseudorabies Virus VP22 Homologue (UL49) Is Dispensable for Virus Growth In Vitro and Has No Effect on Virulence and Neuronal Spread in Rodents". *Journal of Virology* 76.2 (2002).
DOI: 10.1128/jvi.76.2.774-782.2002.

[344] L. Riva et al. "Deletion of the ORF9p Acidic Cluster Impairs the Nuclear Egress of Varicella-Zoster Virus Capsids". *Journal of Virology* 89.4 (2015).
DOI: 10.1128/JVI.03215-14.

[345] L. Riva et al. "ORF9p phosphorylation by ORF47p is crucial for the formation and egress of varicella-zoster virus viral particles." *Journal*

of virology 87.5 (2013).
DOI: 10.1128/JVI.02757-12.

[346] F. J. Rixon and D. McNab. "Packaging-Competent Capsids of a Herpes Simplex Virus Temperature Sensitive Mutant Have Properties Similar to Those of In Vitro-Assembled Procapsids". *Journal of Virology* 73.7 (1999).
DOI: 10.1128/jvi.73.7.5714-5721.1999.

[347] F. J. Rixon et al. "Multiple interactions control the intracellular localization of the herpes simplex virus type 1 capsid proteins". *Journal of General Virology* 77.9 (1996).
DOI: 10.1099/0022-1317-77-9-2251.

[348] B. Roizmann et al. "The family Herpesviridae: an update. The Herpesvirus Study Group of the International Committee on Taxonomy of Viruses." *Archives of virology* 123.3-4 (1992).
DOI: 10.1007/BF01317276.

[349] R. J. Roller et al. "The Herpes Simplex Virus 1 UL51 Gene Product Has Cell Type-Specific Functions in Cell-to-Cell Spread". *Journal of Virology* 88.8 (2014).
DOI: 10.1128/jvi.03707-13.

[350] R. J. Roller and J. D. Baines. "Herpesvirus nuclear egress". In: *Advances in Anatomy Embryology and Cell Biology*. Vol. 223. Springer Verlag, 2017.
DOI: 10.1007/978-3-319-53168-7_7.

[351] R. J. Roller and R. Fetters. "The Herpes Simplex Virus 1 UL51 Protein Interacts with the UL7 Protein and Plays a Role in Its Recruitment into the Virion". *Journal of Virology* 89.6 (2015).
DOI: 10.1128/jvi.02799-14.

[352] B. A. Rous et al. "Role of adaptor complex AP-3 in targeting wild-type and mutated CD63 to lysosomes". *Molecular Biology of the Cell* 13.3 (2002).
DOI: 10.1091/mbc.01-08-0409.

[353] N. Ruel et al. "Alanine substitution of conserved residues in the cytoplasmic tail of herpes simplex virus gB can enhance or abolish cell fusion activity and viral entry". *Virology* 346.1 (2006).
DOI: 10.1016/j.virol.2005.11.002.

[354] T. Russell et al. "Qualitative Differences in Capsidless L-Particles Released as a By-Product of Bovine Herpesvirus 1 and Herpes Simplex Virus 1 Infections". *Journal of Virology* 92.22 (2018).
DOI: 10.1128/jvi.01259-18.

[355] A. Rustom et al. "Nanotubular Highways for Intercellular Organelle Transport". *Science* 303.5660 (2004).
DOI: 10.1126/science.1093133.

[356] S. D. Ryan et al. "Microtubule stability, Golgi organization, and transport flux require dystonin-a2-MAP1B interaction". *Journal of Cell Biology* 196.6 (2012).
DOI: 10.1083/jcb.201107096.

[357] B. J. Ryckman and R. J. Roller. "Herpes Simplex Virus Type 1 Primary Envelopment: UL34 Protein Modification and the US3-UL34 Catalytic Relationship". *Journal of Virology* 78.1 (2004).
DOI: 10.1128/jvi.78.1.399-412.2004.

[358] I. V. Sandoval et al. "Distinct reading of different structural determinants modulates the dileucine-mediated transport steps of the lysosomal membrane protein LIMPII and the insulin-sensitive glucose transporter GLUT4". *Journal of Biological Chemistry* 275.51 (2000).
DOI: 10.1074/jbc.M006261200.

[359] R. A. Santos et al. "Antigenic variation of varicella zoster virus Fc receptor gE: Loss of a major B cell epitope in the ectodomain". *Virology* 249.1 (1998).
DOI: 10.1006/viro.1998.9313.

[360] R. A. Santos et al. "Varicella-zoster virus gE escape mutant VZV-MSP exhibits an accelerated cell-to-cell spread phenotype in both infected cell cultures and SCID-hu mice". *Virology* 275.2 (2000).
DOI: 10.1006/viro.2000.0507.

[361] B. Sato et al. "Requirement of Varicella-Zoster Virus Immediate-Early 4 Protein for Viral Replication". *Journal of Virology* 77.22 (2003).
DOI: 10.1128/jvi.77.22.12369-12372.2003.

[362] K. Sato et al. "Numb controls E-cadherin endocytosis through p120 catenin with aPKC". *Molecular Biology of the Cell* 22 (17 2011).
DOI: 10.1091/MBC.E11-03-0274.

[363] K. S. Schulz et al. "Herpesvirus nuclear egress: Pseudorabies Virus can simultaneously induce nuclear envelope breakdown and exit the nucleus via the envelopment-deenvelopment-pathway". *Virus Res.* 209 (2015).
DOI: 10.1016/j.virusres.2015.02.001.

[364] D. Schumacher et al. "The Protein Encoded by the US3 Orthologue of Marek's Disease Virus Is Required for Efficient De-Envelopment of Perinuclear Virions and Involved in Actin Stress Fiber Breakdown". *Journal of Virology* 79.7 (2005).
DOI: 10.1128/jvi.79.7.3987-3997.2005.

[365] M. T. Sciortino et al. "Of the three tegument proteins that package mRNA in herpes simplex virions, one (VP22) transports the mRNA to uninfected cells for expression prior to viral infection." *Proceedings of the National Academy of Sciences of the United States of America* 99.12

(2002).
DOI: 10.1073/pnas.122231699.

[366] M. T. Sciortino et al. "Replication-Competent Herpes Simplex Virus 1 Isolates Selected from Cells Transfected with a Bacterial Artificial Chromosome DNA Lacking Only the UL49 Gene Vary with Respect to the Defect in the UL41 Gene Encoding Host Shutoff RNase". *Journal of Virology* 81.20 (2007).
DOI: 10.1128/jvi.01239-07.

[367] S. Selvarajan Sigamani et al. "The Structure of the Herpes Simplex Virus DNA-Packaging Terminase pUL15 Nuclease Domain Suggests an Evolutionary Lineage among Eukaryotic and Prokaryotic Viruses". *Journal of Virology* 87.12 (2013).
DOI: 10.1128/jvi.00311-13.

[368] A. K. Sheaffer et al. "Herpes Simplex Virus DNA Cleavage and Packaging Proteins Associate with the Procapsid prior to Its Maturation". *Journal of Virology* 75.2 (2001).
DOI: 10.1128/jvi.75.2.687-698.2001.

[369] G. Sherman et al. "The UL8 subunit of the herpes simplex virus helicase-primase complex is required for efficient primer utilization." *Journal of Virology* 66.8 (1992).
DOI: 10.1128/jvi.66.8.4884-4892.1992.

[370] T. Shimi et al. "Structural organization of nuclear lamins A, C, B1, and B2 revealed by superresolution microscopy". *Molecular Biology of the Cell* 26.22 (2015).
DOI: 10.1091/mbc.E15-07-0461.

[371] D. Shukla and P. G. Spear. "Herpesviruses and heparan sulfate: an intimate relationship in aid of viral entry". *Journal of Clinical Investigation* 108.4 (2001).
DOI: 10.1172/jci13799.

[372] D. Shukla et al. "A novel role for 3-O-sulfated heparan sulfate in herpes simplex virus 1 entry". *Cell* 99.1 (1999).
DOI: 10.1016/S0092-8674(00)80058-6.

[373] M. Simpson-Holley et al. "Identification and Functional Evaluation of Cellular and Viral Factors Involved in the Alteration of Nuclear Architecture during Herpes Simplex Virus 1 Infection". *Journal of Virology* 79.20 (2005).
DOI: 10.1128/jvi.79.20.12840-12851.2005.

[374] R. Singh et al. "Phosphoserine acidic cluster motifs bind distinct basic regions on theμ subunits of clathrin adaptor protein complexes". *Journal of Biological Chemistry* 293.40 (2018).
DOI: 10.1074/jbc.RA118.003080.

[375] C. A. Smibert et al. "Herpes simplex virus VP16 forms a complex with the virion host shutoff protein vhs." *Journal of Virology* 68.4 (1994).
DOI: 10.1128/jvi.68.4.2339-2346.1994.

[376] A. Snyder et al. "Herpes Simplex Virus gE/gI and US9 Proteins Promote Transport of both Capsids and Virion Glycoproteins in Neuronal Axons". *Journal of Virology* 82.21 (2008).
DOI: 10.1128/jvi.01241-08.

[377] B. Sodeik. "Mechanisms of viral transport in the cytoplasm". *Trends in Microbiology* 8.10 (2000).
DOI: 10.1016/S0966-842X(00)01824-2.

[378] P. G. Spear. "Herpes simplex virus: Receptors and ligands for cell entry". *Cellular Microbiology* 6.5 (2004).
DOI: 10.1111/j.1462-5822.2004.00389.x.

[379] P. G. Spear et al. "Three classes of cell surface receptors for alphaherpesvirus entry". *Virology* 275.1 (2000).
DOI: 10.1006/viro.2000.0529.

[380] J. V. Spencer et al. "Assembly of the Herpes Simplex Virus Capsid: Preformed Triplexes Bind to the Nascent Capsid". *Journal of Virology* 72.5 (1998).
DOI: 10.1128/jvi.72.5.3944-3951.1998.

[381] M. L. Spengler et al. "Physical interaction between two varicella zoster virus gene regulatory proteins, IE4 and IE62". *Virology* 272.2 (2000).
DOI: 10.1006/viro.2000.0389.

[382] C. W. Stackpole. "Herpes-Type Virus of the Frog Renal Adenocarcinoma". *Journal of Virology* 4.1 (1969).
DOI: 10.1128/jvi.4.1.75-93.1969.

[383] J. L. Starkey et al. "Elucidation of the Block to Herpes Simplex Virus Egress in the Absence of Tegument Protein UL16 Reveals a Novel Interaction with VP22". *Journal of Virology* 88.1 (2014).
DOI: 10.1128/jvi.02555-13.

[384] T. Stellberger et al. "Improving the yeast two-hybrid system with permutated fusions proteins: the Varicella Zoster Virus interactome". *Proteome science* 8 (2010).
DOI: 10.1186/1477-5956-8-8. arXiv: NIHMS150003.

[385] W. Stoorvogel et al. "Late endosomes derive from early endosomes by maturation". *Cell* 65 (3 1991).
DOI: 10.1016/0092-8674(91)90459-C.

[386] N. D. Stow. "Localization of an origin of DNA replication within the TRS/IRS repeated region of the herpes simplex virus type 1

genome." *The EMBO journal* 1.7 (1982).
DOI: 10.1002/j.1460-2075.1982.tb01261.x.

[387] N. D. Stow and A. J. Davison. "Identification of a varicella-zoster virus origin of DNA replication and its activation by herpes simplex virus type 1 gene products". *Journal of General Virology* 67.8 (1986).
DOI: 10.1099/0022-1317-67-8-1613.

[388] B. L. Strang and N. D. Stow. "Circularization of the Herpes Simplex Virus Type 1 Genome upon Lytic Infection". *Journal of Virology* 79.19 (2005).
DOI: 10.1128/jvi.79.19.12487-12494.2005.

[389] J. Stylianou et al. "Virion incorporation of the herpes simplex virus type 1 tegument protein VP22 occurs via glycoprotein E-specific recruitment to the late secretory pathway." *Journal of virology* 83.10 (2009).
DOI: 10.1128/JVI.00069-09.

[390] T. Suenaga et al. "Myelin-associated glycoprotein mediates membrane fusion and entry of neurotropic herpesviruses". *Proceedings of the National Academy of Sciences of the United States of America* 107.2 (2010).
DOI: 10.1073/pnas.0913351107.

[391] T. Suenaga et al. "Regulation of Siglec-7-mediated varicella-zoster virus infection of primary monocytes by cis-ligands". *Biochemical and Biophysical Research Communications* 613 (2022).
DOI: 10.1016/J.BBRC.2022.04.111.

[392] T. Suenaga et al. "Sialic acids on varicella-zoster virus glycoprotein B are required for cell-cell fusion". *Journal of Biological Chemistry* 290.32 (2015).
DOI: 10.1074/jbc.M114.635508.

[393] T. Suenaga et al. "Siglec-7 mediates varicella-zoster virus infection by associating with glycoprotein B". *Biochemical and Biophysical Research Communications* 607 (2022).
DOI: 10.1016/J.BBRC.2022.03.060.

[394] K. Sugimoto et al. "Simultaneous tracking of capsid, tegument, and envelope protein localization in living cells infected with triply fluorescent herpes simplex virus 1." *Journal of virology* 82.11 (2008).
DOI: 10.1128/JVI.02681-07.

[395] S. Svobodova et al. "Analysis of the Interaction between the Essential Herpes Simplex Virus 1 Tegument Proteins VP16 and VP1/2". *Journal of Virology* 86.1 (2012).
DOI: 10.1128/jvi.05981-11.

[396] B. Taddeo et al. "Interaction of herpes simplex virus RNase with VP16 and VP22 is required for the accumulation of the protein but

not for accumulation of mRNA." *Proceedings of the National Academy of Sciences of the United States of America* 104.29 (2007).
DOI: 10.1073/pnas.0705245104.

[397] K. Takeshima et al. "Identification of the Capsid Binding Site in the Herpes Simplex Virus 1 Nuclear Egress Complex and Its Role in Viral Primary Envelopment and Replication". *Journal of Virology* 93.21 (2019).
DOI: 10.1128/jvi.01290-19.

[398] J. Z. A. Tan and P. A. Gleeson. "Cargo Sorting at the trans-Golgi Network for Shunting into Specific Transport Routes: Role of Arf Small G Proteins and Adaptor Complexes". *Cells* 8.6 (2019).
DOI: 10.3390/cells8060531.

[399] M. Tanaka et al. "Herpes Simplex Virus 1 VP22 Regulates Translocation of Multiple Viral and Cellular Proteins and Promotes Neurovirulence". *Journal of Virology* 86.9 (2012).
DOI: 10.1128/JVI.06913-11.

[400] M. Tanaka et al. "The product of the Herpes simplex virus 1 UL7 gene interacts with a mitochondrial protein, adenine nucleotide translocator 2". *Virology Journal* 5.1 (2008).
DOI: 10.1186/1743-422X-5-125.

[401] P. S. Tarpey et al. "Mutations in the gene encoding the sigma 2 subunit of the adaptor protein 1 complex, AP1S2, cause X-linked mental retardation". *American Journal of Human Genetics* 79.6 (2006).
DOI: 10.1086/510137.

[402] N. S. Taus et al. "The herpes simplex virus 1 U(L)17 gene is required for localization of capsids and major and minor capsid proteins to intranuclear sites where viral DNA is cleaved and packaged". *Virology* 252.1 (1998).
DOI: 10.1006/viro.1998.9439.

[403] D. J. Tenney et al. "The UL8 component of the herpes simplex virus helicase-primase complex stimulates primer synthesis by a subassembly of the UL5 and UL52 components". *Journal of Biological Chemistry* 269.7 (1994).
DOI: 10.1016/s0021-9258(17)37649-4.

[404] J. K. Thurlow et al. "Herpes Simplex Virus Type 1 DNA-Packaging Protein UL17 Is Required for Efficient Binding of UL25 to Capsids". *Journal of Virology* 80.5 (2006).
DOI: 10.1128/jvi.80.5.2118-2126.2006.

[405] G. A. Tipples et al. "New variant of varicella-zoster virus". *Emerging Infectious Diseases* 8.12 (2002).
DOI: 10.3201/eid0812.020118.

[406] R. S. Tirabassi and L. W. Enquist. "Mutation of the YXXL Endocytosis Motif in the Cytoplasmic Tail of Pseudorabies Virus gE". *Journal of Virology* 73.4 (1999).
DOI: 10.1128/jvi.73.4.2717-2728.1999.

[407] B. K. Tischer et al. "Two-step Red-mediated recombination for versatile high-efficiency markerless DNA manipulation in Escherichia coli". *BioTechniques* 40.2 (2006).
DOI: 10.2144/000112096.

[408] K. Toropova et al. "The Herpes Simplex Virus 1 UL17 Protein Is the Second Constituent of the Capsid Vertex-Specific Component Required for DNA Packaging and Retention". *Journal of Virology* 85.15 (2011).
DOI: 10.1128/jvi.00837-11.

[409] L. Trapp-Fragnet et al. "Identification of marek's disease virus VP22 tegument protein domains essential for virus cell-to-cell spread, nuclear localization, histone association and cell-cycle arrest". *Viruses* 11.6 (2019).
DOI: 10.3390/v11060537.

[410] L. M. Traub. "Common principles in clathrin mediated sorting at the Golgi and the plasma membrane". *Biochimica et Biophysica Acta - Molecular Cell Research* 1744.3 SPEC. ISS. (2005).
DOI: 10.1016/j.bbamcr.2005.04.005.

[411] B. L. Trus et al. "The herpes simplex virus procapsid: Structure, conformational changes upon maturation, and roles of the triplex proteins VP19c and VP23 in assembly". *Journal of Molecular Biology* 263.3 (1996).
DOI: 10.1016/S0022-2836(96)80018-0.

[412] B. L. Trus et al. "Allosteric Signaling and a Nuclear Exit Strategy: Binding of UL25/UL17 Heterodimers to DNA-Filled HSV-1 Capsids". *Molecular Cell* 26.4 (2007).
DOI: 10.1016/j.molcel.2007.04.010.

[413] S. Turcotte et al. "Herpes Simplex Virus Type 1 Capsids Transit by the trans -Golgi Network , Where Viral Glycoproteins Accumulate Independently of Capsid Egress Herpes Simplex Virus Type 1 Capsids Transit by the trans-Golgi Network , Where Viral Glycoproteins Accumulate Ind". *Journal of virology* 79.14 (2005).
DOI: 10.1128/JVI.79.14.8847.

[414] A. Turner et al. "Glycoproteins gB, gD, and gHgL of Herpes Simplex Virus Type 1 Are Necessary and Sufficient To Mediate Membrane Fusion in a Cos Cell Transfection System". *Journal of Virology* 72.1 (1998).
DOI: 10.1128/jvi.72.1.873-875.1998.

[415] P. Uetz et al. "Herpesviral protein networks and their interaction with the human proteome". *Science* 311.5758 (2006).
DOI: 10.1126/science.1116804.

[416] I. L. Van Genderen et al. "The phospholipid composition of extracellular herpes simplex virions differs from that of host cell nuclei". *Virology* 200.2 (1994).
DOI: 10.1006/viro.1994.1252.

[417] G. Van Minnebruggen et al. "Internalization of Pseudorabies Virus Glycoprotein B Is Mediated by an Interaction between the YQRL Motif in Its Cytoplasmic Domain and the Clathrin-Associated AP-2 Adaptor Complex". *Journal of Virology* 78.16 (2004).
DOI: 10.1128/jvi.78.16.8852-8859.2004.

[418] S. M. Varnum et al. "Identification of Proteins in Human Cytomegalovirus (HCMV) Particles: the HCMV Proteome". *Journal of Virology* 78.20 (2004).
DOI: 10.1128/jvi.78.20.10960-10966.2004.

[419] V. Vittone et al. "Determination of Interactions between Tegument Proteins of Herpes Simplex Virus Type 1". *Journal of Virology* 79.15 (2005).
DOI: 10.1128/jvi.79.15.9566-9571.2005.

[420] S. E. Vleck et al. "Structure-function analysis of varicella zoster virus glycoprotein H identifies domain-specific roles for fusion and skin tropism". *Proceedings of the National Academy of Sciences of the United States of America* 108.45 (2011).
DOI: 10.1073/pnas.1111333108.

[421] S. A. Walzer et al. "Crystal structure of the human cytomegalovirus pUL50-pUL53 core nuclear egress complex provides insight into a unique assembly scaffold for virus-host protein interactions". *Journal of Biological Chemistry* 290.46 (2015).
DOI: 10.1074/jbc.C115.686527.

[422] L. Wan et al. "PACS-1 defines a novel gene family of cytosolic sorting proteins required for trans-Golgi network localization". *Cell* 94.2 (1998).
DOI: 10.1016/S0092-8674(00)81420-8.

[423] L. Wang et al. "Regulation of the ORF61 Promoter and ORF61 Functions in Varicella-Zoster Virus Replication and Pathogenesis". *Journal of Virology* 83.15 (2009).
DOI: 10.1128/jvi.00118-09.

[424] M. S. Warner et al. "A cell surface protein with herpesvirus entry activity (Hveb) confers susceptibility to infection by mutants of herpes simplex virus type 1, herpes simplex virus type 2, and pseudorabies

virus". *Virology* 246.1 (1998).
DOI: 10.1006/viro.1998.9218.

[425] D. J. Weed and A. V. Nicola. "Herpes simplex virus membrane fusion". In: *Advances in Anatomy Embryology and Cell Biology*. Vol. 223. 2017.
DOI: 10.1007/978-3-319-53168-7_2.

[426] S. P. Weinheimer et al. "Deletion of the VP16 open reading frame of herpes simplex virus type 1." *Journal of Virology* 66.1 (1992).
DOI: 10.1128/jvi.66.1.258-269.1992.

[427] P. Wild et al. "Impairment of Nuclear Pores in Bovine Herpesvirus 1-Infected MDBK Cells". *Journal of Virology* 79.2 (2005).
DOI: 10.1128/jvi.79.2.1071-1083.2005.

[428] E. Wills et al. "The UL31 and UL34 Gene Products of Herpes Simplex Virus 1 Are Required for Optimal Localization of Viral Glycoproteins D and M to the Inner Nuclear Membranes of Infected Cells". *Journal of Virology* 83.10 (2009).
DOI: 10.1128/jvi.02431-08.

[429] N. de Wind et al. "The pseudorabies virus homology of the herpes simplex virus UL21 gene product is a capsid protein which is involved in capsid maturation." *Journal of Virology* 66.12 (1992).
DOI: 10.1128/jvi.66.12.7096-7103.1992.

[430] T. W. Wisner et al. "Herpesvirus gB-Induced Fusion between the Virion Envelope and Outer Nuclear Membrane during Virus Egress Is Regulated by the Viral US3 Kinase". *Journal of virology* 83.7 (2009).
DOI: 10.1128/jvi.01462-08.

[431] E. R. Wonderlich et al. "The tyrosine binding pocket in the adaptor protein 1 (AP-1) μ1 subunit is necessary for Nef to recruit AP-1 to the major histocompatibility complex class I cytoplasmic tail". *Journal of Biological Chemistry* 283.6 (2008).
DOI: 10.1074/jbc.M707760200.

[432] World Health Organization. "Varicella and herpes zoster vaccines: WHO position paper, June 2014 - Recommendations". *Vaccine* 34.2 (2016).
DOI: 10.1016/j.vaccine.2014.07.068.

[433] C. A. Wu et al. "Identification of herpes simplex virus type 1 genes required for origin-dependent DNA synthesis." *Journal of Virology* 62.2 (1988).
DOI: 10.1128/jvi.62.2.435-443.1988.

[434] L. Wu et al. *Alphaherpesvirus Major Tegument Protein VP22: Its Precise Function in the Viral Life Cycle*. 2020.
DOI: 10.3389/fmicb.2020.01908.

[435] S. Wu et al. "Herpes Simplex Virus 1 Induces Phosphorylation and Reorganization of Lamin A/C through the γ 1 34.5 Protein That Facilitates Nuclear Egress". *Journal of Virology* 90.22 (2016).
DOI: 10.1128/jvi.01392-16.

[436] F. Xiao et al. "Interactions between the hepatitis C virus nonstructural 2 protein and host adaptor proteins 1 and 4 orchestrate virus release". *mBio* 9.2 (2018).
DOI: 10.1128/mBio.02233-17.

[437] Y. Xing et al. "A site of varicella-zoster virus vulnerability identified by structural studies of neutralizing antibodies bound to the glycoprotein complex gHgL". *Proceedings of the National Academy of Sciences of the United States of America* 112.19 (2015).
DOI: 10.1073/pnas.1501176112.

[438] F. Xiong et al. "Herpes simplex virus VP22 enhances adenovirus-mediated microdystrophin gene transfer to skeletal muscles in dystrophin-deficient (mdx) mice". *Human Gene Therapy* 18.6 (2007).
DOI: 10.1089/hum.2006.155.

[439] E. Yang et al. "Role for the αV Integrin Subunit in Varicella-Zoster Virus-Mediated Fusion and Infection". *Journal of Virology* 90.16 (2016).
DOI: 10.1128/jvi.00792-16.

[440] E. Yang et al. "The Cytoplasmic Domain of Varicella-Zoster Virus Glycoprotein H Regulates Syncytia Formation and Skin Pathogenesis". *PLoS Pathogens* 10.5 (2014).
DOI: 10.1371/journal.ppat.1004173.

[441] E. Yang et al. "The Glycoprotein B Cytoplasmic Domain Lysine Cluster Is Critical for Varicella-Zoster Virus Cell-Cell Fusion Regulation and Infection". *Journal of Virology* 91.1 (2017).
DOI: 10.1128/jvi.01707-16.

[442] K. Yang and J. D. Baines. "Selection of HSV capsids for envelopment involves interaction between capsid surface components pUL31, pUL17, and pUL25." *Proceedings of the National Academy of Sciences of the United States of America* 108.34 (2011).
DOI: 10.1073/pnas.1108564108.

[443] K. Yang and J. D. Baines. "The Putative Terminase Subunit of Herpes Simplex Virus 1 Encoded by UL28 Is Necessary and Sufficient To Mediate Interaction between pUL15 and pUL33". *Journal of Virology* 80.12 (2006).
DOI: 10.1128/jvi.00125-06.

[444] U. Yasamut et al. "Adaptor protein 1A facilitates dengue virus replication". *PLoS ONE* 10.6 (2015).
DOI: 10.1371/journal.pone.0130065.

[445] D. Yu and S. K. Weller. "Genetic analysis of the UL15 gene locus for the putative terminase of herpes simplex virus type 1". *Virology* 243.1 (1998).
DOI: 10.1006/viro.1998.9041.

[446] X. Yu et al. "Herpes simplex virus type 1 tegument protein VP22 is capable of modulating the transcription of viral TK and gC genes via interaction with viral ICP0". *Biochimie* 92.8 (2010).
DOI: 10.1016/j.biochi.2010.04.025.

[447] X. Yu et al. "Herpes simplex virus type 1 VP22 mediated intercellular delivery of PTEN increases the antitumor activity of PTEN in esophageal squamous cell carcinoma cells in vitro and in vivo". *Oncology Reports* 35.5 (2016).
DOI: 10.3892/or.2016.4694.

[448] S. V. Zaichick et al. "The herpesvirus VP1/2 protein is an effector of dynein-mediated capsid transport and neuroinvasion". *Cell Host and Microbe* 13.2 (2013).
DOI: 10.1016/j.chom.2013.01.009.

[449] T. Zeev-Ben-Mordehai et al. "Crystal structure of the herpesvirus nuclear egress complex provides insights into inner nuclear membrane remodeling". *Cell Reports* 13.12 (2015).
DOI: 10.1016/j.celrep.2015.11.008.

[450] L. Zerboni et al. "Molecular mechanisms of varicella zoster virus pathogenesis". *Nature Reviews Microbiology* 12.3 (2014).
DOI: 10.1038/nrmicro3215.Molecular.

[451] Y. Zhang and J. L. McKnight. "Herpes simplex virus type 1 UL46 and UL47 deletion mutants lack VP11 and VP12 or VP13 and VP14, respectively, and exhibit altered viral thymidine kinase expression." *Journal of Virology* 67.3 (1993).
DOI: 10.1128/jvi.67.3.1482-1492.1993.

[452] Y. Zhang et al. "Role of herpes simplex virus type 1 UL46 and UL47 in alpha TIF-mediated transcriptional induction: characterization of three viral deletion mutants." *Journal of Virology* 65.2 (1991).
DOI: 10.1128/jvi.65.2.829-841.1991.

[453] Z. Zhang et al. "A highly efficient protocol of generating and analyzing VZV ORF deletion mutants based on a newly developed luciferase VZV BAC system." *Journal of virological methods* 148.1-2 (2008).
DOI: 10.1016/j.jviromet.2007.11.012.

[454] C. Zheng et al. "Characterization of the Nuclear Localization and Nuclear Export Signals of Bovine Herpesvirus 1 VP22". *Journal of Virology* 79.18 (2005).
DOI: 10.1128/jvi.79.18.11864-11872.2005.

[455] F. X. Zhu et al. "Virion Proteins of Kaposi's Sarcoma-Associated Herpesvirus". *Journal of Virology* 79.2 (2005).
DOI: 10.1128/jvi.79.2.800-811.2005.

[456] J. Zhu et al. "Nuclear and mitochondrial localization signals overlap within bovine herpesvirus 1 tegument protein VP22". *Journal of Biological Chemistry* 280.16 (2005).
DOI: 10.1074/jbc.M500054200.

[457] L. A. Zhu and S. K. Weller. "The UL5 gene of herpes simplex virus type 1: isolation of a lacZ insertion mutant and association of the UL5 gene product with other members of the helicase-primase complex." *Journal of Virology* 66.1 (1992).
DOI: 10.1128/jvi.66.1.458-468.1992.

[458] Q. Zhu and R. J. Courtney. "Chemical cross-linking of virion envelope and tegument proteins of herpes simplex virus type 1". *Virology* 204.2 (1994).
DOI: 10.1006/viro.1994.1573.

[459] Z. Zhu et al. "Infection of cells by varicella zoster virus: inhibition of viral entry by mannose 6-phosphate and heparin." *Proceedings of the National Academy of Sciences of the United States of America* 92.8 (1995).
DOI: 10.1073/pnas.92.8.3546.